UNIVERSITA' DEGLI STUDI DI FIRENZE

CRANFIELD UNIVERSITY

FRANCESCA BERTI

NEW MICRO- AND NANO-TECHNOLOGIES FOR BIOSENSOR DEVELOPMENT

PhD THESIS

UNIVERSITA' DEGLI STUDI DI FIRENZE

CRANFIELD UNIVERSITY
CRANFIELD HEALTH

DOTTORATO DI RICERCA IN SCIENZE CHIMICHE
XXII CYCLE

PhD THESIS

Academic years 2007-2009

FRANCESCA BERTI

NEW MICRO- AND NANO-TECHNOLOGIES FOR BIOSENSOR DEVELOPMENT

Supervisors:
Professor Giovanna Marrazza (Università di Firenze)
Professor Anthony P.F. Turner (Cranfield University)

This thesis is submitted in partial fulfilment of the requirements for the degree of Doctor of Philosophy under a co-tutela between the University of Firenze and Cranfield University.

ABSTRACT

Recent advances in micro- and nanotechnology have produced a number of new materials which exhibit exceptional potential for the design of novel sensing strategies and to enhance the analytical performance of biosensing systems.

In this thesis three different types of miniaturisation pathways were investigated for electrochemical biosensing applications. Vertically aligned carbon nanotube thin films were designed and tested as platforms for DNA immobilisation and for the development of a model electrochemical genosensor. The sensor format involved the immobilisation of oligoucleotide probes onto the sensor surface, hybridisation with the target sequence and electrochemical detection of the duplex formation. By combining such an electrode platform with an enzyme labeling, a detection limit of oligonucleotide targets in the nanomolar range was achieved.

A novel magnetic particle-based microfluidic sensor was also realised by integrating a microfluidic platform with a new analytical procedure based on the use of paramagnetic beads for the detection of real PCR samples. The hybridisation reaction was carried out on probe-modified beads in a flow-through format, thus enhancing the surface area-to-volume ratio and consequently the sensitivity. Moreover, the magnetic properties of the beads greatly facilitated the delivery and removal of reagents through the microfluidic channels. This format allowed the detection of nanomolar levels of double-stranded DNA sequences, with high reproducibility and fast time of analysis.

Finally, polyaniline nanotubes arranged in an ordered structure directly on gold electrode surfaces were realised and employed to create a model molecularly imprinted polymer(MIP)-sensor for catechol detection. The advantages of using nanostructures in this particular biosensing application have been evaluated by comparing the analytical performance of the sensor with an analogous non-nanostructured MIP-sensor that we had previously developed. A significantly lower limit of detection (one order of magnitude) was achieved, thus

demonstrating that the nanostructures enhanced the analytical performance of the sensor.

ACKNOWLEDGMENTS

I would like to thank Professor Giovanna Marrazza and Professor Anthony Turner, for giving me the possibility to develop this project and for their helpful scientific supervision and support.

I would like to thank Professor Marco Mascini for his wise guidance in the biosensors field and for the opportunity he gave me, together with Professor Turner, to undertake a very useful professional and life experience at Cranfield University (UK).

I wish especially to thank all the staff of Prof. Mascini laboratory for their friendly care and collaboration. Among them a special acknowledgment goes to Dr. Ilaria Palchetti and Dr. Serena Laschi who took part to this project and to Dr. Fausto Lucarelli, Dr. Francesca Bettazzi and Dr. Sonia Centi for their useful advice and true friendship.

I wish also to thank the members of Cranfield Health who warmly welcomed and helped me. In particular I would like to thank Professor Sergey Pilesky for his important scientific support, Dr. Iva Chianella for her kind assistance, my lab and office mates for their friendly aid, and Silvia Todros who shared this experience with me.

TABLE OF CONTENTS

ABSTRACT I
ACKNOWLEDGMENTS III
TABLE OF CONTENTS V
ABBREVIATIONS IX
LIST OF FIGURES XI
LIST OF TABLES XVII

1. INTRODUCTION 1
1.1 Electrochemical biosensors: principles and applications 2
1.1.1 Applications of electrochemical biosensors 5
1.2 Nanomaterials for electrochemical biosensing 8
1.2.1 Carbon nanotubes 9
1.2.1.1 Carbon nanotubes used in catalytic biosensors 11
1.2.1.2 Carbon nanotubes used in affinity biosensors 20
1.2.2 Conductive polymer nanostructures 28
1.2.2.1 Conductive polymer nanostructures used in catalytic biosensors 31
1.2.2.2 Conductive polymer nanostructures used in affinity biosensors 38
1.2.3 Nanoparticles 42
1.2.3.1 Nanoparticles used in catalytic biosensors 43
1.2.3.2 Nanoparticles used in affinity biosensors 44
1.3 Aim and objectives 52

2. MATERIALS AND METHODS 57
2.1 Chemicals 57
2.1.1 DNA sequences: probes and targets 58
2.2 Electrochemical methods 60
2.2.1 Cyclic Voltammetry 60
2.2.2 Differential pulse voltammetry 61
2.2.3 Square wave voltammetry 62

2.2.4 Chronoamperometry 63
2.3 Biosensors preparation and transduction systems 64
2.3.1 Carbon nanotube-based electrochemical genosensor 64
2.3.1.1 CNT Thin Film Fabrication 64
2.3.1.2 Disposable CNT sensors 66
2.3.1.3 Electrochemical apparatus 67
2.3.1.4 Functionalisation of the sensor surface 67
2.3.1.5 Label-free hybridisation assay 68
2.3.1.6 Enzyme-linked hybridisation assay 69
2.3.2 Microfluidc-based genosensor coupled to magnetic beads 70
2.3.2.1 Microfluidic platform 70
2.3.2.2 DNA modification of streptavidin-coated paramagnetic beads 72
2.3.2.3 Enzyme-linked hybridisation assay 73
2.3.2.4 Electrochemical detection: drop-on system 74
2.3.2.5 Electrochemical detection: microfluidic-based platform 76
2.3.3 Catechol MIP-sensor based on one-dimensional polyaniline nanostructures 77
2.3.3.1 Monomer (NPEDMA) preparation 77
2.3.3.2 Template synthesis of PANI nanostructures 78
2.3.3.3 Electrochemical apparatus 78
2.3.3.4 SEM characterisation 79
2.3.3.5 Preparation of the MIP-sensor for catechol detection 79
2.3.3.6 Catechol detection 80

3. CARBON NANOTUBES FOR GENOSENSING 81
3.1 Results 81
3.1.1 Preliminary experiments using disposable carbon electrodes modified with CNTs 81
3.1.2 CNT film characterisation 83
3.1.2.1 Evaluation of CNT adhesion on the growing substrate 83
3.1.2.2 Electrochemical characterisation of the surface 86
3.1.3 Development of the genosensor 88

3.1.3.1 Optimisation of the immobilisation conditions 88
3.1.3.2 Label-free assay 92
3.1.3.3 Enzyme-linked assay 94
3.2 Discussion 95
3.2.1 Optimisation of CNT film construction 95
3.2.2 Electrochemical performance of CNTs 97
3.2.3 CNT for electrochemical biosensing 99
3.2.3.1 Optimisation of immobilisation conditions 99
3.2.3.2 Detection of the hybridisation reaction 102

4. MICROFLUIDIC-BASED GENOSENSOR COUPLED TO MAGNETIC BEADS 105
4.1 Results 105
4.1.1 Optimisation of magnetic bead-genosensor assay using drop-on system 105
4.1.2 Optimisation of the microfluidic platform 107
4.1.2.1 Optimisation of the bead loading step 107
4.1.2.2 Optimisation of the amount of beads 109
4.1.2.3 Optimisation of the substrate concentration 110
4.1.3 Analysis of PCR-amplified samples 111
4.2 Discussion 115
4.2.1 Optimisation of the analytical procedure 116
4.2.2 Analysis of PCR amplified samples 119

5. ONE-DIMENSIONAL POLYANILINE NANOSTRUCTURES FOR MIP-SENSING 123
5.1 Results 123
5.1.1 Synthesis of PANI nanostructures 123
5.1.2 Electrical characterisation 126
5.1.3. Morphological characterisation 127
5.1.4 MIP grafting of polyaniline nanostructures for catechol detection 130
5.1.4.1 Investigation of the electrochemical response of the MIP-sensor 131

5.1.4.2 Evaluation of the analytical performance of the sensor 132
5.2 Discussion 135
5.2.1 Synthesis and characterisation of PANI nanostructures 135
5.2.2 MIP grafting of polyaniline nanostructures for catechol detection 140

6. CONCLUSIONS AND FUTURE WORK 143

BIBLIOGRAPHY 149
PUBLICATIONS 173

ABBREVIATIONS

AChE	acetylcholinesterase
BSA	bovine serum albumin
CNT	carbon nanotube
CV	cyclic voltammetry
CVD	chemical vapour deposition
DEA	diethanolamine
DL	detection limit
DMF	dimethylformamide
DNA	deoxyribonucleic acid
DPV	differential pulse voltammetry
EDAC	*N*-(3-dimethylaminopropyl)-*N*′-ethylcarbodiimide hydrochloride
EDTA	ethylenediaminetetraacetic acid
EIS	electrochemical impedance spectroscopy
FAD	flavin adenine dinucelotide
FET	field effect transistor
GC	glassy carbon
GOx	glucose oxidase
hCG	human chorionic gonadotropin hormone
HRP	horse radish peroxidase
IgG	immunoglublulin G
MIP	molecularly imprinted polymer
MWNT	multiwalled carbon nanotube
NADH	nicotinamide adenine dinucleotide
NIP	non imprinted polymer
NHS	N-hydroxysuccinimide
NMR	nuclear magnetic resonance
NP	nanoparticle

PANI	polyaniline
PBS	phosphate buffer saline
PCR	polymerase chain reaction
PDDA	poly(dimethyldiallyl-ammoniumchloride)
PEDOT	polyethylenedioxythiophene
PPy	polypyrrole
PSS	poly(sodium 4-styrenesulfonate)
PVC	polyvinyl chloride
QD	quantum dot
RNA	ribonucleic acid
$Ru(bpy)_3^{2+}$	tris(2,2'-(bipyridyl)ruthenium(II)
SDS	sodium dodecyl sulphate
SEM	scanning electron microscope
SNPs	single nucleotide polymorphisms
SPE	screen printed electrode
SPE-CNT	screen printed electrodes modified with CNTs
STEM	scanning transimission electron microscope
SWNT	singlewalled carbon nanotube
SWV	square wave voltammetry
TEG	tetra-ethyleneglycol
Tyr	tyrosinase
UV	ultraviolet

LIST OF FIGURES

Figure 1: Diagram of a biosensor. 2

Figure 2: Schematic structures of Single-walled carbon nanotubes (SWNTs) and Multi-walled carbon nanotubes (MWNTs). 10

Figure 3: Main classes of conductive polymers. 31

Figure 4: Schematic representation of four different nanoparticle-based labelling routes: A) conductimetric detection; B) Au dissolving and Au(III) stripping accumulation and detection; C) Silver precipitation, dissolution (with HNO_3) and Ag^+ stripping; D) multi-labelling with different quantum dots and detection of the corresponding ions. 45

Figure 5: Voltage vs time excitation signals used in voltammetry and corresponding current responses: cyclic voltammentry potential (a) and corresponding current response (d); differential pulse voltammetry (b), square wave voltammetry (c) and corresponding peak-shaped current response (e). 61

Figure 6: Chronoamperometry: potential vs time waveform (a), change of concentration profiles (x = distance from the electrode surface) with time (b), the resulting current vs time response (c). 64

Figure 7. Aligned carbon nanotube thin films obtained by CVD. Diagram of the CNT-film grown on a SiO_2 substrate (a) and corresponding SEM image (b). Diagram of the CNT-film grown on a Al/SiO_2 substrate (c) and corresponding SEM image (d). CNT dimensions: Ø = 5-20 nm, length = 3-6 μm, density ≈ 1011 CNT/cm^2. 66

Figure 8. Electrochemical apparatus. Autolab PGSTAT 30(2) digital potentiostat/galvanostat (a). Diagram of the plexiglass well cell used for electrochemical experiments using CNT thin films. An o-ring delimited a circular working electrode surface (Ø = 2mm) on the CNT film (b). 67

Figure 9. Scheme of capture probe immobilisation procedure on CNT thin films. 68

Figure 10. Hybridisation assays performed using CNT thin films as working electrode: label-free (a) and enzyme-linked format (b). 70

Figure 11. Picture of the microfluidic-based Immuspeed™ platform (a) and corresponding technical drawing (b). Diagram of the ImmuChip™ (c). Technical drawing of a microchannel cross-section with flowing magnetic beads being captured by a magnet (d). Technical drawings were 72

kindly provided by DiagnoSwiss S.A. (http://www.diagnoswiss.com).

Figure 12. Scheme of the enzyme-linked hybridisation assay performed on paramagnetic beads. 74

Figure 13. Example of chrono-amperometric detection of enzyme kinetics in a chip. The experiment was performed by adsorbing different amounts of alkaline phosphatase (from 1 to 5 10^{-4} U/mL, in channel from 1 to 8) on the walls of the microchannels and then introducing the enzyme substrate. Each symbol represents a single current acquisition value. 77

Figure 14. Scheme of the template synthesis of PANI nanostructure array. 78

Figure 15. Calibration curve for successive addition of 1mM of H_2O_2 obtained using CNT modified SPE (black line) and bare SPE (red line). Each point is the mean of three amperometric measurement. Applied potential: +700 mV (vs. Ag pseudoreference). Error bars represent the standard deviation of three replicates (n = 3). 82

Figure 16. Evaluation of CNT adhesion during electrochemical measurements in solution (CV in acetate buffer 0.25 M with KCl 10 mM). a) CNT/Ni/SiO_2 (700°C): before (solid line) and after (dashed line) CNT release. b) CNT/Ni/Si_3N_4 (700°C): before (solid line) and after (dashed line) CNT release. c) CNT/Ni/Al/SiO_2 (700°C): six consecutive scans. (CV parameters: start potential 0 V, first vertex potential 1.0 V, second vertex potential 0 V, step potential 0.0244 v, scan rate 0.05 V s^{-1}). 84

Figure 17. Screening of CNT adhesion during a label free hybridisation assay. a) Guanine oxidation signal after the hybridisation with DNA-target 1µM recorded with a CNT/Ni/Si_3N_4 (700°C) sensor. The first signal obtained (solid line) and second signal recorded after CNT release (dashed line). b) Three consecutive cycles of hybridisation/denaturation performed using a CNT/Ni/Al/SiO_2 (700°C) sensor. (DPV parameters: modulation time, 0.05 s; interval time, 0.15 s; step potential, 5mV; modulation amplitude, 70 mV). 86

Figure 18. Electrochemical charecterisation. a) CV of 5 mM $K_3[Fe(CN)_6]$ in KCl 1 M (start potential 0.6 V, first vertex potential -0.2 V, second vertex potential 0.6 V, step potential 0.0244 v, scan rate 0.05 V s^{-1}). (b) CV of 1 mM hydroquinone in acetate buffer 0.25 M with KCl 10 mM (CV parameters: start potential 0.7 V, first vertex potential -0.5 V, second vertex potential 0.7 V, step potential 0.0244 v, scan rate 0.05 V s^{-1}). Signals obtained using CNT-films (black line), carbon screen-printed electrodes (red line) and sensors processed in the CVD reactor, in the absence of one of the precursor gases, thus obtaining only amorphous carbon on the surface (green line). 87

Figure 19. Investigation of oxidation and immobilisation methods. CNT-SPE electrodes were oxidised and inosine-modified probe (5 μM) was immobilised, according to the procedure reported in the text. SWV scan of the immobilised probe was perfomed in 50μL of acetate buffer 0.25 M + KCl 10 mM. (frequency 50 Hz, step potential 15 mV, amplitude 40 mV, potential scan 0.2 V - 1.6V) and Inosine oxidation peak (Pot 1.4 V vs Ag/AgCl) taken as analytical data. Error bars represent the standard deviation of three replicates (n = 3). 89

Figure 20. SWV scans of covalently immobilised inosine based probe (5 μM) using CNT-SPE electrodes (frequency 50 Hz, step potential 15 mV, amplitude 40 mV, potential scan 0.2 V - 1.6 V). CNTs had been oxidised with $K_2Cr_2O_7$ 2.5% HNO_3 10% of 1.5 V (vs Ag/AgCl) for 15" (a), at 1.6 V vs Ag/AgCl for 120" in acetate buffer solution (0.25 M) (b), and with HNO_3 10% for 60" (c). Measurements were performed in 50μL of acetate buffer 0.25 M + KCl 10 mM. 90

Figure 21. SWV measurements in acetate buffer 0.25 M with KCl 10 mM of the 5 μM DNA-probe immobilised on a CNT-film (solid line) and on an amorfous carbon sensor (dashed line). (SWV parameters: frequency 50 Hz, step potential 15 mV, amplitude 40 mV, potential scan 0.2 V - 1.6 V). Measurements were performed in 50μL of acetate buffer 0.25 M + KCl 10 mM. 91

Figure 22. Optimisation of probe concentration. Each value is the mean of three values of guanine oxidation peaks obtained after the hybridisation with DNA target 10 μM or non complementary oligonucleotide 10 μM. Measurements were performed in 50μL of acetate buffer 0.25 M + KCl 10mM. Error bars represent the standard deviation of three replicates (n = 3). (DPV parameters: modulation time, 0.05 s; interval time, 0.15 s; step potential, 5mV; modulation amplitude, 70 mV). 92

Figure 23. Guanine oxidation peaks obtained after the hybridisation with DNA target (concentration range, 0-10 μM) and non complementary oligonucleotide (10 μM). Measurements were performed in 50μL of acetate buffer 0.25 M + KCl 10mM. Inset: linear fit of displayed data: Y = 1.01 X + 0.74, R = 0.99. (DPV parameters: modulation time, 0.05 s; interval time, 0.15 s; step potential, 5mV; modulation amplitude, 70 mV). 93

Figure 24. p-Amino phenol oxidation peaks obtained after the hybridisation with DNA target (concentration range 0-500 nM) and non complementary oligonucleotide (500 nM). Measurements were performed in 400 μL of DEA buffer containing 1mg/mL of p-amino phenyl phosphate after 15 min of incubation with the enzyme labelled 95

hybrid. Inset: linear fit of displayed data: Y = 0.02 X + 0.31, R = 0.98 (DPV parameters: modulation time, 0.05 s; interval time, 0.15 s; step potential, 5mV; modulation amplitude, 70 mV).

Figure 25. Calibration plot for Cor a 1.04 amplicons performed using drop-on system. Probe-modified and biotin-blocked beads were incubated for 15 min with 50 µL of thermally denatured target solutions, diluted to the desired concentration (0, 2, 5, 10, 15, 20, 30 nmol/L) with a solution 0.15 µM of biotinylated signalling probe in phosphate buffer. Other experimental details are avilable in Paragraph 2.3.2.4. Error bars represent the standard deviation of three replicates (n = 3). 106

Figure 26. Optimisation of the "multiple loading protocol". Flow parameters: 20 µL of bead suspension 0.5 mg/mL aspired at at 2 µL/min flow-through for 2 s, 3 s of steady-state without flow, total number of loading: 10, 50, 100, 200 cycles; introduction of 20 µL of 10 mM p-aminophenyl phosphate, 3 s at 10 µL/min flow-through, 2 s of steady-state without flow, 12 cycles. Chronoamperometric measurement: static mode, sequential measured every 2 s for a total acquisition time of 6 min; potential +250 mV vs. Ag/AgCl pseudo-reference. Error bars represent the standard deviation of two replicates (n = 2). 109

Figure 27. Calibration plot for Cor a 1.04 amplicons (a) and example of current vs time plot (b). Probe-modified and biotin blocked beads were incubated for 15 min with 50 µL of thermally denatured target solutions 0, 2, 5, 10, 15, 20, 30 nM and a 30 nM non complementary sequence. Flow parameters: see paragraph 2.3.2.5. Chronoamperometric measurement: static mode, sequential measures every 2 s for a total acquisition time of 3 min; potential +250 mV vs. Ag/AgCl pseudo-reference. Error bars represent the standard deviation of three replicates (n = 3). 112

Figure 28. Total hybridisation assay: calibration plot for Cor a 1.04 amplicons. Probe-modified and biotin blocked beads were loaded in the fluidic system and incubated with thermally denatured target solutions 0, 2, 5, 10, 15, 20, 30 nM and a 30 nM non complementary sequence, according to the procedure illustrated in paragraph 2.3.2.3 and Table 3. Chronoamperometric measurement: static mode, sequential measures every 2 s for a total acquisition time of 3 min; potential +250 mV vs. Ag/AgCl pseudo-reference. Error bars represent the standard deviation of three replicates (n = 3). 114

Figure 29. CV scan of a solution containing NPEDMA 2.4 mM in $HClO_4$ 50 mM. Electrochemical parameters: initial potential -0.4 V, final potential 1.0 V, step potential 0.005 V, scan rate 50 mV/s, 5 (a), 10 (b), 15 (c) cycles, Pot. vs Ag/AgCl. 125

Figure 30. SEM images of Al_2O_3 membranes used as template, with a 127

nominal pore size of 200 nm: (a) Top view of front face, with real pore size of about 20 nm; (b) Top view of back face, with real pore size of 200 nm; (c) Cross sectional view of the funnel-shaped pores

Figure 31. SEM images of membranes after PANI electropolymerisation through cyclic voltammetry in 10 scans (a) and 15 scans (b). 128

Figure 32. SEM image of top view of PANI nanostructures (a), after template dissolution (some residuals of the template still present); vertically aligned PANI nanostructures, after and template dissolution, cross-sectional view (b). The length of the structures is proximately the same of the template thickness (nominal value 60 μm). STEM image of single PANI nanotubes (c). 129

Figure 33. CV of 100 μM catechol in PBS 10 mM, pH 7.4, after loading with 5 mM $CuCl_2$ for 5' (CV parameters: start potential -0.5 V, first vertex potential 0.9 V, second vertex potential -0.5 V, step potential 0.01 V, scan rate 0.05 V s^{-1}; Potential vs. Ag/AgCl). Signals obtained using MIP-grafted sensor (red line), Au-sputtered alumina membrane before electropolymerisation (green line), sensor after growth of PANI nanostructures (black line). 131

Figure 34. CV of catechol and structural analogue potentially interfering compounds. All the solution were prepared using PBS 10 mM, pH 7.4 and cycled after loading the sensor with 5 mM $CuCl_2$ for 5' (CV parameters: start potential -0.5 V, first vertex potential 0.9 V, second vertex potential -0.5 V, step potential 0.01 V, scan rate 0.05 V s^{-1}; Potential vs. Ag/AgCl). 132

Figure 35. Calibration plot of anodic peak current vs catechol concentration for MIP-sensor and corresponding data obtained a non imprinted control sensor. Inset: linear fit of the linea part of the curve (0-2 μM): Y = 35.7 X + 4.77, R = 0.97. Each data point represents the average from three different sensors (n=3). All the solution were prepared using PBS 10 mM, pH 7.4 and cycled after loading the sensor with 5 mM $CuCl_2$ for 5 min. 133

Figure 36. Voltammograms obtained using a MIP-sensor (a) and a NIP-sensor (b). All the solution were prepared using PBS 10 mM, pH 7.4 and cycled after loading the sensor with 5 mM $CuCl_2$ for 5 min. (CV parameters: start potential -0.5 V, first vertex potential 0.9 V, second vertex potential -0.5 V, step potential 0.01 v, scan rate 0.05 V s^{-1}; Potential vs. Ag/AgCl). 134

Figure 37. Scheme of the redox mechanism of N-substituted Polyaniline. 136

LIST OF TABLES

Table 1: Synthetic DNA sequences related to the 35 S promoter. 58

Table 2: Sequences of synthetic oligonucleotides, PCR primers and the PCR fragment related to Cor a 1.04 hazelnut gene. 59

Table 3. Total hybridisation assay working protocol. 75

Table 4. List of the sensors tested for genosensor development. 83

Table 5. Optimisation of the loading step: "back flow protocol". Flow parameters: 20 µL of bead suspension (1 or 3 mg/mL) aspired at a flow rate of 10 µL/min, 2 min; reversed flow 5µL/min, 4 min; introduction of 20 µL of 10 mM p-aminophenyl phosphate, 3 s at 10 µL/min flow-through, 2 s of steady-state without flow, 12 cycles. Chronoamperometric measurement: static mode, sequential measures every 2 s for a total acquisition time of 6 min; potential +250 mV vs. Ag/AgCl pseudo-reference. 108

Table 6. Optimisation of the amount of beads. Flow parameters: 20 µL of bead suspension 0.15, 0.5, 1.0, 3.0 mg/mL aspired at at 2 µL/min flow-through for 2 s, 3 s of steady-state without flow, total number of loading: 100 cycles; introduction of 20 µL of 10 mM p-aminophenyl phosphate, 3 s at 10 µL/min flow-through, 2 s of steady-state without flow, 12 cycles. Chronoamperometric measurement: static mode, sequential measures every 2 s for a total acquisition time of 6 min; potential +250 mV vs. Ag/AgCl pseudo-reference. 110

Table 7. Influence of p-aminophenyl phosphate concentration on the sensitivity of the assay. Flow parameters: 20 µL of bead suspension 0.15 mg/mL aspired at at 2 µL/min flow-through for 2 s, 3 s of steady-state without flow, total number of loading: 100 cycles; introduction of 20 µL of 5, 10, 20 mM p-aminophenyl phosphate, 3 s at 10 µL/min flow-through, 2 s of steady-state without flow, 12 cycles. Chronoamperometric measurement: static mode, sequential measures every 2 s for a total acquisition time of 3 or 6 min; potential +250 mV vs. Ag/AgCl pseudo-reference. 111

Table 8. Electrical resistance measurements between the two sides of the alumina template before and after PANI electrodeposition. 126

Chapter 1

INTRODUCTION

Over the last decade, great attention has been paid to the integration of newly developed nanomaterials such as nanowires, nanotubes and nanocrystals in sensor devices. The reason can be traced to the ability to tailor the size and structure and hence the properties of nanomaterials, thus opening up excellent prospects for designing novel sensing systems and enhancing the performance of bioanalytical assays [1].

The aim of this work was the investigation of different types of nanomaterials, such as carbon nanotubes (CNTs), polymer nanowires and magnetic particles, that could be employed as building blocks for the realisation of new electrochemical biosensors. Biosensors are analytical devices in which the recognition system utilises a biochemical mechanism. They are constituted of a biological element in intimate contact with a transducer which converts the recognition event into a detectable signal (Figure 1) [2, 3].

The interest in coupling these two aspects, nanomaterials and biosensors, derived from the consideration that most biological systems and molecular interactions belong to the nanometre scale. Moreover, nanomaterials possess a technologically important combination of properties, such as high surface area, good electrical properties, chemical stability and ease of miniaturisation, which make them very promising for the realisation of nanoscale bio-electronic devices.

1.1 Electrochemical biosensors: principles and applications

According to the International Union of Pure and Applied Chemistry (IUPAC) an electrochemical biosensor is "a self-contained integrated device, which is capable of providing specific quantitative or semi-quantitative analytical information using a biological recognition element (biochemical receptor) which is retained in direct spatial contact with an electrochemical transduction element" [4]. With respect to other transduction systems (optical, piezoelectric, acoustic, gravimetric, magnetic, calorimetric), electrochemical devices are highly sensitive, inexpensive, easy-to-use, portable and compatible with microfabrication technologies [5]. Thus, they have found application in a large number of clinical and environmental analyses.

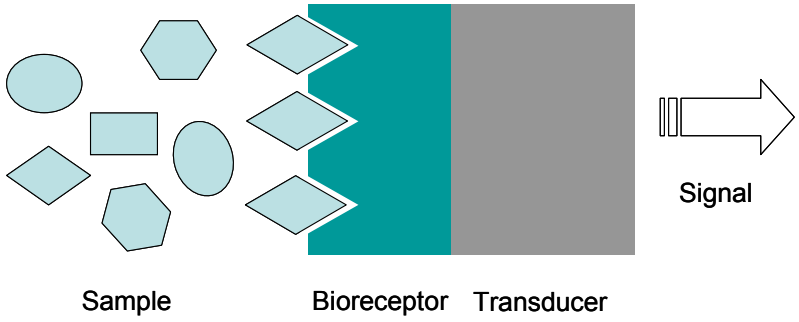

Figure 1. Diagram of a biosensor.

Biosensors can be classified according to the biologically active part into catalytic or affinity biosensors.

Catalytic biosensors are obtained by using biological catalysts such as enzymes, cells, microorganisms or biomimetic catalysts, which promote a reaction involving an organic or inorganic substrate (the analyte) to produce a specie to which the electrode responds [6]. Because of their immediate application in clinical tests and ease of preparation, enzyme-based biosensors have been very popular, with thousands of articles published. In particular, commercial glucose

oxidase-based biosensors have been employed for testing glucose levels in blood since 1975 [7, 8] but a large number of applications have been also found in food and environmental analysis [9, 10].

Affinity biosensors are based on biomolecules able to selectively and reversibly bind specific ligands [11]. In this way, it is possible to monitor and quantify the binding of antibodies to antigens, cell receptors to their ligands, and nucleic acid (DNA, RNA) with a complementary sequence. Biosensors based on antibodies and antigens (immunosensors) have been the most investigated due their high affinity, versatility and commercial availability of the biological elements. Several applications have been developed: from routine clinical tests to diagnostic assays, and from environmental monitoring to food control [12].

However, the use of antibodies in biosensing has also suffered from some limitations [13]: animals are required for their selection and production, which not only constitutes an ethical problem, but antibody generation becomes difficult against molecules which are toxic or not well tolerated by the animal. Moreover, antibodies are labile, the identification and selection of rare antibodies is laborious and the performance of repeat batches of antibodies tends to vary . In order to overcome these limitations, recent progresses in biotechnology and advanced chemical synthesis have lead to the construction of new bio-recognition elements such as molecularly imprinted polymers [14], aptamers [15] and bio-mimetic peptides [16], which able to offer new perspectives for the realisation of affinity biosensors with higher selectivity, sensitivity and stability.

An important class of affinity sensor is also constituted by genosensors, which employ an oligonucleotide sequence as bio-recognition element. In this case recognition derives from complementary base coupling (hybridisation) [17]. The discrimination of specific gene sequences plays a fundamental role in detection of pathogens (viruses, bacteria), genetic diseases, targets of pharmaceutical and industrial interest (i.e., genetically modified organisms) [18]. For this reason, over the past decade, biosensor technology has played a fundamental role in the

realisation of simple and portable devices for DNA and RNA diagnostics. Moreover, new synthetic DNA analogues, such as peptide nucleic acid (PNA) and locked nucleic acid (LNA), have been designed to be employed as new probes, able to hybridise with high stability and selectivity complementary DNA targets in the presence of mismatched sequences, thus allowing the screening of clinically relevant single base polymorphisms (SNPs) and closely related pathogenic species [19].

Both physical and chemical methods have been developed for immobilising the biological element on the sensor surface [20]. Physical strategies comprise adsorption or entrapment in permeable membranes, while chemical methods rely on the covalent binding or cross-linking of reactive residues present within the biomolecule such as amine, carboxylic, aldheydic or thiolic groups. The immobilisation step is a crucial aspect in biosensor development which must be studied and optimised in order to avoid the denaturation of the receptor, with consequent lost of recognition ability, and to control steric hindrance, thus assuring a good accessibility for the analytes.

Another key aspect is the transduction system. Electrochemical biosensors are based on monitoring electro-active species that are bound, produced or consumed by the action of the biological element. They can be divided into five classes: amperometric, voltammetric, conductimetric, potentiometric and field-effect sensors [21, 4]. Amperometry is based on the application of a constant potential between a working electrode and a reference, thus promoting a redox reaction, while in voltammetry current is measured upon varying the potential in a proper range. In both techniques the resulting current is proportional to the bulk concentration of the electroactive species or its production or consumption rate within the adjacent biocatalytic layer. The other three methods are related to ion concentration or charge changes caused by biological reactions (e.g. pH changes due to urease). Conductometric measurements are usually performed by monitoring in parallel the response of biomodified and unmodified sensors. Potentiometry consists of measuring the potential difference between an indicator

electrode and a reference, while no current is passing between them. Finally, surface charge changes can be measured using field-effect transistor systems, constituted by a semiconductor path ("gate") located between two contacts ("source and drain"). A small change in the gate voltage, due to immobilised biomolecules and / or to their interaction with substrates, can cause a large variation in the current flowing from the source to drain.

1.1.1 Applications of electrochemical biosensors

The versatility of biosensors is due to the diverse range of biological elements that can be employed, coupled with the reliability of electrochemical methods and this has lead to an immense number of possible applications in medicine, food control, environmental monitoring and homeland security.

In the clinical field, applications range from diagnosis of pathological conditions, diseases and genetic disorders, to forensic investigations or drug response measurements. [22]. In addition to the aforementioned glucose biosensor, first commercialised in 1975 and employed world-wide for clinical and home testing, many electrochemical sensors have been introduced into the market [7]. Examples include the i-STAT® hand-held clinical analyser (Abbot, USA) which, combines several electrochemical biosensors on a single chip allowing real-time detection of electrolytes and metabolites in clinical samples, and the Ecis-Z (Applied BioPhysics, USA) impedance microarray system for probing cells and cell behaviour.

Considerable utility from the employment of electrochemical devices may also come in the field of detection of cancer biomarkers, which are tumour associated antigens and mutations [23]. Existing methods for cancer screening are still invasive, complex and quite expensive, being based on tissue sampling and cell morphology examination. Bioaffinity electrochemical tests are instead based on simple and rapid detection of a wide range of biomarkers, DNA mutations, RNA

small sequences (micro-RNA), proteins (enzymes and glycoproteins), hormones and other kind of molecules.

Analogous advantages have derived from the application of electrochemical biosensors to food quality control, which has been regulated since 1993, by the Hazard Analysis Critical Control Point system, a protocol which identifies specific hazards and measures in order to assure food safety [24]. The demand for portable, rapid and cost-effective methods to detect biological and chemical contaminants in food and beverages has therefore increased. The traditional procedures for detecting food-borne pathogens, for example, include microbial culturing, isolation and testing thus taking several days. Different types of electrochemical biosensors have been developed for these applications. They can be based on direct impedimetric monitoring of electrical changes due to microbial metabolism as well as on the immobilisation of antibodies able to specifically recognise of microbial cells or on the detection of DNA sequences specific for the main classes of food contaminant bacteria [25-27]. Other important applications have been the development of immunosensors for monitoring of veterinary steroids or growth promoters used in cattle breeding and responsible for toxic effects on consumers, toxins and micotoxins, polychlorinated biphenyls, which have particular affinity for milk and adipose tissues, and toxic proteins expressed by genetically modified organisms (GMO) [12, 28].

Electrochemical biosensors have also been extensively applied to the determination of environmental pollutants, a field which requires sensitive and selective devices, suitable for *in situ* monitoring. Many enzyme-based biosensors have been developed for detection of pesticides, the most abundant environmental pollutants present in water, atmosphere, soil and plants [29]. Other analytes which can be detected using immunosensors or genosensors are polycyclic aromatic hydrocarbons, endocrine disrupting chemicals, genotoxic agents [30, 31].

Finally, an important application which deserves mention is the identification of biological warfare agents, a major challenge for any government organisation.

Analytes in this case include bacteria, viruses and toxins that are spread deliberately in air, food or water to cause disease or death to humans, animals or plants [32].

In the current work, the major focus is the development of model genosensors able to detect specific DNA sequences for food control applications. Traditional methods for nucleic acid detection in clinical or environmental samples are Western and Southern blots and quantitative polymerase chain reaction (PCR)-based techniques (real-time, PCR-ELISA) [33]. Although these assays are very specific and sensitive, they require expensive and time-consuming procedures as well as the use of carcinogenic or radioactive reagents. For these reasons, a flexible and economic alternative is sought in electrochemical DNA hybridisation biosensors [33, 34].

Generally, the sensitivity of most genosensors does not allow the direct analysis of genomic sequences. Detection is thus still dependent on the PCR pre-amplification of the target sequence [18]. PCR is a technique which allows many copies of specific fragments of DNA sequences to be created, starting from a single or a few fragments of nucleic acid. Ordinary PCR results are based on gel electrophoresis separation and so they are only qualitative, not sequence-specific. Therefore, electrochemical genosensing of PCR amplicons is definitely one of the simpler and sensitive way for specific discrimination of particular genomic sequences, which can identify genetic disorders [35], toxic species [36] or bacterial contaminants [27] in food. Among applications which have been developed in our group, two of them were further investigated during this work: hazelnut allergen detection and GMO determination.

As reported by Bettazzi *et al.* [37], food allergy is an emerging public health problem in Western countries where up to 1-2% of the total human population suffers from clinically proven food allergies. Therefore, there is clearly a need for analytical methods which should be highly specific and sensitive, able to detect even traces of allergens; moreover, they need to be rapid, robust, reliable, end-

user friendly and cost-effective. For these reasons, a promising tool for allergen detection is electrochemical detection of PCR fragments of the genes coding for the specific food allergens.

Over the past few years, the determination of GMOs using electrochemical DNA biosensors has also generated great interest [38-40]. GMOs represent one great advance of genomic science and surely can be considered a highly promising tool for farming improvement, but many negative health implications have also been suggested. In Euope, labelling is mandatory for foodstuff containing ingredients derived from genetically modified maize and soy bean in an amount greater than 0.9% [41]. Therefore, also in this case, there is a need for new highly-sensitive analytical methods for GMO detection and control. Gene expression is regulated by specific sequences called "Promoters" and "Terminators". GMOs can thus be identified by detecting promoter P35S and terminator NOS which are the sequences employed in the majority genetic manipulations.

1.2 Nanomaterials for electrochemical biosensing

Recent advances in nanotechnology have lead to the creation of a number of interesting nanoscale materials. Considering that most biological systems, including viruses, membranes and protein complexes are naturally nanostructured materials, and that molecular interactions take place on a nanometre scale, nanomaterials are intuitive candidates for integration into biomedical and bioanalytical devices [42, 43]. Moreover they can pave the way for the miniaturisation of sensors and devices with nanometre dimension (nanosensors and nanobiosensors) in order to obtain better sensitivity, specificity and faster rates of recognition compared to current solutions.

Nanomaterials have dimension in the 1-100 nm range and can be obtained by "top-down" or bottom-up" approaches [44, 45]. The former involves traditional microfabrication equipment, such as photolithography and inkjet printing, to

reduce and shape device dimensions to nanometre sizes or tolerances. The bottom-up approach, in contrast, is based on self-organisation due to chemical properties of the molecules involved in the formation of the nanomaterial (molecular self-assembly). This method is very promising for the production of devices in parallel and is expected to be much cheaper than top-down methods, but could be limited by the the size and complexity of the desired assembly.

The chemical, electronic and optical properties of nano-materials generally depend on both their dimensions and their morphology [46]. A wide variety of nanostructures have been reported in the literature for interesting analytical applications. Among them organic and inorganic nanotubes, nanoparticles and metal oxide nanowires have provided promising building blocks for the realisation of nano-scale electrochemical biosensors due to their biocompatibility and technologically important combination of properties such as high surface area, good electrical properties and chemical stability. Moreover, the integration of nanomaterials in electrochemical devices offers the possibility of realising portable, easy-to-use and inexpensive sensors, due to the ease of miniaturisation of both the material and the transduction system. Over the last decade, this field has been widely investigated and a huge number of papers have been published. This review principally summarises progress made in the last few years (2005 to date) in the integration of nanomaterials such as carbon nanotubes, nanoparticles and polymer nanostructures, in electrochemical biosensing systems.

1.2.1 Carbon nanotubes

Since their discovery in 1991 [47], carbon nanotubes have generated great interest for possible applications in electrochemical devices due to their interesting and technologically important combination of properties such as high surface area, fast heterogeneous electron transfer, chemical stability and ease of miniaturisation [48-50]. Carbon nanotubes are fullerene-like structures (Figure 2) which can be single walled (SWNTs) or multiwalled (MWNTs) [51]. SWNTs are cylindrical

graphite sheets of 0.5-1 nm diameter capped by hemispherical ends while MWNTs comprise several concentric cylinders of these graphitic shells with a layer spacing of 0.3–0.4 nm. MWNTs tend to have diameters in the range 2–100 nm. Carbon nanotubes can be produced by arc-discharge methods [52], laser ablation [53] or chemical vapour deposition (CVD) [54], which has the advantage of allowing the control of the location and alignment of synthesised nanostructures.

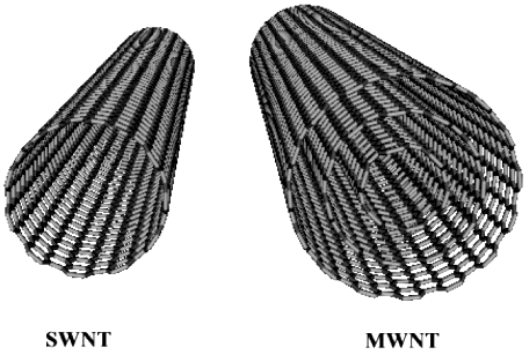

Figure 2. Schematic structures of SWNTs and MWNTs [55].

In a single-walled nanotube every atom is on the surface and exposed to the environment. Moreover, charge transfer or small changes in the charge-environment of a nanotube can cause drastic changes to its electrical properties. The electrocatalytic activity of carbon nanotubes has been related to "topological defects" characteristic of their particular structure; the presence of pentagonal domains in the hemispherical ends or in defects along the graphite cylinder produces regions with charge density higher than in the regular hexagonal network thus increasing electroactivity of CNTs [50, 56, 57]. For these reasons they have found wide application as electrode materials and a huge number of electrochemical biosensors have been described employing CNTs as a platform for biomolecule immobilisation as well as for electrochemical transduction. The only limitation can be their highly stable and closed structure, which does not allow a high degree of functionalisation [58]. Adsorption or covalent immobilisation can only be achieved at the open end of functionalised nanotubes.

For this reason an oxidative pre-treatment of CNTs is required before their chemical modification [59].

Different types of devices have been reported depending on the carbon nanotube electrode constitution, bio-receptor employed (enzymes, antibodies, DNA) and immobilisation strategy (covalent, non covalent). The majority of them have been obtained by modifying carbon electrode surfaces (mainly glassy carbon or carbon paste) with a dispersion of CNTs in polymers or solvents, thus increasing the sensitivity of the analysis by orders of magnitude with respect to the bare electrode surface. Solvents like dimethylformamide (DMF), ethanol or polymeric compounds like Chitosan and Nafion are the most used dispersion matrixes for this kind of process.

1.2.1.1 Carbon nanotubes used in catalytic biosensors

Many carbon nanotube-based enzymatic biosensors have been realised for the determination of various biochemicals (e.g. glucose, cholesterol etc) and environmental pollutants (e.g. organophosphate pesticides). A simple solution was achieved by Carpani *et al.* [60] by dispersing SWNTs in DMF with the aid of ultrasonication and dropping the suspension directly onto the electrochemically activated surface of glassy-carbon (GC) electrodes. Glucose Oxidase (GOx) was immobilised by treatment with glutaraldehyde as a cross linker, both on bare GC- and SWNT-modified electrodes and the response of the two types of sensor to glucose was evaluated. The SWNT-GC/GOx electrodes exhibited a more sensitive response, due to the fact that CNT-based materials enhance electron-transfer reactions and show high electrocatalytic activity towards several biological molecules. However, GC/GOx electrodes exhibited a lower background current, giving rise to a better signal to noise ratio.

Radoi *et al.* [61] modified carbon screen-printed electrodes (SPEs) with a suspension of SWNTs in Ethanol. The nanotubes had been previously oxidised in a strong acid environment to generate carboxyl groups and covalently

functionalised with Variamine blue, a redox mediator, by the carbodiimide conjugation method. The sensor was tested for the detection of nicotinamide adenine dinucleotide (NADH) by flow-injection analysis and the resulting catalytic activity was higher than that obtained using an unmodified screen-printed electrode. Thus nanostructured sensors were subsequently employed for the realisation of NAD+-dependent biosensors (i.e. for lactate detection). Upon detecting similar analytes, Gorton's group [62] reported an interesting study of the sensitivity-enhancing effect of SWNTs in amperometric biosensing, which depended on their average length distribution. They modified carbon electrodes with the enzyme diaphorase (which catalyses the oxidation of NADH to NAD+) and SWNTs using an osmium redox polymer hydrogel and tested the sensor response towards NADH by varying the length of the nanotubes. Surprisingly, the best performance was achieved using SWNTs of medium length. The proposed explanation was a sensitivity-increasing effect caused mainly by the structural and electrical properties of the SWNTs, which have an optimum length (mainly depending on the type of redox enzymes) which allows both efficient blending and charge transport over large distances.

Jeykumari and Narayanan [63] developed a glucose biosensor based on the combination of the biocatalytic activity of GOx with the electrocatalytic properties of CNTs and the redox mediator neutral red for the determination of glucose. MWNTs were functionalised with the mediator through the carbodiimide reaction and mixed with GOx and Nafion as a binder. The suspension was finally deposited on paraffin-impregnated graphite electrodes. Nafion is a perfluorinated ionomer which, because of its unique ion exchange, discriminative and biocompatible properties, has been widely employed for the modification of electrode surfaces and applied to amperometric sensing in many electrochemical sensors and biosensors. The MWNT–Neutral red–GOx–Nafion nanobiocomposite film combined the advantages of the electrocatalytic activity of MWNTs with the capability of the composite material to decrease the electrochemical potential required. In this way the response to interfering substrates such as urea, glycine, ascorbic acid and paracetamol became insignificant. In 2009, the same group [64]

proposed an interesting approach to low-level glucose detection by creating a bienzyme-based biosensor. MWNTs were oxidised, functionalised with the redox mediator toluidine blue and grafted with GOx and hydrogen peroxidase (HRP). The so-functionalised MWNTs were dissolved in a Nafion matrix and deposited on GC electrodes. In this way the substrate glucose reacts with GOx, in the presence of the natural co-substrate O_2, to produce H_2O_2. Hydrogen peroxide, then, serves as substrate for HRP, which is converted to oxidised form by the redox mediator immobilised on MWNTs. The proximity of a mediator which transfers electrons between the enzyme and the electrode reduced the problem of interferences by the other electroactive species. Moreover, the use of multiple enzymes enhanced sensor selectivity and chemically amplified the sensor response.

Another amperometric CNT-Nafion composite was developed by Tsai and Chiu [65] for the determination of phenolic compounds. MWNTs were well dispersed within the Nafion matrix together with the enzyme tyrosinase (Tyr) and deposited on GC electrodes. In this way, MWNTs act as efficient conduits for electrons transfer, Nafion is an electrochemical promoting polymeric binder and tyrosinase is the biological catalyst that facilitates the translation of phenols into o-quinones, which can be electrochemically reduced to catechol without any mediator on an electrode surface. The MWNT-Nafion-Tyr nanobiocomposite modified GC electrode exhibited a three-fold higher sensitive response with respect to the Nafion-Tyr biocomposite modified one, due to the inclusion of MWNTs within Nafion-Tyr matrices. This biosensor was tested for the detection of several phenolic compounds (phenol, o-cresol, p-cresol, m-cresol, catechol, dopamine and ephinephrine) in phosphate buffer solution and the amperometric response was proportional to the concentration of phenol in the analytically important micromolar range. A similar format had already been developed by Deo *et al.* [66] in 2005, by casting with Nafion organophosphorus hydrolase on a carbon nanotube modified transducer. Since the electrochemical reactivity of CNTs is strongly dependent upon their structure and preparation process, an interesting comparison between arc-produced MWNCT and CVD-synthesised MWNT and

SWNT modified electrodes was shown. By comparing their response towards p-nitrophenol, both the SW- and MW-CVD-CNT coated surfaces exhibited a dramatic enhancement of the sensitivity compared to the Arc-produced CNT and bare electrodes. The higher sensitivity of the CVD-CNT-modified electrode reflects a higher density of edge-plane-like defects that lead to higher electrochemical reactivity than previously found [50, 56, 57].

A way to better control the thickness of CNT-polymer films was described by Luo *et al.* [67], who reported a simple and controllable method for the modification of gold electrodes with a chitosan–CNT nanocomposite through electrodeposition. Chitosan is a biological cationic macromolecule with primary amines [68]. It has been widely applied because of its good biocompatibility and film-forming ability. Compared to other solvents, chitosan can prevent biological molecules from denaturing. Moreover, enzymes can be easily attached to chitosan molecules via the primary amines. Upon applying current at the cathode, H^+ ions in the solution were reduced to H_2 thus increasing the pH near the electrode surface. As the solubility of chitosan is pH-dependent, when the pH exceeded the pKa of chitosan (about 6.3), chitosan became insoluble and entrapped CNT onto the cathode surface. In this way, the thickness of the deposited nanocomposite film could be controlled by changing the concentration of the chitosan solution, deposition time and applied voltage. The nanocomposite exhibited excellent electrocatalytic ability for the reduction and oxidation of hydrogen peroxide, thus by simply adding GOx to the CNT-chitosan solution, before the electrodeposition, a glucose biosensor was developed. Chitosan was also employed by Quian and Yang [68] for the development of an amperometric biosensor for hydrogen peroxide detection, based on cross-linking HRP by glutaraldehyde with MWNT/chitosan composite film coated on a glassy carbon electrode. The enzyme-modified electrode exhibited excellent electrocatalytic activity and rapid response for H_2O_2 in the absence of a mediator, good repeatability and absence of interferences by ascorbic acid, glucose, citrate acid and lactic acid. A similar method was developed by Liu *et al.* [69], who prepared nanocomposite laccase/CNT–Chitosan/GC electrodes for detection of 2,2'-azino-bis-(3-

ethylbenzthiazoline-6-sulfonic acid) diammonium salt, catechol and O_2. Unlike peroxidase, laccase does not require hydrogen peroxide to oxidise substrates (electrons are transferred to oxygen to yield water). Its behaviour is strictly dependant on its conformation, thus the CNT–Chitosan composite film resulted in a particularly suitable microenvironment to incorporate the enzyme without using cross-linking reagents, which might alter its conformation and consequently its activity.

In 2007, Rubianes and Rivas [70] demonstrated a highly efficient way to immobilise CNTs on GC electrodes by dispersing them in polyethylenimine. The resulting electrodes showed a dramatic increase in sensitivity for H_2O_2 detection compared to bare GC electrodes and analogous dispersion in Nafion. This was explained by presupposing an irreversible adsorption of polyethylenimine onto the sidewalls of SWNTs, which causes an n-doping of the nanotubes due to the electron-donating ability of amine groups in the polymer. This approach was subsequently exploited by Mascini's group [71] for the modification of carbon screen-printed electrode for the realisation of a disposable glucose biosensor with a wide linear range (0.5–3.0 mM). MWNTs were also coupled with screen-printing technology by Sanchez *et al.* [72], who described a carbon nanotube/polysulfone composite thick-film SPE for amperometric HRP-based biosensing. In this case, MWNTs were mixed with polysulfone and DMF and used as ink for serigraphic deposition on previously printed working electrodes. The result was an interconnected CNT–polymer network, which was highly flexible, porous and biocompatible with immobilised enzyme. Polysulfone is highly resistant in extreme pH conditions as well as thermally stable. HRP was immobilised by a phase inversion process, thus creating a H_2O_2 biosensor. The amperometric signal response was increased in comparison with analogue graphite/polysulfone electrodes, thus demonstrating that the electrocatalytic properties of MWNTs are not diminished by incorporating them in polysulfone matrix. Mineral oil [73], PVC [74], polypyrrole [75] and Teflon [76] were also employed as dispersing matrices by the groups of Rivas, Merkoci, Wang, and Pingarron, respectively, for NADH and glucose detection.

Pingarron's group [77] also synthesised a hybrid composite of MWNTs and the conductive polymer poly(3-methylthiophene) by electrodeposition on GC electrodes and employed them as platform for lactate dehydrogenase immobilisation and lactate detection. The biosensor showed an improved electrochemical oxidation of NADH, used as a cofactor for lactate dehydrogenase, compared to a GC electrode modified either with CNTs or with the conducting polymer separately. The synergistic effect observed with the hybrid material was attributed to the fact that the conducting polymer can immobilise and connect MWNTs, while the presence of MWNTs can interact with the polymer forming aggregates which facilitate charge transfer and increase the conductivity of the polymeric film.

Another highly promising CNT deposition approach is layer-by-layer self-assembly, which is based on electrostatic interactions. The alternate adsorption of negatively and positively charged individual components has become a simple and powerful method for the construction of a suitable microenvironment to retain enzyme activity [78]. Recently, this technique has been used to fabricate a CNT/GOx multilayer composite for glucose biosensors [79-81]. Glucose oxidase is negatively charged at pH 7.4 and can thus be easily incorporated in positively charged multilayer films.

Zhao and Ju [79] developed a multilayer composite CNT network on gold electrodes. A bilayer of the polyelectrolytes poly(dimethyldiallyl-ammoniumchloride) (PDDA) and poly(sodium 4-styrenesulfonate) (PSS) was formed on a 3-mercapto-1-propanesulfonic-acid modified Au electrode. Subsequently, MWNTs wrapped by positively charged PDDA were assembled layer-by-layer with negatively charged glucose oxidase onto the PSS-terminal, until the desired PDDA-MWNTs/GOx bilayer number was achieved. The porous structure obtained showed electrocatalytically reduced dissolved oxygen, mainly due to the assembled MWNTs. Glucose detection was then achieved by exploiting competition between the electrochemical reduction of dissolved oxygen and the

oxidation of glucose by dissolved oxygen (catalysed by the immobilised GOx). In absence of CNTs this process was not observed. This method allowed the detection of glucose at a relatively low applied potential, which excluded interference from ascorbic acid and uric acid.

Another strategy for self-assembling a MWNT–GOx multilayer was elaborated by Yan *et al.* [80] on a flexible, transparent Polyethylene terephthalate substrate. MWNTs were treated with sodium dodecyl sulfate (SDS) in order to facilitate CNT solubilisation and, at the same time, to create a distribution of negative charges on the tube surfaces. After depositing a thin Ti and Au layer on the polymer substrate, an organic monolayer was formed on it via alternative electrostatic adsorption of the positively charged PDDA with negatively charged SDS–MWNTs and GOx. In this way the amperometric response could be controlled by varying the quantity of MWNTs and GOx by adding or reducing the layers. The glucose sensor obtained showed a linear response to glucose in the concentration range of 0.02–2.2 mM, with a very low detection limit of 10 μM. This particular format allowed great flexibility, light-weight, portability and low cost, and is well suited to commercial applications such as *in vivo* implantation, monitoring of changes in disease states and the effects of therapeutic agents. A layer-by-layer approach was also developed by Liu and Lin [81], for monitoring organophosphate pesticides by self-assembling acetylcholinesterase on a GC electrode. CNTs were oxidised and kept at pH 8 in order to achieve negatively charged carboxylate anions, dispersed in N,N-dimethylformamide and deposited on a GC electrode surface. The enzyme acetylcholinesterase (AChE) was immobilised on the negatively charged CNT surface by alternatively assembling a cationic PDDA and AChE thus obtaining a nanometre composite layer (thickness ~9 nm) which provided a favourable microenvironment to maintain the bioactivity of AChE. The developed biosensor integrated with an amperometric flow-injection system was used to detect paraoxon and a limit of detection (0.4 pM), 2.5 times better than that achieved with a nanoporous carbon matrix was obtained.

MWNT-Polylisine polycationic layers have been realised by Jalit *et al.* [82] for adsorption of GOx. GC electrodes were modified with MWNTs dispersed in polylisine forming a platform for self-assembly of multiple layers of the polyelectrolytes and glucose oxidase (GOx). In this case, the presence of MWNTs appeared necessary to obtain a more efficient arrangement of the multilayer system and to decrease the barrier effects observed when using polylisine directly assembled on GC electrodes.

Despite progresses made with layer-by-layer techniques, the main drawback of CNT-modified macroelectrodes is the low reproducibility of the nanostructured layer. Moreover, charge–charge attraction or hydrophobic interactions, which are the basis of enzyme entrapment, often lead to conformational changes of the protein that diminish its electrocatalytic function. A great improvement in this respect has been obtained by creating vertically aligned carbon nanotube arrays, which on the one hand work as electrode surface by themselves, while on the other hand provide a suitable platform for highly ordered immobilisation of biosensing elements.

A possible approach has been demonstrated by Viswanathan *et al.* [83], who realised self-assembled monolayers of SWNTs on gold electrode surfaces by wrapping them with thiol-terminated single-strand oligonucleotide. A polyaniline matrix was then electropolymerised on them for AChE immobilisation and subsequent organophosphorous insecticides detection. The presence of SWNTs not only provided the conductive pathways to promote the electron transfer, but also increased the surface area and the flexibility of the enzyme supporting layer. One limitation of such an assembly is that the highly conductive CNTs were not in direct contact with the electrode surface thus electron transfer could be hindered.

A really powerful solution to this problem is directly aligned CNT fabrication, normally achieved by CVD technology. Up to now only a few papers have reported this kind of approach for the creation of enzyme-biosensors. Lin *et al.*

[84] reported a glucose biosensor based on carbon nanotube nanoelectrode ensembles made of low-site density aligned CNTs grown on a Cr-coated Si substrate by plasma-enhanced CVD, using Ni nanoparticles as a catalyst. An epoxy-based polymer was then spin-coated on the substrate and covered half of the CNTs. Finally the protruding parts of the CNTs were removed by polishing. In this way, each nanotube worked as an individual nanoelectrode and signal-to-noise ratio as well as detection limits could be improved. Moreover, good electrical conductivity was ensured by directly growing CNTs on the conductive substrate. Glucose oxidase was immobilised directly on the broken tips of CNTs via carbodiimide chemistry for glucose detection, thus eliminating the need for permselective membrane barriers and mediators for delivering electrons from the enzyme centre to the electrode. A different CNT array was realised by Withey and co-workers [85] using anodised aluminum oxide as template. MWNTs grown by CVD from hexagonally patterned template features were virtually identical in length, diameter and spacing. Within the array, each individual tube was physically separated and electrically insulated by the insulating aluminium oxide template, and a direct electrical contact for each tube was made by sputtering the backside of the array with a layer of gold. Sensor response to glucose detection was evaluated by covalently linking GOx to the nanotube tips or non-covalently adsorbing the enzyme to the side walls. The first format exhibited a higher level of bioelectrocatalytic activity due to the highly ordered array configuration. Despite the need for more advanced technology, these last two approaches appear the most suitable way to obtain nanoscale sensors.

One really innovative strategy in this field has recently been reported by Boo *et al.* [86] who fabricated a nanoneedle consisting of a MWNTs attached to the end of an etched tungsten tip, which is the smallest needle-type biosensor reported to date (diameter = 30 nm, length = 2-3 μm). A tungsten tip was electrochemically etched to form a sharp, long-tip geometry, to which a MWNT was coupled using a field-emission scanning electron microscope equipped with two piezoelectric nanomanipulators. The nanoneedle tungsten portion was sealed with a UV-hardening polymer to insulate it from the solution under study (only the MWNT

was exposed) and to provide mechanical support. Glutamate oxidase was electropolymerised on the nanoelectrode and the amperometric biosensor was able to respond to the neurotransmitter glutamate in the 100-500 μM range. Due the sensitivity and the nanoscale, such a tool could offer considerable opportunities to investigate cell signalling and the dynamics of living cells.

1.2.1.2 Carbon nanotubes used in affinity biosensors

Despite the huge amount of papers published over the past few years regarding enzymatic biosensors, there has been little research done on CNT-based electrochemical immunosensors. In this case antibody orientation is crucial for molecular recognition. For this reason, despite some interesting work reporting casting of antibodies on screen-printed electrodes [87-91], most of the work has been realised by preparing highly ordered vertical aligned CNTs arrays [92-98] with well-defined properties and uniform length and diameter, which also provide unique controllability of nanotube spatial density and conductivity, if compared to powder type CNT electrodes.

In 2007, Sanchez *et al.* [87] reported the fabrication of a carbon nanotube/polysulfone/rabbit-immunoglobuline (IgG) "immunocomposite" on carbon screen-printed electrodes. The construction procedure was similar to the one described by the same group for HRP-biosensor development [72], in which serigraphy was employed to print the MWNT/Polysulfone/rabbit-IgG immunocomposite onto the reaction region of carbon SPE working electrodes. The biosensor was based on a competitive assay between free and labelled anti-IgG for the available binding sites of immobilised rabbit IgG. The electrochemical transduction was performed by labelling with HRP enzyme and using hydroquinone as mediator. Upon comparing the electrochemical response obtained using MWNTs with different length and diameter, 200 μm long nanotubes exhibited a sensitivity five fold higher then bare graphite, thus demonstrating that carbon nanostructures maintained their highly conducting properties even though they were immersed in a polysulfone matrix modified with

rabbit-IgG antibody. The immunosensor was able to discriminate anti-rabbit-IgG concentrations ranging from 2 to 5 μg/ml, showing lower unspecific adsorption of anti-rabbit-IgG-HRP.

Buch and Rishpon [88] employed protein A to improve anti-C-Reactive protein-antibody orientation on SPEs modified with multi-walled carbon nanotubes. After modifying carbon surfaces with CNTs, polyethylenimine and glutaraldehyde crosslinker, Protein A was covalently immobilised on the electrodes in order to facilitate the orientation of the bound immunoglobulin. The electrodes were then immersed in human serum solutions containing different concentrations of protein, and finally labelled with goat anti-C-Reactive protein antibody conjugated with HRP. This format allowed the determination of C-Reactive protein down to a concentration of 0.5 ng mL^{-1}, 20 fold lower than that obtained using unmodified electrodes (10 ng mL^{-1}), due to the improved electron-transfer kinetics and increased surface available for immobilisation. In this way, higher dilution of the samples could be achieved thus reducing interferences given by serum matrix. A similar modification strategy was developed by Viswanathan *et al.* [89] for the design of a disposable electrochemical immunosensor for the detection of carcinoembryonic antigen, a cancer marker glycoprotein. Polyethylenimine chains were ionically wrapped on the surface of carboxylic acid-functionalised MWNT and dropped on carbon SPEs. The amine groups present in the polymer chains were further used for anti-carcinoembryonic antibodies immobilisation and a sandwich immunoassay was performed with antigens and antibodies tagged ferrocene carboxylic acid encapsulated liposomes. Square Wave Voltammetry (SWV) was employed to analyse the Faradaic redox responses of the released ferrocene carboxylic acid from the immunoconjugated liposomes on the electrode surface. This process was demonstrated to be highly facilitated by the intimate connection with MWNTs, which provides a highly precise and sensitive determination of carcinoembryonic antigen in human blood serum and saliva samples. Another tumour marker, prostate specific antigen, was detected by Panini *et al.* [90], by using an immunosensing microfluidic system formed by a GC electrode modified with MWNT dispersed in a mixture of

methanol, water and Nafion. GC electrodes were also modified by He *et al.* [91] with MWNTs covalently linked to clenbuterol, a poisonous animal feed additive, for quantitative determination of the molecule using a competitive mechanism.

In addition to these interesting results, recent advances in nanotechnology and in semiconductor processing have made it possible to fabricate carbon nanotube arrays with extremely high density and compatibility for improved nano-immunosensors. Such an innovative platform for bio-electroanayltical applications was reported by Okuno *et al.,* in 2007 [92]. They developed a CNT-based compact sensor by growing SWNTs directly on Pt electrodes, by thermal CVD. Pt and Ti were patterned on a SiO_2 substrate and covered with a second SiO_2 passivation film (100 nm). The film was partially etched using photolithography, thus creating an array of microelectrodes onto which SWNTs were synthesised by a thermal CVD method using a Fe-containing catalyst. In this way, an array of 30 microelectrodes, with SWNT modification, was built on a single substrate. Electrochemical measurements of $K_3[Fe(CN)_6]$ and amino acids revealed that the electrochemical signals achieved using SWNT-arrayed microelectrodes were about 100-fold higher than those obtained using bare Pt microelectrodes. After this encouraging result, the chip was further employed by the same group [93] for the label-free detection of the cancer marker, total prostate-specific antigen, using differential pulse voltammetry (DPV). Total prostate-specific monoclonal antibodies were covalently immobilised on SWNTs and the amount of antigen detected by monitoring the increase of current signals, derived from the oxidation of tyrosine and tryptophan residues. High peak current signals were clearly observed using the SWNT-modified microelectrodes, whereas no signal was obtained with the bare Pt ones, thus indicating total prostate-specific antigen and the correspondin antibody were not non-specifically adsorbed on the bare Pt microelectrodes. The detection limit for total prostate-specific antigen was determined as 0.25 ng/mL, 16-fold lower than the cut-off limit between prostate hyperplasia and cancer, thus proving promising for clinical applications.

CVD was also employed by Yun *et al.* [94] for the construction of CNT arrays cast in epoxy. Highly aligned multiwalled carbon nanotubes were grown on a $Fe/Al_2O_3/SiO_2/Si$ substrate. The substrate was subsequently patterned in blocks of 100 μm^2, and carbon nanotube towers up to 2 mm in height were grown within the blocks. Nanotubes were then peeled off the silicon substrate and cast in epoxy. Both ends were polished: one end for electrical connection, and the other end for chemical activation and covalent modification with Anti-mouse IgG for an immunosensing application. Electrochemical impedance spectroscopy (EIS) was used for label-free detection of the binding of mouse IgG to its specific antibody immobilised on the nanotube electrode surface, by monitoring the enhancement of electron transfer resistance with increase of analyte concentration (DL = 200 ng/L). This procedure also facilitated scaling down the size of electrodes, thus improving the sensitivity and possibility of biomedical applications. A further step forward was achieved by same group in 2008 [95], by using a similar method to fabricate 8 mm-long aligned multi-walled carbon nanotube-array electrodes and electrochemically depositing gold nanoparticles onto the nanotube tips at the top of the array. This new approach could be the foundation for further nanobiosensor development using self-assembled monolayers and bio-conjugation of antibodies on gold.

Other ways to obtain a so called "SWNTs nanoforest" were based on SWNTs vertically assembled from DMF dispersions onto thin iron hydroxide-decorated Nafion conductive films [96-98]. Yu *et al.* [96] developed an alternative biosensor design based on orthogonally-oriented SWNTs on conductive substrates, with higher packing density and thus superior mechanical properties than vertical SWNTs grown by chemical vapour deposition. These "forests" were assembled on pyrolytic graphite by forming a thin layer of Nafion on the surfaces onto which aqueous acidic (pH 1.7–1.9) $FeCl_3$ was adsorbed to precipitate Fe(OH)x on the surface. After the immersion of the substrates into DMF dispersions of shortened and oxidised SWNTs, vertical assemblies of nanotubes are formed (SWNT forests). The initial driving force for the formation of SWNT forests originated from acid–base neutralisation between one of the two SWNT ends with basic

Fe(OH)x domains formed by slow precipitation on Nafion-adsorbed Fe^{3+} ions, involving trace amounts of water during the DMF washing step. The lateral bundled growth of the vertical SWNT domains was driven by the tendency of the assembly to reduce the overall hydrophobic surface area that originates from SWNT side walls. Protein immunosensors were obtained by covalently attaching antibodies to the carboxylated ends of nanotube forests and applied to the detection human serum albumin and cancer biomarkers [97, 98], with detection limits in the picomolar range.

Another really appealing aspect in the field of carbon nanotube-based electrodes is their employment for DNA sensing (nano-genosensors). Nano-scale geno-electronics represents the ideal molecular interfacing approach which, by exploiting DNA recognition event, could allow the realisation of arrays able to measure the expression patterns of thousands of genes in parallel, helping to identify appropriate targets for therapeutic intervention and to monitor changes in gene expression in response to drug treatments [99]. Over the last five years, several genosensors have been realised employing CNTs as a platform for DNA immobilisation and electrochemical transduction. While several platforms have been created by dispersing CNTs in polymers and solvents, only a few papers have reported genosensors based on self-standing CNT films.

Erdem *et al.* [100] reported a comparison between glassy carbon and graphite pencil electrodes modified with a suspension of DMF, by monitoring changes in the oxidation signal of guanine in a label-free assay based on the immobilisation of a guanine-free DNA probe [101, 102]. MWNTs were oxidised, dispersed in DMF and deposited on the carbon surfaces. Both kind of CNT-modified electrodes displayed higher voltammetric responses over their bare counterparts and especially over modified graphite pencil electrodes. The improved behaviour was explained as originating from the highly porous composite structure of the graphite pencil electrode which allowed a higher inclusion of CNTs and consequently a higher surface area. A signal enhancement of 89% in comparison to bare unmodified electrodes was achieved. This aspect was further exploited by

the same authors [103] for the study of the interaction between DNA and anticancer drugs, using SWNT-modified graphite pencil electrodes and covalently coupling amine group in the guanine bases of DNA to the carboxylated ends of nanotubes. Moreover, they tested commercial carboxylated-MWNT (MWNT-COOH) based screen-printed electrodes for the detection of specific DNA sequences related to Hepatitis B virus [104]. Also in this case, a guanine-free amine-modified DNA probe was covalently immobilised onto MWNT-COOH and the amount of hybridised target detected by measuring the guanine oxidation peak (guanine was present only in target). The presence of CNTs in the electrode composition facilitated surface coverage with the DNA probe and, consequently, guanine loading from the hybridised target: the higher is guanine loaded the higher is the signal, directly correlated to the amount of analyte. Moreover, by promoting electron transfer, the current response was increased resulting in a sensitivity of 1.74 nmol L^{-1}, a good discrimination between full-match sequence and a single-base mismatch (signal 50% lower) and a negligible signal in the presence on a non-complementary sequence.

As already reported for other biosensors, several polymeric matrixes have been employed to fix CNTs on electrode surfaces. A dispersion of MWNTs in chitosan was combined with ZrO_2 nanoparticles by Yang *et al.* [105], in order obtain a composite layer on GC electrodes which, with its large surface area and good charge-transport characteristics, provided a synergistic increase of DNA loading, current response towards the redox indicator employed (daunomicine) and improved detection sensitivity for DNA hybridisation compared to MWNTs/Chitosan- or ZrO_2/Chitosan-modified GC electrode. Chitosan was also employed by Yang *et al.* [106] for the modification of GC electrodes with a highly performing nanocomposite based on MWNT and Polyaniline (PANI) nanofibres. Electrochemical characterisation showed a great enhancement in conductivity and electrochemical activity of the sensors due to the synergistic effect of the two nanostructured components. Moreover, the very large surface area of the composites greatly increased the loading of the DNA probe, thus allowing a highly sensitive detection specific of DNA sequences related to

transgenic genes in genetically modified crops, such as the phosphinothricin acetyltransferase gene and the terminator of nopaline synthase gene. Other composite coatings were obtained on carbon paste electrode surfaces by casting CNT, nafion and tris(2,2'-(bipyridyl)ruthenium(II) ($Ru(bpy)_3^{2+}$) layers [107]. The genosensing format involved physical sorption of DNA onto an electrode surface and guanine and adenine oxidation, catalysed by $Ru(bpy)_3^{2+}$ present in the film.

Due to its negatively charged backbone, DNA can also be easily immobilised by electrostatic interaction. For this reason, cationic polymers also proved particularly appealing for CNT dispersion. Jang *et al.* [108] electropolymerised poly-L-lysine with well-dispersed SWNTs (in DMF) on GC electrodes to prepare poly-L-lysine/SWNT/GC films for EIS detection of PCR fragments. Carboxylic functionalised SWNTs were firstly dispersed in DMF, deposited on GC electrodes, then poly-L-lysine films were electropolymerised on them by cyclic voltammetry (CV). DNA probes were easily immobilised on the poly-l-lysine films via electrostatic adsorption, since the amino groups of poly-l-lysine can bind the phosphate skeleton of DNA via electrostatic forces. The hybridisation event was detected by monitoring the increasing of electron transfer resistance using electrochemical impedance spectroscopy, in the presence of an anionic redox couple as indicator, $[Fe(CN)_6]^{3-/4-}$. Electropolymerisation was also used by Xu *et al.* [109], who reported an analogue electrochemical-impedance based DNA biosensor by using a composite material of polypyrrole (PPy) and MWNTs to modify a GC electrode. PPy was electropolymerised onto GC electrode by CV in the presence of MWNTs with terminal carboxylic groups and amino-linked DNA probe was covalently coupled to the surface. As a result of the PPy/MWNTs modification, the electrode showed properties characteristic of both constituent components, such as large surface area, as well as mechanical stability and efficient thermal/electrical conduction. A detection limit of 5.0×10^{-12} mol L^{-1} was achieved as well as good selectivity towards one-base mismatched sequence (the signal was 35.5% of the one obtained with the complementary sequence).

A really interesting application of nanostructured genosensors was shown by Huska *et al.* [110] who coupled gel electrophoresis, a standard and reliable separation technique, with CNT-based screen printed electrodes for quantification of PCR amplified sequences ("off-line coupling"). Carbon SPEs and carbon modified analogues were placed in the wells of the agarose electrophoretic gel and the amount of migrated amplicons detected by SWV. By using this approach, amplicons obtained after two cycles were detected in the presence on CNTs (and after 10 cycles without CNTs).

Even greater advantage may be derived from the employment of highly ordered and vertically aligned carbon nanotube surfaces. Vertical orientation of the nanostructures could in turn greatly facilitate vertical orientation of the immobilised probe, making it more accessible for the complementary sequence. Moreover, technologies required for the construction of such surfaces are compatible with device miniaturisation, thus allowing the realisation of nano-scale genomic arrays. He *et al.* [111] proposed a genosensor obtained by covalently grafting DNA on the tip and wall of Au-supported aligned CNTs, generated from pyrolysis of Fe(II) phtalocyanine in acetic acid atmosphere. Upon using ferrocene carboxaldehyde as a redox indicator, the hybridisation event was achieved with high sensitivity and selectivity

Another very interesting platform was realised in 2002, by Meyyappan and co-workers [112]. It consisted of nanoelectrodes arrays obtained by embedding vertically aligned CNTs in a SiO_2 matrix, thus providing structural support to the nanostructures and improving their chemical coupling to nucleic acid. MWNTs were grown using plasma enhanced CVD process and oxidised, for further covalent DNA immobilisation using a plasma treatment. This process was found to compromise the mechanical stability of the nanotubes, often leading to total collapse of the aligned CNTs. For this reason, after CNT growth, a film of spin-on glass was used to fill the gaps between the individual CNTs in the array, thus providing structural support to the carbon nanotubes, enabling them to retain their vertical configuration during the purification and tip opening process and also

served as a dielectric material, able to insulate the individual nanotubes from their neighbours. This format, in combination with $Ru(bpy)_3^{2+}$ mediated guanine oxidation was employed for the determination of a few attomoles of oligonucleotide DNA [113] as well as PCR amplicons with a sensitivity comparable with florescence-based DNA microarray techniques (hundreds of hybridised targets per spot) [114]. Recently this method has been further developed [115] by coupling optical and electron beam lithography with CVD in order to obtain a chip formed of nine individually addressable arrays of vertically aligned carbon nanofibres. Thanks to the combination of the three techniques, nanofibres were precisely grown on 100 nm Ni dots deposited with 1μm spacing on each of the nine micro pads which formed the array. The sensor was tested for the electrochemical detection of DNA targets from *E. Coli* by exploiting the array format for simultaneously testing a positive control (mismatch probe), a negative control (no probe) and specific hybridisation. The proposed method has the potential to be scaled up to N×N arrays (with N up to 10), which could be ideal for detecting hundreds of different organisms.

1.2.2 Conductive polymer nanostructures

Another class of organic nanomaterials, which in the last few years has found a greatly increasing number of applications, is constituted by conductive polymer nanostructures.

Conducting polymers are multifunctional materials which can be employed as receptors as well as transducers or immobilisation matrix in electrochemical biosensing. They are characterised by an extended π-conjugation along the polymer backbone which promotes an intrinsic conductivity, ranging between 10^{-14} and 10^{2} S cm^{-1} [116]. Their electrical conductivity, in fact, results from the formation of charge carriers ("doping") upon oxidising (p-doping) or reducing (n-doping) their conjugated backbone [117]. In this way they assume the electrical properties of metals, while having the characteristics of organic polymers such as

light weight, resistance to corrosion, flexibility and ease of fabrication [118]. When formed as nanostructures, conductive polymers assume further appealing properties: ease of preparation by chemical or electrochemical methods, sensitivity towards a wide range of analytes, great signal amplification due to their electrical conductivity and fast electron transfer rate. Moreover, with respect to other nanostructures (i.e. CNTs), they allow an easier chemical modification of their structure in order to obtain high specificity towards different compounds and are amenable to fabrication procedures which greatly facilitate miniaturisation and array production [119].

Nanostructured conductive polymers can be obtained by "template" or "template free" methods of synthesis, as widely reviewed [120-124]. Among template approaches, "hard template" and "soft template" strategies can be distinguished. "Hard template" synthesis involves the employment of physical templates such as fibres or membranes. In the first case, polymer nanotubes can be obtained by assembling monomers around a template constituted by degradable fibres produced by electrospinning [120]. However, the most widespread method for polymer nanostructures preparation is based on the use of nanoporous membranes (polycarbonate, silica or alumina) as template. Monomer solution fills cylindrical pores of the membrane, thus allowing the formation of monodisperse polymer nanocylinders or tubes with accurate control of length (in the order of microns) and diameter (between 10 and 200 nm) [121]. Polymerisation can be carried out by electrochemical oxidation within the pores of the membranes after coating one side of the membrane with a metal film, or by immersing the membrane in a solution of the monomer and an oxidising agent [122]. The polymer generally nucleates and grows on the pore walls because of the electrostatic attraction between the growing polycationic polymer and anionic sites along the pore walls of the membrane itself [123].

"Soft template" synthesis, instead, involves the employment of chemical template processes, such as emulsion with surfactants, interfacial polymerisation, radiolytic synthesis, sonochemical and rapid mixing reaction methods, liquid crystals and

biomolecules [124]. Although they are very popular, these methods have the drawback of requiring a post-synthesis process for the integration of the nanostructures into the device system and, in case of membrane-based methods, there is a limitation on the dimensions derived from the shape of the pores [119, 122]. For these reasons, recent progress in nanotechnology has led to the development of "template-free" direct fabrication of nanomaterial-integrated systems based on nanolithography and other nanopatterning techniques [122, 124].

As stated above, conductive polymers are very easy to functionalise, thus proving particularly promising for biosensing applications. However, an important aspect to be considered, when using them in the design of electrochemical sensors, is the integration between the electron transfer mechanism at the electrode surface and the subsequent charge transport through the polymer backbone [124]. Both covalent and non-covalent strategies have been developed and reviewed for this purpose [125-127].

Covalent approaches may comprise grafting of polymer nanostructures with functional groups. This strategy ensures that the nano-morphology is unaffected [128]. Alternatively, properly functionalised monomers can be used which, after polymerisation, confer specific binding sites for different bioreceptors (such as antibodies, enzymes, nucleic acids, aptamers or cells). Moreover, covalent binding processes often require aqueous buffer solutions which preserve the catalytic activity or the recognition properties of the biomolecule [126]. Non-covalent methods are mainly based on physical entrapment or electrostatic interactions between the polycationic matrix (consisting of the oxidised polymer) and negative biomolecules such as DNA or proteins (enzymes, antibodies), provided that the pH is higher than the isoelectric point (pI) [125]. The drawback in this case is worse control of the orientation of the bioreceptor which can lead to a less accessibility for the substrate.

The following sections will provide an overview of progress made in the application of conductive polymers in biosensor field, with particular attention to polyaniline, which was one of the polymers used to form the nanostructures investigated in this thesis. In Figure 3 the main classes of conductive polymers are illustrated.

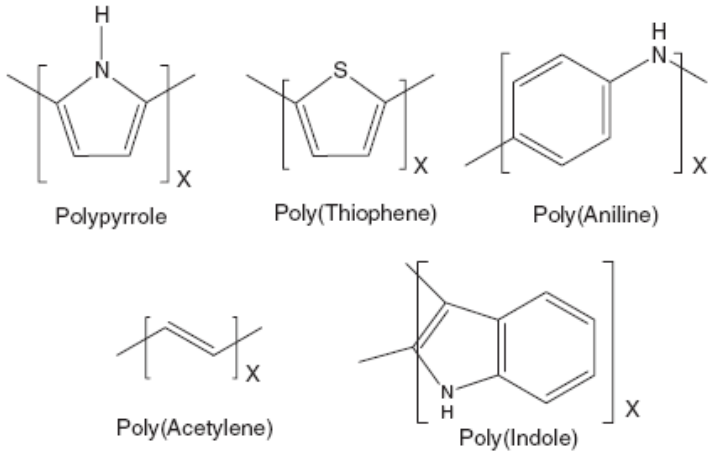

Figure 3. Main classes of conductive polymers [125].

1.2.2.1 Conductive polymer nanostructures used in catalytic biosensors

Among conductive polymers, polypyrrole (PPy) is arguably the most widely employed in biosensing, especially as an immobilisation substrate for biomolecules. Compared to other polymers such as Polyaniline and Polythiophene, PPy can be easily polymerised in a neutral environment, thus proving particularly suitable for biological matrixes [129].

The first example of the use of PPy for enzyme immobilisation in biosensors was reported in 1992 by Koopal *et al.* [130], who described template synthesis of PPy microtubules inside track-etch membranes for glucose biosensing. Glucose oxidase was adsorbed within the tubules and glucose was then measured

amperometrically. The interesting aspect of this work was the observation that the enzyme was immobilised only inside the tubules and not on the surface of the membrane, because the corrugation of the interior surface of the PPy tubules matched the dimension of GOx and thus resulted in an intimate connection between the transducer and the bioreceptor.

A nanoporous glucose biosensor was also later developed by Ekanayake *et al.* [131] using Pt plated-alumina substrates. PPy was electrochemically deposited on the top surface as well as inside walls of the Pt nano holes, thus obtaining a PPy nanotube array and, consequently, a greatly enhanced surface area for GOx immobilisation by simple physical adsorption. A significant improvement was demonstrated in the amperometric responses compared to analogous non-nanostructured PPy films created on indium-tin-oxide electrodes.

Carboxylated PPy monomers were also employed by Shamsipur *et al.* [132] in order to obtain cauliflower-like nanostructures by electropolymerisation on Pt disks. Impedance studies of the nanostructured films before and after the immobilisation of Cytochrome C showed good features for the development of a novel H_2O_2 biosensor with good sensitivity, dynamic range, detection limit (0.25 μM) and stability.

A higher sensitivity was obtained by Lupu *et al.* [133] using a new sensor platform based on nanoarrays of PPy nanopillars, obtained using nanosphere lithography. Polystyrene beads deposited on a gold surface were reduced in size by plasma etching, covered with an insulating layer and subsequently removed, thus leaving nanoholes on the surface. PPy nanopillars were grown into the holes and the redox mediator Prussian Blue–(ferric ferricyanide) incorporated in the polypyrrole network by electropolymerisation ("artificial peroxidase" sensor). In this way, as polypyrrole is conductive in the potential range where the mediator is electroactive, charge propagation across Prussin Blue redox centres was enhanced and very low concentrations of hydrogen peroxidase (10^{-9}M) was detected using chronoamperometry.

One of the drawbacks of polypyrrole is its poor long-term stability and, in particular, the decrease of electrical conductivity with the increase of temperature and humidity [134]. For this reason, several groups found in polythiophene and derivates, such as polyethylenedioxythiophene (PEDOT), a valid alternative for the realisation of nanotubes and nanowires with better environmental stability and easier control of electrical and optical properties [135]. The first example was reported by Kros *et al.* [136] who reported an amperometric glucose biosensor based on track-etched membranes coated with PEDOT nanotubules. The sensor was designed in order to increase the electrostatic interaction between the negatively charged GOx and the positively charged conducting polymer to obtain a biosensor with a higher response to glucose, due to more efficient electron transfer. In order to obtain a high density of positive charges, polymerisation of 3,4-ethylenedioxythiophene was carried out in the presence of the polycation poly-(N-methyl-4-pyridine). Subsequently GOx was immobilised inside the polymer-coated pores and the membranes mounted in a three-electrode cell incorporated in a flow system. A sensitivity of 45 nA $mmol^{-1}$ L^{-1} was achieved with the same sensor over a period of 30 days, thus demonstrating a high stability and suitability for long-term glucose measurements.

The influence of a nanostructured polythiophene morphology in amperometric glucose sensing was also investigated by Liu and co-workers [137]. They produced nanostructured films by electrochemical copolymerisation of 3-methylthiophene and thiophene-3-acetic acid and found that once the copolymer film grew over a critical thickness, a spontaneous formation of nanostructures occurred, probably depending on changes in the chain length of deposited oligomers and formation of a branched structure as the film thickened.

Another interesting glucose biosensor was demonstrated by Park *et al.* [138] who fabricated a nanotubular array upon electrochemically polymerising 3,4-ethylenedioxythiophene into a template polycarbonate membrane fixed onto an indium tin oxide electrode. Polymer coated pores formed nanotubes which were loaded with glucose oxidase solution, then sealed with a PEDOT/PSS composite

cap in order to block the enzyme inside the tubules, but at the same time to allow analytes and oxygen to permeate into the sensing system. In this way the dynamic range of the sensor was enhanced (0-8 mM) and a good selectivity towards interfering compounds (ascorbate and acetaminophen) was achieved.

More recently, a new composite consisting of PEDOT nanofibres and palladium nanoparticles was obtained by a new methodology involving a micellar "soft template" approach [139]. A surfactant (sodium dodecyl sulphate) and an ionic liquid (1-butyl-3-methylimidazolium tetrafluoroborate) were used to form cylindrical micelles which, after monomer addition, were electrodeposited onto the electrode surface, thus obtaining PEDOT nanofibres. Further addition of Pd nanoparticles and GOx led to the creation of a glucose biosensor, the sensitivity of which was enhanced by the synergistic effect of the nanofibrous PEDOT and the nanoparticles (DL 75μM). The sensor was also tested with real samples and the results were found to be in good agreement with a reference commercial glucose meter (error 3.24%).

A remarkable *in-vivo* study was reported by Rahman *et al.* who developed a PEDOT nanoparticle-based biosensor for monitoring the change in extracellular glutamate levels in response to cocaine exposure [140]. A layer (100nm) of PEDOT nanoparticles was obtained on a Pt microelectrode by CV at high scan rate (1V s^{-1}). Subsequently, glutamate oxidase was immobilised in the presence of ascorbate oxidase (to eliminate the ascorbate interference) through the formation of covalent bonds between the carboxylic acid groups of the polymer and the amine groups of the enzymes. The resulting glutamate biosensor was firstly tested *in vitro* with very good results (linear range between 0.2 and 100 μM, DL 0.1μM), then employed to monitor the extracellular fluctuation of glutamate. For this purpose, the micro-biosensor was implanted in a rat's brain and, after repeated injections of cocaine, the increase of basal glutamate levels was monitored.

Among conducting polymers, the class of compounds which recently has been widely investigated for sensing applications is polyaniline (PANI) because of its

inexpense, the easy availability of raw materials for its synthesis, ease of processing, high conductivity and simple doping process [141].

Despite its extensive application in electrochemical biosensors, mostly as an enzyme or antibody immobilisation matrix [126], the performance of conventional PANI films is strongly thickness dependant: the higher the thickness, the poorer is the diffusion of analytes towards the sensing element and consequently the sensitivity of measurements decreases [142]. For this reason, considerable attention has been paid to the realisation of one-dimensional polymer nanostructures which, due to their greater exposure area, offer the possibility of enhancing the diffusion of analyte towards the transducer. Polyaniline nanofibre sensors have been employed in gas and chemical detection and, in all cases, nanostructures performed better than conventional thin films [143, 144].

Upon coupling PANI nanostructures with biologically functional materials (i.e. enzymes, bio- or synthetic receptors), high-performance composites for bio-analytical applications have been obtained.
One of the first examples was reported by Morrin *et al*. in 2004 [145], who described the use of PANI nanoparticles for the modification of glassy-carbon electrode surfaces flowed by immobilisation of horseradish peroxidase for H_2O_2 sensing. Such nanoparticles were obtained in aqueous media using dodecylbenzene sulfonic acid as doping agent and electrochemically deposited on the electrode surface, thus forming a highly conductive nanostructured film which allowed a uniform electrostatic adsorption of enzyme. Results obtained for H_2O_2 biosensing were compared with an analoguous non-nanostructured film deposited from bulk monomer solutions. The nanostructured surface proved more efficient, both in terms of protein immobilisation (it required a concentration six-fold lower for homogeneous coverage) and signal-to-noise ratio (3:1).

Another interesting nanostructured surface was obtained by Luo *et al.* [146] on carbon screen-printed electrodes. Polystyrene nanoparticles (diameter 100nm) were self-assembled on SPEs and acted as templates for the electropolymerisation

of a PANI layer (thickness 10-30 nm), which assumed a cauliflower-like nanostructured shape providing a very large immobilisation surface. HRP was further deposited using chitosan as immobilisation matrix and amperometric determination of H_2O_2 was carried out. The biosensor exhibited a fast response time of about 5 s, a detection limit of 0.36 mM and a high sensitivity of 41.0 mA mM^{-1}, due to the benefits of the nanostructured PANI.

Another HRP-based biosensor was recently developed by Du et al. [147] using polyaniline nanofibres synthesised by interface polymerisation in the presence 4-toluensulfonic acid as dopant. Nanofibres were dispersed in chitosan together with HRP and cast onto GC electrodes. Good analytical performances (linear range $1x10^{-5}$ -$1.5x10^{-3}$, DL $5x10^{-7}$) were obtained due to the highly efficient enzyme loading and rapid electron transfer rate between the active centre and electrode, favoured by the presence of PANI nanofibres.

PANI nanoparticles were employed by Wang and co-workers [148] for the realisation of a new immobilisation and detection platform for H_2O_2 biosensing based on an Au-Pt nanoparticle/nanoPANI composite on GC electrodes. Au-Pt alloy nanoparticles and nano-PANI exhibited a synergistic effect on electron transfer, thus facilitating a fast response time (< 2s) and wide linear range (1.0-2200 μM).

An Au nanoparticle/PANI nanorod composite was also developed by the Willner group [149] in order to provide a highly enhanced surface area with superior charge transport properties for efficient contacting of GOx with the electrode surface. PANI nanorods were obtained by a template synthesis inside porous alumina templates coated on one side with an Au layer. Au nanoparticles were further incorporated inside the pores before removing the template and GOx biocatalytic activity was then studied. From the electrochemical characterisation of the system a 4-fold increase of anodic currents was observed, in comparison with analogous non-composite homogeneous PANI layers. The higher bioelectrocatalytic activity of the Au-Nanoparticle/PANI nanorod assembly was

attributed to the enhanced charge transport properties of the Au-NP/polymer matrix.

The enhancement of GOx catalytic activity in the presence of a polymeric nanostructured surface was also investigated by Zhao et al. [150]. They reported the creation of PANI nanofibres obtained by interfacial polymerisation in the presence of ammonium peroxydisulfate and cast on GC electrodes. The GOx-nanoPANI/GC electrode was fabricated by covalently attaching GOx on the surface of the polyaniline nanofibres via a carbodiimide coupling reaction. The interesting aspect of this work was a voltammetric study of the biocatalytic activity of GOx immobilised onto the nanostructured composite electrodes, which showed a six-fold higher electron transfer rate with respect to previous reported GOx modified electrodes.

A simple and effective new route for PANI nanowire construction and application in glucose biosensing was shown by Horng *et al.* [151]. Polyaniline was directly grown on carbon cloth via electrochemical polymerisation, thus obtaining free-standing, template-independent nanowires. Carbon cloth was specifically selected as a support because of its high porosity, chemical stability, high conductivity, cost-effectiveness and flexible nature, which could be suitable for designing *in vivo* devices. The template-free nanostructure construction consisted of a first nucleation stage, upon applying a proper potential (by linear sweep voltammetry), and subsequent growth under galvanostatic conditions. GOx was electrostatically adsorbed and glucose sensing was performed with excellent sensitivity (2.5 mA mM^{-1} cm^{-2}) over a detection range claimed to be adequate for clinical monitoring of human glucose levels (0-8mM).

The kinetics of a different enzyme was studied by Somerset *et al.* [152], who chose acetylcholinesterase in combination with polyaniline nanorods as an innovative tool for pesticide biosensing. In order to obtain better solubility, polyanilines bearing particular substituent groups were synthesised (poly o-methoxy aniline, poly 2,5-dimethoxy aniline) and AChE was encapsulated in the

nanopolymeric composite deposited on a gold electrode. The biosensor was applied to the study of the inhibition caused by diazinon and carbofuran pesticides and a detection limit of 0.14 ppb and 0.06 ppb, respectively, was calculated.

Polyaniline nanotubes were fabricated via electrophoretic deposition on indium tin oxide electrodes by Dhand *et al*. [153] and utilised for covalent immobilisation of lipase for triglyceride detection. From impedimetric investigation they found that charge transfer resistance decreases linearly with increased triglyceride concentration because lipase hydrolyses tributyrin, thus generating proton and fatty acid in addition to glycerol. The consequent lowering of pH resulted in increased positively charged quinoid moieties on the PANI-nanowire backbone, thus enhancing the charge transfer rate (resistance decreased). The biosensor was tested both in pure solution and in serum and exhibited a discordance of only 5.4%, thus indicating a negligible interference of proteins and other moieties present in the real matrix.

1.2.2.2 Conductive polymer nanostructures used in affinity biosensors

Besides the more common catalytic enzyme-based biosensors, a number of DNA-biosensors have also been developed using polypyrrole and polyaniline nanostructures.

Ozcan *et al.* [154] prepared polypyrrole nanofibre-modified pencil graphite (PG) electrodes for the investigation of double stranded-DNA electrochemical oxidation. Nanofibres were obtained by electropolymerisation of pyrrole in the presence of Na_2CO_3 and $LiClO_4$ upon applying a constant potential. Under the same conditions, but in the absence of carbonate, a PPy film was obtained and results were compared with those obtained with nanofibres, which exhibited a shift to the more cathodic potential of the guanine and adenine bases as a result of the catalytic effect of nanofibre PPy.

Ko *et al.* [155] reported the formation of carboxylic acid-functionalised polypyrrole nanotubes using aluminum oxide membranes and their application for DNA measurement. After soaking with an oxidant solution (iron chloride), membranes and pyrrole-3-carboxylic acid monomers were placed in a reactor and allowed to polymerise under high pressure. In this way, the authors obtained nanofibres covered with carboxylic groups, which acted as binding sites for amino-tethered oligonucleotides. Conductance changes after the hybridisation with different amounts of complementary DNA sequence were measured by depositing functionalised fibres on gold pads and high sensitivity at low analyte concentration was obtained (1 nM). Moreover, this particular sensor design showed promise for future application as a nanosensor and for lab-on-a-chip technology, due the possibility of manipulating and contacting a sigle nanofibre to act as sensor.

In 2006, Zhu *et al*. [156] fabricated PANI nanowires and modified them with oligonucleotides probes for DNA hybridisation detection. Nanowires of a diameter of 80-100nm were directly synthesised on GC electrodes thorough a three-step electrodeposition of monomer containing solution. In the first polymerisation step the polymer was deposited on the electrode surface as small particles, which served as seeds for the growth of nanoframeworks during the following steps, consisting of two continued polymerisations at reduced current density. Oligonucleotides were covalently immobilised through the formation of phosphoramidate bonds between the amino groups of the polyaniline and phosphate groups at the 5' end. The hybridisation event was measured by DPV, using methylene blue as indicator. A good discrimination between complementary and non-complementary DNA sequences was achieved, with a detection limit of 1.0×10^{-12} mol L^{-1}.

Chang *et al*. [157] reported the realisation of a PANI nanotube array as platform for immobilisation and sensitive detection of oligonucleotide sequences. A good aligned and orientated PANI nanotube array was obtained on graphite electrodes using alumina nanoporous layers as template. As already stated in the case of

CNTs, vertical alignment greatly favours orientation and accessibility of DNA probes. Oligonucleotide probes were covalently immobilised on the surface of inner and outer walls of PANI nanotubes, making each PANI nanotube work like a signal amplification nanodevice for the hybridisation event. After labelling the hybrid with daunorubicin, the DPV response showed that the PANI nanotube array had a signal enhancement capability, allowing the detection of target oligonucleotides at femto molar level and a good differentiation between perfect match and one-base mismatched sequences.

Polyaniline nanostructures and metal nanoparticle composites were also used for the development of a DNA biosensor. Feng and co-workers [158] created gold nanoparticle/polyaniline nanotube (diameter ~100 nm) membranes on glassy carbon electrodes for the impedimetric investigation of the hybridisation event. Also in this case the synergistic effect of the two nanomaterials dramatically enhanced the sensitivity and detection limit (1×10^{-13}mol L^{-1}) of specific DNA sequences with respect to other DNA biosensors realised by the same group. In addition to gold nanoparticles, Zhou *et al.* [159] incorporated also CNTs in the polyaniline nanofibre composite in order to further enhance electron transfer rate and the available surface for oligonucleotide immobilisation. PCR amplicons related to transgenically modified products were determined with label-free impedance measurements, achieving a detection limit of 5×10^{-13} mol L^{-1}.

Another class of polymeric compounds which should be mentioned in the present section consists of nanostructures and nanocomposites of molecular imprinted polymers (MIPs). Molecularly Imprinted Polymers (MIPs) are synthetic polymers with artificial recognition cavities [160-162]. The imprinting technique consists of using the target molecule as a template for synthesising polymers. Polymerisation of functional monomers occurs in the presence of the template, which directs the positioning and orientation of the material structural components by a self-assembly mechanism. Subsequent removal of the template leaves specific recognition sites in the MIP matrix which are capable of rebinding the target molecules in preference to other closely related molecules. The particular interest

this class of compounds has generated is due to three main characteristics: their high affinity and selectivity (similar to those of natural receptors such as enzymes and antibodies), a unique stability, which can't be found in natural biomolecules, and an ease of preparation, suitable for mass production [163]. The main challenge in designing MIP-based electrochemical sensors is the integration between the recognition and the transduction element. Imprinted polymers, in fact, are mainly based on acrylic or vinylic compounds, which are electrical insulators: this feature could strongly limit their use as receptors in electrochemical sensors, because of the lack of a direct path for conduction from the active sites to the electrode. For this reason conductive and semiconductive MIPs, such as imprinted polypyrrole, aniline and aminophenyl boronic acid, have been extensively investigated [164-166]. These MIPs can be directly integrated with the transducer surface using electropolymerisation, thus obtaining substrate-selective electrodes (*in situ* imprinting). Moreover, with respect to other immobilisation techniques, electropolymerisation allows the deposition of receptors at precise spots on the transducer and the regulation of thickness and polymer density by simply varying electrochemical parameters [14].

Molecular imprinting technology appears, therefore, a highly promising tool to realise nano-sized devices. The advantage can be found not only in the size itself, but also in the increase of equilibrium rate with the analyte and significant enhancement of accessible complementary cavities per material weight [167]. MIP nanofibres and nanowire arrays have been made using the classical approach of template synthesis with alumina nanoporous membranes [168-170]. Another approach to produce polymer nanostructures is electrospinning (ejection of a liquid seed material from a capillary tube at high voltage), which has been employed for the preparation of MIP nanofibres with diameters of 100-300 nm for the recognition of theophylline and estradiol [171, 172].

In order to apply these materials for sensor construction, MIPs have to be patterned on chip surfaces and interfaced with the transducers. Patterning techniques, mainly based on photolithography, soft-lithography and micro-

spotting, have been developed [167], but research in this field is still very challenging and opens great opportunities for future development of highly sensitive and miniaturised electrochemical devices.

1.2.3 Nanoparticles

Nanoparticles (NPs) have been employed in an enormous variety of bioanalytical formats; in only the last five years, more than 300 papers have been published in the main international scientific journals, illustrating the versatile range of application of nanoparticles as quantification tags, immobilisation substrates, for signal amplification and as carriers. For this reason, this section will present only a brief overview of the fundamental characteristics which have made nanoparticles so interesting for biological sensing, with some examples of the more interesting applications.

Depending on their composition (metal, semiconductor, magnetic), nano-size particles (or beads) exemplify different functions in electroanayltical applications. Metal nanoparticles provide three main functions: enhancement of electrical contact between biomolecules and electrode surface, catalytic effects and, together with semiconductor ones, labelling and signal amplification [173]. They are typically obtained by chemical reduction of corresponding transition metal salts in the presence of a stabiliser (self-assembled monolayers, microemulsions, polymers matrixes), which give the surface stability and proper functionalisation, in order to modulate charge and solubility properties [174].

Magnetic particles act mainly as functional components for immobilisation of biomolecules, separation and delivery of reactants. The magnetic core-shell is commonly constituted by iron oxides, obtained by co-precipitation of Fe (II) and Fe (III) aqueous salts by addition of a base. Upon modulating synthetic parameters, it is possible to obtain the required characteristics for biomedical and bioengineering applications, such as uniform size (smaller than 100 nm), specific

physical and chemical properties and high magnetisation [175]. Moreover, with proper surface coating, biomodification and biocompatibilty can be achieved.

Among metal nanoparticles, the most widely used have been gold nanoparticles (Au-NP) because of their unique biocompatibility, structural, electronic and catalytic properties.

1.2.3.1 Nanoparticles used in catalytic biosensors

Gold nanoparticle-enzyme hybrid systems have been widely investigated by the Willner group [176, 177] in order to overcome the lack of electrical communication often observed between redox enzymes and an electrode surface. Biocatalytic electrodes were prepared by conjugation of apo-GOx (apoprotein form) with Au nanoparticles functionalised with a FAD cofactor unit extracted from active GOx and self-assembled on a dithiol-modified Au electrode. In this way, NPs were implanted in intimate contact with the active site of the enzyme, thus forming an hybrid architecture which facilitated the electrocatalysed oxidation of glucose, thanks to highly efficient electron transport.

Other Au-NP-enzyme composites were investigated by the Pingarròn group [178, 179]. A xanthine oxidase biosensor for hypoxanthine detection was realised using carbon paste electrodes modified with electrodeposited Au nanoparticles, onto which the enzyme was cross-linked with glutaraldehyde and BSA [178]. This format allowed the determination of hypoxanthine at lower potential (0 V) thus minimising interference by ascorbic acid. Another enzyme biosensor was fabricated using graphite-Teflon electrodes in which tyrosinase and Au-NPs were incorporated [179]. The presence of colloidal Au particles enhanced kinetics of both the enzyme reaction and the electrochemical reduction of the analyte (*o*-quinones) at the electrode, thus providing a high sensitivity for catechol and other phenolic compounds detection (20nM).

A multilayer technique was developed by Yang *et al.* [180] for the construction of GOx/AuNPs films on Au electrodes. A biosensor realised with six bilayers of GOx/AuNPs showed a wide linear response to glucose (range of 10 μM–0.013 M) and a fast response (4 s).

Magnetic nanoparticles have also been involved in the construction of composite biocatalytic assays. A biosensor based on Fe_3O_4 nanoparticles–chitosan nanocomposite was developed for the determination of phenolic compounds [181]. The large surface area of nanoparticles and the porous morphology of chitosan allowed a better loading of enzyme without compromising its bioactivity. The biosensor exhibited a linear range from 8.3×10^{-8} to 7.0×10^{-5} mol L^{-1}, and a detection limit of 2.5×10^{-8} mol L^{-1} for catechol detection. Mavré *et al.* [182] prepared self-assembled aggregates of iron oxide NPs, avidin, and a biotinylated diaphorase oxidoreductase for bioelectrocatalytic oxidation of NADH. This method represented a very simple, fast and efficient route for the construction of highly loaded enzyme electrodes. Upon applying a magnet, the magnetic enzyme aggregate was collected on a carbon SPE and catalytic currents recorded by cyclic voltammetry. The response obtained was much higher than that measured at an electrode directly coated with a packed film of diaphorase.

Further advantages have been demonstrated to come from the combination of gold nanoparticles with CNTs [76] or conductive polymers such as polypyrrole and polyaniline [183].

1.2.3.2 Nanoparticles used in affinity biosensors

Many particle-based routes have been investigated for gene detection and immunosensing. These protocols are based on colloidal Au tags but also on polymer carrier beads, quantum dot tracers (QD, semiconductor nanocrystals ranging from 2-10 nm in diameter). With respect to traditional labelling techniques, nanoparticles offer several advantages: higher stability (enzyme-label and isotope lifetime is limited), possible combination of different tags for simultaneous analysis of various analytes and suitability for multiplexed array construction.

The most effective approaches, especially for DNA sensing, rely on the voltammetric or potentiometric stripping of nano-metal/semiconductor tracers This method, as extensively reviewed by Merkoci and co-workers [184-186], consists of different strategies, as illustrated in Figure 4. One possibility is monitoring the enhancement of conductivity after accumulation of silver or gold on AuNPs anchored to conventional genosensors (Figure 4A). Another strategy has been the stripping analysis of gold directly, as well as Au(III) ions released after acid treatment with HBr/Br_2 (Figure 4B) or of silver, previously deposited un Au-NPs (Figure 4C). Finally, multilabelling with three different quantum dots and simultaneous detection of the released different metals (figure 4D) has found to be useful for simoultaneous analysis of different compounds. Usually, the DNA probe is immobilised directly on the transduction platform as well as on paramagnetic beads and successively magnetically confined on the electrode surface. Labelling with nanoparticles is performed upon hybridisation of target DNA in the presence of NP-modified secondary probes (sandwich hybridisation assay), previously prepared. Thiol-Au covalent binding and streptavidin-biotin affinity reactions are the most common procedures for the immobilisation of biological molecules, such as oligonucleotides and antibodies, on nanoparticles.

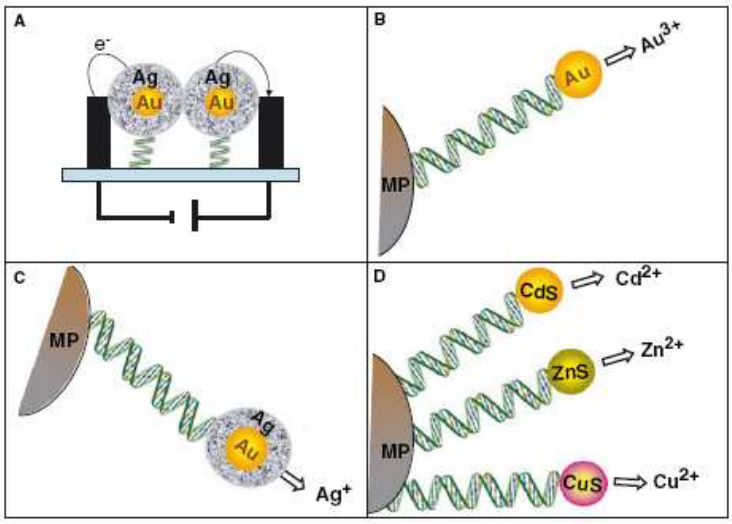

Figure 4. Schematic representation of four different nanoparticle-based labelling routes: A) conductimetric detection; B) Au dissolving and Au(III) stripping accumulation and detection; C) Silver precipitation, dissolution (with HNO_3) and Ag^+ stripping; D) multilabelling with different quantum dots and detection of the corresponding ions. [183]

One of the first examples was reported by the Wang group in 2001 [187], who described the immobilisation of a DNA probe on streptavidin-coated magnetic beads and hybridisation with a biotinylated target, which was able to bind streptavidin coated Au-NPs (5nm in diameter). Dissolved gold was quantified by potentiometric stripping analysis on carbon electrodes, obtaining a detection limit of 4 nM for segments related to breast cancer. A better detection limit (femtomolar level) was achieved by the same group [188] by using the silver enhancement method, based on the precipitation on Ag on Au-NPs, its dissolution with HNO_3 and potentiometric detection.

More recently, Pumera *et al*. [189] reported a NP-based system using magnetically induced direct electrochemical detection of gold QD tracers (Au67, diameter 1.4nm) linked to the DNA target in 1:1 ratio. The assay was performed on paramagnetic beads, further collected on magnetic graphite-epoxy composite electrodes and Au67-QD was directly quantified by DPV, achieving a nanomolar detection limit. The two main advantages of this platform were: the direct detection of QDs, without the need for dissolution and absence of an interconnected 3D network of Au-DNA duplex–paramagnetic beads, which may decrease the sensitivity because of the sharing of one gold tag by several DNA strands. A similar approach was applied by the Ozsoz group [190] for the analysis of PCR real samples and an even lower detection limit (femtomolar level) was achieved.

Rochelet-Dequaire *et al.* [191] investigated a new route for DNA detection avoiding previous PCR amplification, by realising a new genosensor for the determination a 35-base human cytomegalovirus nucleic acid target. Target was adsorbed in polystyrene microwells and hybridised with an Au-NP modified detection probe, to be detected by anodic stripping of the chemically oxidised gold label at screen printed electrodes. Further enhancement of the hybridisation signal was obtained upon incubating with mixture of Au (III) and hydroxylamine, which induced the autocatalytic reductive deposition of ionic gold on the surface of the AuNPs labels. This strategy allowed the detection of DNA concentrations

as low as 600 aM. A singular signal amplification was more recently achieved by Du *et al.* [192] who realised a sandwich hybridisation assay in which Au nano-tags were further linked to DNA modified PbS nano-spheres ("bio bar code") and lead ions were detected using anodic stripping voltammetry, thus achieving a detection of 5×10^{-15} M for oligonucleotide target.

Metal sulfides QDs were employed by Liu *et al.* [193] for the simultaneous detection of different single nucleotide polymorphisms. The format consisted of linking ZnS, CdS, PbS and CuS NPs to adenosine, cytidine, guanosine, and thymidine mononucleotides, respectively. Monobase-conjugated nanocrystals were then incubated with the hybrid-coated magnetic-bead solution and each mutation captured different nanocrystal-mononucleotides. In this way, for each single nucleotide polymorphism, distinct voltammetric stripping signals were obtained.

A similar approach was also reported by the same authors for simultaneous immunosensing of β_2-microglobulin, IgG, BSA and C-reactive protein [194]. The multianalyte sandwich immunoassay involved a dual binding event of primary and secondary antibodies onto QDs tags (ZnS, CdS, PbS and CuS) and magnetic beads, respectively. A carbamate-base linkage was used for conjugating the hydroxyl-terminated nanocrystals with the secondary antibodies. Each biorecognition event generated a distinct voltammetric peak, the position and size of which was specific of the type and concentration of the corresponding antigen.

Other immunoassays were developed exploiting Au-NP labelling. Liao *et al.* [195] reported a highly sensitive assay based on the autocatalytic deposition of Au (III) onto AuNPs for the determination of rabbit IgG with square-wave stripping voltammetry (detection limit 1.6 fM). Chu *et al*. [196] were able to detect a concentration of 1ng mL^{-1} of human IgG using the method based on the precipitation of silver on colloidal gold labels. Direct electrical detection of Au was instead employed by Idegami *et al.* [197] for the design of an immunosensor for the detection of a pregnancy marker (human chorionic gonadotropin hormone,

hCG). Primary antibody was immobilised on screen-printed carbon strips and the captured antigen was sandwiched with Au-NP labelled secondary antibody. Gold nanoparticles were exposed to a preoxidation process and then reduced via DPV. Urine samples of pregnant and non-pregnant adults were tested and results compared with a standard ELISA test with good agreement, as evidenced by the fact that both tests were not able to detect any hCG in the urine sample of non-pregnant women.

Au-NPs have been not only employed for labelling, but also for the enhancement of electrical properties. An example is the label-free immunoassay based on impedimetric measurements developed by Tang *et al.* [198] for the detection of carcinoembryonic antigen. Carcinoembryonic antibody was covalently attached to AuNPs and the composite immobilised on Au electrode by electrocopolymerisation with *o*-aminophenol. Electrochemical impedance spectroscopy studies demonstrated that the formation of antibody–antigen complexes increased the electron-transfer resistance of $[Fe(CN)_6]^{3-/4-}$ redox probe at the poly-*o*-aminophenol/Carcinoembryonic antibody-AuNPs/Au electrode, thus monitoring of carcinoembryonic antigen concentration could be performed (detection limit 0.1 $ngmL^{-1}$).

An alternative application of Au-NPs was also reported by He *et al.* [199] for the development of label-free sensors for thrombin detection using aptamers. Aptamers are DNA (or RNA) oligonucleotides, able to recognise a variety of targets such as proteins, peptides, small molecules [15]. Anti-thrombin antibodies were immobilised on the microtitre plates to bind thrombin and the complex was sandwiched with aptamers conjugated to Au nanoparticles ("bio bar code"). After washing, a basic treatment allowed the collection of the "bar code" aptamers, which were further degraded and the amount of Adenine (proportional to the amount of bound thrombin) quantified by DPV. This assay takes advantage of the amplification potential of Au nanoparticles carrying numerous aptamer tags.

Another important use of nanoparticles is their employment as platforms for the immobilisation of biological elements. Their large surface area greatly increases biomolecule loading. Moreover, with respect to confinement on an electrode surface, the higher mobility achieved favours delivering of reactants and recognition reactions. Due to the ease of functionalisation with thiol groups, gold nanoparticles have also been widely employed in this field. The greatest contribution to the improvement of sensitivity and reliability of electrochemical biosensors has been provided by magnetic micro and nano-particles (or beads). A recurring problem in electrochemical biosensing is the background interference due to aspecific adsorption of ligands or enzymatic/chemical labels at the electrode surface. Moreover, passivation and fouling of electrodes is the most important problem in all electroanayltical techniques [200]. To overcome these obstacles, in the last decade, magnetic beads have represented a very elegant and effective solution. Many groups exploited the possibility of performing the recognition event on the surface of paramagnetic micro- and nano-beads, thus realising highly sensitive electrochemical immunosensors [201-204] and genosensors [205-213], which are also called immunomagnetic and genomagnetic sensors, respectively. This approach offers several advantages. Firstly, by performing the bio-recognition and the transduction step at different surfaces (i.e. magnetic beads and unmodified electrodes), the non-specific adsorption of analytes and other reagents can be significantly reduced. Moreover, upon employing receptor-modified particles freely moving in solution, random collisions between reagents are favored and the efficiency of coupling rises. Finally, magnetic separation of the particles from the solution facilitates washing steps, thus improving the removal of non-specifically adsorbed reagents.

Centi *et al.* [201-203] reported several interesting immunosensors and aptasensors in which the analytical performances of the assay were significantly improved by immobilising antibodies (or aptamers) on paramagnetic beads rather than directly onto the working electrode surface. As demonstrated also by Sakar *et al.* [204] in the determination of free prostate specific antigen, this method has great potential to be used as a diagnostic tool because, after binding with the analyte, particles

can be magnetically separated from the sample medium (blood, serum) and thus the electrode can be preserved from fouling or interference problems.

Palacek and Wang can be considered the pioneers of genomagnetic assays with tens of papers and reviews published over the last decade, exploring both label-free and enzyme-linked methods [205-208]. An interesting combination of magnetic, polymeric and gold nanoparticles was reported by Kawde and Wang [209], who achieved a detection limit of 0.1 ng/mL using oligonucleotides functionalised with polymeric beads carrying gold nanoparticles. This strategy involved the hybridisation of the oligonucleotide probe (captured on magnetic beads) to the DNA target labelled with the Au-loaded sphere, and subsequent dissolution and stripping-potentiometric detection of the Au tracer. Lermo *et al*. [210] developed a genomagnetic assay for the detection of food pathogens based on a graphite-epoxy composite magneto electrode as electrochemical transducer. The assay was performed in a sandwich format by double labelling the amplicon ends during PCR, with a biotinylated capture probe, to achieve the immobilisation on streptavidin-coated magnetic beads and with a digoxigenin signalling probe, to achieve further labelling with the enzyme marker (anti-digoxigenin horseradish peroxidase). Erdem *et al.* [211] proposed a genomagnetic assay based on label-free electrochemical detection of hepatitis B virus DNA in PCR amplicons, using pencil graphite electrodes as transducers. They obtained a detection limit in the femtomolar range. The same group reduced the magnetic bead dimension to the nano-scale to further increase the sensitivity of the assay [212]. The magnetite (Fe_3O_4) nanoparticles (average dimension of 125 and 225 nm) were prepared by co-precipitation technique, and functionalised for coating with streptavidin. A label-free DNA hybridisation assay was developed by immobilising guanine-free biotinylated probe and monitoring the guanine oxidation peak after hybridisation. Very small diameter magnetic beads (18 nm) were also prepared by Zhu *at al.* [213]. After immobilisation of DNA, probe nanoparticles were deposited on pyrolitic graphite electrodes, incubated with target and the hybridisation event was monitored by cyclic voltammetry using the redox couple $K_3[Fe(CN)_6]/K_4[Fe(CN)_6]$ as indicator (redox peaks decreased after base pair

coupling). Over the whole hybridisation period, a magnetic field was applied over or below the electrode. NPs were either repelled or attracted from or to the surface of the electrode, thus working as a magneto-switch as NPs were released once hybridisation occurred.

Other applications of magnetic NPs have involved the construction of composite or layer-by-layer films for immunomagnetic assay design.
Three-layer nanoparticles composed of a ferrite magnetic core, covered with Prussian blue and gold were realised by Zhuo *et al.* [214] to be applied as a mobile platform for the immobilisation of a secondary antibody and a bienzyme labelling system (HRP and GOx) for immunosensing. Primary antibodies were immobilised on a hydrogel composite Au electrode and, after incubation with Carcinoembryonic antigen, labelling could be easily performed with the multifunctionalised nanoparticles. In this way the immunosensor could be regenerated by simply applying an external magnetic field, thus obtaining a dramatic improvement in reproducibility.

A different type of magnetic composite nanobead was developed by Pale *et al.* [215] to act as an immunomagnetic concentrator of *Bacillus Anthracis* spores from food samples as well as an electrical transducer. Magnetic iron oxide nanoparticles (100nm in diameter) were coated with a conductive polyaniline layer, linked to a detector antibody and added to the contaminated food sample. After binding the spores, beads were magnetically removed and deposited on a pad, placed between silver electrodes, where a secondary antibody had been previously immobilised. The presence of conductive particles increases conduction between the two Ag electrodes and was proportional to the amount of analyte, which could be detected at concentrations as low as 4.2×10^2 spores mL^{-1}.

These examples show attractive features, especially for automation of analytical biosystems. Magnetic beads, in fact, also offer great advantages in flow systems where magnetic properties may facilitate the delivery and removal of reagents through the channels and help in the miniaturisation of the whole sensing

apparatus. The main problem for miniaturisation of analytical systems lies mostly in the preliminary operations (sampling, sample introduction and treatment). By contrast, detection and signal transduction, as well as data acquisition and processing, can achieve a high degree of miniaturisation [216]. Thus, coupling new micro and nanotechnologies with emerging nanostructures, "smart" nanosensors able of electrochemical coding could be the basis for the construction of a tiny ''chemical lab'' (lab-on-a-bead) [186] able to detect and analyse a unique ligand in a complex mixture.

1.3 Aim and objectives

The above literature review highlights the exceptional potential of nanomaterials for the design of novel sensing technologies and to enhance the analytical performance of biosensing systems. On the basis of these observations, the present work was focused on the investigation of different types of micro- and nano-materials (carbon nanotube thin films, polyaniline nanotubes and magnetic particles) and their application in highly sensitive sensing systems. The choice of these particular materials and specific applications for each of them derived from the insertion of the present research activity in projects and collaborations in which our research group has been involved (Italian project PRIN 2005 "Quasi mono dimensional nanosensors for label free ultra sensitive biological detection", collaboration with DiagnoSwiss S.A. company; research activity within the cotutela program in Smart Materials, Cranfield Health, Cranfield University)

The first part of the research activity was focused on the designing and testing of new vertical aligned MWNTs thin films as candidate working electrodes for DNA immobilisation and for the development of an electrochemical genosensor. The vertical orientation of the nanostructures, in fact, was supposed to facilitate the loading of DNA probe as well as the access of the analyte towards the immobilised probe, thus increasing the sensitivity of the analysis. Despite these advantages, there are still few papers [111-115] reporting the application of well

oriented CNTs film for DNA electrochemical biosensing. Self-assembled aligned MWNT thin films were prepared by CVD onto insulators (SiO_2 or Si_3N_4) and metallic (Al) substrates, using acetylene and ammonia as precursor gases and nickel particles as catalyst. So far these devices themselves have been used only for gas sensing (based on changes in the electrical resistance of the CNT film) for the detection of nitrogen dioxide, ammonia and ethanol [217, 218]. The aim of the current work, therefore, was their employment, for the first time, for electrochemical measurements in solution. In order to determine the most suitable film format for our purposes, different growing substrates and temperatures were tested. For this purpose, a preliminary characterisation was performed using cyclic voltammetry (CV), in order to investigate their electrochemical behaviour in solution. Subsequently, in order to investigate their performances as biosensing platforms, a genosensor was developed using synthetic oligonucleotides related to the 35S promoter, a typical genetic construct present in the majority of GMOs, target of great interest in biosensor-based food analysis [38-40].

DNA detection was also the target of another sensing system developed during this three year research activity. A novel magnetic particle-based microfluidic sensor was realised by integrating an existing technology developed by DiagnoSwiss S.A. [219] with a new analytical procedure based on the use of paramagnetic beads for the detection of real PCR samples [37]. As widely discussed in paragraph 1.2.3, paramagnetic beads offer unique advantages in electrochemical biosensing: reduction of non-specifically adsorbed reagents on the electrode surface, higher coupling efficiency, easier washing steps etc. However, a significant challenge for all biosensor systems is minimising sample preparation, requirements, operational complexity and time. Microfluidic-based platforms show great potential in responding to these demands due to significantly decreased sample/reagent consumption and cost, and dramatically reduced time. Therefore microfluidic devices have found great application in the proteomic [220, 221] and genomic area [222, 223]. Further advantages have been demonstrated by incorporating paramagnetic beads as transportable solid support [224, 225]: analytes were captured by probe (i.e. DNA or antigen)-modified beads

in flowthrough format. Small-diameter particles, in fact, help to enhance the surface area-to-volume ratio thus increasing the sensitivity. Moreover, magnetic properties greatly facilitate the delivery and removal of reagents through the microfluidic channels. Only few examples of analytical procedures based on microfluidic platform coupled to paramagnetic beads for hybridisation electrochemical detection were reported in literature [226, 227]. Baeumner and co-workers [227] reported an interesting approach based on liposomes entrapping the electrochemical marker (ferro/ferricyanide couple).
The novelty of the proposed procedure was the combination of a sensitive electrochemical platform and a proper microfluidic with a simple and effective enzyme signal amplification system, which can pave to way to further investigation for dimension reduction, in line with the concept of lab-on-a-chip-technology.

Finally, polyaniline nanostructures were developed and characterised for highly sensitive bioanalytical application. Among conductive polymers, polyaniline (PANI) has generated great interest because of its inexpense, the easy availability of raw materials for its synthesis, ease of processing, high conductivity and simple doping process. Therefore, the research activity was focused on the development and characterisation of polyaniline (PANI) nanostructures, obtained by electrochemical polymerisation of aniline monomers using alumina nanoporous membranes as template. After an electrochemical and morphological (SEM) characterisation, nanostructures were employed for the realisation of a model MIP-sensor for catechol detection. To our knowledge, this is the first example of integration between molecular imprinted polymers and PANI nanostructured electrodes. The idea was to develop a sensor based on polyaniline nanowires or nanotubes grafted with MIP receptors using a novel hybrid material, N-phenylethylene diamine (NPEDMA) [228] as monomer. This molecule combines two orthogonal polymerisable functionalities, an aniline group and a methacrylamide. In this way, the polymerisation of NPEDMA results in a conductive nanowires which allow direct electrical connection between the electrode and the MIP. The conducting nanostructures were synthesised inside the

pores of a membrane by electropolymerisation of the aniline function. The MIP, a Tyrosinase-mimicking polymer, imprinted with catechol, was photochemically grafted over the polyaniline, via iniferter activation of the methacrylamide groups. Thus, hybrid catalytic material electrodes were prepared and characterised. Finally the ability to detect catechol was evaluated and compared with the analogue sensor developed by Lakshmi *et al.* [229], based on a NPEDMA non-nanostructured thin layer, in order to evaluate if the presence of nano-structures facilitates an improvement of the analytical performance.

Chapter 2

MATERIALS AND METHODS

2.1 Chemicals

Acetic acid, sodium acetate, potassium chloride, potassium ferricyanide, nitric acid, disodium hydrogenphosphate, were obtained from Merck (Milan, Italy). *N*-(3-dimethylaminopropyl)-*N*′-ethylcarbodiimide hydrochloride (EDAC), urea, streptavidin-alkaline phosphatase, bovine serum albumin (BSA), magnesium chloride and diethanolamine (DEA) were purchased from Sigma-Aldrich (Milan, Italy). Catechol, resorcinol, hydroquinone, (-)-epinephrine, serotonin hydrochloride, ethylene glycol dimethacrylate, N-phenyl ethylenediamine, methacrylic anhydride, acetonitrile, dimethylformamide, perchloric acid, sodium hydroxide, phosphate buffered saline (PBS) tablets and methanol were purchased from Sigma-Aldrich (Gillingham, U.K.). N-hydroxysuccinimide (NHS) and sodium dodecyl sulphate (SDS) were obtained from Fluka (Milan, Italy). p-Aminophenyl phosphate was purchased from DiagnoSwiss S. A. (Monthey, Switzerland). Diethyl dithiocarbamic acid benzyl ester was purchased from TCI (Oxford, U.K.). Copper chloride and ethylenediaminetetraacetic acid (EDTA) were obtained from Fisher Scientific (Loughborough, UK). NMR solvents were obtained from Goss Scientific (Chelmsford, U.K.). TE buffer 20× (200 mmol/L Tris/HCl; 20 mmol/L EDTA; pH 7.5), Picogreen and λ-DNA standard solution (100 μg/mL), used for fluorescent measurements, were obtained from Invitrogen (Milan, Italy). Streptavidin-coated paramagnetic beads (iron oxide particles with the diameter of approximately 1.0±0.5 μm) were purchased from Promega (Milan, Italy).

Ultrapure water (Millipore) was used for preparing all the solutions.

2.1.1 DNA sequences: probes and targets

Synthetic oligonucleotides were obtained from Eurofins MWG (Ebersberg, Germany).

Sequences related to the 35 S promoter [38, 39] were employed for the development of genosensors based on carbon nanotube thin films and are listed in Table 1.

35 S Promoter (GMO)
Capture probe (25 mer)
5'-NH_2–$(CH_2)_6$-GGCCATCGTTGAAGATGCCTCTGCC–3'
Inosine-substituted capture probe (25 mer)
5'-NH_2–$(CH_2)_6$-IICCATCITTIAAIATICCTCTICC– 3'
Target (25 mer)
5'- GGCAGAGGCATCTTCAACGATGGCC- 3'
Biotinylated target (25 mer)
5'- biotin-TEG*-GGCAGAGGCATCTTCAACGATGGCC- 3'
Non-complementary sequence (24 mer)
5' - GGAGATCGACCACGCAAACTTCAA – 3'
Non-complementary biotinylated sequence (24 mer)
5' – biotin – TEG- AGGCCCTGCGAGCAACATCTCATG –3'
* TEG (tetra-ethyleneglycol) was used as spacer arm

Table 1. Synthetic DNA sequences related to the 35 S promoter.

The sequences of synthetic oligonucleotides, PCR primers and the PCR fragment related to Cor a 1.04 hazelnut gene [37], employed for the development of the magnetic-particles based microfluidic sensor, are listed in Table 2. Genomic DNA from dried hazelnut fruits was extracted using the commercial kit, Sure Food PREP-Allergen (Congen, Berlin, Germany), according to the manufacturer's instructions. The conditions for the PCR amplification of the gene sequence codifying for Cor a 1.04 allergen were adapted from the procedure reported in literature [230]. All the reagents for the PCR reaction were obtained from Takara (Takara Bio Europe, Saint-Germain-en-Laye, France). The PCR reaction was

carried out in a final volume of 50 μL containing PCR buffer 1×, 1.5mM $MgCl_2$, 1.2 U/mL of *Taq* polymerase, 200 μM of deoxyribonucleotide triphosphates mixture, 0.25 μM of forward primer, 0.25 μM of reverse primer and 500 ng of genomic DNA. The PCR was performed with a MJ Research PTC 150 thermocycler (MJ Research Inc., Bruno, Canada) using the following conditions: activation of *Taq* polymerase at 95 ◦C for 5min, followed by a 40 two-step cycles (94°C for 30 s, 63°C for 30 s) and a final extension at 72°C for 10 min. Prior to use, PCR amplicons were purified using Millipore Montage PCR centrifugal filter devices according to the manufacturer's protocol (Millipore, Milan, Italy). Their concentration was finally determined by fluorescence measurements using Picogreen dye and a TD-700 fluorimeter (Analytical Control, Milan, Italy).

Cor a 1.04 (hazelnut allergen)

Capture probe (24 mer)
5'-biotin-TEG*-GGAGATCGACCACGCAAACTTCAA-3'
Signaling probe (20 mer)
5'-ATACTGCTACAGCATCATCG-TEG-biotin-3'
Forward primer (24mer)
5'-GGAGATCGACCACGCAAACTTCAA-3'
Reverse primer (23 mer)
5'-CCTCCTCATTGATTGAAGCGTTG-3'
PCR amplified fragment of the Cor a 1.04 gene (182 bp)
5'-GGAGATCGACCACGCAAACTTCAAATACTGCTACAGCATCATCGAGGGAG GTCCATTGGGGCACACACTGGAGAAGATCTCTTACGAGATCAAGATGGCGGC AGCCCCTCATGGAGGAGGATCCATCTTGAAGATCACCAGCAAGTACCACACC AAGGGCAACGCTTCAATCAATGAGGAGG-3'.
* TEG (tetra-ethyleneglycol) was used as spacer arm

Table 2. Sequences of synthetic oligonucleotides, PCR primers and the PCR fragment related to Cor a 1.04 hazelnut gene.

2.2 Electrochemical methods

All electrochemical measurements were performed using a three-electrode system, either arranged in a well-cell or in planar cells obtained through screen-printing or lithographic techniques. The cell consisted of working electrode, reference electrode and counter electrode. The potential applied to the working electrode was referred to an Ag/AgCl reference electrode. Current passed between the working and the counter electrode and, in this way, a constant potential was maintained between the working electrode and the reference electrode. The applied potential induced the transformation (oxidation or reduction) of the analyte at the working electrode and a current proportional to the analyte concentration was generated.

2.2.1 Cyclic voltammetry

Cyclic voltammetry (CV) is a widely used electroanalytical technique which has been mainly applied to the investigation of mechanisms and kinetics of redox reactions as well as to the characterisation of electrode surfaces [231]. In CV experiments the current response derives from the application (in an unstirred solution) of a triangular potential waveform (figure 5 a), which produces a forward and a reverse scan. Each experiment can consist of one full cycle, a partial cycle or several cycles. The interval of potential scanned in every experiment depends on the voltage at which diffusion-controlled oxidation or reduction of the sample can be observed.

The most useful parameters in a cyclic voltammogram are the cathodic peak potential, E_{pc}, the anodic peak potential, E_{pa}, the cathodic peak current, i_{pc}, and the anodic peak current, i_{pa} (Figure 5 d). They allow determination of the reversibility of the electron transfer reaction and the consequent similarity of the system to a Nernstian behaviour [232]. For a reversible electrode reaction, the ratio between anodic and cathodic peak currents should be equal to 1. Moreover, at 25°C the difference in peak potentials, ΔE_p, is expected to be 0.059/n, where n is the

number of electrons involved in the half-reaction. Higher ΔE_p indicates irreversibility due to slow electron transfer kinetics.

Quantitative information can be obtained from the Randles-Sevcik equation, which, at 25°C, is:

$$i_p = (2.69 \times 10^5)\, n^{3/2} A D^{1/2} C v^{1/2}$$

where i_p is the peak current, A is the electrode area in cm^2, D is the diffusion coefficient in cm^2/s, C is the concentration in mol/cm^3, and v is the scan rate in V/s. In this way it is possible to calculate one of the parameters, if the others are known.

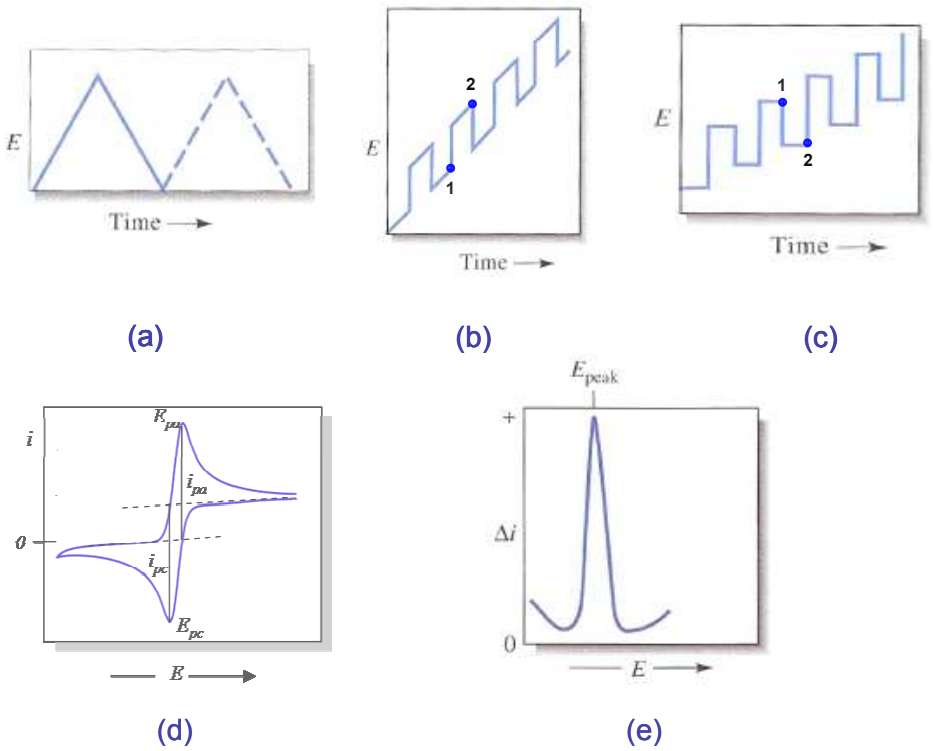

Figure 5. Voltage vs time excitation signals used in voltammetry and corresponding current responses: cyclic voltammentry potential (a) and corresponding current response (d); differential pulse voltammetry (b), square wave voltammetry (c) and corresponding peak-shaped current response (e). *Adapted from [231, 233]*

2.2.2 Differential pulse voltammetry

In differential pulse voltammetry the applied potential (shown in Figure 5 b) derives from the superimposing of a periodic pulse (amplitude 10-100 mV) to a

linear scan. Current is sampled twice: just before the pulse application (1, Figure 4 b) and just before the end (2, Figure 5b). The difference between the two current values (i_2-i_1) is plotted versus the linear increase of the voltage, thus obtaining a voltammogram consisting of peaks (Figure 5e). The height of the peak is directly proportional to the concentration of the analyte, while its position is characteristic of the species.

One of the advantages of this technique is the peak-shaped response which allows the discrimination of species differing by as little as 50 mV. Moreover, by taking the difference between current samples, DPV allows a significant reduction of background current contributions, thus achieving higher sensitivity and lower detection limits with respect to other non-pulsed methods [231, 233]. This is the main advantage of all pulsed techniques, which exploit the faster decay of capacitive current with respect to faradic current. Thus, sampling current response at points where has considerably decayed can greatly increase the signal-to-noise ratio.

In the present work DPV measurements were employed for the monitoring of the hybridisation event in carbon nanotube based genosensors (see paragraph 2.3.1), upon applying the following parameters:

- modulation time 0.05 s
- interval time 0.15 s
- step potential 5 mV
- modulation amplitude 70 mV

2.2.3 Square wave voltammetry

Square wave voltammetry is a pulsed technique in which the potential applied to the working electrode is composed of a large symmetrical square wave pulse (> 100 mV) superimposed on a staircase scan, as shown in Figure 5c. Current is sampled twice during each square wave cycle, once at the end of the first half of the square wave (1, Figure 5c), which is in the direction of the staircase scan and

once at the end of the reverse pulse (2, Figure 5c). The difference between the two measurements is plotted versus the base stair case potential and a peak-shaped voltammogram is obtained. The main advantage of SWV is the speed of each measurement, which derives from the product of the square-wave frequency and the staircase step height [231]. The consequence is a consistent reduction of analysis time: a complete voltammogram can be recorded in a few seconds, as compared with 2-3 minutes requested by DPV, upon applying similar pulse parameters.

In this work SWV was used for the investigation of the immobilised DNA probe on carbon nanotube thin films. Experimental parameters are reported below:

- frequency 50 Hz
- step potential 15 mV
- amplitude 40 mV

2.2.4 Chronoamperometry

Chronoamperometry is based on stepping the potential (Figure 6a) and monitoring the resulting current derived from faradic processes at the working electrode, as a function of time. As these experiments are carried out in unstirred solutions, mass transport is governed solely by diffusion. In this way, the consuming of reactants in the proximity of the working electrode causes an expansion of the diffusion layer and hence a decrease of the slope of the concentration profile as time progresses [233], as illustrated in Figure 6b. Consequently, current decays with time, as shown in Figure 6 c, according to the Cottrell equation:

$$i(t) = \frac{nFACD^{1/2}}{\pi^{1/2} t^{1/2}} = kt^{1/2}$$

where n is the number of electrones involved in the reaction, F is the Faraday constant (96500 C mol^{-1}), A the area of the electrode (cm^2), C the concentration, D the diffusion coefficient (cm^2 s^{-1}), t the time (s). This technique is often employed in addition to CV, for measuring the diffusion coefficient of electroactive species or the effective area of the working electrode.

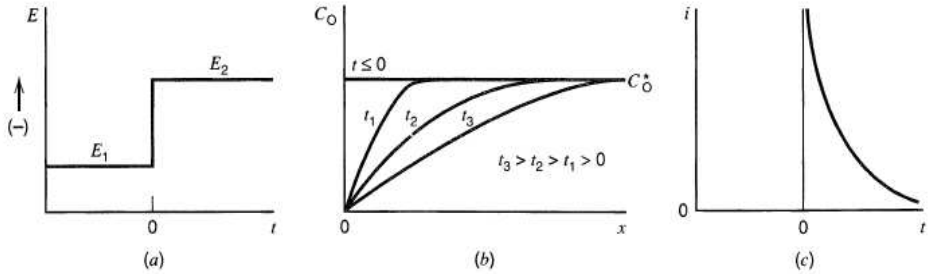

Figure 6. Chronoamperometry: potential vs time waveform (a), change of concentration profiles (x = distance from the electrode surface) with time (b), the resulting current vs time response (c). [232]

Chronoamperometric measurements consist of applying repetitively a fixed potential at the working electrode and monitoring the current resulting from each pulse at fixed time intervals, which is directly proportional to the analyte concentration.

In bioanalysis this technique is often employed for studying the kinetics of enzymatic reaction. For this reason chronoamprometry was chosen for the monitoring of the enzymatic reaction in the microfluidic genosensor developed in this work (see paragraph 2.3.2). A potential of 250 mV (vs Ag/AgCl) was applied in order to oxidise the enzymatic product. The resulting current was plotted as a function of time and the slope of the linear portion of the plot used as analytical data.

2.3 Biosensors preparation and transduction systems

2.3.1 Carbon nanotube-based electrochemical genosensor

2.3.1.1 CNT Thin Film Fabrication

Multi-walled carbon nanotube thin films were obtained (in collaboration with Prof. Santucci's group, University of l'Aquila, Italy) by chemical vapour deposition using acetylene and ammonia as precursor gases and nickel particles as

catalyst. Different substrates were used: commercially available SiO_2 (Figure 7a and 7b) and Si_3N_4 layers (100 and 150 nm thick, respectively) on silicon, as well as Al (100 nm) layer grown by sputtering onto a Si substrate (Figure 7c and 7d), with a thin native silicon dioxide layer. A thin (3 nm) film of Ni catalyst was deposited by high vacuum (10^{-6} Torr) thermal evaporation onto the substrate. Then the substrate was introduced in the CVD reactor. The CVD reactor was pumped down up to about 10^{-6} Torr, mainly to remove oxygen. Then, the pressure was raised up to about 3 Torr introducing ammonia (100 standard cubic centimetre for minute, sccm) and the substrate was heated to 500°C or 700°C for 20 minutes in ammonia environment, in order to induce the cluster formation of the catalyst layer and to remove the nickel oxide layer derived from the air exposure of the sample during the transfer from the evaporation system to the CVD reactor. Keeping the ammonia flux unchanged, acetylene was flowed (20 sccm) for 10 min thus enabling the CNT growth. Two different CNT growing temperatures, 500°C and 700°C, were used. In the case of MWCNT grown on SiO_2 and Si_3N_4 substrate a gold film was also deposited by thermal evaporation on one side of the film, for the realisation of the metallic contact.

All the samples were morphologically characterised (Figures 7b and 7d) by means of a scanning electron microscope (SEM) equipped with a field emission gun (LEO 1530, LEO Inst., Germany).

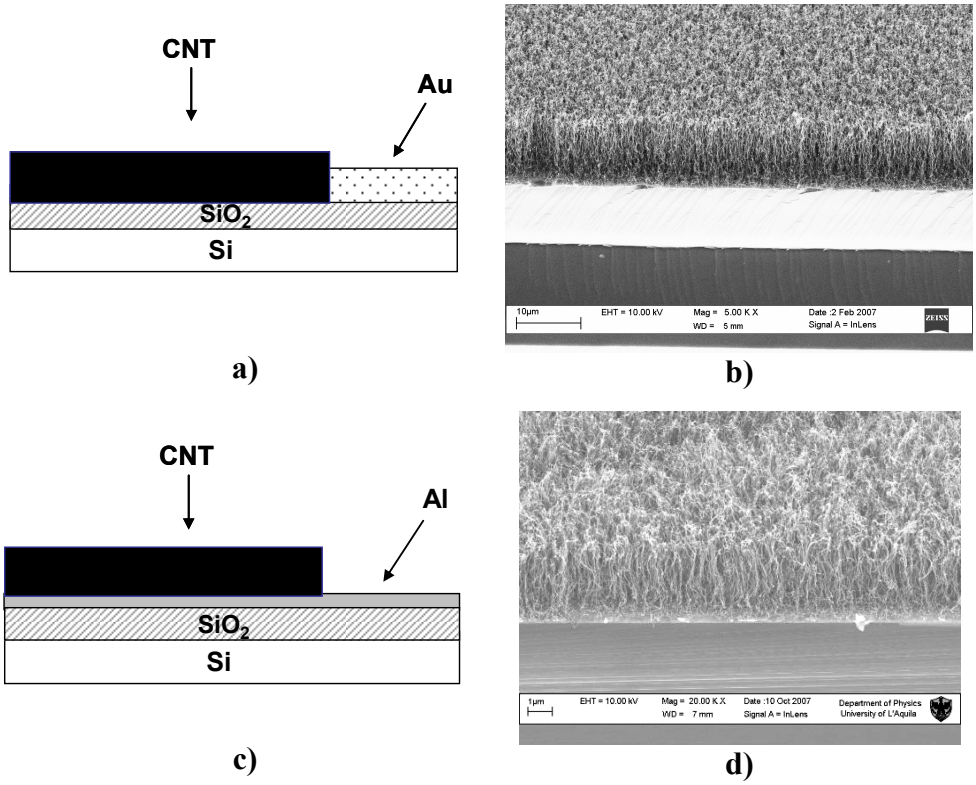

Figure 7. Aligned carbon nanotube thin films obtained by CVD. Scheme of the CNT-film grown on a SiO_2 substrate (a) and corresponding SEM image (b). Scheme of the CNT-film grown on a Al/SiO_2 substrate (c) and corresponding SEM image (d). CNT dimensions: Ø = 5-20 nm, length = 3-6 µm, density ≈ 1011 CNT/cm^2.

2.3.1.2 Disposable CNT sensors

Carbon screen printed electrodes modified with carbon nanotubes (SPE-CNT) were also employed. They were obtained by modifying in-house produced disposable cells with a dispersion of MWNTs according to the procedure reported in [71]. The dispersion was obtained by dispersing 5.0 mg of MWCNTs (NanoLab, Newton, USA, Ø = 30±10 nm, length = 1-5 µm) within 1.0 mL of 5.0 mg/mL PEI solution (prepared in 50:50 v/v ethanol/water) followed by sonication for 15 min. An aliquot of 10 µL was dropped on the working electrode and allowed to dry for 90 min. Each cell consisted of a CNT-modified carbon working electrode, a carbon counter electrode and a silver pseudo-reference

electrode. Materials and procedures to screen-print the transducers are described elsewhere [234].

2.3.1.3 Electrochemical apparatus

Electrochemical experiments were performed with an AUTOLAB PGSTAT 30(2) digital potentiostat/galvanostat (figure 8a) with a GPES 4.8 software package (EcoChemie, Utrecht, Netherlands). A Plexiglass three electrode well cell (made in our laboratory) with the carbon nanotube thin film as working electrode (Ø = 2 mm), an Ag/AgCl wire as reference electrode and a platinum coil as counter electrode was employed (figure 8b). All the potentials were referred to the Ag/AgCl reference electrode. All the experiments were carried out at room temperature (25°C).

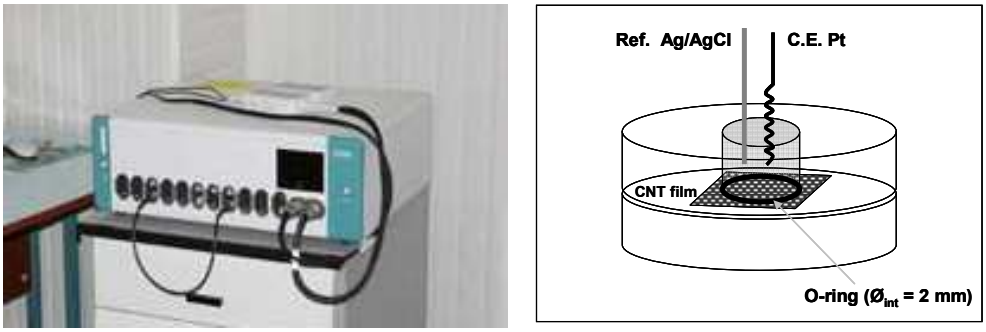

Figure 8. Electrochemical apparatus. Autolab PGSTAT 30(2) digital potentiostat/galvanostat (a). Diagram of the plexiglass well cell used for electrochemical experiments using CNT thin films. An o-ring delimited a circular working electrode surface (Ø = 2mm) on the CNT film (b).

2.3.1.4 Functionalisation of the sensor surface

Each cycle of measurement consisted of three steps: capture probe immobilisation, hybridisation and electrochemical investigation of the surface. After biosensor regeneration a new cycle was performed. Synthetic guanine-containing as well as inosine-modified oligonucleotides, having a six-carbon

spacer arm and a terminal amino group, were covalently immobilised onto CNTs, according to the procedure illustrated in Figure 9. Carboxylic groups were introduced onto the carbon nanotubes by oxidation with HNO_3 10%. Carboxylic goups were activated by interaction with 30 µL of an aqueous solution containing 5 mmol/L EDAC and 8 mmol/L NHS for 1 h [235]. Finally, 30 µL of capture-probe 10 µM in phosphate buffer 0.5 M pH 7.0, were deposited overnight (~16 h). The immobilisation proceeded through the formation of amide bonds between the carboxylic moiety at the electrode surface and the amino-terminal end of the oligonucleotides. The residual reactive groups were blocked by depositing 30 µL of ethanolamine 100 mM for 20'. Then the biosensor was rinsed 3 times with 100 µL of phosphate buffer.

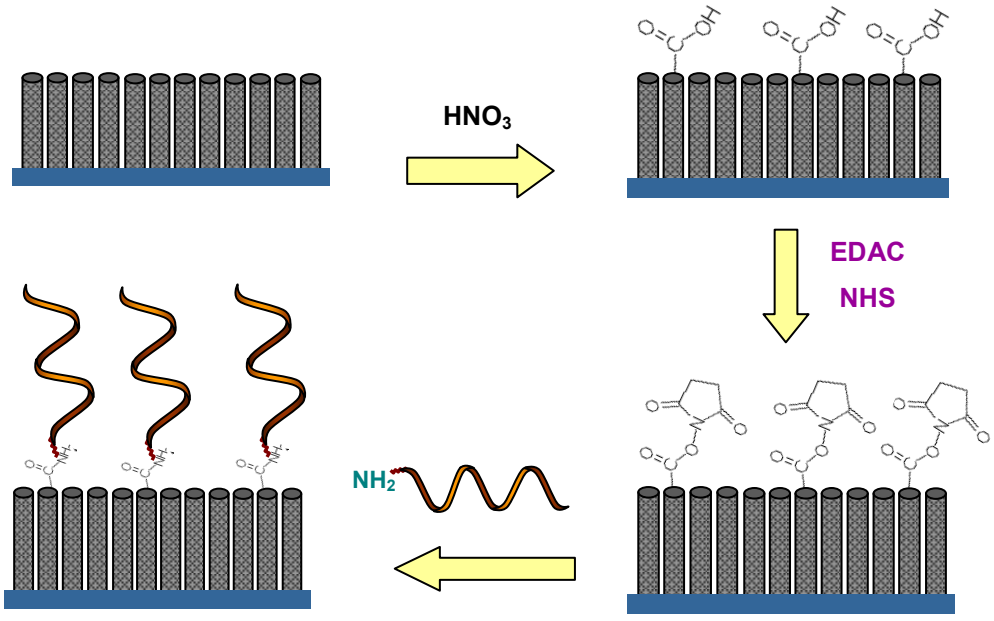

Figure 9. Scheme of capture probe immobilisation procedure on CNT thin films.

2.3.1.5 Label-free hybridisation assay

Figure 10a shows the procedure for label-free detection of the hybridisation event. The inosine-substituted immobilised probe was hybridised for 30 min with 30 µL of a convenient amount of guanine containing oligonucleotide target in phosphate buffer 0.5 M pH 7.0. An analogous solution of non-complementary sequence was

employed as control of the non-specific signal. After 20 minutes the sensor was washed 3 times with 100 µL of acetate buffer 0.25 M, pH 4.7 (containing 10 mM of KCl). The guanine electrochemical oxidation was performed by DPV, after placing the sensor in the cell and closing the circuit with 50 µL of acetate buffer (modulation time, 0.05 s; interval time, 0.15 s; step potential, 5mV; modulation amplitude, 70 mV; potential scan from 0.70 V to 1.05 V).
Finally the genosensor was regenerated with 50 µL of a denaturant solution containing urea 5 M and SDS 0.05%, for 5 min.

2.3.1.6 Enzyme-linked hybridisation assay

The hybridisation experiments were carried out using a biotinylated target, following the procedure illustrated in Figure 10b. Control experiments were carried out using non-complementary biotinylated sequences to evaluate the non-specific signal. The probe-modified sensor was incubated for 30 min with 30 µL of oligonucleotide target solution, diluted to the desired concentration with phosphate buffer 0.5 M pH 7.0. After hybridisation, the sensor was washed three times with 100 µL of DEA buffer (0.1 M diethanolamine, 1 mM $MgCl_2$, 0.1 M KCl; pH 9.6) and incubated with 30 µl of a solution containing 0.75 U/ml of the streptavidin-alkaline phosphatase conjugate and 10 mg/ml of BSA (blocking agent) in DEA buffer. After 20 minutes the surface was washed 3 times with 100 µL of DEA buffer. The electrochemical measurements were performed by placing the sensor in the cell and closing the circuit with 50 µL of DEA buffer containing 1 mg/mL of enzymatic substrate, p-amino phenyl phosphate. After 10 min, the electrochemical signal of the enzymatically produced p-amino phenol was measured by DPV (modulation time, 0.05 s; interval time, 0.15 s; step potential, 5mV; modulation amplitude, 70 mV; potential scan from -0.20 V to 0.30V). Regeneration of the genosensor surface was performed by washing the surface with distilled water to remove the enzymatic product and by treating with 50 µL of a denaturant solution containing urea 5M and SDS 0.05%, for 5 min.

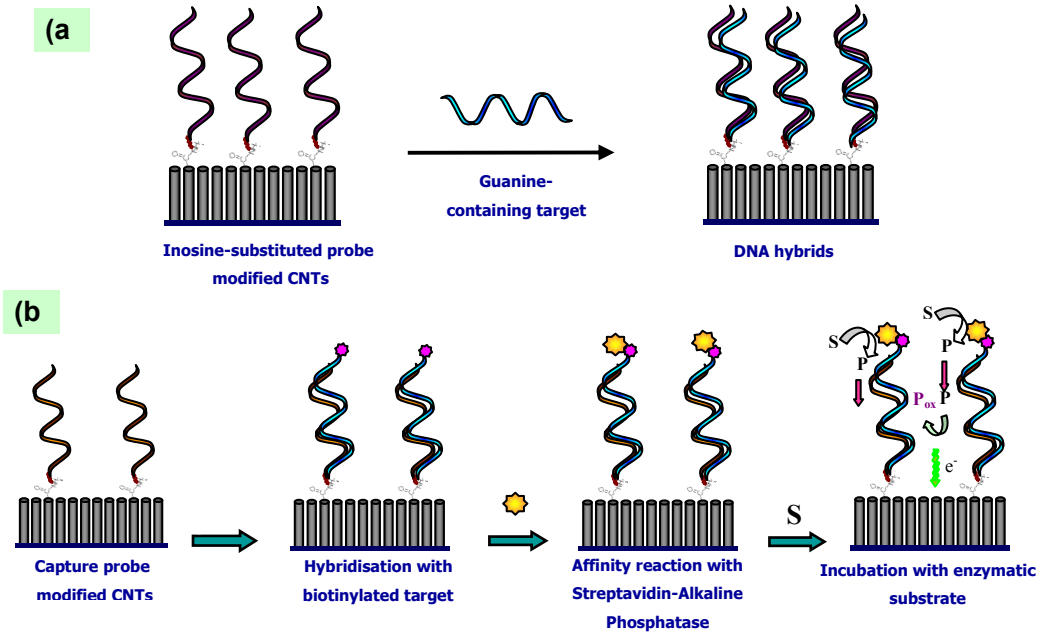

Figure 10. Hybridisation assays performed using CNT thin films as working electrode: label-free (a) and enzyme-linked format (b).

2.3.2 Microfluidc-based genosensor coupled to magnetic beads

2.3.2.1 Microfluidic platform

The microfluidic system employed in this work had been previously developed by by DiagnoSwiss S.A. for automated ELISA tests and we implemented and optimised it for DNA detection using magnetic beads. The system combines a disposable cartridge (ImmuChip^{TM}), with a computer controlled instrument (ImmuSpeed^{TM}) which manages the fluidics and the electrochemical detection. A picture and a scheme of the instrumentation are reported in Figures 11a and 11b.

The ImmuChip^{TM} consists of eight parallel microchannels etched in a polyimide substrate (Figure 11c). The fabrication process of the microchannel systems has been described elsewhere [219, 220, 221]. Each microchannel contains a housing with a sample deposition reservoir (well) etched in a polyimide body with inlet/outlet in contact with microelectrode tracks. The microchannels have a

length of 1 cm, a diameter of 40 µm and a total volume of 65 nL. The upper part of each channel contains an array of 48 gold working microelectrodes. A counter electrode and an Ag/AgCl pseudo-reference electrode are placed at the bottom of the well, near the channel entrance.

ImmuSpeed™ is composed of an interface into which the disposable cartridge can be plugged, a temperature controller, a multichannel pumping device and valves as well as a multiplexed electrochemical detector for sequential detection of reactions occurring in each of the eight channels (Figure 11b). Custom software (ImmuSoft™) integrates the fluidic and electrochemical detection systems. Moreover, it allowed independent protocols for the different channels to be developed. Sample and reagent solutions are thus aspirated from the inlet reservoir through the reaction channel to waste. The solution flow can be directed in both directions, allowing the construction of protocols with back flow. The sample can be introduced into the channels by using different methods; parameters that can be varied are the time during which the liquid should flow through the channels at a pre-set flow rate or remain static, as well as the turnover at which this mode should be repeated (loading cycles). At the end of the procedure, chronoamperometric detection parameters were introduced. These included the value of the potential to apply, the duration of each measurement and, in order to follow the kinetics of the enzyme reaction, the time interval between two chronoamperometric measurements as well as the number of such measurements cycles. In this particular application, the chip was integrated with a dedicated magnet to capture the beads into the channel, as described in Figure 11d. Eight cylindrical magnets, supported in a bar, were inserted between the chip and instrument interface in order to capture the beads flowing through the channel at the electrode position. All experiments were carried out at 37°C.

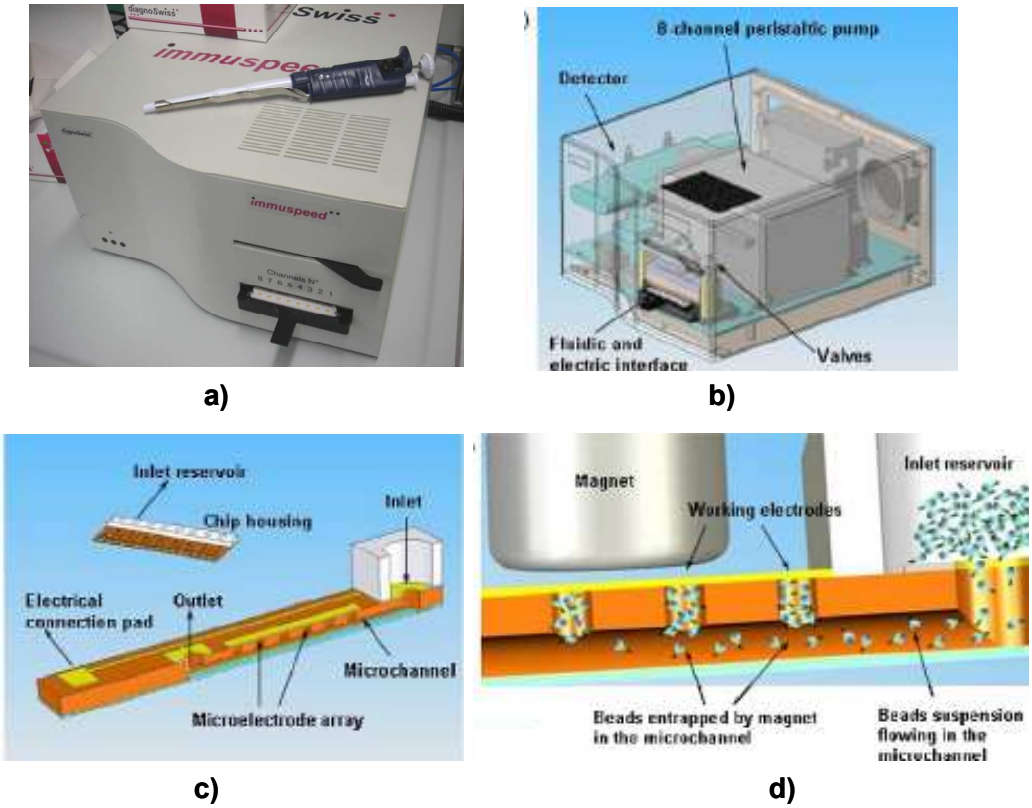

Figure 11. Picture of the microfluidic-based Immuspeed™ platform (a) and corresponding technical drawing (b). Diagram of the ImmuChip™ (c). Technical drawing of a microchannel cross-section with flowing magnetic beads being captured by a magnet (d). Technical drawings were kindly provided by DiagnoSwiss S.A. (http://www.diagnoswiss.com).

2.3.2.2 DNA modification of streptavidin-coated paramagnetic beads

The modification of the beads with biotinylated capture probe was carried out using aliquots of 0.75 mL, containing 1 mg/mL of beads. The beads were washed three times with 600 µL of phosphate buffer 0.5M, pH 7.0 (using a magnetic particle concentrator, MagneSphere Magnetic Separation Stand, Promega, Milan, Italy) and re-suspended in 500 µL of buffer containing 1.0 nmol of capture probe/mg of beads. After incubation for 30 min, under continuous mixing, the beads were washed three times with phosphate buffer. Finally, the modified beads were incubated for 15 minutes with 500 µL of a 500µM solution of biotin in phosphate buffer, to block the remaining streptavidin active sites on the probe-

functionalised surface, in order to prevent the undesired binding of other biotinylated oligonucleotides. After the treatment beads were washed three times with phosphate buffer and re-suspended to 1mg/ml in buffer. The modified beads can be stored at 4°C until use.

2.3.2.3 Enzyme-linked hybridisation assay

The enzyme-linked hybridisation procedure, illustrated in Figure 12, was developed for the analysis of PCR amplified fragments of Cor a 1.04, the major hazelnut allergen. Hybridisation event was carried out in a sandwich-like format using PCR amplicons diluted with a solution 0.15 µM of a biotinylated signalling probe in phosphate buffer. The double-stranded DNA was thermally denaturated by using a boiling water bath (5 min at 100°C); amplicon strand re-annealing was retarded by cooling the sample in an ice-water bath for 1 min. Both the PCR blank and non-complementary PCR products were used as negative controls.

A first approach consisted of performing hybridisation and enzyme labelling before introducing beads in the micro-fluidic system. In this case, for every assay 20 µl of probe-modified beads were employed. Using the magnetic particle concentrator, the buffer was removed carefully and then the beads were incubated with 50 µL of the hybridisation solution for 15 minutes. After hybridisation, the beads were washed three times with 100 µL of DEA buffer, in order to remove non-specifically adsorbed sequences. Beads were subsequently incubated with 50 µl of a solution containing 0.75 U/ml of the streptavidin-alkaline phosphatase conjugate and 10 mg/ml of BSA (blocking agent) in DEA buffer and, after 20 minutes, washed 3 times with 100 µL of DEA buffer. At this point beads were loaded in the fluidic system for incubation with the enzymatic substrate and electrochemical detection.

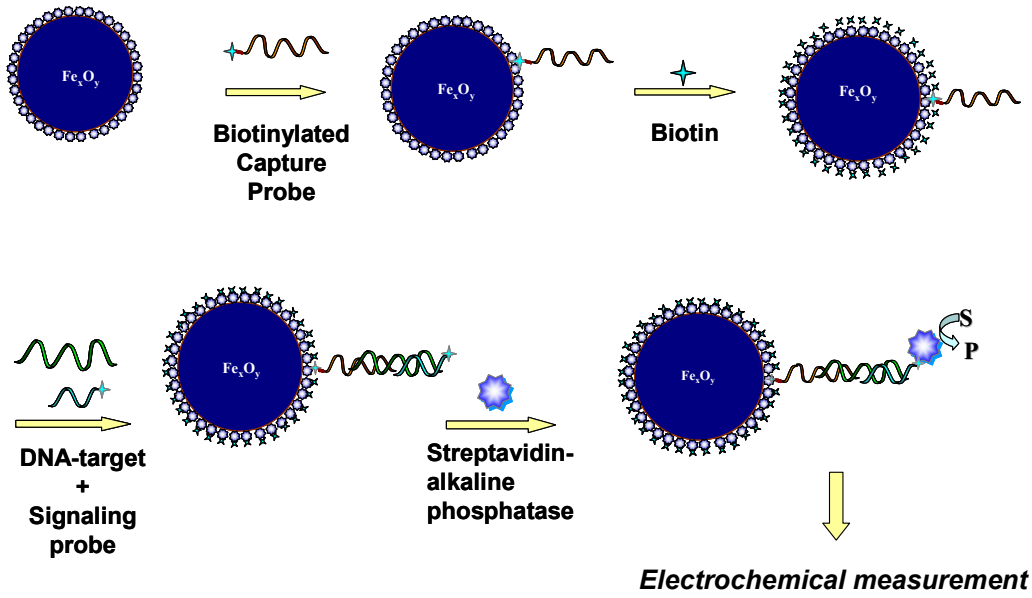

Figure 12. Scheme of the enzyme-linked hybridisation assay performed on paramagnetic beads.

A second approach, called "Total hybridisation assay" consisted of performing both the hybridisation and the incubation with the enzyme in flow. A volume of 20 µL of probe-modified bead suspension was added in each inlet reservoir of the ImmuChip™. The solutions were introduced in the microchannels by applying the optimised loading cycles reported in Table 3. During the loading cycles, a suitable magnet was used in order to allow the blocking of the beads within each microchannel.

2.3.2.4 Electrochemical detection: drop-on system

Preliminary experiments for the optimisation of the hybridisation assay were carried out without using the microfluidic apparatus. For this purpose, in-house produced screen printed electrochemical cell were employed.

Total hybridisation assay

Bead Loading	2s at 2 µL/min flow-through, 3s of steady-state without flow. Total number of loading: 100 cycles.
Target + signalling probe loading	3s at 10 µL/min flow-through, 2s of steady-state without flow. Number of loading cycles: 24
Enzyme-conjugate loading	3s at 10 µL/min flow-through, 2s of steady-state without flow. Number of loading cycles: 24

Table 3. Total hybridisation assay working protocol.

Each cell consisted of a carbon working electrode, a carbon counter electrode and a silver pseudo-reference electrode. Materials and procedures to screen-print the transducers are described elsewhere [234].

Electrochemical measurement were performed by keeping cells horizontally and a magnet holding block was placed on the bottom part of the electrode, to better localise the beads onto the working surface. In the following sections, these disposable electrochemical sensors will be called a “drop-on system”.

After washing, the beads were re-suspended in 25 µL of DEA buffer. A 10 µl drop of enzyme-labelled bead suspension was deposited onto the working electrode surface, and the liquid was carefully removed with a pipette without touching the electrodes. Then, the planar electrochemical cell was covered with 50 µL of 10 mM p-aminophenyl phosphate in DEA buffer. After 5 min, the electrochemical signal of the enzymatically produced p-aminophenol was measured by DPV (modulation time 0.05 s; interval time 0.15 s; step potential 5 mV; modulation amplitude 70 mV; potential scan from 0 to +0.6 V). The DPV electrochemical measurements were performed using a µAutolab type II PGSTAT with a GPES 4.9 software package (Metrohm, Rome, Italy). All potentials were referred to the Ag/AgCl pseudo-reference electrode. All experiments were carried out at room temperature (25°C).

Upon scanning the potential, p-aminophenol was oxidised; the height of its oxidation peak was taken as the analytical signal. Reported results are the average of at least three measurements and the error bars correspond to the standard deviation.

2.3.2.5 Electrochemical detection: microfluidic-based platform

After washing, the beads were re-suspended in 135 µL. A volume of 20 µL of enzyme-labelled bead suspension was added in each inlet reservoir of the ImmuChip™. The solution was then introduced in the microchannels by applying the optimised loading cycles (2s at 2 µL/min flow-through, 3s of steady-state without flow. Total number of loading: 100 cycles); during the loading cycles, a suitable magnet was used in order to allow for the blocking of the beads within each microchannel. In case of "total hybridisation assay" this step had already been performed, before hybridisation.

Once all the suspensions were introduced and the beads captured, the substrate solution, p-aminophenyl phosphate (10 mM in DEA buffer), was added. The enzyme kinetics were monitored by chrono-amperometric measurements performed in a static mode, i.e. without flow. The eight channels were sequentially measured, each for 2 s, at a potential of +250 mV vs. Ag/AgCl, for a total acquisition time of 3 min; in this way many measuring cycles were recorded, and a plot of current as function of time was obtained for each channel. An example of enzyme kinetics acquisition data, obtained by adsorbing only alkaline phosphatase enzyme in the microchannels, is reported in Figure 13. The slope of the linear portion of the plot, which is a direct measure of the p-aminophenol concentration and hence of the enzyme concentration, was used as analytical data. The data elaboration was performed using the software incorporated in the DataFitX fitting tool (Oakdale Engineering, USA).

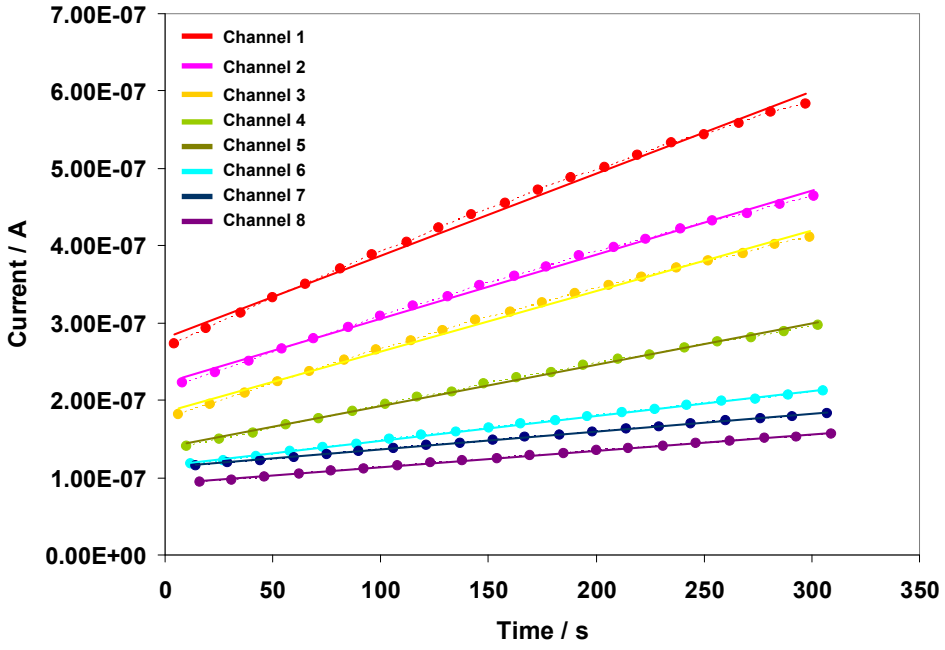

Figure 13. Example of chrono-amperometric detection of enzyme kinetics in a chip. The experiment was performed by adsorbing different amounts of alkaline phosphatase (from 1 to 5 10^{-4} U/mL, in channel from 1 to 8) on the walls of the microchannels and then introducing the enzyme substrate. Each symbol represents a single current acquisition value.

2.3.3 Catechol MIP-sensor based on one-dimensional polyaniline nanostructures

2.3.3.1 Monomer (NPEDMA) preparation

N-phenylethylenediamine methacrylamide (NPEDMA) monomer was prepared following a procedure reported by Lakshmi *et al.* [228]. N-phenylethylenediamine (3.0 g) was dissolved in methanol (60 mL) and cooled on ice before methacrylic anhydride (3.3 g) addition. The stirred mixture was held at 0°C for 3h before warming to room temperature. The solvent was removed using a rotary evaporator and the residue dispersed in diethyl ether (25 mL). The ether phase was washed with 0.1 M NaOH (4 times x 25 mL) and then water (1 time x 25 mL), dried over anhydrous magnesium sulphate and evaporated. The product was a light brown oil

which crystallised by standing in a refrigerator. The monomer was characterised by recording ^{1}H-NMR spectra using deuterated chloroform ($CDCl_3$) as solvent.

2.3.3.2 Template synthesis of PANI nanostructures

Polyaniline nanostructures were electrochemically synthesised using nanoporous alumina membranes as template, as shown in Figure 14. A gold layer was sputtered (180", 20 mA, in Ar atmosphere, using an Auto sputter coater, Agar Scientific, Stansted, UK) on one side of an alumina nanoporous membrane employed as template (Whatman Anopore membrane, Ø = 0.02µM), in order to improve electrical conductivity. The aniline monomer (NPEDMA) was electro-polymerised by cycling the Au sputtered membrane between -0.4 V and +1.0 V (vs. Ag/AgCl, scan rate 50 mV/s, 10 cycles) in a solution 2.4 mM NPEDMA (previously dissolved in methanol) in 50 mM $HClO_4$. In order to obtain an array of nanostructures, template was removed by dissolving the membrane in NaOH 3M for 30 minutes. For sensing application, in order to facilitate MIP grafting and placement in the cell, the membrane was kept as rigid framework.

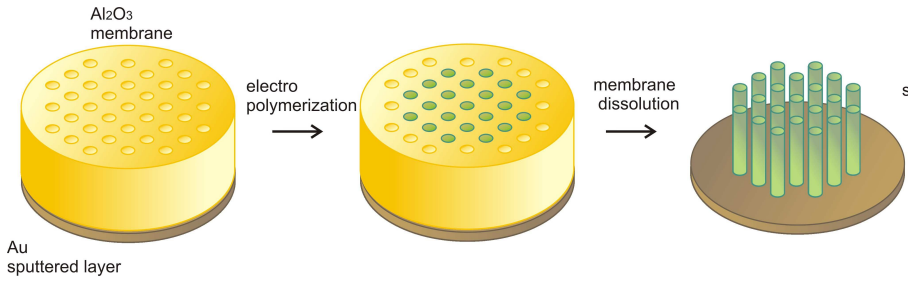

Figure 14. Scheme of the template synthesis of PANI nanostructure array.

2.3.3.3 Electrochemical apparatus

All electrochemical experiments were performed with a AUTOLAB PGSTAT 10 digital potentiostat/galvanostat with a GPES 4.8 software package (Eco Chemie, Utrecht, Netherland). A plexiglass three electrode well cell made in our

laboratory, and similar to the one shown in Figure 8b, was employed. It consisted of the sputtered membrane as working electrode (Ø= 8 mm), an Ag/AgCl reference electrode and a platinum wire as counter electrode.

All potentials were referred to the Ag/AgCl reference electrode. All the experiments were carried out at room temperature (25°C).

2.3.3.4 SEM characterisation

SEM analysis was carried out by field-emission LEO 1525 microscope, equipped with In-Lens detector (LEO Inst., Nano Technology Systems Division of Carl Zeiss SMT, Germany) for secondary-electron imaging, with a STEM detector (KE Development, UK) on the back of the sample holder to acquire transmitted electron beam and with a X-ray detector (Oxford Inst. Inca 250, UK) for EDX analysis.

2.3.3.5 Preparation of the MIP-sensor for catechol detection

The MIP composition had been developed by Piletsky *et al.* [236], as a Tyrosinase-mimicking polymer, imprinted with catechol. MIP was photochemically grafted over the polyaniline nanostructures, via N,N′-diethyldithiocarbamic acid benzyl ester (iniferter) activation of the methacrylamide groups of NPEDMA monomer, according to the following procedure.

Iniferter immobilisation: a solution of (0.0015g/10 mL acetonitrile) of diethyl dithiocarbamic acid benzyl ester, was prepared in a glass petri dish (Ø = 10 cm) and oxygen was removed from the solution by purging with argon for 10 minutes. After dipping the electro-polymerised membranes in the iniferter solution, the petri dish was covered with a flat glass plate, using some Parafilm to improve the

adhesion and sealing. Irradiation with a Philips UV lamp, mounted at 8 cm from the surface of the samples, for 20 minutes was used to photochemically attach the iniferter to the PANI nanostructures. The membrane was then washed with methanol and dried in Argon gas.

MIP/NIP grafting: 375µmol (62.3 mg) of urocanic acid ethyl ester, 62.5 µmol (6.9 mg) of catechol and 1 mmol of $CuCl_2$ (134.45 mg) were dissolved with 2.50 g DMF in a 30 mL thick walled tube glass followed by the addition of 1.20 g (6.06 mmol) of ethylene glycol dimethacrylate. The reaction mixture was well mixed and then sonicated for 10 minutes. The iniferter grafted electropolymerised membrane was dipped in the aforementioned reaction mixture in a glass petri dish. After the removal of the oxygen by purging with argon for 4 minutes, the petri dish was covered with a flat glass plate sealed with Parafilm. Irradiation with UV light for 30 minutes (same exposure set-up as above) was then used to graft MIP on the samples. Template was subsequently removed by washing 5-6 times membranes with EDTA 0.1M. Membranes were then rinsed with DMF and dried in air. Following the same procedure, NIP (non-imprinted polymer) was also prepared using the same recipe without the addition of template (catechol).

2.3.3.6 Catechol detection

Different concentrations of catechol were detected by cyclic voltammetry. Firstly 1 mL of $CuCl_2$ was added in the cell for 5 minutes. After washing with PBS, fresh solutions of catechol (in PBS, pH 7.4), were added to the electrochemical cell containing the Cu-loaded hybrid electrode. CVs were recorded by applying the following parameters: start potential -0.5 V, first vertex potential 0.9 V, second vertex potential 0.5 V, step potential 0.01 V, scan rate 0.05 V s^{-1}; Potential vs. Ag/AgCl. The height of the anodic peak was taken as analytical signal. Analogous interference substances were measured according to the same procedure.

Chapter 3

CARBON NANOTUBES FOR GENOSENSING

The first part of the research activity was devoted to the design and testing of aligned carbon nanotube thin films as candidate platforms for DNA immobilisation and for the development of a model electrochemical genosensor.
The films were prepared by chemical vapour deposition (CVD) using acetylene and ammonia as precursor gases and nickel particles as catalyst. A preliminary electrochemical characterisation was performed using cyclic voltammetry since, so far, these films have been used only for gas sensing. The surface was then covalently functionalised with a DNA oligonucleotide probe, complementary to the sequence of the most common inserts in GMOs: the Promoter 35S. The genosensor format involved the immobilisation of the probe onto the sensor surface, hybridisation with the target-sequence and electrochemical detection of the duplex formation. For the detection of the hybridisation event, both label-free and enzyme-labelled methods were investigated.

3.1 Results

3.1.1 Preliminary experiments using disposable carbon electrodes modified with CNTs

Disposable CNT-based sensors were often employed for preliminary screenings and characterisations in order to limit the waste of CNT films, which required a more refined technology to be produced. For this reason a good model surface

was found to be disposable electrodes modified with CNTs (SPE-CNT), realised in house, according to the procedure reported in paragraph 2.3.1.2.

The first investigation of CNT performance was carried out by comparing the amperometric response towards H_2O_2 of SPE-CNT and unmodified SPEs. A calibration plot for successive additions of 100mM H_2O_2 is reported in Figure 15. A dramatic enhancement of the sensitivity was achieved in the presence of the nanotubes (black curve), while signal variation after consecutive additions of H_2O_2 was negligibile when bare SPEs were used. (red curve).

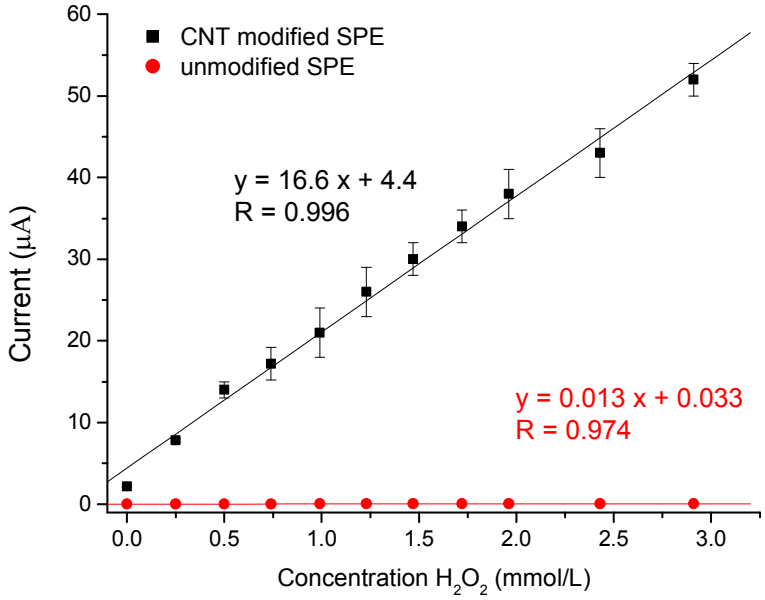

Figure 15. Calibration curve for successive addition of 1mM of H_2O_2 obtained using CNT modified SPE (black line) and bare SPE (red line). Each point is the mean of three amperometric measurement. Applied potential: +700 mV (vs. Ag pseudoreference). Error bars represent the standard deviation of three replicates (n = 3).

This result was highly encouraging and clearly established the improvement CNTs could potentially bring to biosensing. CNT-modified SPEs were also employed in further experiments as model nanotube-based platforms for functionalisation studies.

3.1.2 CNT film characterisation

3.1.2.1 Evaluation of CNT adhesion on the growing substrate

Different patterns of CNT films (Table 5), grown on different substrates (SiO_2, Si_3N_4, Al) and at different temperatures (500°C, 700°C) were tested.
All the CNT films used for this purpose were firstly characterised by cyclic voltammetric scans in buffer solution.

Sensor	**Growth temperature**
CNT/Ni/SiO_2	500°
CNT/Ni/SiO_2	700°
CNT/Ni/Si_3N_4	500°
CNT/Ni/Si_3N_4	700°
CNT/Ni/Al/SiO_2	500°
CNT/Ni/Al/SiO_2	700°

Table 5. List of the sensors tested for genosensor development.

The first kind of sensor was obtained on SiO_2 substrates (CNT/Ni/SiO_2) by firstly evaporating gold contacts, then depositing the catalyst particles (Figure 7a); finally the CNTs were grown. These sensors showed remarkable problems of adhesion once in solution and CNTs were released after few potential scans. Besides being clearly visible by an optical inspection, this phenomenon was also demonstrated by comparing CV scans recorded before and after CNT release. As reported in Figure 16, a decrease of the capacitive current was observed. It is obvious that the mechanical resistance of the surface and, in particular, the adhesion of CNTs to the growth substrate is crucial. The release of nanotubes during the assay changes the surface properties with consequent loss of reliability of the measurements. A little improvement in CNT adhesion was achieved, for both the temperatures applied, by changing the growth substrate by substituting

SiO_2 with Si_3N_4 (CNT/Ni/Si_3N_4), as shown in Figure 16 b. However, CNTs were also released in this case with increasing number of CV scans.

The introduction of an Aluminum layer on the SiO_2 substrate (CNT/Ni/Al/SiO_2, Figure 7c), which serves as growth substrate as well as electrical contact, facilitated improved film stability. As reported in the literature [84, 237], carbon nanotubes synthesised on metallic substrates have been demonstrated to exhibit excellent properties as electrode materials.

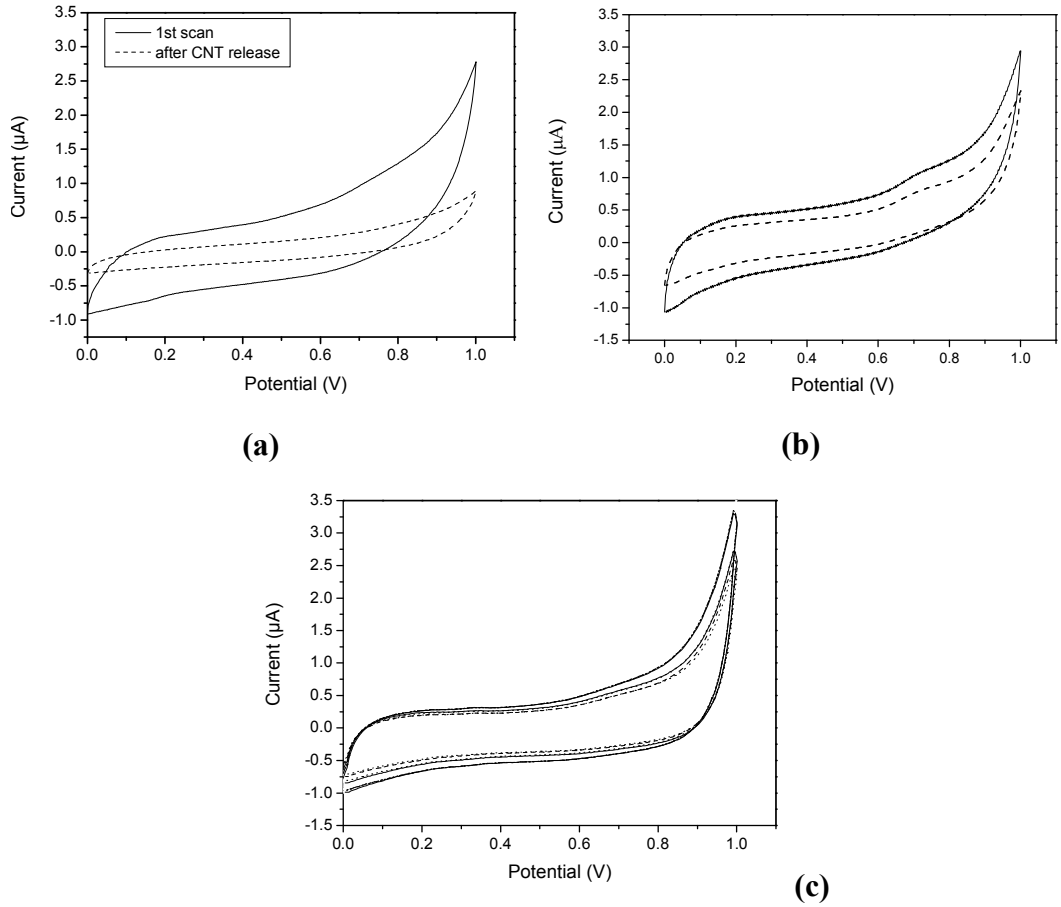

Figure 16. Evaluation of CNT adhesion during electrochemical measurements in solution (CV in acetate buffer 0.25 M with KCl 10 mM). **a)** CNT/Ni/SiO_2 (700°C): before (solid line) and after (dashed line) CNT release. **b)** CNT/Ni/Si_3N_4 (700°C): before (solid line) and after (dashed line) CNT release. **c)** CNT/Ni/Al/SiO_2 (700°C): six consecutive scans. (CV parameters: start potential 0 V, first vertex potential 1.0 V, second vertex potential 0 V, step potential 0.0244 v, scan rate 0.05 V s^{-1}).

Moreover, the stability of the film guarantees the possibility of regeneration of the immobilised probe, in order to perform different analyses on the same surface. Thus, mechanical stability was also controlled by performing consecutive label-free hybridisation experiments (procedure reported in paragraph 2.3.1.5).

A strategy for regeneration of the genosensor was developed in order to perform different analyses using the same functionalised surface. In particular, the immobilised probe was regenerated by denaturing the hybrid with an aqueous solution containing urea 5 M and SDS 0.05% and re-hybridising with a new target sequence.

Figure 17a shows the results obtained using Si_3N_4 as substrates. The guanine signal recorded after the second hybridisation (with an equal amount of target) was negligible, due the detachment of nanotubes during the denaturation and following washes. This behaviour was similar for both the growth temperatures (700°C and 500°C). In case of CNT/Ni/Al/SiO_2, CNTs grown at 500°C were weakly adhered at the surface so they were released in solution just after the immobilisation step, but a high stability was achieved using films grown at 700°C. Figure 17b shows that the signal obtained after the second hybridisation is similar to the first one and that the sensor maintained a good response even for the third measurement. Thus CNT/Ni/Al/SiO_2 was used for all further experiments.

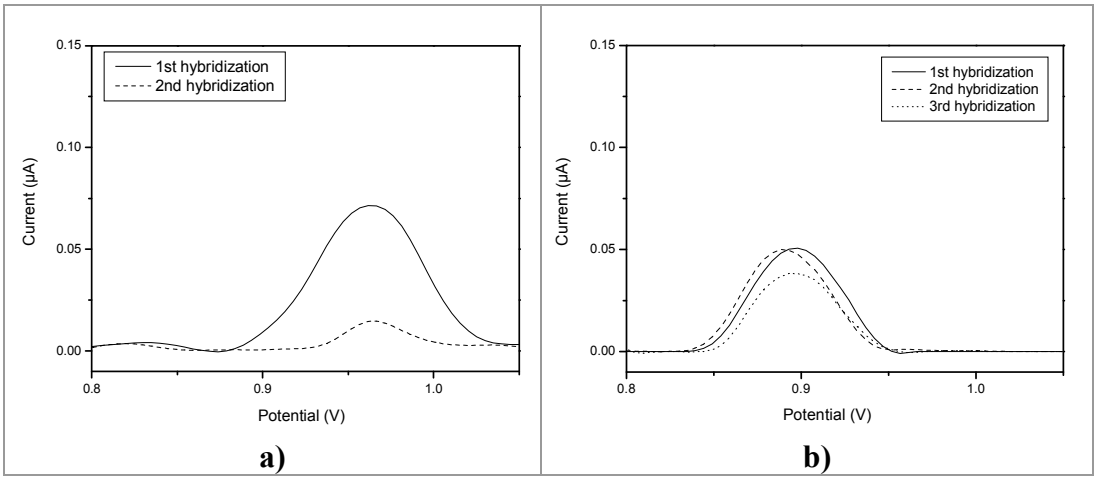

Figure 17. Screening of CNT adhesion during a label-free hybridisation assay. **a)** Guanine oxidation signal after the hybridisation with DNA-target 1μM recorded with a CNT/Ni/Si_3N_4 (700°C) sensor. The first signal obtained (solid line) and second signal recorded after CNT release (dashed line). **b)** Three consecutive cycles of hybridisation/denaturation performed using a CNT/Ni/Al/SiO_2 (700°C) sensor. (DPV parameters: modulation time, 0.05 s; interval time, 0.15 s; step potential, 5mV; modulation amplitude, 70 mV).

3.1.2.2 Electrochemical characterisation of the surface

In order to investigate the electron-transfer properties of these sensors in solution, CV experiments were performed. For this purpose two different redox mediators such as potassium ferricyanide and hydroquinone were used. Signals obtained using CNT-films were compared with the ones obtained using graphite screen-printed electrodes, with the same geometric area, and an amorphous carbon sensor obtained by processing the substrate in the CVD reactor, in the absence of one of the precursor gases. As known, for a Nernstian wave the ratio of peak currents (i_{pa}/i_{pc}) is 1, regardless of scan rate, and the separation of peak potential (ΔE_p) is always close to 59/n mV (where n is the number of exchanged electrons) [232]. An increase in the reversibility was observed at CNT-film surfaces for both the mediators tested, thus demonstrating that the presence of nanostructures enhances electron transfer at the electrode-solution interface.

Results obtained using potassium ferricyanide as redox mediator are reported in Figure 18a. In this case the improvement of i_{pa}/i_{pc} and ΔE_p were less remarkable (i_{pa}/i_{pc} = 1.23 for the amorphous carbon surface, 1.18 for graphite SPE, 1.08 for the CNT-film; ΔE_p = 307 mV for the amorphous carbon surface, 264 mV for graphite SPE, 188 mV for the CNT-film).

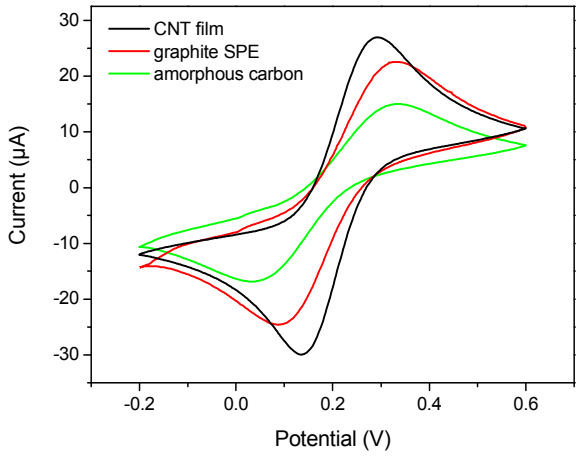

(a)

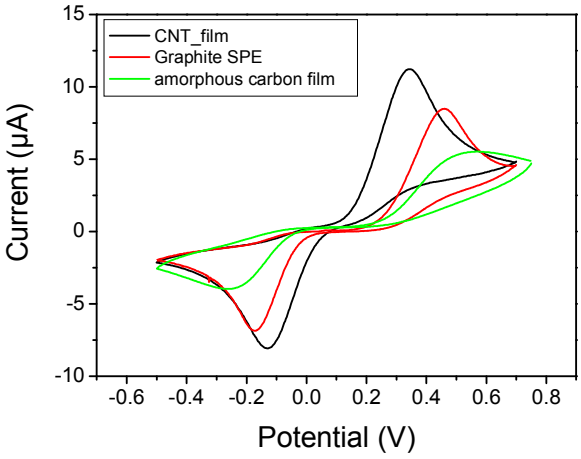

(b)

Figure 18. Electrochemical charecterisation. **a)** CV of 5 mM $K_3[Fe(CN)_6]$ in KCl 1 M (start potential 0.6 V, first vertex potential -0.2 V, second vertex potential 0.6 V, step potential 0.0244 v, scan rate 0.05 V s^{-1}). **(b)** CV of 1 mM hydroquinone in acetate buffer 0.25 M with KCl 10 mM (CV parameters: start potential 0.7 V, first vertex potential -0.5 V, second vertex potential 0.7 V, step potential 0.0244 v, scan rate 0.05 V s^{-1}). Signals obtained using CNT-films (black line), carbon screen-printed electrodes (red line) and sensors processed in the CVD reactor, in the absence of one of the precursor gases, thus obtaining only amorphous carbon on the surface (green line).

The increase in reversibility was more pronounced in the case of hydroquinone (Figure 18b). The values obtained show an improvement of the ratio of peak currents and a significant decrease of the separation of peak potential of about 100 mV with respect to carbon electrode and about 400 mV with respect to the amorphous carbon surface (i_{pa}/i_{pc} = 1.47 for the amorphous carbon surface, 1.08 for graphite SPE, 1.02 for the CNT-film; ΔE_p = 869 mV for the amorphous carbon surface, 576 mV for graphite SPE, 467 mV for the CNT-film).

3.1.3 Development of the genosensor

3.1.3.1 Optimisation of the immobilisation conditions

As the electrochemical characterisation demonstrated highly promising electrical properties, CNT-films were then investigated as platforms for DNA immobilisation and electrochemical transduction. Firstly, the oligonucleotide immobilisation conditions were studied in depth. In fact, control of the surface chemistry and coverage is essential for assuring high reactivity, orientation, accessibility and stability of the surface-confined probe as well as for minimising non-specific adsorption events [5]. Two properties of CNT-films make them particularly suitable to serve these purposes: the good alignment of nanostructures and the high reactivity of their fullerene-like tips, which allow an easy end-modification of the nanotubes with functional groups (e.g. –COOH, -OH, -C=O) [238].

A preliminary screening of the possible oxidation methods was performed using SPE-CNTs as working electrode surface, assembled in the three electrode well cell employed for CNT-films. Three different approaches were investigated: a strong oxidation using $K_2Cr_2O_7$ 2.5%, HNO_3 10% and applying a potential of 1.5V (vs Ag/AgCl) for 15” [234], an electrochemical oxidation (1.6 V vs Ag/AgCl for 120”) in acetate buffer solution (0.25 M), and a milder treatment with HNO_3 10% for 60”. Moreover, two strategies of immobilisation of the

amine-modified probe were investigated: direct and through the classical method of diimide activated amidation using EDAC and NHS. All these possibilities were compared by immobilising an inosine modified probe and evaluating current values of inosine oxidation peak obtained by SWV.

Results are reported in reported in Figures 19 and 20. In all of the three cases, covalent functionalisation though carbodiimide activation gave higher peak currents, thus demonstrating a more efficient immobilisation of the probe. Oxidation with $K_2Cr_2O_7$ seems to make the immobilisation highly irreproducible, as confirmed also by the noisy base line reported in Figure 20a. Electrochemical and HNO_3 oxidation gave similar results in terms of inosine peak intensity. However the second one was chosen for further experiments with CNT-films because the milder conditions could allow a longer stability of sensors, considering the problems of adhesion illustrated in the previous paragraph.

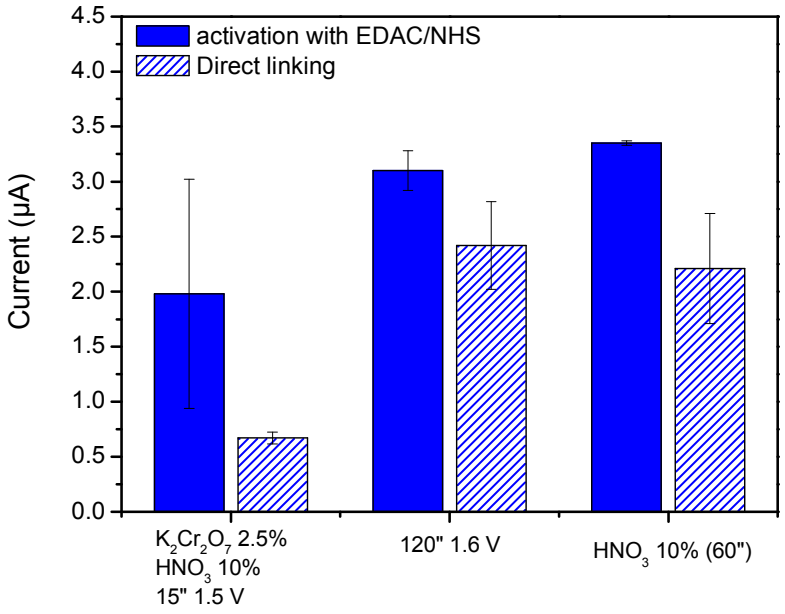

Figure 19. Investigation of oxidation and immobilisation methods. CNT-SPE electrodes were oxidised and inosine-modified probe (5µM) was immobilised, according to the procedure reported in the text. SWV scan of the immobilised probe was perfomed in 50µL of acetate buffer 0.25 M + KCl 10mM. (frequency 50 Hz, step potential 15 mV, amplitude 40 mV, potential scan 0.2V-1.6V) and Inosine oxidation peak (Pot 1.4 V vs Ag/AgCl) taken as analytical data. Error bars represent the standard deviation of three replicates (n = 3).

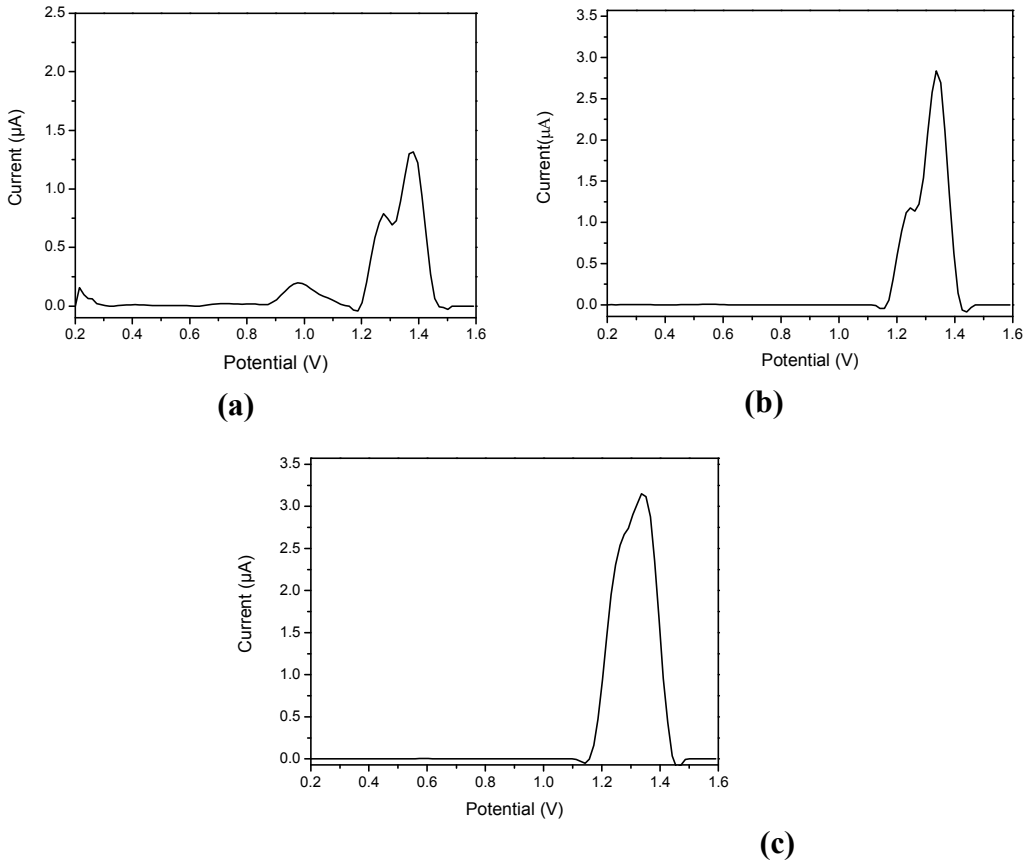

Figure 20. SWV scans of covalently immobilised inosine based probe (5 μM) using CNT-SPE electrodes (frequency 50 Hz, step potential 15 mV, amplitude 40 mV, potential scan 0.2 V - 1.6 V). CNTs had been oxidised with $K_2Cr_2O_7$ 2.5% HNO_3 10% at 1.5 V (vs Ag/AgCl) for 15" **(a)**, at 1.6 V vs Ag/AgCl for 120" in acetate buffer solution (0.25 M) **(b)**, and with HNO_3 10% for 60" **(c)**. Measurements were performed in 50μL of acetate buffer 0.25 M + KCl 10 mM.

Thus in further experiments amino-linked DNA-probe was covalently immobilised by the classical method of diimide activated amidation after introducing carboxylic groups on the nanotube ends by oxidation with HNO_3 10%.

A SWV scan of a guanine containing immobilised probe is reported in Figure 21 (solid line) where oxidation peaks of guanine (E_{peak} = 0.91 V vs Ag/AgCl) and adenine (E_{peak} = 1.28 V vs Ag/AgCl) can be observed. The dashed line represents the DPV scan obtained after applying the same immobilisation protocol for the functionalisation of an amorphous carbon sensor. The absence of any oxidation

peak of the purine bases demonstrates that no chemisorption or physisorption event occurs in the absence of nanostructures or at the underlying growing aluminum substrate.

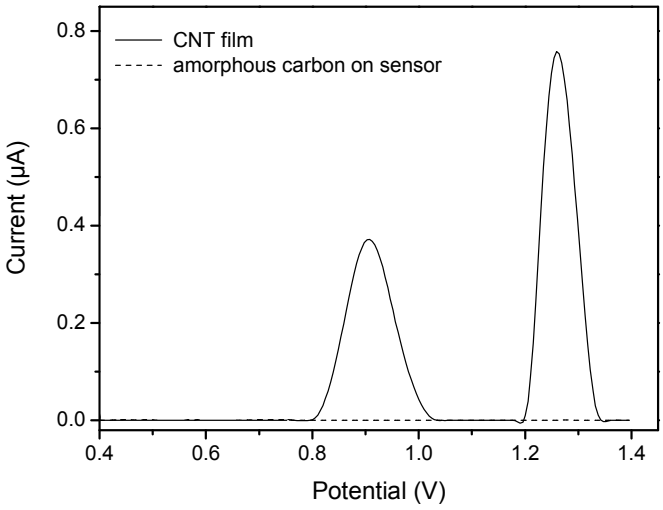

Figure 21. SWV measurements in acetate buffer 0.25 M + KCl 10 mM of the 5 µM DNA-probe immobilised on a CNT-film (solid line) and on an amorphous carbon sensor (dashed line). Measurements were performed in 50µL of acetate buffer 0.25 M + KCl 10 mM. (SWV parameters: frequency 50 Hz, step potential 15 mV, amplitude 40 mV, potential scan 0.4 V - 1.4 V)

Finally, the influence of the probe concentration on the hybridisation reaction was investigated. Electrode surfaces with lower probe densities show, a limited number of biorecognition sites, whereas higher surface densities can cause steric and electrostatic interference between packed probes and the incoming target DNA fragment [38]. The optimal surface coverage was experimentally assessed by performing label-free hybridisation experiments varying the capture probe concentration in a range between 5 and 20µM. A different sensor for each concentration was employed and three cycles of hybridisation/denaturation were performed. The means of guanine oxidation peak intensities are reported in Figure 22. The higher hybridisation yield was obtained using a 10 µM solution of amino-linked probe (Guanine oxidation peak height vs. Ag/AgCl: i_p = 247±18 nA for target 1µM, i_p = 51.4±11 nA for a 1µM non complementary sequence, specific vs. non specific ratio ~1:5), thus this concentration was chosen for further measurements.

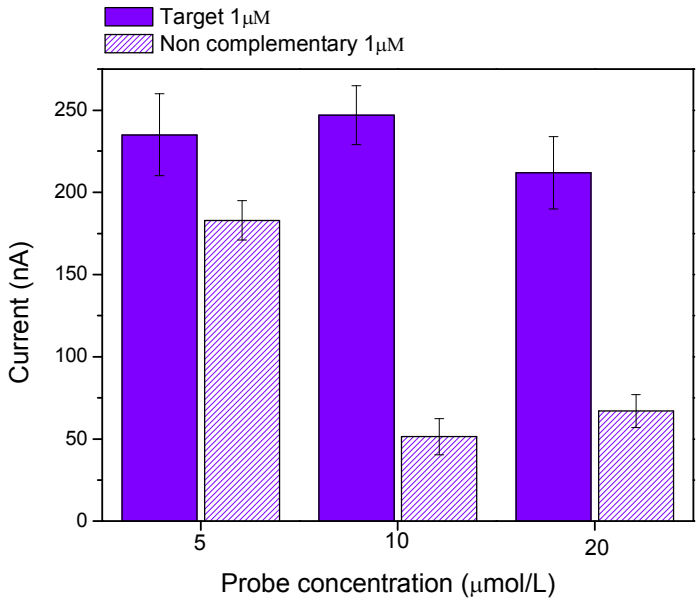

Figure 22. Optimisation of probe concentration. Each value is the mean of three values of guanine oxidation peaks obtained after the hybridisation with DNA target 10 μM or non complementary oligonucleotide 10 μM. Measurements were performed in 50μL of acetate buffer 0.25 M + KCl 10 mM. Error bars represent the standard deviation of three replicates (n = 3). (DPV parameters: modulation time, 0.05 s; interval time, 0.15 s; step potential, 5mV; modulation amplitude, 70 mV).

3.1.3.2 Label-free assay

Two different approaches were investigated for the electrochemical detection of the hybridisation reaction. The first, a label free assay, was based on the intrinsic electrochemical activity of the guanine moiety. The format involved the immobilisation of an inosine-modified (guanine-free) probe onto the sensor. The inosine moiety preferentially formed base-pair with the cytosine residue, but its oxidation signal is well separated from that of guanine (ΔE_p ~ 400 mV). After hybridisation, duplex formation is indicated by the oxidation signal of the guanine bases, present only in the target sequence. The performances of the genosensor thus obtained were investigated by testing different amounts of DNA-target. A CNT-film sensor was modified with the inosine probe according to the optimised conditions and then subsequent cycles of hybridisation/denaturation were

performed, increasing target concentration. As reported in Figure 23, guanine oxidation peaks recorded in the presence of different DNA-target, in a concentration range between 0 and 10µM, exhibited a good directly proportional relationship between concentration and electrochemical response (from the linear fit of displayed data: Y = 1.01 X + 0.74, R = 0.99). The non-specific signal, obtained using a non-complementary sequence (10µM), resulted more than three times lower than the lowest investigated concentration, thus confirming the selectivity of the genosensor.

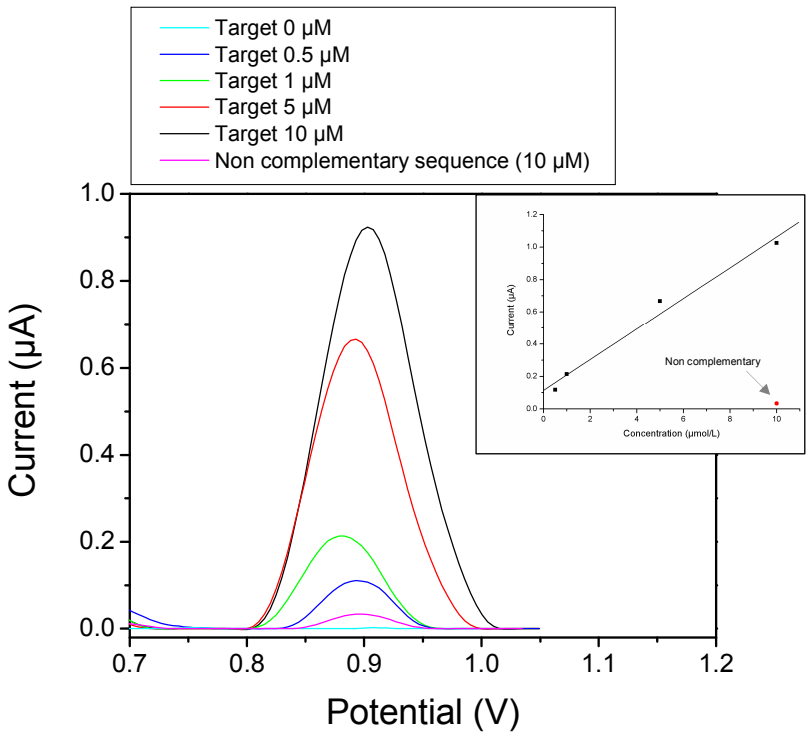

Figure 23. Guanine oxidation peaks obtained after the hybridisation with DNA target (concentration range, 0-10 µM) and non-complementary oligonucleotide (10 µM). Measurements were performed in 50 µL of acetate buffer 0.25 M + KCl 10 mM. Inset: linear fit of displayed data: Y = 1.01 X + 0.74, R = 0.99. (DPV parameters: modulation time, 0.05 s; interval time, 0.15 s; step potential, 5mV; modulation amplitude, 70 mV).

The reproducibility of this kind of measurement was evaluated as relative standard deviation over 3 measurements for a 1 µmol/L solution and resulted 20% within the same sensor (for successive cycle of hybridisation), 26% when using different sensors .

3.1.3.3 Enzyme-linked assay

An enzyme-linked approach was also developed. The biocatalytic activity of the enzyme label cause a great amplification of the hybridisation signal, thus increasing the sensitivity of DNA electrochemical detection. Moreover, non-specific signals can be minimised by using an appropriate enzymatic conjugate (streptavidin-AP) coupled with an efficient blocking agent (BSA) [39].

After the immobilisation, the probe was hybridised with a biotinylated target. The biotinylated hybrid was then labelled with streptavidin-alkaline phosphatase and incubated with a substrate, whose product of enzymatic hydrolysis is electroactive and can be detected by DPV. p-Amino-phenyl phosphate was selected among other substrates because the oxidation product, p-amino phenol, does not form electropolymerised products and can be easily washed away thus allowing the reusability of the sensor.

The performance of the enzyme-labelled format was tested by recording the enzymatic product signals obtained in the presence of different concentrations of DNA-target. As reported in Figure 24, the voltammetric response increased linearly with the target concentration up to 200 nmol/L (from the linear fit of displayed data $Y = 0.02\ X + 0.31$, $R = 0.98$). The non-specific signal, obtained using a non-complementary sequence, was negligible even at the highest concentration investigated (200nM), thus confirming the good selectivity of the genosensor. Thus target concentrations at nanomolar levels could be easily detected.

In this case, the reproducibility of the measurements (evaluated as relative standard deviation over 3 results for a 1 μmol/L solution) was 11% within the same sensor (for successive cycle of hybridisation) and 18% when using different sensors.

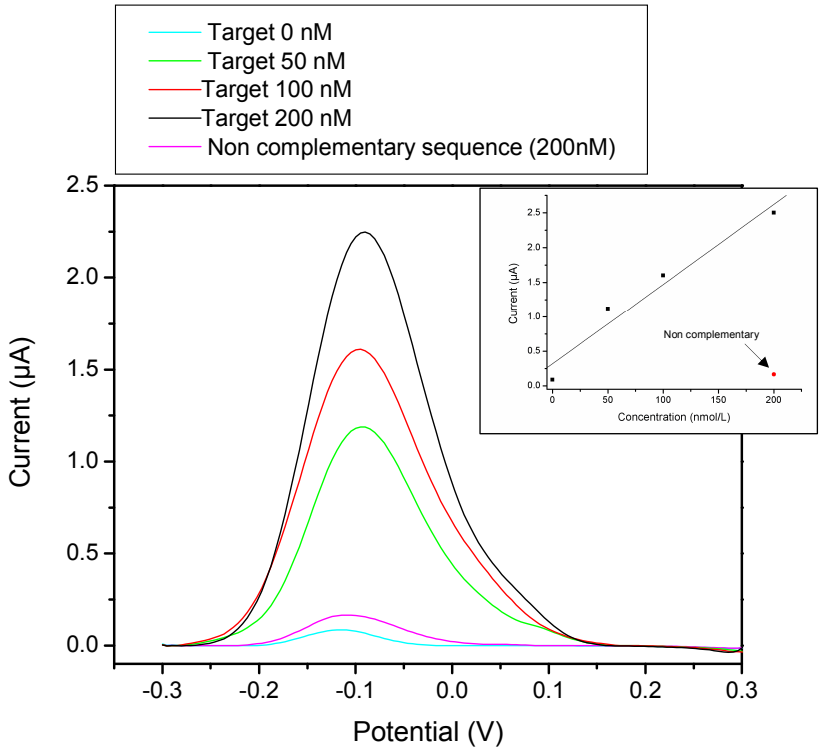

Figure 24. p-amino phenol oxidation peaks obtained after the hybridisation with DNA target (concentration range 0-500 nM) and non-complementary oligonucleotide (500 nM). Measurements were performed in 400 µL of DEA buffer containing 1mg/mL of p-amino phenyl phosphate after 15 min of incubation with the enzyme-labelled hybrid. Inset: linear fit of displayed data: Y = 0.02 X + 0.31, R = 0.98. (DPV parameters: modulation time, 0.05 s; interval time, 0.15 s; step potential, 5mV; modulation amplitude, 70 mV).

3.2 Discussion

3.2.1 Optimisation of CNT film construction

CNT films employed throughout this study were realised in collaboration with the group of Prof. Santucci, University of L'Aquila (Italy). They had been initially developed for gas sensing, based on changes in the electrical resistance of the CNTs in the presence of nitrogen dioxide, ammonia and ethanol [217, 218]. In

this work, such sensors were employed for electrochemical measurements for the first time, thus, their behaviour in solution was the first critical aspect to be investigated.

Self-assembled aligned MWCNT thin films were prepared by CVD at different growth temperatures (500°C, 700°C) onto insulators (SiO_2 or Si_3N_4) and metallic (Al) substrates, using acetylene and ammonia as precursor gases and nickel particles as catalyst (Table 5). Preliminary tests of CNT adhesion during electrochemical measurements in solution were carried out by performing CV scans in buffer solution. In case of SiO_2 and Si_3N_4 substrates a consistent release of nanotubes was clearly visible by an optical inspection. Data displayed in Figure 16 show a decrease of the capacitive current when comparing CV scans recorded before and after CNT release, evidence that detachment of nanotubes occurred. This phenomenon is consistent with studies on wettability of vertically aligned CVD-grown CNTs reported in literature [239, 240], which demonstrated a compression of nanostuctures upon water contact and a consequent compromising of their mechanical stability. Moreover, Nguyen *et al.* [112] reported that oxidative treatment for chemical functionalisation of the open ends of nanotubes further contributed to weakening mechanical stability, even leading to a collapse of vertically aligned nanostructures. To overcome this problem, they developed a new approach based on filling gaps between nanostructures with a spun-on glass coating able to provide structural support. Similarly, Yun *et al.* [94, 95] cast CNTs in an epoxy resin and polished the two ends of the nanotubes, one to be attached to an electrical contacting pad and one for functionalisation, in order to obtain highly ordered nanoelectrode arrays.

While very interesting, these solutions require highly advanced technology based on lithography and nanomanipulation. For this reason, the approach we decided to investigate was the synthesis of carbon nanotube on metallic substrates, a strategy which had been demonstrated as a way to obtain excellent electrode materials [237]. Examples are reported in literature of aligned CNT growth on Pt [92, 93], Cr [84, 113] or Au [241] substrates, based on plasma enhanced CVD, in which the

necessary energy for the chemical reaction is introduced by heated plasma instead of heating the whole reaction chamber [242]. In the present work Al was chosen as substrate and a much more accessible method for CNT growth was employed: thermal CVD, which requires only a basic tube furnace and gas manifold, and therefore offers advantages in terms of expense and numbers of samples that can be prepared per run. The increase of stability at the higher temperature (500°C or 700°C) chosen for this work results from a partial inclusion of Ni particles into the metal as aluminum is melted at 700°C, and this may root CNTs deeper in the Al substrate [243].

Figure 16c and 17b show the higher stability which can be achieved using these optimised conditions; even after six consecutive scans the surface remain stable, as well as the response after three cycle of denaturation/hybridisation.

3.2.2 Electrochemical performance of CNTs

The improvement of electrochemical performance due to the presence of carbon nanotubes has been discussed in the Introduction (Paragraph 1.2.1). Several authors [50, 56, 57, 95] attributed this phenomenon to defects in nanotube structure as well as to the open ends, which make the conductivity particularly favourable by acting as electrocatalytic sites for the electron transfer process.
Preliminary experiments reported in Figure 15 confirmed this affirmation. With respect to bare SPEs, a dramatic increase of current after consecutive additions of H_2O_2 was achieved when using an analogous CNT-modified disposable electrode. This is consistent with similar experiments reported in literature by Rubianes *et al.* [70] and Laschi *et al.* [71], which also found that the polymer (PEI) employed for CNT casting on carbon electrode surfaces contributed to an increase in the electroactivity of the sensor, due to the electron-donating ability of amine groups of PEI.

The investigation of the electrochemical behaviour of CNT films was particularly interesting. Initial useful information can be obtained from the CV experiments performed in buffer for the study of CNT adhesion, reported in Figure 16. The capacitive current due to the double layer formation at the electrode interface is normally proportional to the effective surface area [232] thus the high value obtained when using CNT films is consistent with a dramatic increase of surface area due to the nanostructures. Indirect confirmation of this was the decrease of the capacity current after nanotube detachment, a phenomenon which considerably decreased the active surface.

The study of the electron transfer properties of these sensors was performed using two commonly used redox mediators, potassium ferricyanide and hydroquinone. Figure 18 shows a comparison between signals obtained using CNT films, graphite screen-printed electrodes with the same geometric area, and an amorphous carbon sensor obtained by processing the substrate in the CVD reactor in the absence of one of the precursor gases. The shape of the voltammograms obtained with the nanostructured sensors appears consistent with that reported in literature concerning densely packed vertical CNTs electrodes [244]; the diffusion layers of individual nanostructures overlap thus generating a peak-shaped CV scan, similar to a solid planar macroelectrode.

Quasi-reversible behaviour was observed at CNT-film surfaces for both the mediators tested as indicated by the improvement of i_{pa}/i_{pc} and ΔE_p. Values obtained for potassium ferricyanide were: i_{pa}/i_{pc} = 1.23 for the amorphous carbon surface, 1.18 for graphite SPE, 1.08 for the CNT-film; ΔE_p = 307 mV for the amorphous carbon surface, 264 mV for graphite SPE, 188 mV for the CNT-film. For hydroquinone: i_{pa}/i_{pc} = 1.47 for the amorphous carbon surface, 1.08 for graphite SPE, 1.02 for the CNT-film; ΔE_p = 869 mV for the amorphous carbon surface, 576 mV for graphite SPE, 467 mV for the CNT-film.

The improvement in reversibility of electron transfer due to the presence of CNTs has been extensively reported in literature [49, 244-246] and the results obtained

are in good accordance with those published. One particularly relevant previous observation concerns the peculiar electron transfer properties observed in vertical aligned CNTs. According to Li *et al.* [113], the electrochemical properties of carbon nanotubes are highly dependant on their construction and orientation. The open ends exhibit a fast electron transfer rate, similar to a graphite edge-plane electrode, while the sidewalls present a slower rate and low specific capacitance similar to the graphitic basal plane. For this reasons highly ordered vertical aligned nanotubes behave as "conductive wires" which establish an electrical channel between the underlying metal film and the redox couple solution, in intimate contact with the active open ends, thus accelerating the electron transfer and decreasing the surface resistance [244].

3.2.3 CNT for electrochemical biosensing

3.2.3.1 Optimisation of immobilisation conditions

The immobilisation step is crucial for the overall performance of a biosensor. Both oligonucleotide immobilisation and orientation need to be carefully controlled in order to achieve the best conditions for DNA target recognition, i.e. high reactivity, accessibility and stability of the surface-bound probe and minimisation of non-specific adsorption of non-complementary sequences [5]. An appropriate immobilisation strategy is covalent functionalisation, which prevents desorption of the probes from the sensing layer. Chemical functionalisation of carbon surfaces is usually quite difficult to achieve because it requires a strong oxidant and random adsorption of a significant fraction of surface-confined strands often tends to occur, due to the porosity of graphite layers [18]. In this light, CNT films emerged as particularly suitable immobilisation platform. On the one hand, their vertical alignment could improve the vertical orientation of the immobilised probe thus increasing its accessibility. On the other hand, the high reactivity of their fullerene-like tips allows an easy end-modification of the nanotubes with functional groups such as –COOH, -OH, -C=O [238]. Among

these, the introduction of carboxylic acid groups is often the best choice because they can undergo a variety of reactions and are easily created on CNTs via oxidising treatment [245]. Shortening by ultrasonication with oxidising acid mixtures is also frequently used to functionalise CNTs [60, 68, 105], but this method is clearly not applicable to films.

In the current work, three different oxidation strategies were investigated: a strong oxidation using $K_2Cr_2O_7$ 2.5%, HNO_3 10% and applying a potential of 1.5 V (vs Ag/AgCl) for 15 munutes, an electrochemical oxidation (1.6 V vs Ag/AgCl for 120") in acetate buffer solution (0.25 M), and a milder treatment with HNO_3 10% for 60 minutes. At the same time, two strategies for chemical functionalisation were investigated: the direct linking of an amine-modified oligonucleotide probe and the classical method of carbodiimide/*N*-hydroxy-succinimide (EDC/NHS) covalent coupling. The comparison was carried out upon immobilising the inosine substituted amine-linked probe, scanning the potential in the range 0.2-1.6 V and evaluating the inosine peak intensity. In this way two pieces of information can be deduced, the amount of immobilised probe and the shape of the baseline, in order to check that no interfering peaks appear in the potential range of interest. From the comparison of peak intensities reported in Figure 19, it is evident that carbodiimide activation is a more robust chemistry for functionalisation, giving rise to higher currents whatever was the oxidising process. EDC and NHS convert the carboxylic acid into a reactive ester intermediate and, in the presence of an amino-linked oligonucleotide, an amide bond is formed [245, 246].

Investigation of oxidation processes indicated that treatment with $K_2Cr_2O_7$ was too irreproducible (RDS% = 52). This method was reported by Mikkelsen [34, 235] for the oxidation of glassy carbon electrodes, which require a strongly oxidising environment. In the case of CNTs, it may result in random detachment of CNTs from the electrode surface and this could be responsible for the irreproducibility. Also the noisy baseline reported in Figure 20a, with an anomalous peak corresponding to the guanine oxidation potential (0.9 V, as shown in Figure 21) confirms the inadequacy of this procedure in this case.

Electrochemical oxidation has been used for the introduction of carboxylic groups on carbon electrode surfaces [33, 102] as well as on nanotubes [113]. Results were comparable with those obtained using HNO_3. However, the latter method was preferred due to the milder conditions and consequent lower stress on the CNT film surface. During electrochemical treatment, generation of bubbles due to the electrolysis of water could be observed and this could be responsible for further detachment of nanotubes from the surface. Moreover, according to the literature, acid treatment should enhance oxide defects on the side walls and make the CNT film more hydrophilic, thus improving the contact between the aqueous solution and the surface with a consequent increase in the electron transfer rate [244, 247].

Once the immobilisation conditions were optimised, the influence of the probe concentration on the hybridisation reaction was investigated. This step must be carefully controlled, especially for the label-free assay based on the determination of Guanine signal, in order to reduce the contribution of non-specifically adsorbed (i.e. not hybridised) target sequences [102]. Hence the optimal surface coverage depends on the chemistry of functionalisation and concentration of the probe.

Figure 22 shows the results (the mean peak intensities for Guanine signal, n=3) obtained with label-free hybridisation experiments by varying the capture probe concentration in the range 5-20μM. The effect of probe concentration on immobilisation efficiency was evaluated by estimating the ratio between the target and non-complementary sequence guanine signal. A higher hybridisation yield was obtained using a 10 μM solution of amino-linked probe (~1:5), thus this concentration was chosen for further measurements. The trend observed in Figure 22 was consistent with that reported in literature by Lucarelli *et al.* [33]. For low probe concentration surface coverage is insufficient to avoid adsorption of target sequences thus resulting in high specific/non-specific ratio. The decrease of the same ratio at higher concentration has been explained elsewhere as due to the

higher surface densities which may cause steric and electrostatic interference between tightly packed probes and incoming target DNA [36].

3.2.3.2 Detection of the hybridisation reaction

Two approaches were investigated for the electrochemical detection of the hybridisation event: a label-free and an enzyme-linked method. A label-free option is normally preferable because it greatly simplifies the sensing protocol and avoids the use of toxic or carcinogenic compounds usually used as indicators [5].

The assay was based on the measurement of the intrinsic electrochemical signal of the guanine moiety [33, 101, 102]. An inosine-modified (guanine-free) probe was immobilised onto the sensor. Inosine also preferentially formed a specific base-pair with the cytosine residue, but its oxidation signal is well separated from that of guanine ($\Delta E_p \sim 400$ mV) and appears as a shoulder of Adenine signal (as observable in Figure 20). After hybridisation, duplex formation was detected by measuring the oxidation signal of guanine, which was present only in the target sequence. Once the experimental procedure had been elaborated, the analytical performance of the assay was determined by measuring different concentrations of target and controlling the non-specific signal. Probe was immobilised onto the CNT-film surface according to the optimised protocol and increasing concentrations of target were detected by performing subsequent cycles of hybridisation/denaturation on the same sensor. The trend reported in Figure 23 exhibited a good directly proportional relationship between concentration and current response. An estimate of the sensitivity was made using a the linear fit of displayed data (0.95 A/mol L^{-1}). The non-specific signal obtained using a non-complementary sequence (10μM), was more than three times lower than the lowest investigated concentration (0.5μM), thus confirming the selectivity of the genosensor.

These experiments generally characterised the overall analytical performance of the sensor. A more accurate determination would have required a statistically valid number of experiments, which was not possible to achieve due the limited number of sensors available and the initial problems with the experimental set up described in Paragraph 3.2.1.
A comparison with the results reported in the literature for label-free detection of oligonucleotide sequences reveals good agreement even though the technologies employed to obtain the nanostructured surfaces are different. Karadeniz *et al.* [104] reported a detection limit of nearly 100 nM, a sensitivity of 103 nA/µg L^{-1} (corresponding to nearly 1 A/mol L^{-1}) and specific/non-specific ratio 1:~3, using commercial available carbon SPEs modified with MWNT-COOH. Better performance (a few attomoles of oligonucleotide DNA) were obtained by the Meyyappan group [113, 114] using nanoelectrodes arrays obtained by embedding vertically aligned CNTs in a SiO_2 matrix in combination with a detection method based on amplified guanine oxidation using $Ru(bpy)_3^{2+}$ as mediator.

The disadvantage of a label-free method is the small amount of electroactive molecules available to be oxidised (i.e. Guanine bases present in the hybridised target). Evidently, the electrocatalytic activity attributed to CNTs was not sufficient to achieve the expected improvement in sensitivity, with our technology. Therefore, in order to improve the selectivity and the sensitivity of the assay an enzyme-linked approach (Figure 10b) was investigated. In this configuration, the biocatalytic activity of the enzyme can be exploited to amplify the hybridisation signal [36-39].

A normal guanine-containing probe was immobilised onto the sensor and hybridised with a biotinylated target. In this way the biotinylated hybrid can be easily labelled with streptavin-alkaline phosphatase exploiting the highly stable affinity reaction between streptavidin and biotin ($K_a = 10^{15}$ mol^{-1}). After incubation with the enzymatic substrate, the product of the biocatalytic reaction was detected by DPV. Once again, the overall performance of the assay was evaluated by recording the current response at different concentrations of DNA

target, in the range 0-200 nM as shown in Figure 24. A linear response was observed and an increase in sensitivity was achieved as can be seen from the slope of the graph (20 A/mol L^{-1}). Target concentrations at nanomolar levels could be easily detected and the good selectivity of the genosensor was confirmed by the negligible signal obtained using a non-complementary sequence, even at the highest concentration investigated (200nM).

Comparison with the literature is difficult in this case because enzyme-amplified assays performed on CNT-based electrodes have not previously been reported. Different labels and indicator strategies have been investigated: methylene blue [241], ferrocene carboxaldehyde [111], daunomicine [105, 252]. The lowest detection limit (0.1 nM) was reported by Cai *et al.* [248] and all these workers reached nanomolar levels of sensitivity. These results are also comparable with those obtained in our group using a similar enzyme-linked method with non-nanostructured surfaces such as carbon or gold SPEs [27, 35-37].

The conclusion which can be gathered from this work is that CNTs thin films represent a new and interesting alternative for electrochemical measurements. From the comparison with performance obtained with non-nanostructured electrodes, it emerged that our sensors provide an enhancement in sensitivity towards small molecules such as hydrogen peroxidase, potassium ferricianide and hydroquinone freely moving in solution and able to easily penetrate the nanotube forest. On the other hand, biosensor formats developed in this work did not exhibit a substantial enhancement of sensitivity due to the physical properties of the nanostructures. However, these results open the way for further investigation of possible exploitation of the electrochemical activity of CNTs by employing a different enzyme label, such as HRP [19], in conjunction with hydrogen peroxidase detection or redox mediators, which gave encouraging results in this work (Figures 15 and 18).

Chapter 4

MICROFLUIDIC-BASED GENOSENSOR COUPLED TO MAGNETIC BEADS

This work concerned the development of a novel rapid and sensitive electrochemical genosensor obtained by integrating a microfluidic platform with an analytical procedure based on the use of paramagnetic beads for the detection of real PCR samples.

The procedure, reported in details in Paragraph 2.3.2, was based on the functionalisation of streptavidin-coated paramagnetic microbeads with a biotinylated capture probe. This procedure was briefly optimised using screen-printed electrodes as a transduction system. Subsequently the loading conditions within the microfluidic system and the electrochemical detection were optimised. Finally the analytical parameters (sensitivity, reproducibility, limit of detection) of the assay were evaluated by realising a calibration curve of a PCR amplified fragment of Cor a 1.04, the major hazelnut allergen.

4.1 Results

4.1.1 Optimisation of magnetic bead-genosensor assay using drop-on system

Preliminary experiments were performed using disposable electrochemical sensors as transducers in order to evaluate the reliability of the magnetic bead-based assay and to optimise some parameters before combining this method with the microfluidic system. The experiments were performed using solutions of

hazelnut amplicon corresponding to Cor a 1.04 gene according to the procedure reported in Paragraph 2.3.2.4.

Most of the optimisations (i.e. modification of beads, assay times and procedures) were carried out during my master degree thesis [249] and therefore they will not be shown in this context. With respect to these previous experiments, a different enzymatic substrate was required for the employment of the magnetic bead assay in the microfluidic system. p-Amino-phenyl phosphate was selected among other substrates because the oxidation product, p-amino phenol, does not form electropolymerised products and can be easily washed away, thus allowing the Immuchip to be reused. The feasibility of the assay was therefore investigated by performing a calibration experiment of PCR amplicons using the new enzymatic substrate and the previously optimised conditions. Figure 25 shows that the voltammetric response increased linearly with the target concentration up to 10 nmol/L and then slowly decreased.

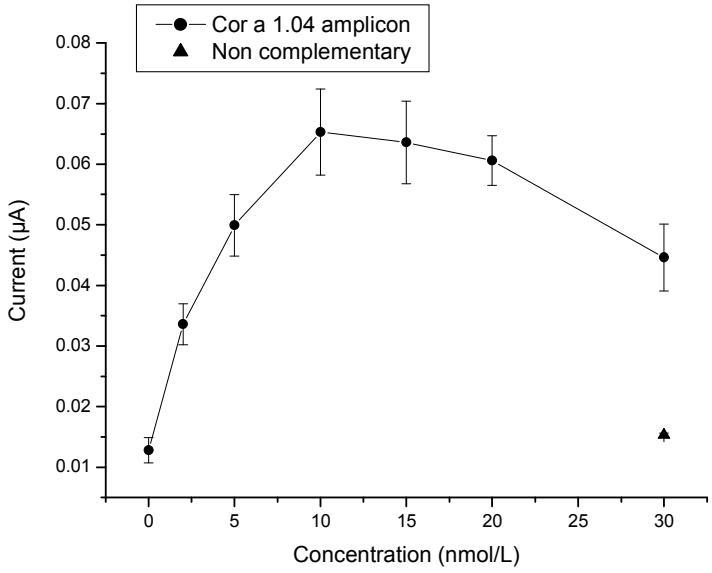

Figure 25. Calibration plot for Cor a 1.04 amplicons performed using drop-on system. Probe-modified and biotin-blocked beads were incubated for 15 min with 50 µL of thermally denatured target solutions, diluted to the desired concentration (0, 2, 5, 10, 15, 20, 30 nmol/L) with a solution 0.15 µM of biotinylated signalling probe in phosphate buffer. Other experimental details are avilable in Paragraph 2.3.2.4. Error bars represent the standard deviation of three replicates (n = 3).

The non-specific signal, obtained using a non-complementary sequence, proved negligible even at the highest investigated concentration, thus confirming the good selectivity of the genosensor. A detection limit of 0.6 nM was calculated considering the linear portion of the calibration curve (0-10 nM) and using the following equation: $Y = 1.51 \times 10^{-8} X + 6.02 \times 10^{-9}$ ($R = 0.96$) the mean of the blank solution response plus three times its standard deviation [240]. The reproducibility of the measurements (evaluated as relative standard deviation over 3 results for a 10 nmol/L solution) was 8%.

4.1.2 Optimisation of the microfluidic platform

This microfluidic platform had been originally developed for automated ELISA tests [221]. The integration of the existing technology with the magnetic bead-based genosensor required the optimisation of some key parameters such as the procedure for bead capture in the microchannel of the chip and protocols for the electrochemical evaluation of the enzyme kinetic.

These experiments were performed using beads modified with a target concentration of 10 nM and labelled with the enzymatic conjugate following the conditions optimised in paragraph 4.1.1. The electrochemical detection step was performed using a real-time chronoamperometric technique, in which the kinetics of the enzyme-labelled reaction were followed, by measuring the current alternatively on each channel and then reporting it vs. time, as shown in the example reported in Figure 13.

4.1.2.1 Optimisation of the bead loading step

The first set of experiments was designed to develop a suitable procedure for bead capture within the microchannels. For this reason, two different loading operations were compared. The experiments were performed by depositing a volume of 20 μL of modified bead suspension into each of the 8 inlet reservoirs of

a chip. In the first loading protocol ("back flow protocol"), after placing the magnet, a flow rate of 10 µL/min was applied for 2 minutes until the bead suspension was completely introduced into each channel. The flow was, then, reversed and kept at a rate of 5 µL/min in order to allow the complete capture of the beads. The idea was that a repeated passage of beads over the magnet might increase capturing efficiency.

After 4 minutes, the solution was removed from the wells and 20 µL of 10 mM p-aminophenyl phosphate were introduced into the channel at a flow rate of 2 µL/min. After 30 s, the flow was stopped and sequential chrono-amperometric measurements were carried out every 2 s for a total time of 6 min. The same experiment was performed using two different bead suspension amounts (1 and 3 mg/mL respectively), each placed in four of the eight channels (n = 4). Results reported in Table 5 demonstrated that this strategy was characterised by low reproducibility for both amounts and thus it was not considered useful.

Beads amount (mg/mL)	Linear slope (A/s)	R^2
1 mg/mL	$(2.4 \pm 2) \times 10^{-6}$	$R^2 = 0.78 \pm 0.21$
3 mg/mL	$(3{,}2 \pm 3) \times 10^{-6}$	$R^2 = 0.63 \pm 0.38$

Table 5. Optimisation of the loading step: "back flow protocol". Flow parameters: 20 µL of bead suspension (1 or 3 mg/mL) aspired at a flow rate of 10 µL/min, 2 min; reversed flow 5µL/min, 4 min; introduction of 20 µL of 10 mM p-aminophenyl phosphate, 3 s at 10 µL/min flow-through, 2 s of steady-state without flow, 12 cycles. Chronoamperometric measurement: static mode, sequential measures every 2 s for a total acquisition time of 6 min; potential +250 mV vs. Ag/AgCl pseudo-reference.

Thus, more loading cycles were introduced and the reverse phase was eliminated, in order to increase the efficiency of the assay ("multiple loading protocol"). In this approach, each loading step comprised 2 s at 2 µL/min flow-through and 3 s of steady-state without flow. The number of loading cycles was optimised by testing 4 different numbers of cycles (10, 50, 100, 200). Figure 26 shows that a

total number of 100 loading cycles allowed the higher sensitivity, thus this parameter was used for further experiments.

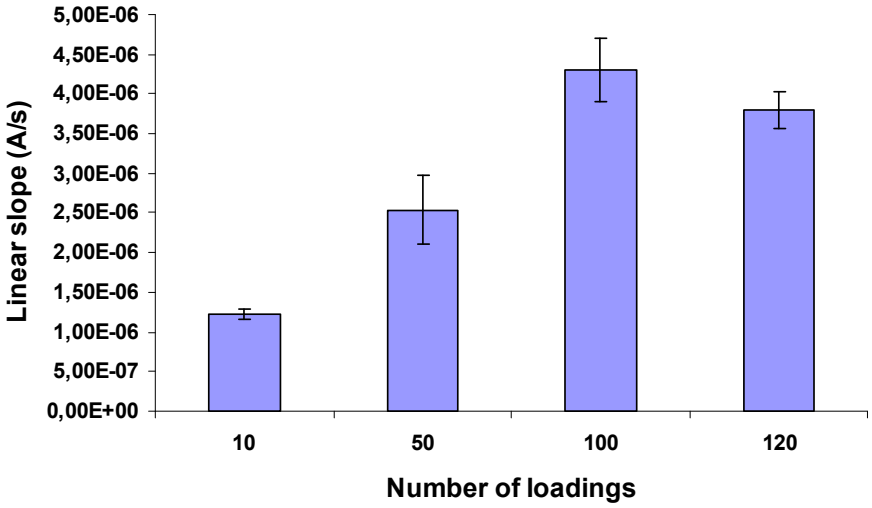

Figure 26. Optimisation of the "multiple loading protocol". Flow parameters: 20 µL of bead suspension 0.5 mg/mL aspired at at 2 µL/min flow-through for 2 s, 3 s of steady-state without flow, total number of loading: 10, 50, 100, 200 cycles; introduction of 20 µL of 10 mM p-aminophenyl phosphate, 3 s at 10 µL/min flow-through, 2 s of steady-state without flow, 12 cycles. Chronoamperometric measurement: static mode, sequential measured every 2 s for a total acquisition time of 6 min; potential +250 mV vs. Ag/AgCl pseudo-reference. Error bars represent the standard deviation of two replicates (n = 2).

4.1.2.2 Optimisation of the amount of beads

Four different bead suspensions (0.15, 0.5, 1.0, 3.0 mg/ml) were tested. As reported in Table 6, the higher sensitivity was obtained by decreasing the amount of beads. These results could be due to the fact that a high amount of beads reduced the flow efficiency into the microchannels, which were partially obstructed by the particles. For 0.5 mg/mL bead suspension, a sensitivity of (4±1) $\times$ 10^{-6} A/s was observed; this was the highest sensitivity obtained, but was associated with a large standard deviation (RSD% = 25, n=8). The best result was obtained for a concentration of 0.15 mg/mL, where a lower slope was observed (2

$\times 10^{-6}$ A/s) but with the highest reproducibility (RSD% = 10, n= 8). This amount of beads was then used for further experiments.

Beads amount (mg/mL)	Linear slope (A/s)	R^2
0.15 mg/mL	$(2.0 \pm 0.3) \times 10^{-6}$	$R^2 = 0.95 \pm 0.01$
0.5 mg/mL	$(4.0 \pm 1) \times 10^{-6}$	$R^2 = 0.83 \pm 0.06$
1.0 mg/mL	$(1.4 \pm 0.7) \times 10^{-6}$	$R^2 = 0.68 \pm 0.14$
3.0 mg/mL	*Not detectable*	-

Table 6. Optimisation of the amount of beads. Flow parameters: 20 µL of bead suspension 0.15, 0.5, 1.0, 3.0 mg/mL aspired at at 2 µL/min flow-through for 2 s, 3 s of steady-state without flow, total number of loading: 100 cycles; introduction of 20 µL of 10 mM p-aminophenyl phosphate, 3 s at 10 µL/min flow-through, 2 s of steady-state without flow, 12 cycles. Chronoamperometric measurement: static mode, sequential measures every 2 s for a total acquisition time of 6 min; potential +250 mV vs. Ag/AgCl pseudo-reference.

4.1.2.3 Optimisation of the substrate concentration

Finally, the concentration of p-aminophenyl phosphate was optimised in order to get the higher sensitivity and to avoid the inhibition of the enzymatic activity due to a substrate excess. During the electrochemical measurement step, three different concentrations of p-aminophenyl phosphate were used, in combination with two different acquisition times. Table 7 shows that, among the three substrate concentrations tested (20, 10 and 0.5 mM), the best a linear slope trends were obtained for the 20 mM concentration (R^2= 0.94 for 6 minutes of acquisition time, R^2= 0.999 for 3 minutes). Otherwise, by decreasing the data acquisition time from 6 to 3 min, a high sensitivity with a good linear correlation (r^2= 0.990) was obtained also for 10 mM as substrate concentration. Thus, this concentration was then used for the assay, taking advantage of the reduced reagent consumption coupled with a shorter detection time.

	Acquisition time: 6 min		Acquisition time: 3 min	
[Substrate] (mM)	**Linear slope (A/s)**	**R^2**	**Linear slope (A/s)**	**R^2**
20 mM	$(1.1 \pm 0.2) \times 10^{-7}$	$R^2 = 0.94 \pm 0.07$	$(9.4 \pm 0.3) \times 10^{-8}$	$R^2 = 0.999 \pm 0.001$
10 mM	$(3.6 \pm 0.3) \times 10^{-6}$	$R^2 = 0.66 \pm 0.29$	$(4.2 \pm 0.6) \times 10^{-6}$	$R^2 = 0.990 \pm 0.008$
5 mM	*Not detectable*	-	$(5.1 \pm 1.2) \times 10^{-7}$	$R^2 = 0.55 \pm 0.08$

Table 7. Influence of p-aminophenyl phosphate concentration on the sensitivity of the assay. Flow parameters: 20 µL of bead suspension 0.15 mg/mL aspired at at 2 µL/min flow-through for 2s, 3s of steady-state without flow, total number of loading: 100 cycles; introduction of 20 µL of 5, 10, 20 mM p-aminophenyl phosphate, 3s at 10 µL/min flow-through, 2s of steady-state without flow, 12 cycles. Chronoamperometric measurement: static mode, sequential measured every 2 s for a total acquisition time of 3 or 6 min; potential +250 mV vs. Ag/AgCl pseudo-reference.

4.1.3 Analysis of PCR-amplified samples

After the optimisation, the analytical performance of the system for PCR samples detection was investigated. Different amplicon concentrations (0, 2, 5, 10, 15, 20, 30 nM) and a 30 nM of non-specific sequence (negative control) solution were analysed. Each concentration was tested in a different channel. After measurement, the magnet was removed and the microchannels were washed with deionised water for 5 min with a flow rate of 5 µl/min. Then, fresh aliquots of beads were added in the microchannels and measurements were repeated. This procedure was performed three times. As reported in Figure 27, the response increased with the target concentration up to 10 nmol/L, and then slowly decreased.

The reproducibility of the measurements (evaluated as relative standard deviation over 3 results for a 10 nM solution) was 6%.

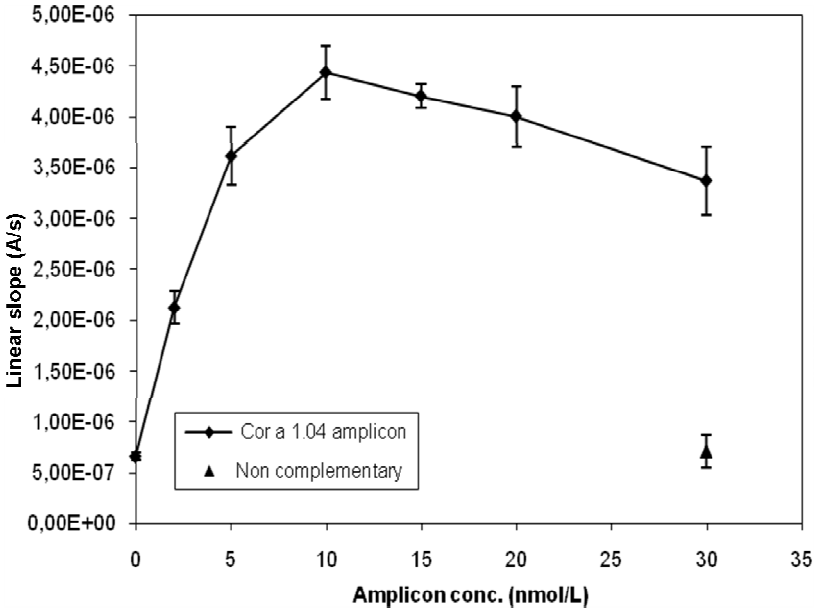

(a)

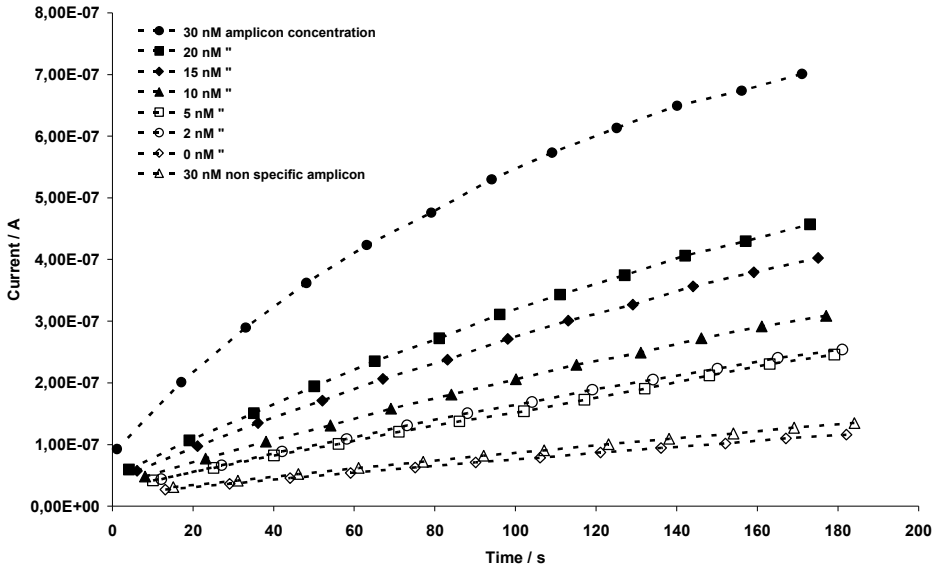

(b)

Figure 27. Calibration plot for Cor a 1.04 amplicons (a) and corresponding example of current vs time plot (b). Probe-modified and biotin blocked beads were incubated for 15 min with 50 µL of thermally denatured target solutions 0, 2, 5, 10, 15, 20, 30 nM and a 30 nM non complementary sequence. Flow parameters: see paragraph 2.3.2.5. Chronoamperometric measurement: static mode, sequential measures every 2 s for a total acquisition time of 3 min; potential +250 mV vs. Ag/AgCl pseudo-reference. Error bars represent the standard deviation of three replicates (n = 3).

A detection limit of 0.2 nM was calculated considering the slope of the linear portion of the calibration curve (0-5 nM), fitting in the following equation: $Y = 6.1 \times 10^{-7} X + 9.3 \times 10^{-7}$ ($R = 0.99$) the mean of the blank solution response plus three times its standard deviation [250]. Moreover, the reliability of the method was also demonstrated by the signal of the non-specific sequence, nearly one ordered of magnitude lower than the specific one, measured at the higher concentration (30 nM). The procedure (loading and measurement) took approximately 12 minutes.

Finally, a total hybridisation assay was developed by performing the hybridisation and the enzyme labelling steps in the flowing stream. In this case signal depends also on the number of target DNA and enzyme conjugate loadings. The same conditions for substrate injection were adopted (3 s at 10 μL/min flow-through, 2 s of steady-state without flow), with the only difference that the number of cycles was doubled, in order to increase the contact with reagents. The volume of solutions employed was decreased to 5 μL in each channel, thus limiting the consumption of reagents.

Once again, different amplicon concentrations (0, 1, 2, 5, 10, 15, 20) and a 20 nM of non-specific sequence solution were tested in different channels. After measurement, the magnet was removed and the microchannels were washed, fresh aliquots of beads were added in the microchannels and measurements were repeated. This procedure was performed for three times. Results obtained from this experiment are reported in Figure 28.

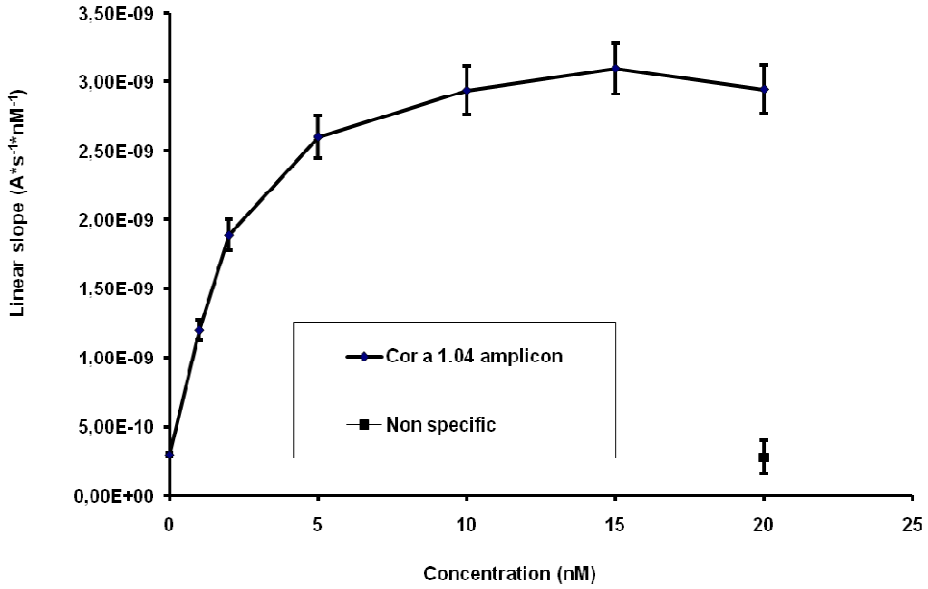

Figure 28. Total hybridisation assay: calibration plot for Cor a 1.04 amplicons. Probe-modified and biotin blocked beads were loaded in the fluidic system and incubated with thermally denatured target solutions 0, 2, 5, 10, 15, 20, 30 nM and a 30 nM non complementary sequence, according to the procedure illustrated in paragraph 2.3.2.3 and Table 3. Chronoamperometric measurement: static mode, sequential measures every 2 s for a total acquisition time of 3 min; potential +250 mV vs. Ag/AgCl pseudo-reference. Error bars represent the standard deviation of three replicates (n = 3).

In this case, the response increased with the target concentration up to 5 nmol/L, then slowly kept increasing until 15 nmol/L and finally decreased. From the interpolation of the linear part of the curve (0-5 nM) a detection limit of 0.1 nM was calculated fitting in the following equation: $Y = 4.2 \times 10^{-10} X + 6.2 \times 10^{-10}$ ($R = 0.94$) the mean of the blank solution response plus three times its standard deviation [250]. The non-specific signal due to the non-complementary sequence tested was negligible even at the higher concentration tested thus demonstrating the selectivity of the method. The reproducibility of the measurements (evaluated as relative standard deviation over 3 results for a 10 nM solution) was 7%.

Thus, the analytical performance of the total hybridisation assay was comparable to the previous system studied with the further advantage of a consistent reduction

of analysis time down to nearly 16 minutes, including the hybridisation and labeling steps.

4.2 Discussion

Coupling a microfluidic device with paramagnetic beads represents an attractive strategy for the development of highly sensitive biosensor formats, due to the combination of advantages which results. The advantages of micro- and nano-magnetic beads have been discussed in Paragraph 1.2.3.3 and include minimising non-specifically adsorbed reagents on the electrode surface, higher coupling efficiency and easier washing steps. Microfluidics used in combination with automation of the analysis (separation, delivering and mixing of reagents, detection) and requiring volumes in the micro-scale range, offer advantages in reducing consumption of reagents, speeding up reactions and time of analysis, and increasing sensitivity [251]. Moreover, fabrication technology enables parallel processing and easy integration with the most important transduction systems (i.e. electrochemical and optical).

One of the first examples of this highly promising combination was developed by Baeumner's group [252], who realised an optical genosensor using a microfluidic device comprising disposable microchannels made of polydimethylsiloxane integrated in a glass chip and a sandwich assay based on paramagnetic beads for probe immobilisation and a secondary probe labelled with dye-loaded liposome. Subsequently, this procedure was converted by the same group from an optical to an electrochemical format by integrating an interdigitated ultramicroelectrode array in the glass chip, downstream of the capturing magnet and labelling the hybrid with liposomes filled with an electrochemical marker, which could be oxidised or reduced at the electrode surface [227, 253]. A similar approach, based on Silicon electrical chip arrays coupled to interdigitated ultramicroelectrodes, was reported by Gabig *et al.* [226] for the recognition of the RNA of infectious bacteria. In this case, the DNA probe was captured on streptavidin coated beads

and labelled with a secondary probe functionalised with digoxigenin. After incubation with an anti-digoxigenin antibody conjugated with alkaline phosphatase, an enzyme amplified detection of the hybridisation event was performed.

Our approach involved the combination of a micro-electroanalytical device, previously developed for automated ELISA tests, with a new analytical procedure based on paramagnetic beads for the rapid screening of PCR amplicons obtained from the genes coding for specific food allergens. In particular, the system was applied to the detection of a 182 bp fragment of Cor a 1.04, the major hazelnut allergen. This application had been extensively investigated by our group by developing an electrochemical DNA-array based on gold screen printed electrodes [37]. Thus, we found it interesting to compare results obtained with the micro-fluidic device with those ones previously obtained.

4.2.1 Optimisation of the analytical procedure

At the beginning of this work preliminary experiments were performed using disposable electrochemical sensors as transducers, according to the procedure illustrated in Figure 12. This allowed us to control the reliability of the bead-based magnetic assay using an experimental set-up that had already been tested in our group for other analytical applications [28, 201-203] and thus avoiding any effect due to flow conditions. Most of the optimisation stages have been part of previous research activity and have been reported elsewhere [249, Publication n. 1].
Figure 25 shows a calibration experiment with PCR amplicons obtained by recording the signal given by the enzymatic oxidation of the product at different concentrations, in the range 0-30 nM. As shown, the voltammetric response increased linearly with the target concentration up to 10 nmol/L and then slowly decreased. This behaviour is fairly typical when analysing long double-stranded DNA sequences and has been explained elsewhere as a consequence of the re-annealing of the two complementary strands [36, 39]. When the amount of target

in solution is relatively high, random collisions of reagents favour re–annealing of the two complementary sequences over formation of the probe-amplicon hybrid.

In order to integrate this new protocol with the existing technology developed by Rossier *et al.* (Immuswiss S.A.) [219], a magnetic tool constituted of eight cylinder magnets supported in a bar, was designed and inserted between the chip and the instrument interface. In this way, beads flowing through the channel were captured at the transduction interface position, thus facilitating the diffusion of the released electroactive product towards the nearby electrode surface. Some basic flow parameters, such as substrate loading rate, chronoamperometric measurement modality and acquisition time had been previously optimised by the manufacturer [220, 221] and were maintained. However, the combination with the magnetic sensing platform required the optimisation of some key parameters such as the procedure for bead capture in the microchannels, the amount of beads and the protocol for the hybridisation assay. This set of experiments was performed using beads modified with a target concentration of 10 nM and labelled with the enzymatic conjugate according to the protocol optimised in Paragraph 4.1.1.

Firstly two different loading procedures were compared: a “back flow” and a “multiple loading” steps protocol. The former consisted of pumping the whole bead suspension inside the channel and subsequently reversing the flow in order to make the suspension pass several times over the magnet. In this way, the efficiency of bead capture was expected to be increase due to repeated passage of the suspension in proximity to the magnet. Results reported in Table 5 show poor reproducibility for both the bead amounts tested (RDS% = 83 for 1mg/mL of beads, RDS% = 93 for 3 mg/mL of beads). A possible explanation is that upon aspiring all the suspension at high flow rate (10 µL/min, 2 min), beads were placed randomly over the magnet and the reverse flow was in turn too quick (5µL/min, 4 min), thus causing a partial detachment of the beads. The highest reproducibility was achieved in the multiple loading step modality (represented by the error bars in Figure 26) and seems to confirm this assumption. The method consisted of eliminating the reverse phase and applying more loading cycles

comprising 2 s at 2 µL/min flow-through and 3 s of steady-state without flow. In this way, a small amount of beads was aspired during each loading step and the steady state without flow allowed an ordered placement of them over the magnet and hence over the electrochemical interface. As demonstrated in Figure 26, the highest response was achieved by increasing the number of cycles up to 100 loading steps. The increase of current response with the increase of loading steps appears logical because the higher the number of cycles, the larger is the amount of beads loaded inside the channel, as the same volume (20µL) was deposited in the inlet reservoir. It is more difficult to explain the decrease obtained at the highest number of steps tested (120). Upon comparing these results with those obtained for the optimisation of bead amount (Table 6) this phenomenon can be attributed to an excessive accumulation of beads in the channel, which could obstruct the efficiency of substrate flow . More loading steps, without varying the flow rate, results in a larger number of beads confined within the channel.

A further confirmation of this explanation has been reported by Goral *et al.* [253] who found a disadvantageous signal to noise ratio by increasing the amount of beads loaded in a microfluidic system. For similar reasons, when testing four different bead suspensions (Paragraph 4.1.2.2), higher sensitivity was obtained when using a smaller amount of beads, in contradiction with the assumption that more beads would result in more catalytic sites for substrate interaction. Actually, data reported in Table 6 sows that for 0.5 mg/mL of bead suspension, a higher signal was observed, but was exhibited a large standard deviation (RSD% = 25, n=8). While using a lower bead amount (0.15 mg/mL) resulted in higher reproducibility (RSD% = 10, n=8) even though a smaller slope was observed.

Finally, three different concentrations of p-aminophenyl phosphate, in combination with two different acquisition times, were investigated. The concentration of enzymatic substrate is another parameter to be carefully controlled in order to avoid the inhibition of the enzymatic activity due to a substrate excess [39]. Data reported in Table 7 shows that the shallowest slope were obtained using a 20 mM substrate solution. Another aspect of note is that by

decreasing the data acquisition time from 6 to 3 min, an overall improvement of the sensitivity was obtained. A possible explanation is that p-aminophenyl phosphate, which is known to be light-sensitive, is partially converted to p-aminophenol if not kept in the dark [226]. Thus, by reducing acquisition time the risk of degradation was limited and the reliability of the measurement increased.

4.2.2 Analysis of PCR amplified samples

The analytical performance of the microfluidic platform was tested by recording a calibration curve varying the PCR amplicons concentration in the range 0-30 nM. Firstly, an approach based on performing hybridisation and enzyme labelling before introducing beads in the micro-fluidic system was verified. Results reported in Figure 27 show behaviour consistent with that observed using the "drop-on-sensor" (Figure 25), as would be expected considering that the protocol for modification of the beads was the same for both strategies. Once again this trend can be ascribed to the re-annealing of the two complementary strands which it is likely to occur at high concentrations [36, 39]. The calculated detection limit was 0.2 nM and the signal produced by the non-specific sequence measured at the higher concentration (30 nM) was nearly one order of magnitude lower than the specific one, thus demonstrating the high selectivity of the assay. The procedure (bead loading and measurement) took approximately 12 minutes. Thus the total duration of the assay was approximately 50 minutes, comprising hybridisation, enzyme labelling and washing steps (nearly 40 minutes).

In order to enhance the efficiency of the analysis, a second procedure called "Total hybridisation assay", was designed. In this approach also the hybridisation and the incubation with the enzyme label were performed in flow. A consistent gain in terms of duration of the assay and consumption of reagents (only 5 μL of solution per channel were employed) was therefore achieved. Figure 28 shows the calibration plot obtained by testing different concentration of PCR amplicons. The slope was nearly three orders of magnitude lower than those obtained with the

first approach and this is probably a consequence of the smaller number of sample molecules loaded. The chronoamperometric response appears similar to the ones shown in Figure 27 and Figure 25, even if the linear range appears reduced. The slope increased linearly with the sample concentration up to 5 nmol/L, then slowly kept increasing until 15 nmol/L and finally decreased slowly. This phenomenon can be attributed to the change of the hybridisation reaction kinetics [252]. By pumping the sample solution through the channel, complementary strands needed a little time to reach the probe immobilised on the beads, thus diffusion from the bulk was consistently favoured. For this reason hybridisation required a smaller time to take place and the re-annealing effect was reduced. A detection limit of 0.1 nM was calculated and a negligible non-specific signal was obtained at the higher concentration tested, confirming that the assay was selective and that the risk of non-specific adsorption of enzyme molecules within the channel was limited.

The analytical performance of the two hybridisation assays was analogous. The detection limit reported by Bettazzi *et al.* [37] using gold SPEs arrays for the analysis of the same samples was ten times higher (1 nM). A nanomolar level of sensitivity was also reported by Lermo *et al.* [210] and by Erdem et *al.* [211-212], who respectively developed an enzyme-linked and a label-free assay based on magnetic beads (in static conditions) for the determination of PCR amplicons. Besides being highly sensitive, a further advantage of the total hybridisation method is the consistent reduction of the time of analysis down to nearly 16 minutes, comprising the hybridisation and labeling steps. According to the literature, this value was lower than the time required to complete analoguous sets of measurement based on fluidic systems and magnetic beads, which range from 30 minutes [253] to 4 hours [226].

In summary, an innovative sensing system for the development of DNA assays was realised using magnetic beads as an immobilisation platform and microfluidic technology for automation of the analysis steps and transduction system. The device was user-friendly, requiring low sample volume and delivering fast

detection time, high sensitivity and eight simultaneous analyses. Future work should be focussed on further miniaturisation of the system by reducing the size of the instrumentation and the dimensions of the immobilisation platform by employing nanoparticles.

Chapter 5

ONE-DIMENSIONAL POLYANILINE NANOSTRUCTURES FOR MIP-SENSING

The aim of this work was the development and characterisation of conductive polyaniline (PANI) nanostructures for applications in electrochemical sensing. A simple, cheap and fast route to grow polyaniline (PANI) nanotubes arranged in an ordered structure directly on an electrode surface was investigated. The deposited nanostructures were electrochemically and morphologically characterised and then used as a functional substrate for the development of a molecularly imprinted polymer-based sensor. Thus, we were able to exploit the intrinsic advantages of nanostructures as optimal transducers and the well known benefits of molecularly imprinted polymers (MIPs) as receptors. In particular, the hybrid nanostructured-MIP obtained was applied to the molecular recognition of catechol.

5.1 Results

5.1.1 Synthesis of PANI nanostructures

Polyaniline nanostructures were electrochemically synthesised using nanoporous alumina membranes as template, a technique which has the advantage of careful control of the shape and dimensions of polymerised objects.

A recently designed aniline monomer, NPEDMA [229], was employed for nanostructure construction. The peculiarity of this compound is the simultaneous presence of orthogonal polymerisable moieties, an aniline group and a methacrylamide, which allow the growth of PANI nanostructures as well as easy functionalisation with bioreceptors.

Electrochemical deposition inside the pores of the membrane was carried out as reported in Figure 14. A gold layer was sputtered on one side of an alumina nanoporous membrane in order to achieve electrical conductivity (Figure 14a). The aniline monomer was electropolymerised (Figure 14b) by CV after placing the membrane as working electrode in a three-electrode well cell.

Cycles of 5, 10 and 15 scans were tested in order to find the best condition for obtaining well defined nanowires. A low number of cycles could cause an incomplete filling of the pores. On the other hand, after too many scans polymer could fill the pores and form a layer over the membrane. Figure 29 shows voltammograms obtained after 5, 10, and 15 consecutive scans. From observation of these we were able to assume that 5 cycles were not enough to obtain consecutive reproducible scans, thus polymerisation was not complete. SEM characterisation, which will be reported in the next paragraph, was helpful in choosing 10 cycles as the best condition for growth.

In all the three cases, a reversible redox couple, absent in the first scan and increasing with increasing number of cycles until a constant intensity was observed, at E_{pa}=400 mV and E_{pc}=200 mV; this can be attributed to the Leucoemeraldine (completely reduced form)-Emeraldine (partially oxidized form) transition [254]. An oxidation peak, without corresponding cathodic peak on the reverse sweep, appeared at 650 mV and decreased until disappearing with increasing number of cycles.

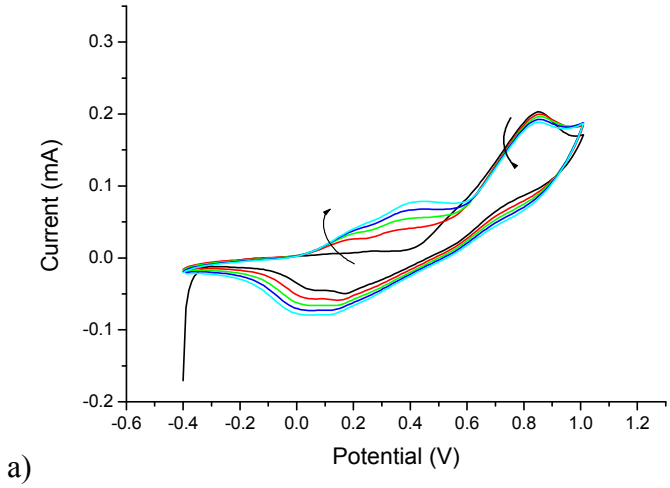

a)

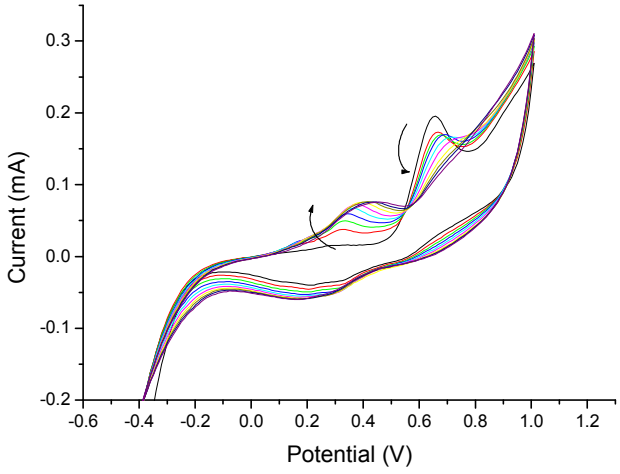

b)

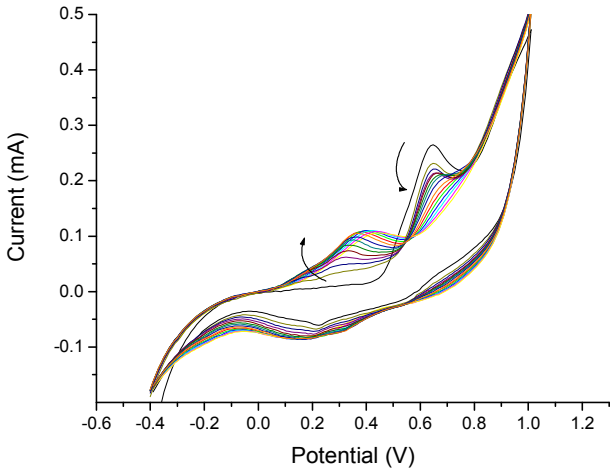

c)

Figure 29. CV scan of a solution containing NPEDMA 2.4 mM in $HClO_4$ 50 mM. Electrochemical parameters: initial potential -0.4 V, final potential 1.0 V, step potential 0.005 V, scan rate 50mV/s, 5 (a), 10 (b), 15 (c) cycles, Pot. vs Ag/AgCl.

5.1.2 Electrical characterisation

Once electro-polymerised polyaniline was formed, the conductivity between the two side of the membrane was measured in order to evaluate if the pores were filled with the conductive polymer or not. Two electrical contacts were attached, using an Ag paint, onto each side of the membrane and the electrical resistance measured between them.

Firstly resistance was measured between the two sides of a bare membrane, after having sputtered one of them with a gold layer, thus demonstrating that even if a small amount of gold penetrates the pores it was not enough to contact the two sides.

When testing membranes after the electropolymerisation of aniline inside the pores, electrical conductivity was demonstrated upon recording resistance values in the range 0.2-2.6 MΩ, thus demonstrating the presence of electrical "wires" connecting the two side of the membrane. Resistance values obtained, were quite changeable from one membrane to the another, as reported in Table 8.

Sample	R (Ω) Au-Al_2O_3	R (Ω) Au-PANI	Comments
Bare membrane	-	-	insulated
Au sputtered (180")	∞		
Au sputtered + PANI 1 mM	∞	26.3M	A lower concentration of monomer was employed, thus probably less polymer was formed. This could explaine the higher resistance
Au sputtered + PANI 2.4 mM	∞	10.3M	
Au sputtered + PANI 2.4 mM	∞	2 – 8 M	R not stable, value increased during the measurement

Table 8. Electrical resistance measurements between the two sides of the alumina template before and after PANI electrodeposition.

5.1.3. Morphological characterisation

In order to evaluate the morphology of electrochemically obtained PANI nanostructures, Scanning Electron Microscopy (SEM) analysis was carried out. SEM imaging was first performed on alumina membranes (templates), in order to understand if their real features are consistent with the nominal ones, declared by the supplier. Pictures reported in Figure 30 show clearly that the pores of the membranes are not cylindrical, but funnel-shaped. Therefore it is extremely important to carry out the electro-polymerisation on the surface where the pore diameter is larger.

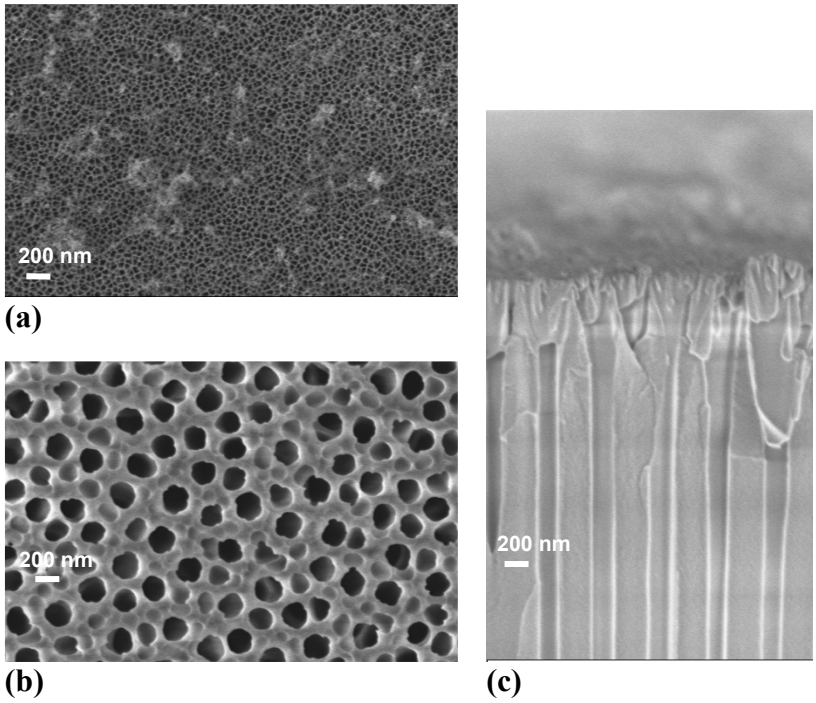

Figure 30. SEM images of Al_2O_3 membranes used as template, with a nominal pore size of 200 nm: (a) Top view of front face, with real pore size of about 20 nm; (b) Top view of back face, with real pore size of 200 nm; (c) Cross sectional view of the funnel-shaped pores.

Alumina membranes were analysed using SEM after electrochemical polymerisation of NPEDMA monomer in order to verify the presence of nanostructures grown inside the pores of the membranes and to understand the role of the number of CV deposition cycles (5, 10, 15) on material structure.

Comparing top views of membranes before and after electro-polymerisation, it was clearly that the pores were not completely filled by the polymer, even if some new structure could be found on the surface after the deposition. This effect was more pronounced the higher is the number of cycles in the deposition: in 5-cycle samples there were no remarkable variations of the membrane surface morphology, in 10-cycle samples, just a few small particles appeared (Figure 31a), while after 15-cycles a discontinuous film of polymer partially covered the membrane surface (Figure 31b). For this reason, 10-cycle depositions were selected as optimised conditions for growth.

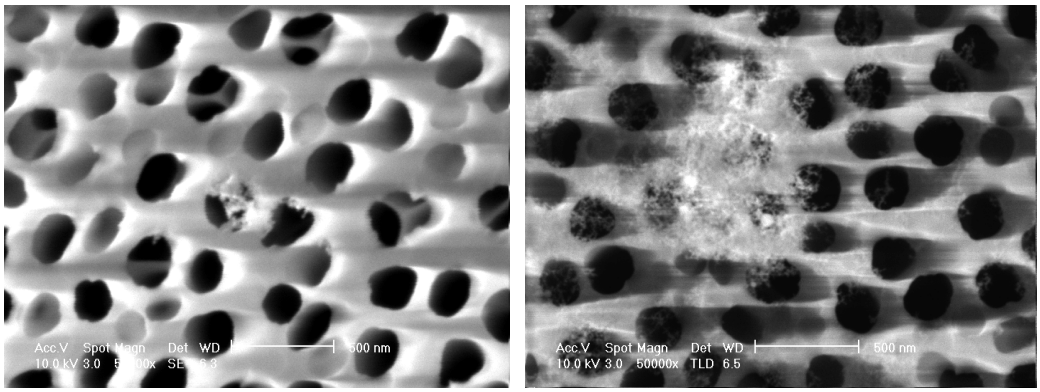

(a) **(b)**

Figure 31. SEM images of membranes after PANI electropolymerisation through cyclic voltammetry using 10 scans (a) and 15 scans (b).

The membranes were then dissolved in NaOH 3M for 30 minutes and analysed again, in order to obtain a morphological characterisation of the PANI nanostructures and to evaluate their durability after membrane dissolution. The resulting structures after membrane dissolution are shown in Figure 32. Polymer quasi-monodimensional nanostructures, of approximate diameter of 150 nm and length up to 50 μm, covered the surface uniformly. These structures were vertically aligned on the substrate surface, even if after membrane dissolution, small mechanical relaxation of the polymer could be observed. They were semiconductive, as could be deduced from weak charging effects under illumination with the electron beam, except in areas where some residuals of the alumina membrane were still present or the glass sample holder was uncovered.

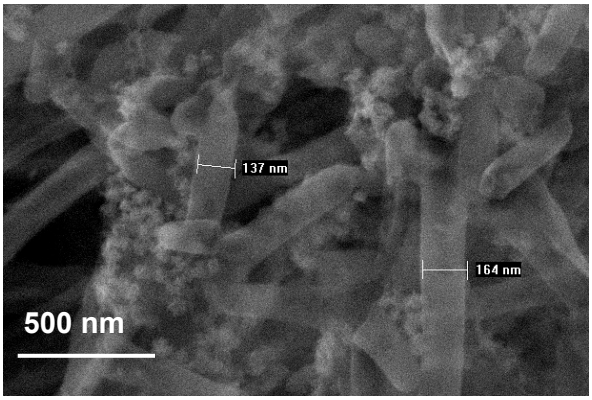

(a)

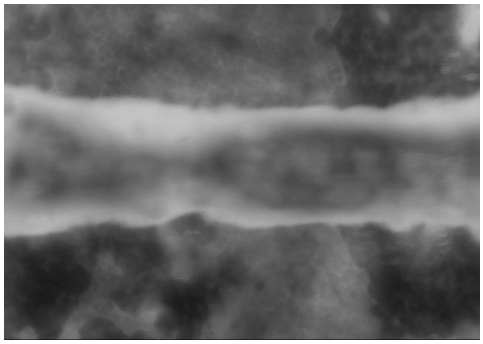

(c)

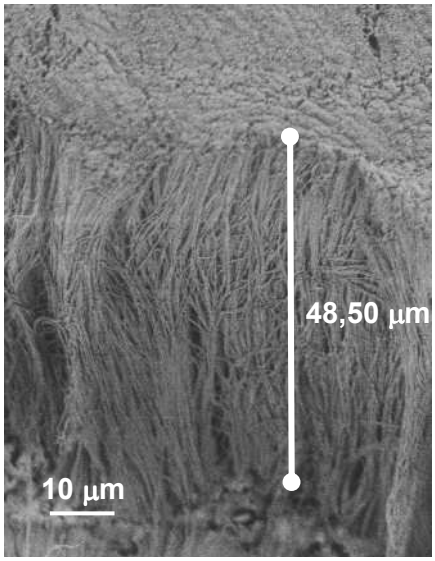

(b)

Figure 32. SEM image of top view of PANI nanostructures (a), after template dissolution (some residuals of the template still present); vertically aligned PANI nanostructures, after and template dissolution, cross-sectional view (b). The length of the structures is proximately the same of the template thickness (nominal value 60 μm). STEM image of a single PANI nanotube (c)

However, from SEM characterisation it was not clear if these structures were nanowires/nanorods, i.e. whether the pores of the membrane were completely filled with polymer, or were nanotubes with an empty core (i.e. the polymer starts depositing on the pore surface towards the interior).

To obtain a deeper understanding of this issue, Scanning Transmission Electron Microscopy (STEM) analysis was carried out (with the kind contribution of the CNR-INFM Sensor Lab, University of Brescia, Italy).

Small portions of membranes were prepared in the shape of thin samples, transparent to high energy electrons, in order to perform STEM analysis: fragments of electro-polymerised membranes were placed on TEM grids and then

dissolved in NaOH, resulting in single nanostructures suspended on the grid. The microscope was then operated at high voltage (20 kV).

As can be clearly seen in Figure 32 c, STEM analysis showed the presence of dark areas near the centre of a single nanostructure, imputable to the existence of porosities and with an empty core in the middle of the structure. Thus it can be inferred that these polymer nanostructures are tubes with a variable pore size depending on the number of deposition cycles.

5.1.4 MIP grafting of polyaniline nanostructures for catechol detection.

The nanostructured sensors obtained were tested by realising a model MIP biomimetic sensor for catechol detection, by adapting a procedure previously developed in our group by Lakshmi and co-workers [229]. Our purpose was to compare sensors formed using a well optimised grafting method on our new nanostructures with the ones previously obtained on conventionally formed polymer structures. To our knowledge, this is the first MIP-sensor realised using a nanostructured conductive polymer-based platform for electrochemical transduction. The MIP composition had been previously developed by our team [236] as a Tyrosinase-mimicking polymer, imprinted with catechol. It is based on the simultaneous coordination of a catechol molecule with Cu(II) and the imidazole moiety of the functional monomer (urocanic acid ethyl ester), thus reproducing the active site of the enzyme tyrosinase, capable of oxidising o-diphenols to o-quinones, in the presence of oxygen.
PANI nanowires were grafted with MIP and NIP via iniferter activation of the methacrylamide groups (as reported in paragraph 2.3.3.5), without removing the alumina membrane, in order to have a rigid framework which facilitated the placement in the electrochemical cell. After grafting, the catechol employed as template in MIP construction, was removed using EDTA. In this way sensors

were ready to be employed following loading with Cu (II) before the interaction with the analyte.

5.1.4.1 Investigation of the electrochemical response of the MIP-sensor

The electrochemical behaviour of the nanostructured sensor in the presence of catechol, was investigated upon comparing CV scans before and after MIP grafting. Figure 33 shows CV scans of a 100 µM solution of catechol in PBS buffer recorded using an Au-sputtered alumina membrane before electropolymerisation (red line), the same membrane after PANI nanostructures growing (green line), and the MIP-grafted sensor (black line). An oxidation and a reduction peak are visible at +0.3 V and +0.1 V respectively, only when using a MIP-grafted sensor, thus demonstrating that recognition and catalytic oxidation of catechol occur only in the presence of MIP and NPEDMA polymeric nanowires, which enable electrons exchange between the catalytic centre and the electrode.

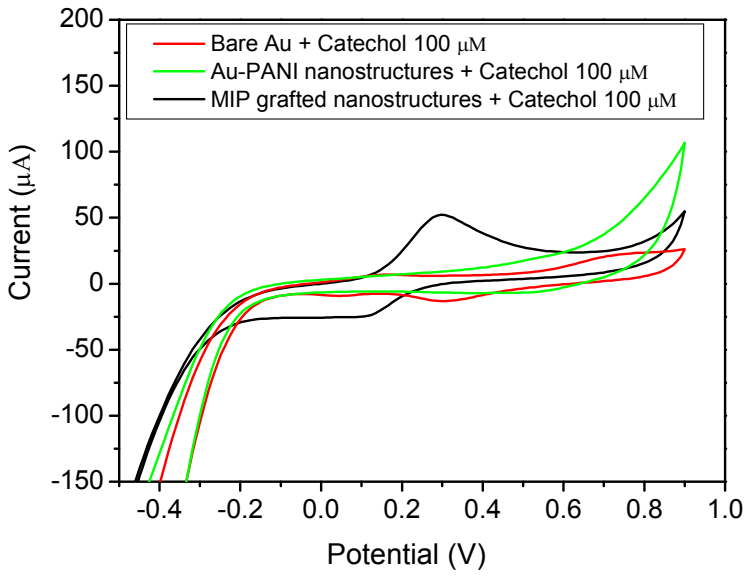

Figure 33. CV of 100 µM catechol in PBS 10 mM, pH 7.4, after loading with 5mM $CuCl_2$ for 5 min (CV parameters: start potential -0.5 V, first vertex potential 0.9 V, second vertex potential -0.5 V, step potential 0.01 V, scan rate 0.05 V s^{-1}; Potential vs. Ag/AgCl). Signals obtained using MIP-grafted sensor (red line), Au-sputtered alumina membrane before electropolymerisation (green line), sensor after growth of PANI nanostructures (black line).

Compounds structurally related to catechol were also examined by CV, in order to evaluate the possible interference of analogues. Results reported in Figure 34 show that even testing concentrations ten-fold higher then catechol reference solution, no peaks were detected for any of these compounds, in the potential window of catechol oxidation, thus demonstrating the high selectivity of the sensor.

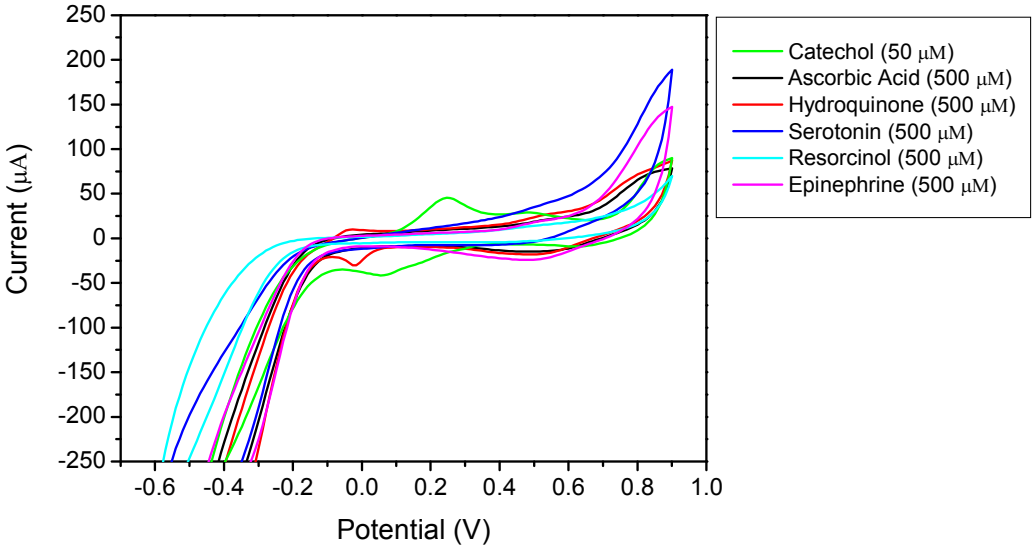

Figure 34. CV of catechol and structural analogue potentially interfering compounds. All the solution were prepared using PBS 10 mM, pH 7.4 and cycled after loading the sensor with 5 mM $CuCl_2$ for 5 min (CV parameters: start potential -0.5 V, first vertex potential 0.9 V, second vertex potential -0.5 V, step potential 0.01 V, scan rate 0.05 V s^{-1}; Potential vs. Ag/AgCl).

5.1.4.2 Evaluation of the analytical performance of the sensor

The analytical performance of the sensor was investigated by producing a calibration curve correlating the catechol concentration (in the range 1-100 μM) with the anodic peak current obtained by CV (Figure 35). The experiment was performed using the same sensor for different concentrations: immobilised catechol was removed with EDTA after each measurement and then another concentration was tested, after loading with Cu(II) in order to recreate the active site of tyrosinase. Each data point reported was calculated as the average of three

different sensors. Moreover, corresponding data were collected using non-imprinted (NIP) control nanostructured electrodes, obtained with the same procedure of MIP, without adding the template.

As shown in Figure 35, sensors grafted with MIP exhibited a near linear response in the concentration range 0-5µM, then the signal increased more slowly, but still increasing in proportional to the concentration. In case of non-imprinted control sensors the signal was negligible, thus demonstrating the selectivity of the MIP. Corresponding voltammograms for MIP and NIP are reported in Figure 36. From the interpolation of the linear part of the curve (0-2 µM) (Figure 35, inset), a limit of detection of 12 nM for catechol was calculated using the following equation: Y = 35.7 × + 4.77 (R=0.97) and considering the mean of the blank solution response plus three times its standard deviation [250].

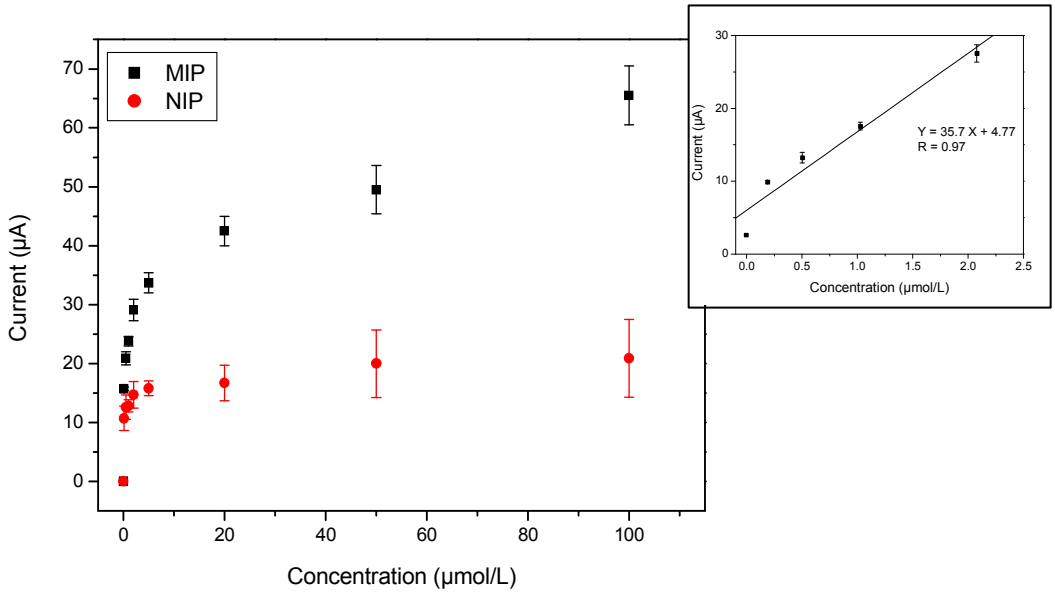

Figure 35. Calibration plot of anodic peak current vs catechol concentration for MIP-sensor and corresponding data obtained a non imprinted control sensor. Inset: linear fit of the linea part of the curve (0-2 µM): Y = 35.7 X + 4.77, R = 0.97. Each data point represents the average from three different sensors (n=3). All the solution were prepared using PBS 10 mM, pH 7.4 and cycled after loading the sensor with 5 mM $CuCl_2$ for 5 min.

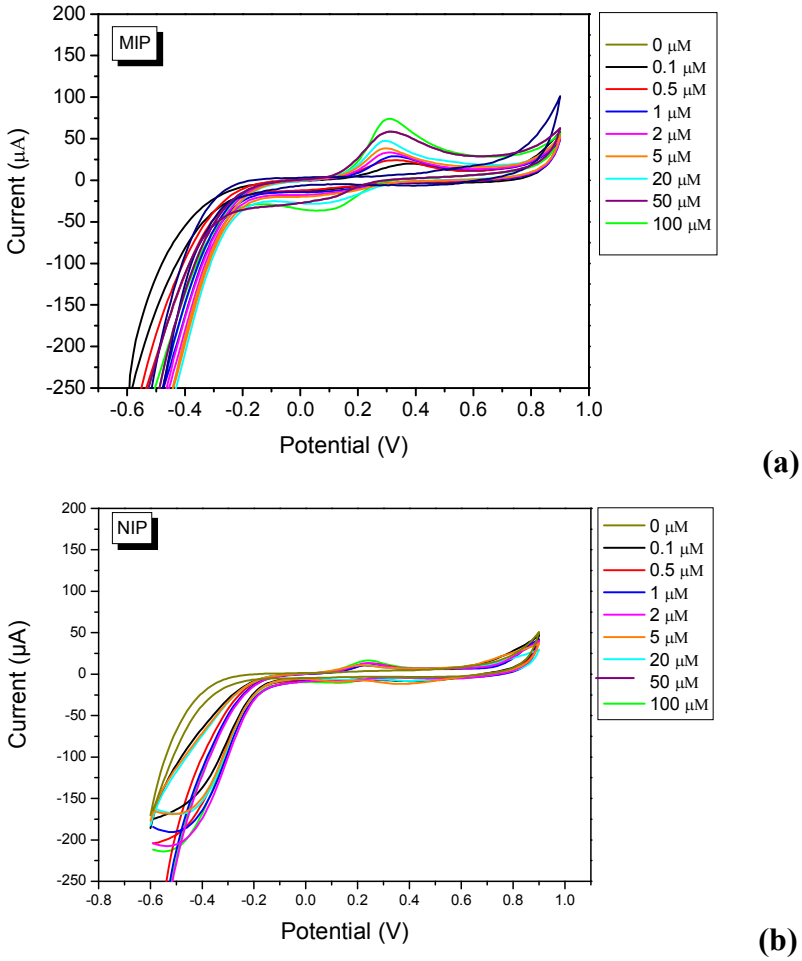

Figure 36. Voltammograms obtained using a MIP-sensor (a) and a NIP-sensor (b). All the solution were prepared using PBS 10 mM, pH 7.4 and cycled after loading the sensor with 5 mM $CuCl_2$ for 5 min. (CV parameters: start potential -0.5 V, first vertex potential 0.9 V, second vertex potential -0.5 V, step potential 0.01 v, scan rate 0.05 V s^{-1}; Potential vs. Ag/AgCl).

5.2 Discussion

This work was focused on the realisation and characterisation of polyaniline nanostructures and mainly on the investigation of the possible advantages of such nanomaterial compared to current non-nanostructured alternatives.

PANI nanostructures were used as functional substrate for the development of a MIP-based sensor for catechol detection. Paragraph 1.2.2 highlights the many advantages of nanostructured conductive polymers in chemical sensing. Moreover, the intimate integration of MIPs with the transducers through the PANI nanostructure represents a reliable solution to overcome one of the main drawbacks to the employment of MIPs in electrochemical sensing, i.e.: their limited electrical conductivity. In fact, most common imprinted polymers are based on acrylic or vinylic compounds, which produce electrical insulators. Different ways have been reported to overcome this problem, such as the direct realisation of conductive and semi-conductive MIPs, based on imprinted polypyrrole and polyaniline [164, 165] or the integration of MIPs with polymeric conductors, thus taking advantage of both materials [255].

The coupling of molecularly imprinting technology with polyaniline nanostructures does not appear to have been reported previously. Moreover, this particular application allowed a direct comparison with an analogous non-nanostructured, sensor previously developed by Lakshmi *et al.* [229].

5.2.1 Synthesis and characterisation of PANI nanostructures

Template synthesis of nanoporous membranes is a highly versatile, inexpensive and feasible method to obtain monodisperse polymer nanostructures with accurate control of length and diameter [121-123]. As excellently illustrated by Martin [123], each pore can be viewed as beaker in which the desired material is synthesised. The cylindrical shape of the pores determines the nanocylinder shape

of synthesised objects, while the membrane composition and the chemistry of pores affect their solid or hollow internal structure.

In this work polymerisation, was carried out by electrochemical oxidation within the pores of a commercially available alumina nanoporous membrane (declared pore diameter = 20 nm). After coating one side of the membrane with a Au film, the membrane was placed as working electrode in a three-electrode well cell and the aniline monomer (NPEDMA) was electropolymerised by CV.

Figure 29 shows voltammetric scans obtained after 5 (Figure 29a), 10 (Figure 29b) and 15 cycles (Figure 29c). In all the three cases, a reversible redox couple, absent in the first scan and increasing with increasing number of cycles until a constant intensity was observed (E_{pa}=400 mV, E_{pc}=200 mV). This behaviour is consistent with that shown by Lakshmi *et al.* [229] for an analoguous NPEDMA polymerisation on a Au coated glass surface. The literature reports that this is typical for N-substituted polyanilines (in our case N = methacrylamide group [228]) and can be attributed to the Leucoemeraldine-Emeraldine transition [254] . The redox mechanism is shown below in Figure 37.

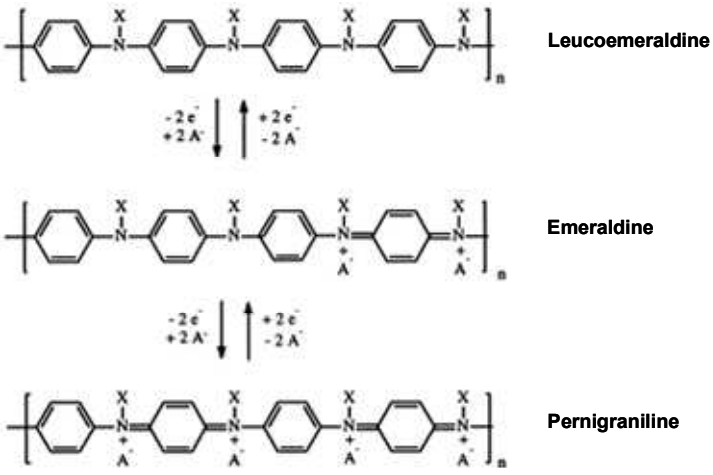

Figure 37. Scheme of the redox mechanism of N-substituted Polyaniline. *Adapted from [254]*.

Moreover, an oxidation peak, without corresponding cathodic peak on the reverse sweep, appeared at 650 mV and decreased until disappearing with increasing number of cycles. According to the literature [256], this can be ascribed to the oxidation of aniline to cation radicals, which are gradually deposited on the electrode surface, thus preventing aniline from being further oxidised. The determination of the appropriate number of cycles required to obtain well defined nanostructures was subject to SEM morphological investigation discussed below.

An indirect proof of the replenishment of pores was represented by electrical resistance measurements across the membrane. For this purpose, each side of the membrane was contacted using an Ag paint to fix the conducting wire. Table 8 reports resistance values obtained before and after gold sputtering and at the end of the electrochemical polymerisation. As expected, no conductivity was observed before electropolymerisation, thus confirming that even if a small amount of gold penetrates the pores it was not enough to contact the two sides. Data recorded after PANI synthesis are in the range 0.2-2.6 MΩ, thus demonstrating that nanostructures are able to create an electrical connection between the two sides of the membrane. The variability of resistance from one membrane to another can be ascribed to the crude apparatus employed for the measurement (i.e. Ag paint, wires and voltmeter). Similarly Martin [257], while measuring the variation of electrochemical resistance with the variation of pores size, observed consistent problems of irreproducibility whenworking in uncontrolled conditions (i.e. temperature, pressure).

An in depth investigation of the morphology of the electrochemically obtained PANI nanostructures was performed using Scanning Electron Microscopy (SEM) and Scanning Transmission Electron Microscopy (STEM). SEM [258] is a technique based on the emission of electrons which scan the sample, with typically energies of 2-40 keV. The electrons interact with the atoms of the sample, thus producing information on surface topography, crystalline structure, chemical composition and electrical behaviour of the surface. STEM is a variant of transmission electron microscopy in which electrons pass through the sample

but, similarly to SEM, the optical system focuses the beam into a narrow spot (probe) which is scanned over the specimen mounted on a grid [259]. STEM has many advantages: the focus does not change as the magnification is changed and the signal can be amplified to produce a highly visible image. Moreover, better high-resolution chemical analysis can be performed because the probe size is finer and has a high current (more than 0.5 nA focused on to less than 1 nm^2). In this work SEM was operated at 1-3 kV accelerating voltage range in order to prevent the electrostatic charging of both alumina and polymer and to avoid polymer degradation under the impinging beam.

Firstly, a brief investigation of the alumina templates was performed in order to verify the exact shape and dimension of the pores which determine the size of PANI structure. Images shown in Figure 30 demonstrate that pore appear funnel-shaped, thus careful attention was paid in carrying out the electrochemical synthesis on the side were the diameter was larger, in order to allow a proper replenishment of the pores with the monomer solution.
SEM characterisation greatly facilitated the choice of the better number of deposition cycles to obtained well defined nanowires. From the observation of top views of the membranes before and after the polymerisation it was clear that after a few number of cycles an insufficient filling of the pores was achieved, while on increasing the number of CV scans some structures emerged from the pores (Figure 31). Five-cycle samples, in fact, exhibited no substantial variations of the upper side surface morphology (image not reported). This is consistent with the CV scans reported in Figure 29a, where it is clear that 5 scans were not enough to obtain consecutive reproducible voltammograms, evidence that polymerisation was not complete. On the contrary, SEM images (Figure 31b) show that after 15-cycles a discontinuous film of polymer partially covered the membrane surface. Even if this condition had been considered suitable for the realisation of a continuous and homogenous film of poly-(NPEDMA) in Lakshmi's work [229], in this case it was evidently excessive to obtain well-defined nanostructures. For this reason 10-cycle depositions was chosen as the optimal electropolymerisation condition, since only a few small particles appeared to emerge from the pores.

Finally, the nanostructures morphology was investigated after dissolving the template with NaOH 3M for 30 minutes. Figure 32a shows a SEM image of the top view of PANI nanostructures, where an approximate diameter of 150 nm can be measured. Small grains covering the nanowires have been recognised as alumina residuals of the template. Figure 32b shows a cross-sectional view in which vertically aligned PANI nanostructures covered the surface uniformly and exhibited a homogeneous length of approximately 50 μm.

However, SEM characterisation turned out to be inappropriate to clarify whether the obtained nanostructures were hollow (nanotubes) or completely full (nanowires/nanorods). A better understanding was achieved by performing STEM analysis of thin portions of membranes placed on a grid and then dissolved in order to obtain single nanostructures suspended on the holder. In Figure 32c, dark areas are clearly visible in the centre of a single nanostructure, imputable to the empty core in the middle of the structure. Thus it can be inferred that these polymer nanostructures are tubes with a variable pore size depending on the number of deposition cycles. This assumption is consistent with an analoguous example reported in the literature by Chang *et al.* [157], who fabricated PANI nanotubes on graphite electrodes though an alumina template electro-synthesis for DNA biosensor construction. According to Martin [123, 257], a solvophobic effect rules polymerisation inside membranes: although monomers are soluble in aqueous media, the polycationic forms of polymers are completely insoluble. Moreover, an electrostatic component influences the interaction between the conductive polymer and the template: polymer generally nucleates and grows on the pore walls because of the electrostatic attraction between the growing polycationic polymer and anionic sites along the pore walls of the membrane itself, thus a hollow tubule is obtained. The same author reported that in case of polyaniline, the end of the nanostructure remains opened, even for long polymerisation times, while for example, polypyrrole tents to form end-capped nanofibrils.

5.2.2 MIP grafting of polyaniline nanostructures for catechol detection

Catechol imprinted polymer mimicking the enzyme Tyrosinase was first reported by Piletsky *et al.* in 2005 [236]. Tyrosinase is a copper-containing monooxygenase enzyme which catalyses the oxidation of o-diphenols to their corresponding o-quinones [260]. The electrochemical reduction of these quinones has been been widely exploited for the construction of biosensors for the detection of phenolic compounds, a class of chemicals which requires to be carefully monitored due to toxic effects which have been found in animals and plants [65, 179, 261]. Moreover, related compounds, such as catecholamines are of great importance in biology and medicine since they are involved in neurotransmission processes [262].

The MIP was designed in order to simulate the enzyme active site, based on the simultaneous coordination of a catechol molecule with Cu(II) and the imidazole moiety of the functional monomer (in our case: urocanic acid ethyl ester). MIP grafting of PANI nanotubes was carried out following a previously reported procedure [229] based on the iniferter activation of the methacrylamide substituent. Control non-imprinted sensors were realised using the same protocol without adding the template (catechol) in the reaction mix.

The electrochemical behaviour and reliability of the nano-MIP sensor was firstly tested by recording CV scans before and after MIP grafting, as reported in Figure 33. CV scans of a 100 μM solution of catechol obtained using an Au-sputtered alumina membrane before electropolymerisation (red line), after PANI nanostructures were grown (green line) and after MIP grafting (black line) were compared. A redox couple (E_{pa} = +0.3 V, E_{pc} = +0.1 V), corresponding to the catalytic oxidation of catechol, was observed only when using a MIP-grafted sensor. A similar behaviour has been also observed for the realisation of catalytic biosensors for catechol detection based on the entrapment of the enzyme Tyrosinase on the electrode surface [261, 263]. Cyclic voltammetry experiments performed using enzyme modified or non-modified electrodes showed that only in

the presence of Tyrosynase did catechol redox peaks appear. Thus, recognition and catalytic activity of the imprinted receptor was confirmed as well as the poly-NPEDMA nanotubes' role as wires which enable electron exchange between the catalytic centre and the electrode.

A recurrent problem for Tyrosinase based biosensors is the interference of structurally related compounds. Fore this reason, most of them have been designed for the determination of classes of phenolic compounds [65, 179, 262, 263]. In contrast, however, a catechol imprinted sensor is intended to offer the possibility of selective detection of the analyte, even in the presence of analogue interferents. Figure 34 shows CV scans recorded in the presence of catechol and of structurally similar molecules, ten-fold more concentrated. Since no peaks were detected for any of these compounds in the potential window of catechol oxidation, we were able to establish the high selectivity of the MIP-sensor in the presence of potential interferences. For resorcinol, hydroquinone and serotonin, this aspect has previously been explained [229] as a lack of interaction with the MIP because these compounds are devoid of the ortho-dihydroxy motif required for the formation of the complex with copper. While in case of ascorbic acid and epinephrine, this was probably due to their lower propensity to oxidation or to steric hindrance [65] which prevents a good fit inside the recognition cavity. This result may open the way for possible application in the monitoring in physiological fluids, where interference of ascorbic acid or catecholamine can be high.

Finally, the analytical parameters of the nanostructured sensor were investigated. For this purpose, a calibration plot (Figure 35) correlating the catechol concentration with the anodic peak current was constructed. In order to have a further confirmation of MIP selectivity, corresponding data obtained using non-imprinted (NIP) control nanostructured sensors were also plotted. The voltammetric response of MIP-grafted sensors increased nearly linear with concentration in the range 0-5μM and then kept increasing more slowly, while remaining proportional to the increase in amount of analyte. The signal from the

NIP-sensor remained negligible and constant, thus confirming the fundamental role of template for the correct assembly of the enzyme mimic active site.

The detection limit, calculated according to the 3(standard deviation of the blank)/slope criterion was 12 nM and the sensitivity was 35.7 A/mol L^{-1}. These results were compared with analytical parameters previously obtained by our team [229] using an analoguous non-nanostructured MIP-sensor for catechol detection by depositing thin films of poly-(NPEDMA) on gold electrodes. Despite the wider range of linearity obtained in that case (228 nM-144 μM), in the present work a lower limit of detection was achieved (1 order of magnitude less), thus demonstrating that the presence of nanostructures increases the capability of the sensor to detect lower concentrations, due to the enhanced surface area and improved electron transfer properties.

Moreover it could be interesting to qualitatively compare these results with the ones reported by other authors who reported creative combinations of Tyrosinase and nanostructured materials such as carbon nanotubes [65] and gold nanoparticles [179, 263] for the detection of catechol and related compounds. The lower detection limit reported by Pingarron's group [179], using a composite graphite-teflon electrode modified with Au nanoparticles, was nearly 20 nM. Other publications report detection limits in the order of hundreds of nmol L^{-1}. These results provide indirect proof of not only the enhancement of exchange area, but the synergistic contribution of shape (nanotubes), material (polyaniline) and receptor (MIP) that made our novel sensor particularly promising for highly sensitive clinical analysis.

Chapter 6

CONCLUSIONS AND FUTURE WORK

The combination of micro- and nano-technology with molecular recognition described in this work has been shown to offer excellent possibilities for designing novel sensing systems and enhancing the performance of bioanalytical assays. Three different miniaturisation pathways were investigated for electrochemical biosensing applications: the employment of carbon nanotube thin films, the combination of a microfluidic system coupled to magnetic particles and the construction of polyaniline nanotube arrays. The sensor devices described generally resulted in better sensitivity, specificity and faster response compared to current solutions.

Vertically aligned MWNTs thin films were designed and tested as platform for DNA immobilisation and for the realisation of electrochemical genosensors. Sensors were realised by CVD onto insulators (SiO_2, Si_3N_4) and metallic substrates using acetylene and ammonia as precursor gases and nickel particles as catalyst. Prior to this work, such materials had only been used for gas sensing and the aim of the current investigation was to explore alternative applications in electrochemical biosensors for measurements in solution. A preliminary electrochemical characterisation demonstrated that carbon nanotube growth onto insulators showed considerable problems of adhesion once in solution. On the contrary when using aluminum as substrate and high growth temperature (700°C), a higher stability was achieved and the reusability of the sensor was assured. Cyclic voltammetry experiments performed using two different redox mediators (potassium ferricyanide and hydroquinone) demonstrated that the presence of well-aligned CNTs greatly improved electron transfer properties with respect to other carbon based electrodes.

Subsequently, a model genosensor was developed using synthetic oligonucleotides related to the 35S promoter, a typical genetic construct present in the majority of GMOs [38-40]. Different methods of chemical functionalisation of the nanostructures with the oligonucleotide DNA-probe were investigated in depth to achieve the best reactivity, orientation and stability of the surface-bound probe and minimise non-specific adsorption events. An oxidising treatment with HNO_3 followed by a carbodiimide coupling of the amino-linked oligonucleotide probe was shown to be the optimal immobilisation strategy due to the high reactivity of nanotube fullerene-like tips, which allow an easy end-modification of the nanotubes with carboxylic moiety. Moreover, the good alignment of the tubes favoured a vertical orientation, and thus the accessibility of the probe.

For the detection of the hybridisation event a label-free assay, based on the oxidation of the guanine moiety, was initially developed. Good levels of sensitivity and selectivity were achieved, but the electrocatalytic activity of the CNTs was not sufficient to achieve the expected improvement in sensitivity. The analytical performance of the assay was improved by moving to an enzyme-linked approach, thus exploiting the biocatalytic activity of the enzyme to amplify the hybridisation signal [36-39]. In this configuration the sensitivity of the measurement was increased by nearly one order of magnitude and target concentration at the nanomolar level could be easily detected. Moreover, good selectivity of the genosensor was confirmed by the negligible signal obtained using a non-complementary sequence, even at the highest concentration investigated (200nM). However, the overall performance of the genosensor was similar to analoguous non-nanostructured devices, suggesting that the use of these nanostructures could not enhance the sensitivity of this particular assay. Whereas, when measuring small molecules such as hydrogen peroxidase, potassium ferricianide and hydroquinone, which move freely in solution and are able to easily penetrate the nanotube forest, a remarkable improvement in the electron transfer rate and a consequent enhancement of sensitivity were observed. This aspect could be further exploited by using enzyme labels, such as HRP [19], based on hydrogen peroxidase detection or redox mediators. By combining such an

electrode platform with improved enzyme labelling, applications involving gene expression and highly sequence specific (single base mismatch) DNA analysis could be accomplished. Moreover CNT thin films may represent a new and interesting alternative for electrochemical detection of trace redox chemicals (i.e. heavy metals, toxic contaminants, drugs, etc), immunoassay based detection schemes and as electrochemical detectors in microfluidic devices.

A novel electrochemical genosensor was also realised by integrating an existing microfluidic platform developed by DiagnoSwiss S.A. [219] with a new analytical procedure based on the use of paramagnetic beads. This innovative system for the development of affinity assays combines a special cartridge containing gold microelectrodes embedded in eight polymer microchannels, with a computer-controlled instrument for the control of fluidics. The advantages derived by incorporating paramagnetic beads as a transportable solid support in microfluidic devices were demonstrated for the detection of real PCR samples obtained from the genes coding for the major hazelnut allergen (Cor a 1.04). Analytes were captured by probe-modified beads in flow-through format, thus enhancing the surface area-to-volume ratio and consequently the sensitivity. Moreover, the magnetic properties greatly facilitate the delivery and removal of reagents through the microfluidic channels.

The procedure was based on the functionalisation of streptavidin-coated paramagnetic microbeads with a biotinylated capture probe. After a brief investigation of the modification procedure using screen-printed electrodes, some key parameters such as the procedure for bead capture within the microfluidic system, the amount of beads, the protocol for the hybridisation assay and the electrochemical detection were optimised. Among the loading protocols tested, the best efficiency was achieved upon applying a multiple loading step modality, which consisted of applying a series of loading cycles of flow-through periods and steady-states without flow.

Two different hybridisation assays were developed. Firstly, an approach based on performing hybridisation and enzyme labelling before introducing beads in the

micro-fluidic system was verified. Quantitative determinations of the analyte concentrations were obtained by loading the beads, then the enzymatic substrate and following the kinetics of the enzymatic reaction within each channel. In this format a detection limit of 0.2 nM for a 182 bp PCR amplicon and a reproducibility of 6% (n=3, for a 10nM solution) were obtained. The procedure (bead loading and measurement) took approximately 12 minutes. Thus, the total duration of the assay was approximately 50 minutes, comprising hybridisation, enzyme labelling and washing steps. A second procedure named "Total hybridisation assay", was designed with the intention of performing both the hybridisation and the incubation with the enzyme label in flow. A consistent gain in terms of duration of the assay (from 50 to 16 minutes) and consumption of reagents (only 5 μL of solution per channel were employed) was thus achieved. A detection limit of 0.1 nM was calculated and a negligible non-specific signal was obtained at the higher concentration tested, confirming that the assay was selective and that the risk of non-specific adsorption of enzyme molecules within the channel was limited. The reproducibility of the measurements (n=3 for a 10 nM solution) was 7%.

The conclusion which can be gathered from this work is that microfluidic devices used in combination with automation of the analysis (separation, delivering and mixing of reagents, detection) and magnetic immobilisation supports, offer advantages in reducing consumption of reagents, speeding up reactions, time of analysis and increasing sensitivity. This particular platform also offered the further advantage of eight simultaneous analyses. Future work should be devoted to investigating the possibility of automating the modification of the beads and on further miniaturisation of the system by reducing the size of the instrumentation and the dimensions of the immobilisation platform (i.e. by employing nanoparticles), in line with the concept of lab-on-a-chip technology. Moreover, even though the procedure was developed for DNA detection, other assays using affinity biomolecules (i.e. antibodies) or new mimetic bioreceptors such as aptamers or molecularly imprinted polymers could undoubtedly benefit from the

use of paramagnetic beads integrated in a microfluidic-based platform, using the set-up developed in this work.

Finally, a simple, inexpensive and rapid method for the formation of novel polyaniline (PANI) nanostructures was developed and applied to a new biosensor design. The idea was to develop a nanostructured sensor based on polyaniline nanowires or nanotubes grafted with molecularly imprinted polymer (MIP) receptors using a novel hybrid material, N-phenylethylene diamine (NPEDMA) [228] as monomer. This molecule combines two orthogonal polymerisable functionalities, an aniline group and a methacrylamide. In this way, the polymerisation of NPEDMA resulted in conductive nanowires which allow direct electrical connection between the electrode and the MIP.

The nanostructures were synthesised by electropolymerisation of the aniline function using alumina nanoporous membranes as template. An electrochemical and physical (SEM and STEM imaging) characterisation were subsequently accomplished in order to find out the best conditions for nanostructure growth as well as to reveal their morphological features. Polymer nanostructures exhibiting a diameter of 150 nm and length of up to 50 μm, uniformly covered the surface and were vertically aligned with respect to the growth substrate. Moreover, from STEM characterisation it could be inferred that they are tubes with a variable pore size depending on the number of deposition cycles. Their high aspect-ratio is extremely favourable for sensing applications, because they provide an extended surface area of active sites which could significantly increase the sensitivity. This assumption was proved by grafting MIPs on polymer nanowires to create a specific and selective model MIP-sensor for catechol detection. The MIP, a Tyrosinase-mimicking polymer [236], imprinted with catechol, was photochemically grafted over the polyaniline, via iniferter activation of the methacrylamide groups. The ability to detect catechol was investigated as well as the selectivity of the sensor in the presence of structurally related compounds (ascorbic acid, hydroquinone, serotonin, resorcinol, epinephrine).

The advantages which can derive from using nanostructures in this particular biosensing application were evaluated by comparing the analytical performance of the sensor with an analogous non-nanostructured MIP-sensor that we had previously developed [229]. A significantly lower limit of detection (one order of magnitude) was achieved (12 nmol L^{-1}) thus demonstrating that the nanostructures enhance the analytical performance of the sensor. This improvement was attributed to the synergistic contribution of shape (nanotubes), material (polyaniline) and receptor (MIP) that made our novel sensor particularly promising for highly sensitive clinical analysis. In addition, the nanostructures could be connected directly to single or double electrical contacts for applications in chemical gas sensing by exploiting the variation in resistance of the polymer in the presence of different oxidising and reducing gases.

In summary, this work highlighted interesting opportunities for the employment of nanomaterials in electrochemical biosensing. Carbon nanotubes exhibited highly improved electron transfer properties with respect to other carbon based electrodes; in the case of polyaniline, the improvement resulting from the miniaturisation of the sensing surface was particularly evident. This in-depth investigation of some of the most representative nano- and micro- technologies paves the way for the realisation of novel sensing strategies using interesting combination of materials. Coupling polyaniline nanostructures with CNTs or nanoparticles for highly conductive nanocomposite construction and employing CNTs as nano-transducers in fluidic systems for facilitating miniaturisation to nanoscale levels are just a couple of examples of the potential permutations that these materials can offer.

BIBLIOGRAPHY

[1] Wang J. (2005) Nanomaterial-based electrochemical biosensors. *Analyst* **130**, 421-426.

[2] Turner A. P. F., Karube I., Wilson G. S. (1987) Biosensors: Fundamentals and applications. *Oxford University Press*, Oxford, U. K.

[3] Griffiths D., Hall G. (1993) Biosensor – what real progress in being made? *Trends in Biotechnology* **11**, 122-130.

[4] Thevenot D. R., Toth K., Durst R. A., Wilson G. S. (1999) Electrochemical biosensors: recommended definitions and classification (Technical Report). *IUPAC, Pure and Applied Chemistry* **71**, 2333-2348.

[5] Lucarelli F, Marrazza G., Turner A. P. F., Mascini M. (2004) Carbon and gold electrodes as electrochemical transducers for DNA hybridisation sensors. *Biosensors and Bioelectronics* **19**, 515–530.

[6] Cammann K. (1977) Bio-Sensors Based on Ion-Selective Electrodes. *Fresenius Zeitschrift Analytische Chemie* **287**, 1-9.

[7] Luong J. A. T., Male K. B., Glennon J. D. (2008) Biosensor technology: Technology push versus market pull. *Biotechnology Advances* **26**, 492-500.

[8] Turner A. P. F. (2000) Biosensors--Sense and Sensitivity. *Science* **290**, 1315-1317.

[9] De Luca S., Florescu M., Ghica M. E.. Lupu A., Palleschi G., Brett C. M. A., Compagnone D. (2005) Carbon film electrodes for oxidase-based enzyme sensors in food analysis. *Talanta* **68**, 171–178.

[10] Laschi S., Ogonczyk D., Palchetti I., Mascini M. (2007) Evaluation of pesticide-induced acetylcholinesterase inhibition by means of disposable carbon-modified electrochemical biosensors. *Enzyme and Microbial Technology* **40**, 485–489.

[11] Leech, D. (1994) Affinity biosensors. *Chemical Society Reviews* **23**, 205-213.

[12] Ricci F., Volpe G., Micheli L., Palleschi G. (2007) A review on novel developments and applications of immunosensors in food analysis. *Analytica Chimica Acta* **605**, 111-129.

[13] Jayasena S. D. (1999) Aptamers: an emerging class of molecules that rival antibodies in diagnostics. *Clinical Chemistry* **45**, 1628–1650.

[14] Piletsky S. A., Turner A. P. F. (2006) Electrochemical sensors based on molecularly imprinted polymers. *Electroanalysis* **14**, 317-323.

[15] Tombelli S., Minunni M., Mascini M. (2005) Analytical applications of aptamers. *Biosensors and Bioelectronics* **20**, 2424–2434.

[16] Mascini M., Del Carlo M., Compagnone D., Cozzani I., Tiscar P. G., Mpmhanga C. P., Chen B. (2006) Piezoelectric sensors based on biomimetic peptides for the detection of heat shock proteins (HSPs) in mussels. *Analytical Letters* **39**, 1627-1642.

[17] Palecek E. (2002) Past Present and future of nucleic acids electrochemistry. *Talanta* **56**, 809–19

[18] Lucarelli F., Tombelli S., Minunni M., Marrazza G. Mascini M. (2008) Electrochemical and piezoelectric DNA biosensors for hybridisation detection. *Analytica Chimica Acta* **609**, 139-159.

[19] Laschi S., Palchetti I., Marrazza G., Mascini M. (2009) Enzyme-amplified electrochemical hybridisation assay based on PNA, LNA and DNA probe-modified micro-magnetic beads. *Bioelectrochemistry* **76**, 214–220.

[20] Mascini M., Guilbault G. G. (1986) Clinical uses of enzyme electrode probes. *Biosensors* **2**, 147-172.

[21] Farré M., Kantiani L., Pérez S., Barcelo D. (2009) Sensors and biosensors in support of EU directives. *Trends in Analytical Chemistry* **28**, 170-185.

[22] Ahmed M. U, Hossain M. M., Tamiya E. (2008) Electrochemical biosensors for medical and food applications. *Electroanalysis* **20**, 616 – 626.

[23] Tothill I. E. (2009) Biosensors for cancer markers diagnosis. *Seminars in Cell and Developmental Biology* **20**, 55–62.

[24] van Schothorst M., Jongeneel S. (1994) Line monitoring, HACCP and food safety. *Food Control* **5**, 107-110.

[25] Yang L., Bashir R. (2008) Electrical/electrochemical impedance for rapid detection of foodborne pathogenic bacteria. *Biotechnology Advances* **26,** 135–150.

[26] Tully E., Higson S. P., O'Kennedy R. (2008) The development of a 'labeless' immunosensor for the detection of *Listeria monocytogenes* cell surface protein, Internalin B. *Biosensors and Bioelectronics* **23**, 906–912.

[27] Farabullini F., Lucarelli F., Palchetti I., Marrazza G., Mascini M. (2007) Disposable electrochemical genosensor for the simultaneous analysis of different bacterial food contaminants. *Biosensors and Bioelectronics* **22**, 1544-1549.

[28] Centi S., Silva E., Laschi S., Palchetti I., Mascini M. (2007) Polychlorinated biphenyls (PCBs) detection in milk samples by an electrochemical magneto-immunosensor (EMI) coupled to solid-phase extraction (SPE) and disposable low-density arrays. *Analytica Chimica Acta* **594**, 9–16.

[29] Trojanowicz M. (2002) Determination of pesticides using electrochemical enzymatic biosensors. *Electroanalysis* **14**, 1311-1328

[30] Badihi-Mossberg M., Buchner V., Rishpon J. (2007) Electrochemical biosensors for pollutants in the environment. *Electroanalysis* **19**, 2015-2028.

[31] Palchetti I., Mascini M. (2008) Nucleic acid biosensors for environmental pollution monitoring. *Analyst* **133**, 846–854.

[32] Shah J., Wilkins E. (2003) Electrochemical biosensors for detection of biological warfare agents. *Electroanalysis* **15**, 157-167.

[33] Lucarelli F., Marrazza G., Palchetti I., Cesaretti S. , Mascini M. (2002) Coupling of an indicator-free electrochemical DNA biosensor with polymerase chain reaction for the detection of DNA sequences related to the apolipoprotein E. *Analytica Chimica Acta* **469,** 93–99.

[34] Mikkelsen S. (1996) Electrochemical biosensors for DNA sequence detection. *Electroanalysis* **8**,15-19.

[35] Lucarelli F., Capponcelli S., Marrazza G., Sangiorgi L., Mascini M. (2009) Split hybridisation probes for electrochemical typing of single-nucleotide polymorphisms. *Analyst* **134**, 52–59.

[36] Del Giallo M. L., Lucarelli F., Cosulich E., Pistarino E, Santamaria B., Marrazza G., Mascini M. (2005) Steric factors controlling the surface hybridisation of PCR amplified sequences, Analytical Chemistry **77**, 6324-6330.

[37] Bettazzi F., Lucarelli F., Palchetti I., Berti F., Marrazza G., Mascini M. (2008) Disposable electrochemical DNA-array for pcr amplified detection of hazelnut allergens in foodstuff. *Analytica Chimica Acta* **61**4, 93–102.

[38] Lucarelli F., Marrazza G., Mascini M. (2005) Enzyme-based impedimetric detection of PCR products using oligonucleotide-modified screen-printed gold electrodes. *Biosensors and Bioelectroics*. **20**, 2001-2009.

[39] Carpini G., Lucarelli F., Marrazza G., Mascini M. (2004) Oligonucleotide-modified screen-printed gold electrodes for enzyme-amplified sensing of nucleic acids, *Biosensors and Bioelectroics* **20**, 167-175.

[40] Meric B., Kerman K., Marrazza G., Palchetti I., Mascini M., Ozsoz M., (2004) Disposable genosensor, a new tool for the detection of NOS-terminator, a genetic element present in GMOs. *Food Control* **15**, 621-626.

[41] European Commision Regulation N. 641/2004, (April 2004) *Official Journal of the European Union.*

[42] Xu T., Zhang N., Nichols H. L., Shi D., Wen X. (2007) Modification of nanostructured materials for biomedical applications. *Materials Science and Engineering C* **27**, 579–594.

[43] Fortina P., Kricka L. J., Surrey S., Grodzinski P. (2005) Nanobiotechnology: the promise and reality of new approaches to molecular recognition. *Trends in Biotechnology* **23**, 168-173.

[44] Niemeyer C. M. (2007) Functional devices from DNA and proteins. *Nanotoday* **2**, 42-52.

[45] Hamley I. W. (2003) Nanotechnology with Soft Materials. *Angewandte Chemie International Edition* **42**, 1692 –1712.

[46] Suni I. I. (2008) Impedance methods for electrochemical sensors using nanomaterials. *Trends in Analytical Chemistry* **27**, 604-611.

[47] Iijima S. (1991) Helical microtubules of graphitic carbon. *Nature* **354**, 56-58.

[48] Baughman R.H., Zakhidov A., De Heer W.A. (2002) Carbon Nanotubes--the Route Toward Applications. *Science* **297**, 787-792.

[49] Valentini F., Orlanducci S., Terranova M. L., Amine A., Palleschi G. (2004) Carbon nanotubes as electrode materials for the assembling of new electrochemical biosensors. *Sensors and Actuators B* **100**, 117–125.

[50] Rivas G. A., Rubianes M. D., Rodrìguez M. C., Ferreyra N. F., Luque G. L., Pedano M. L., Miscoria S. A., Parrado C. (2007) Carbon Nanotubes for electrochemical biosensing. *Talanta* **74**, 291–307.

[51] Merkoci A., Pumera M., Leopis X., Péres B., Del Valle M., Alegret S. (2005) New materials for electrochemical sensing VI: Carbon nanotubes. *Trends in Analytical Chemistry* **4**, 826-838.

[52] Iijima S., Ichihashi T. (1993) Single-shell carbon nanotubes of 1-nm diameter. *Nature* **363**, 603-605.

[53] Guo T., Nikolaev P., Thess A., Colbert D.T., Smalley R.E. (1995) Catalytic growth of single-walled manotubes by laser vaporization. *Chemical Physics Letters* **243**, 49-54.

[54] Che G., Lakshmi B. B., Martin C. R., Fisher E. R. (1998) Chemical Vapor Deposition (CVD)-Based Synthesis of Carbon Nanotubes and Nanofibers Using a Template Method. *Chemistry of Materials* **10**, 260-267.

[55] Web source: Immunologie et chimie therapeutiques CNRS universitè de Strasbourg
http://www-ibmc.u-strasbg.fr/ict/vectorisation/nanotubes_eng.shtml

[56] Banks C. E., Davies T. J., Wildgoose G. G., Compton R. G. (2005) Electrocatalysis at graphite and carbon nanotube modified electrodes: edge-plane sites and tube ends are the reactive sites. *Chemical Communications*, 829–841.

[57] Britto P. J., Santhanam K. S. V., Rubio A., Alonso J. A., Ajayan P. M. (1999) Improved charge transfer at carbon nanotube electrodes. *Advanced Materials* **11**, 154-157.

[58] Sotiropoulou S., Chaniotakis N. A. (2003) Carbon nanotube array-based biosensor. *Analytical and Bioanalytical Chemistry* **375**, 103-105.

[59] Hirsch A. (2002) Functionalization of Single-Walled Carbon Nanotubes. *Angewandte Chemie International Edition* **41**, 1853-1859.

[60] Carpani I., Scavetta E., Tonelli D. (2008) Amperometric Glucose Biosensors Based on Glassy Carbon and SWCNT-Modified Glassy Carbon Electrodes. *Electroanalysis* **1**, 84-90.

[61] Radoi A., Compagnone D., Valcarcel M.A., Placidi P., Materazzi S., Moscone D., Palleschi G. (2008) Detection of NADH via electrocatalytic oxidation at single-walled carbon nanotubes modified with Variamine blue. *Electrochimica Acta* **53**, 2161–2169.

[62] Tasca F., Gorton L., Wagner J. B., Noll G. (2008) Increasing amperometric biosensor sensitivity by length fractionated single-walled carbon nanotubes. *Biosensors and Bioelectronics* **24**, 272–278.

[63] Jeykumari D. R. S., Narayanan S. S. (2008) A novel nanobiocomposite based glucose biosensor using neutral red functionalized carbon nanotubes. *Biosensors and Bioelectronics* **23**, 1404–1411.

[64] Jeykumari D.vR. S., Narayanan S. S. (2009) Functionalized carbon nanotube-bienzyme biocomposite for amperometric sensing. *Carbon* **47**, 957-996.

[65] Tsai Y., Chiu C. (2007) Amperometric biosensors based on multiwalled carbon nanotube-Nafion-tyrosinase nanobiocomposites for the determination of phenolic compounds. *Sensors and Actuators B* **125**, 10–16.

[66] Deo R. P., Wang J., Block I., Mulchandani A., Joshi K. A., Trojanowicz M., Scholz F., Chen W., Lin Y. (2005) Determination of organophosphate pesticides at a carbon nanotube/organophosphorus hydrolase electrochemical biosensor. *Analytica Chimica Acta* **530**, 185–189.

[67] Luo X., Xu J., Wang J., Chen H. (2005) Electrochemically deposited nanocomposite of chitosan and carbon nanotubes for biosensor application. *Chemical Communications*, 2169–2171.

[68] Qian L., Yang X. (2006) Composite film of carbon nanotubes and chitosan for preparation of amperometric hydrogen peroxide biosensor. *Talanta* **68**, 721–727.

[69] Liu Y., Qu X., Guo H., Chen H., Liu B., Dong S. (2006) Facile preparation of amperometric laccase biosensor with multifunction based on the matrix of carbon nanotubes–chitosan composite. *Biosensors and Bioelectronics* **21**, 2195–2201.

[70] Rubianes M. D., Rivas G. A. (2007) Dispersion of multi-wall carbon nanotubes in polyethylenimine: a new alternative for preparing electrochemical sensors. *Electrochemistry Communications* **9**, 480–484.

[71] Laschi S., Bulukin E., Palchetti I., Cristea C., Mascini M. (2008) Disposable electrodes modified with multi-wall carbon nanotubes for biosensor applications. *ITBM-RBM* **29**, 202–207.

[72] Sanchez S., Pumera M., Cabrujac E., Fabregas E. (2007) Carbon nanotube/polysulfone composite screen-printed electrochemical enzyme biosensors. *Analyst* **132**, 142–147.

[73] Rivas G. A., Rubianes M. D., Pedano M. L., Ferreyra N. F., Luque G. L., Rodriguez M. C., Miscoria S. A. (2007) Carbon nanotubes paste electrodes. A new alternative for the development of electrochemical sensors. *Electroanalysis* **19**, 823 – 831.

[74] Perez-Lopez B., Sola J., Alegret S., Merkoci A. (2008) A carbon nanotube PVC based matrix modified with glutaraldehyde suitable for biosensor applications. *Electroanalysis* **20**, 603 – 610.

[75] Wang J., Musameh M. (2005) Carbon-nanotubes doped polypyrrole glucose biosensor. *Analytica Chimica Acta* **539**, 209–213.

[76] Manso J., Mena M. L., Yanez-Sedeno P., Pingarron J. (2007) Electrochemical biosensors based on colloidal gold–carbon nanotubes composite electrodes. *Journal of Electroanalytical Chemistry* **603**, 1–7.

[77] Aguì L., Eguìlaz M., Pena-Farfal C., Yanez-Sedeno P., Pingarron J. M. (2009) Lactate dehydrogenase biosensor based on a hybrid carbon nanotube-conducting polymer modified electrode. *Electroanalysis* **21**, 386 – 391.

[78] Wang J., Lin Y. (2008) Functionalized carbon nanotubes and nanofibers for biosensing applications. *Trends in Analytical Chemistry* **27**, 619-626.

[79] Zhao H., Ju H. (2006) Multilayer membranes for glucose biosensing via layer-by-layer assembly of multiwall carbon nanotubes and glucose oxidase. *Analytical Biochemistry* **350**, 138–144.

[80] Yan X.B., Chen X.J., Tay B.K., Khor K.A. (2007) Transparent and flexible glucose biosensor via layer-by-layer assembly of multi-wall carbon nanotubes and glucose oxidase. *Electrochemistry Communications* **9**, 1269–1275.

[81] Liu G., Lin Y. (2006) Biosensor based on self-assembling acetylcholinesterase on carbon nanotubes for flow injection/amperometric detection of organophosphate pesticides and nerve agents. *Analytical Chemistry* **78**, 835-843.

[82] Jalit Y., Rodriguez M. C., Rubianes M. D., Bollo S., Rivas G. A. (2008) Glassy carbon electrodes modified with multiwall carbon nanotubes dispersed in polylysine. *Electroanalysis* **20**, 1623 – 1631.

[83] Viswanathan S., Radecka H., Radecki J. (2009) Electrochemical biosensor for pesticides based on acetylcholinesterase immobilized on polyaniline deposited on vertically assembled carbon nanotubes wrapped with ssDNA. *Biosensors and Bioelectronics* **24**, 2772–2777.

[84] Lin Y., Lu F., Tu Y., Ren Z. (2004) Glucose biosensors based on carbon nanotube nanoelectrode ensembles. *Nano Letters* **4**, 191-195.

[85] Withey G. D., Lazareck A. D., Tzolov M. B., Yina A., Aich P., Yeh J. I., Xua J. M. (2006) Ultra-high redox enzyme signal transduction using highly ordered carbon nanotube array electrodes. *Biosensors and Bioelectronics* **21**, 1560–1565.

[86] Boo H., Jeong R., Park S., Kim K. S., An K. H., Lee Y. H., Han J. H., Kim H. C., Chung, T. D. (2006) Electrochemical nanoneedle biosensor based on multiwall carbon nanotube. *Analytical Chemistry* **78**, 617-620.

[87] Sanchez S., Pumera M., Fabregas E. (2007) Carbon nanotube/polysulfone screen-printedel ectrochemical immunosensor. *Biosensors and Bioelectronics* **23**, 332–340.

[88] Buch M., Rishpon J. (2008) An electrochemical immunosensor for C-reactive protein based on multi-walled carbon nanotube-modified electrodes. *Electroanalysis* **20**, 2592 – 2594.

[89] Viswanathana S., Rani C., Anand A. V., Ho J. A. (2009) Disposable electrochemical immunosensor for carcinoembryonic antigen using ferrocene liposomes and MWCNT screen-printed electrode. *Biosensors and Bioelectronics* **24**, 1984–1989.

[90] Panini N. V., Messina G. A., Salinas E., Fernandez H., Raba J. (2008) Integrated microfluidic systems with an immunosensor modified withcarbon nanotubes for detection of prostate specific antigen (PSA) in human serum samples. *Biosensors and Bioelectronics* **23**, 1145–1151.

[91] He P., Wang Z. I., Zhang L., Yang W. (2009) Development of a label-free electrochemical immunosensor based on carbon nanotube for rapid determination of clenbuterol. *Food Chemistry* **112**, 707–714.

[92] Okuno J., Maehashi K., Matsumoto K., Kerman K., Takamura Y., Tamiya E. (2007) Single-walled carbon nanotube-arrayed microelectrode chip for electrochemical analysis. *Electrochemistry Communications* **9**, 13–18.

[93] Okuno J., Maehashi K., Kerman K., Takamura Y., Matsumoto K., Tamiya E. (2007) Label-free immunosensor for prostate-specific antigen based on single-walled carbon nanotube array-modified microelectrodes. *Biosensors and Bioelectronics* **22**, 2377–2381.

[94] Yun Y., Bange A., Heineman W. R., Halsall H. B., Shanov V. N., Dong Z., Pixley S., Behbehani M., Jazieh A., Tu Y., Wong D. K.Y., Bhattacharya A., Schulz M. J. (2007) Nanotube array immunosensor for direct electrochemical detection of antigen–antibody binding. *Sensors and Actuators B* **123**, 177–182.

[95] Yun Y., Dong Z., Shanov V. N., Doepke A., Heineman W. R., Halsall H. B., Bhattacharya A., Wong D. K. Y., Schulz M. J. (2008) Fabrication and characterisation of carbon nanotube array electrodes with gold nanoparticle tips. *Sensors and Actuators B* **133**, 208–212.

[96] Yu X., Kim S. N., Papadimitrakopoulos F., Rusling J. F. (2005) Protein immunosensor using single-wall carbon nanotube forests with electrochemical detection of enzyme labels. *Molecular Biosystems* **1**, 70–78.

[97] Yu X., Munge B., Patel V., Jensen G., Bhirde A., Gong J. D., Kim S. N., Gillespie J., Gutkind J. S., Papadimitrakopoulos F., Rusling J. F. (2006) Carbon nanotube amplification strategies for highly sensitive immunodetection of cancer biomarkers. *Journal of the American Chemical Society* **128**, 11199-11205

[98] Rusling J. F., Sotzing G., Papadimitrakopoulosa F. (2009) Designing nanomaterial-enhanced electrochemical immunosensors for cancer biomarker proteins. *Bioelectrochemistry* **76**, 189-194.

[99] Erdem A. (2007) Nanomaterial-based electrochemical DNA sensing strategies. *Talanta* **74**, 318–325.

[100] Erdem A., Papakonstantinou P., Murphy H. (2006) Direct DNA hybridisation at disposable graphite electrodes modified with carbon nanotubes. *Analytical Chemistry* **78**, 6656-6659.

[101] Palecek E., Fojta M., Tomschik M., Wang J. (1998) Electrochemical biosensors for DNA hybridisation and DNA damage. *Biosensor and Bioelectronics* **13**, 621-628.

[102] Wang J., Rivas G., Fernandes J. R., Lopez Paz J. L., Jiang M., Waymire R. (1998) Indicator-free electrochemical DNA hybridisation biosensor. *Analytica Chimica Acta* **375** 197-203.

[103] Erdem A., Karadeniz H., Caliskan A. (2009) Single-walled carbon nanotubes modified graphite electrodes for electrochemical monitoring of nucleic acids and biomolecular interactions. *Electroanalysis* **21**, 464 – 471.

[104] Karadeniz H., Erdem A., Caliskan A. (2008) Electrochemical monitoring of DNA hybridisation by multiwalled carbon nanotube based screen printed electrodes. *Electroanalysis* **20**, 1932 – 1938.

[105] Yang Y., Wang Z., Yang M., Li J., Zheng F., Shen G., Yu R. (2007) Electrical detection of deoxyribonucleic acid hybridisation based on carbon-nanotubes/nano zirconium dioxide/chitosan-modified electrodes. *Analytica Chimica Acta* **584**, 268–274.

[106] Yang T., Zhou N., Zhang Y., Zhang W., Jiao K., Li G. (2009) Synergistically improved sensitivity for the detection of specific DNA sequences using polyaniline nanofibers and multi-walled carbon nanotubes composites. *Biosensors and Bioelectronics* **24**, 2165–2170.

[107] Wei H., Du Y., Kang J., Wang E. (2007) Label free electrochemiluminescence protocol for sensitive DNA detection with a tris(2,20-bipyridyl)ruthenium(II) modified electrode based on nucleic acid oxidation. *Electrochemistry Communications* **9**, 1474-1479.

[108] Jiang C., Yang T., Jiao K., Gao H. (2008) A DNA electrochemical sensor with poly-l-lysine/single-walled carbon nanotubes films and its application for the highly sensitive EIS detection of PAT gene fragment and PCR amplification of NOS gene. *Electrochimica Acta* **53**, 2917-2924.

[109] Xu Y., Ye X., Yang L., He P., Fang Y. (2006) Impedance DNA biosensor using electropolymerized polypyrrole/multiwalled carbon nanotubes modified electrode. *Electroanalysis* **18**, 1471 – 1478.

[110] Huska D., Hubalek J., Adam V., Kizek R. (2008) Miniaturized electrochemical detector as a tool for detection of DNA amplified by PCR. *Electrophoresis* **29**, 4964–4971.

[111] He P., Li S., Dai L. (2005) DNA-modified carbon nanotubes for self-assembling and biosensing applications. *Synthetic Metals* **154**, 17–20.

[112] Nguyen C. V., Delzeit L., Cassell A. M., Li J., Han J., Meyyappan M. (2002) Preparation of nucleic acid functionalized carbon nanotube arrays. *Nano Letters* **2**, 1079-1081.

[113] Li J., Ng H. T., Cassell A., Fan W., Chen H., Ye Q., Koehne J., Han J.,. Meyyappan M. (2003) Carbon nanotube nanoelectrode array for ultrasensitive DNA detection. *Nano Letters* **3**, 597-602.

[114] Koehne J., Chen H., Li J., Cassell A. M., Ye Q., Ng H. T., Han J., Meyyappan M. (2003) Ultrasensitive label-free DNA analysis using an electronic chip based on carbon nanotube nanoelectrode arrays. *Nanotechnology* **14**, 1239-1245.

[115] Arumugam P. U., Chen H., Siddiqui S., Weinrich J. A. P., Jejelowo A., Li J., Meyyappan M. (2009) Wafer-scale fabrication of patterned carbon nanofiber nanoelectrode arrays: a route for development of multiplexed, ultrasensitive disposable biosensors. *Biosensors and Bioelectronics* **24**, 2818–2824.

[116] Bidan G. (1992) Electro conducting conjugated polymers: new sensitive matrices to build up chemical or electrochemical sensors. A review. *Sensors and Actuators B* **6**, 45–56.

[117] Lange U., Roznyatovskaya N. V., Mirsky V. M. (2008) Conducting polymers in chemical sensors and arrays. *Analytica Chimica Acta* **614**, 1-26.

[118] Palaniappan S., John A. (2008) Polyaniline materials by emulsion polymerization pathway. *Progress in Polymer Science* **33**, 732-758.

[119] Yoon H. and Jang J. (2009) Conducting-polymer nanomaterials for high-performance sensor applications: issues and challenges. *Advanced Functional Materials* **19**, 1567–1576.

[120] Kuchibhatla S. V.N.T., Karakoti A.S., Bera D., Seal S. (2007) One dimensional nanostructured materials. *Progress in Materials Science* **52**, 699–913.

[121] Cho S., Lee S. B. (2008) Fast electrochemistry of conductive polymer nanotubes: synthesis, mechanism, and application. *Accounts of Chemical Research* **41**, 699-707.

[122] Cao G., Liu D. (2008) Template-based synthesis of nanorod, nanowire, and nanotube arrays. *Advances in Colloid and Interface Science* **136**, 45–64.

[123] Martin C. R. (1996) Membrane-Based Synthesis of Nanomaterials. *Chemistry of Materials* **8**, 1739-1746.

[124] Chen J., Xu Y., Zheng Y., Dai L., Wu H. (2008) The design, synthesis and characterisation of polyaniline nanophase materials. *Comptes Rendus Chimie* **11**, 84-89.

[125] Ahuja T., Mir I. A., Kumar D., Rajesh (2007) Biomolecular immobilisation on conducting polymers for biosensing applications. *Biomaterials* **28**, 791–805.

[126] Cosnier S. (1999) Biomolecule immobilisation on electrode surfaces by entrapment or attachment to electrochemically polymerized films. A review. *Biosensors and Bioelectronics* **14**, 443–456.

[127] Teles F.R.R., Fonseca L.P. (2008) Applications of polymers for biomolecule immobilisation in electrochemical biosensors. *Materials Science and Engineering C* **28**, 1530–1543.

[128] Lahiff E., Woods T., Blau W., Wallace G. G., Diamond D. (2009) Synthesis and characterisation of controllably functionalised polyaniline nanofibers. *Synthetic Metals* **159**, 741–748.

[129] Ramanavicius A., Ramanaviciene A., Malinauskas A. Electrochemical sensors based on conducting polymer-polypyrrole. *Electrochimica Acta* **51**, 6025-6037.

[130] Koopal C. G. J., Feiters M. C., Nolte R. J. M., de Ruiter B., Schasfoort R. B. M. (1992) Glucose sensor utilizing polypyrrole incorporated in tract-etch membranes as the mediator. *Biosensors and Bioelectronics* **7**, 461-471.

[131] Ekanayake E. M. I. M., Preethichandra D. M. G., Kaneto K. (2007) Polypyrrole nanotube array sensor for enhanced adsorption of glucose oxidase in glucose biosensors. *Biosensors and Bioelectronics* **23**,107–113.

[132] Shamsipur M., Kazemi S. H., Mousavi M. F. (2008) Impedance studies of a nano-structured conducting polymer and its application to the design of reliable scaffolds for impedimetric biosensors. *Biosensors and Bioelectronics* **24**, 104–110.

[133] Lupu A., Lisboa P., Valsesia A., Colpo P., Rossi F. (2009) Hydrogen peroxide detection nanosensor array for biosensor development. *Sensors and Actuators B* **137**, 56–61.

[134] Kros A., Nolte R.J.M., Sommerdijk N.A.J.M. (2002) Conducting polymers with confined dimensions: track-etch membranes for amperometric biosensor applications. *Advanced Materials* **14**, 1779-1782.

[135] Park D.H., Kim B.H., Jang M.K., Bae K.Y., Lee S.J., Joo J. (2005) Synthesis and characterisation of polythiophene and poly (3-methylthiophene) nanotubes and nanowires. *Synthetic Metals* **153**, 341-34.

[136] Kros A., van Hövell S. W. F. M, Sommerdijk N. A. J. M., Nolte R. J. M (2001) Poly(3,4-ethylenedioxythiophene)-based glucose biosensors. *Advanced Materials* **13**, 1555-1557.

[137] Liu C., Kuwahara T., Yamazaki R., Shimomura M. (2007) Covalent immobilisation of glucose oxidase on films prepared by electrochemical copolymerization of 3-methylthiophene and thiophene-3-acetic acid for amperometric sensing of glucose: effects of polymerisation conditions on sensing properties. *European Polymer Journal* **43**, 3264–3276.

[138] Park J., Kim H. K., Son Y. (2008) Glucose biosensor constructed from capped conducting microtubules of PEDOT. *Sensors and Actuators B* **133**, 244–250.

[139] Santhosh P., Manesh K. M., Uthayakumar S., Komathi S., Gopalan A. I., Lee K. P. (2009) Fabrication of enzymatic glucose biosensor based on palladium nanoparticles dispersed onto poly(3,4-ethylenedioxythiophene) nanofibers. *Bioelectrochemistry* **75**, 61–66.

[140] Rahman M. A., Kwon N., Won M., Choe E. S., Shim Y. (2005) Functionalized conducting polymer as an enzyme-immobilizing substrate: an amperometric glutamate microbiosensor for in vivo measurements. *Analytical Chemistry*. **77**, 4854-4860.

[141] Ding S., Chao D., Zhang M., Zhang W. (2008) Structure and electrochemical properties of polyamide and polyaniline. *Journal of Applied Polymer Science* **107**, 3408-3412.

[142] Zhang D., Wang Y., (2006) Synthesis and applications of one-dimensional nano-structured polyaniline: an overview. *Material Science and Engineering B* **134**, 9-19.

[143] Virji S., Huang J., Kaner R. B., Weiller B. H. (2004) Polyaniline nanofiber gas sensors: examination of response mechanism. *Nano Letters* **4**, 491–496.

[144] Huang J., Virji S., Weiller B.H., Kaner R.B. (2004) Nanostructured polyaniline sensors. *Chemistry – A European Journal* **10**, 1314–1319.

[145] Morrin A., Ngamna O., Killard A. J., Moulton S. E., Smyth M. R., Fallace G. G. (2005) An amperometric enzyme biosensor fabricated from polyaniline nanoparticles. *Electroanalysis* **17**, 423-430.

[146] Luo X., Vidal G. D., Killard A. J., Morrin A., Smyth M. R. (2007) Nanocauliflowers: a nanostructured polyaniline-modified screen-printed electrode with a self-assembled polystyrene template and its application in an amperometric enzyme biosensor. *Electroanalysis* **19**, 876 – 883.

[147] Du Z., Li C., Li L., Zhang M., Xu S., Wang T. (2009) Simple fabrication of a sensitive hydrogen peroxide biosensor using enzymes immobilized in processable polyaniline nanofibers/chitosan film. *Materials Science and Engineering C* **29**, 1794–1797.

[148] Wang X., Yang T., Feng Y., Jiao K., Li G. (2009) A novel hydrogen peroxide biosensor based on the synergistic effect of Gold-Platinum alloy Nanoparticles/ PolyanilineNanotube/ Chitosan nanocomposite membrane. *Electroanalysis* **21**, 819 – 825.

[149] Granot E., Katz E., Basner B., Willner I. (2005) Enhanced bioelectrocatalysis using Au-nanoparticle/ polyaniline hybrid systems in thin films and microstructured rods assembled on electrodes. *Chemistry of Materials* **17**, 4600–4609.

[150] Zhao M., Wu X., Cai C. (2009) Polyaniline nanofibers: synthesis, characterisation and application to direct electron transfer of glucose oxidase. *Journal of Physical Chemistry C* **113**, 4987–4996.

[151] Horng Y., Hsu Y., Ganguly A., Chen C., Chen L., Chen K. (2009) Direct-growth of polyaniline nanowires for enzyme-immobilisation and glucose detection. *Electrochemistry Communications* **11**, 850–853.

[152] Somerset V., Klink M., Akinyeye R., Michira I., Sekota M., Al-Ahmed A., Baker P., Iwuoha E. (2007) Spectroelectrochemical reactivities of novel polyaniline nanotube pesticide biosensors. *Macromolecular Symposia* **255**, 36–49.

[153] Dhand C., Solanki P. R., Sood K. N., Datta M., Malhotra B. D. (2009) Polyaniline nanotubes for impedimetric triglyceride detection. *Electrochemistry Communications* **11**, 1482–1486.

[154] Ozcan A., Sahin Y., Ozsoz M., Turan S., (2007) Electrochemical Oxidation of ds-DNA on Polypyrrole Nanofiber Modified Pencil Graphite Electrode. *Electroanalysis* **19**, 21, 2208 – 2216.

[155] Ko S., Jang J. (2008) Label-free target DNA recognition using oligonucleotide-functionalized polypyrrole nanotubes. *Ultramicroscopy* **108**, 1328– 1333.

[156] Zhu N., Chang Z., Heb P., Fang Y. (2006) Electrochemically fabricated polyaniline nanowire-modified electrode for voltammetric detection of DNA hybridisation. *Electrochimica Acta* **51**, 3758–3762.

[157] Chang H., Yuan Y., Shi N., Guan Y. (2007) Electrochemical DNA biosensor based on conducting polyaniline nanotube array. *Analytical Chemistry* **79**, 5111-5115.

[158] Feng Y., Yang T., Zhang W., Jiang C., Jiao K. (2008) Enhanced sensitivity for deoxyribonucleic acidelectrochemical impedance sensor: Gold nanoparticle/polyaniline nanotube membranes. *Analytica Chimica Acta* **616**, 144–151.

[159] Zhou N., Yang T., Jiang C., Du M., Jiao K. (2009) Highly sensitive electrochemical impedance spectroscopic detection of DNA hybridisation based on Au_{nano}–CNT/PANnano films. *Talanta* **77**, 1021–1026.

[160] Mosbach K. (1994) Molecular Imprinting. *Trends in Biochemical Science* **19**, 9-14.

[161] Holliger P., Hoogenboom H. R. (1995) Artficial antibodies and enzymes: mimicking nature and beyond. *Trends in Biotechnology* **13**, 7-9.

[162] Wullf G. (1993) The role of binding-site interactions in the molecular imprinting of polymers. *Trends in Biotechnology* **11**, 85-87.

[163] Piletsky S., Turner N. W., Laitenberger P. (2006) Molecularly imprinted polymers in clinical diagnostics—Future potential and existing problems. *Medical Engineering and Physics* **28**, 971–977.

[164] Deore B., Chen Z., Nagaoka T. (1999) Overoxidized polypyrrole with dopant complementary cavities as a new molecularly imprinted polymer matrix. *Analytical Sciences* **15** , 827-828.

[165] Sreenivasan K. (2007) Synthesis and evaluation of multiply templated molecularly imprinted polyaniline. *Journal of Material Science* **42**, 7575-1578.

[166] Deore B., Freund M.S. (2003) Saccharide imprinting of poly(aniline boronic acid) in the presence of fluoride. *Analyst* **128**, 803-806.

[167] Tokonami S., Shiigi H., Nagaoka T. (2009) Review: Micro- and nanosized molecularly imprinted polymers for high-throughput analytical applications. *Analytica Chimica Acta* **641**, 7–13.

[168] Li Y.. Yin X. F,. Chen F. R., Yang H. H., Zhuang Z. X., Wang X. R. (2006) Synthesis of magnetic molecularly imprinted polymer nanowires using a nanoporous alumina template. *Macromolecules* **39**, 4497-4499.

[169] Xie C., Zhang Z., Wang D., Guan G., Gao D., Liu J. (2006) Surface molecular self-assembly strategy for TNT imprinting of polymer nanowire/nanotube arrays. *Analytical Chemistry* **78**, 8339-8346.

[170] Vandevelde F., Belmont A.S., Pantigny J., Haupt K. (2007) Hierarchically nanostructured polymer films based on molecularly imprinted surface-bound nanofilament. *Advance Materials* **19**, 3717-3720.

[171] Agarwal S., Wendorff J. H., Greiner A., Use of electrospinning technique for biomedical applications. *Polymer* **49,** 5603–5621.

[172] Chronakis S., Jakob A., Hagstrom B., Ye L. (2006) Encapsulation and selective recognition of molecularly imprinted theophylline and 17β-estradiol nanoparticles within electrospun polymer nanofibers. *Langmuir* **22**, 8960-8965.

[173] Katz E., Willner I., Wang J. (2004) Electroanalytical and bioelectroanalytical systems based on metal and semiconductor nanoparticles. *Electroanalysis* **16**, 19-42.

[174] Guo S., Wang E. (2007) Synthesis and electrochemical applications of gold nanoparticles. *Analytica Chimica Acta* **598**, 181–192.

[175] Gupta A. K., Gupta M. (2005) Synthesis and surface engineering of iron oxide nanoparticles for biomedical applications. *Biomaterials* **26**, 3995–4021.

[176] Willner I., Basnar B., Willner B. (2007) Nanoparticle-enzyme hybrid systems for nanobiotechnology. *FEBS Journal* **274**, 302–309.

[177] Yan Y., Tel-Vered R., Yehezkeli O., Cheglakov Z., Willner I. (2008) Biocatalytic growth of Au nanoparticles immobilized on glucose oxidase enhances the ferrocene-mediated bioelectrocatalytic oxidation of glucose. *Advanced Materials* **20**, 2365–2370.

[178] Aguì L., Manso J., Yanez-Sedeno P., Pingarron J. M. (2006) Amperometric biosensor for hypoxanthine based on immobilized xanthine oxidase on nanocrystal gold–carbon paste electrodes. *Sensors and Actuators B* **113**, 272-280.

[179] Carralero C., Mena M. L., Gonzalez-Cortes A., Yanez-Sedeno P., Pingarron J. M. (2006) Development of a high analytical performance-tyrosinase biosensor based on a composite graphite–Teflon electrode modified with gold nanoparticles. *Biosensors and Bioelectronics* **22**, 730-736

[180] Yang W., Wang J., Zhao S., Sun Y., Sun C.(2006) Multilayered construction of glucose oxidase and gold nanoparticles on Au electrodes based on layer-by-layer covalent attachment. *Electrochemistry Communications* **8**, 665–672.

[181] Wang S., Tan Y., Zhao D., Liu G. (2008) Amperometric tyrosinase biosensor based on Fe_3O_4 nanoparticles–chitosan nanocomposite. *Biosensors and Bioelectronics* **23**, 1781-1787.

[182] Mavré F., Bontemps M., Ammar-Merah S., Marchal D., Limoges B. (2007) Electrode surface confinement of self-assembled enzyme aggregates using magnetic nanoparticles and its application in bioelectrocatalysis. *Analytical Chemistry* **79**, 187-194.

[183] Pingarron J. M., Yanez-Sedeno P., Gonzalez-Cortes A. (2008) Gold nanoparticle-based electrochemical biosensors. *Electrochimica Acta* **53**, 5848–5866.

[184] Merkoci A. (2007) Electrochemical biosensing with nanoparticles. *FEBS Journal* **274**, 310–316.

[185] Castaneda M. T., Alegret S., Merkoci A. (2007) Electrochemical sensing of DNA using gold nanoparticles. *Electroanalysis* **19**, 743 – 753.

[186] Merkoci A., Aldavert M., Marìn S., Alegret S. (2005) New materials for electrochemical sensing V: Nanoparticles for DNA labelling. *Trends in Analytical Chemistry* **24**, 341-350.

[187] Wang J., Xu D., Kawde A., Polsky R. (2001) Metal nanoparticle-based electrochemical stripping potentiometric detection of DNA hybridisation. *Analytical Chemistry* **73,** 5576–5581.

[188] Wang J., Xu D., Polsky R. (2002) Magnetically-induced solid-state electrochemical detection of DNA hybridisation. *Journal of the American Chemical Society* **124**, 4208–4209.

[189] Pumera M., Castaneda M.T, Pividori M.I., Eritja R., Merkoci A., Alegret S. (2005) Magnetically trigged direct electrochemical detection of DNA hybridisation based Au67 Quantum Dot-DNA-paramagnetic bead conjugate. *Langmuir* **21**, 9625-9629.

[190] Ozsoz M., Erdem A., Kerman K., Ozkan D., Tugrul B., Topcuoglu N., Erken H., Taylan M. (2003) Electrochemical genosensor based on colloidal gold nanoparticles for the detection of factor V Leiden Mutation using disposable pencil graphite electrodes. *Anaytical. Chemistry* **75**, 2181–2187.

[191] Rochelet-Dequaire M., Limoges B., Brossier P. (2006) Subfemtomolar electrochemical detection of target DNA by catalytic enlargement of the hybridized gold nanoparticle labels. *Analyst* **131**, 923-929.

[192] Du P., Li H., Cao W. (2009) Construction of DNA sandwich electrochemical biosensor with nanoPbS and nanoAu tags on magnetic microbeads nanoAu tags on magnetic microbeads. *Biosensors and Bioelectronics* **24**, 3223–3228.

[193] Liu G., Lee T. M. H., Wang J. (2005) Nanocrystal-based bioelectronic coding of single nucleotide polymorphisms. *Journal of the American Chemical Society* **127**, 38–39.

[194] Liu G, Wang J, Kim J & Jan MR (2004) Electrochemical coding for multiplexed immunoassays of proteins. *Analytical Chemistry* **76**, 7126–7130.

[195] Liao K. T., Huang H. J. (2005) Femtomolar immunoassay based on coupling gold nanoparticle enlargement with square wave stripping voltammetry. *Analytica Chimica Acta* **538**, 159-164.

[196] Chu X., Fu X., Chen K., Shen G. L., Yu R. Q. (2005) An electrochemical stripping metallo-immunoassay based on silver-enhanced gold nanoparticle label. *Biosensors and Bioelectronics* **20**, 1805-1812.

[197] Idegami K., Chikae M., Kerman K., Nagatani N., Yuhi T., Endo T., Tamiya E. (2008) Gold nanoparticle-based redox signal enhancement for sensitive detection of human chorionic gonadotropin hormone. *Electroanalysis* **20**, 14-21.

[198] Tang H., Chen J. H., Nie L. H., Kuang Y. F., Yao S. Z. (2007) A label-free electrochemical immunoassay for carcinoembryonic antigen (CEA) based on gold nanoparticles (AuNPs) and nonconductive polymer film. *Biosensors and Bioelectronics* **22**, 1061-1067.

[199] He P., Shen L., Cao Y., Li D. (2007) Ultrasensitive electrochemical detection of proteins by amplification of aptamer-nanoparticle bio bar code. *Analytical Chemistry* **79**, 8024-8029.

[200] Solé S., Merkoci A., Alegret s. (2001) New materials for alectrochemical sensing III. Beads. *Trends in Analytical Chemistry* **20**, 102-110.

[201] Centi S., Laschi S., Mascini M. (2007) Improvement of analytical performances of a disposable electrochemical immunosensor by using magnetic beads. *Talanta* **73**, 394-399.

[202] Centi S., Tombelli S., Minunni M., Mascini M. (2007) Aptamer-based detection of plasma proteins by an electrochemical assay coupled to magnetic beads. *Analytical Chemistry* **79**, 1466-1473.

[203] Centi S., Bonel Sanmartin L., Tombelli S., Palchetti I., Mascini M. (2009) Detection of C Reactive Protein (CRP) in serum by an electrochemical aptamer-based sandwich assay *Electroanalysis* **21**, 1309 – 1315.

[204] Sarkar P., Ghosh D., Bhattacharyay D., Setford S. J., Turner A. P. F. (2008) Electrochemical immunoassay for free prostate specific antigen (f-PSA) using magnetic beads. *Electroanalysis* **20**, 1414 – 1420.

[205] Wang J., Kawde A., Erdem A., Salzar M. (2001) Magnetic bead-based label free electrochemical detection of DNA hybridisation. *Analyst* **126**, 2020-2024.

[206] Wang J., Xu D., Erdem A., Polsky R., Salazar M.A. (2002) Genomagnatic electrochemical assays of DNA hybridisation. *Talanta* **56**, 931-938.

[207] Palecek E., Billovà S., Havran L., Kizek R., Miculkova A., Jelen F. (2002) DNA hybridisation at microbeads with cathodic stripping voltammetric detection. *Talanta* **56**, 919-930.

[208] Palecek E., Fojta M. (2007) Magnetic beads as versatile tools for electrochemical DNA and protein biosensing. *Talanta* **74**, 276-290.

[209] Kawde A. N., Wang J. (2004) Amplified electrical transduction of DNA hybridisation based on polymeric beads loaded with multiple gold nanoparticle tags. *Electroanalysis* **16**, 101-107.

[210] Lermo A., Campoy S., Barbè J., Hernadez S., Alegret S., Pividori M.vI. (2007) *In situ* DNA amplification with magnetic primers for the electrochemical detection of food pathogens. *Biosensors and Bioelectronics* **22,** 2010-2017.

[211] Erdem A., Ariksoysal D. O., Karadeniz H., Kara P., Sengonul A., Sayiner A. A., Ozsoz M. (2005) Electrochemical genomagnetic assay for the detection of hepatitis B virus DNA in polymerase chain reaction amplicons by using disposable sensor technology. *Electrochemistry Communications* **7**, 815-820.

[212] Erdem A., Sayar F., Karadeniz H., Guven G., Ozsoz M., Piskin E. (2007) Development of streptavidin carrying magnetic nanoparticles and their applications in electrochemical nucleic acid sensor systems. *Electroanalysis* **19**, 798-804.

[213] Zhu X., Han K., Li G. (2006) Magnetic nanoparticles applied in electrochemical detection of controllable DNA hybridisation. *Analytical Chemistry* **78**, 2447-2449.

[214] Zhuo Y., Yuan P., Yuan R., Chai Y., Hong C. (2009) Bienzyme functionalized three-layer composite magnetic nanoparticles for electrochemical immunosensors. *Biomaterials* **30**, 2284–2290.

[215] Pal S., Alocilja E. C. (2009) Electrically active polyaniline coated magnetic (EAPM) nanoparticle as novel transducer in biosensor for detection of *Bacillus anthracis* spores in food samples. *Biosensors and Bioelectronics* **24**, 1437–1444.

[216] Rìos A., Escarpa A., Gonzàlez M. C., G. Crevillén A. G. (2006) Challenges of analytical microsystems. *Trends in Analytical Chemistry* **25**, 467-479.

[217] Valentini L., Lozzi L., Cantalini C., Armentano I., Kenny J. M., Ottaviano L., Santucci S. (2003) Effects of oxygen annealing on gas sensing properties of carbon nanotube thin films. *Thin solid films* **436**, 95-100.

[218] Valentini L., Armentano I., Kenny J. M., Cantalini C., Lozzi L., Santucci S. (2003) Sensors for sub-ppm NO_2 gas detection based on carbon nanotube thin films. *Applied Physics Letters* **82**, 961-963.

[219] Rossier J. S., Vollet C., Carnal A., Lagger G., Gobry V., Girault H. H., Michel P, Reymond F. (2002) Plasma etched polymer microelectrochemical systems. *Lab Chip* **2**, 145-150.

[220] Rossier J. S. and Reymond F. (2007) Microfluidic Based Electrochemical Platform for Rapid Immunological Analysis in Small Volumes. In: *Comprehensive Analytical Chemistry Vol 49,* edited by S. Alegret and A. Merkoçi, Elsevier, p. 885-905.

[221] Hoegger D., Morier P., Vollet C., Heini D., Reymond F., Rossier J. S. (2007) Disposable microfluidic ELISA for rapid determination of folic acid content in food products. *Analytical and bioanalytical chemistry* **387**, 267-275.

[222] Liu R. H., Yang J., Lenigk R., Bonanno J., Grodzinski P. (2004) Self-contained, fully integrated biochip for sample preparation polymerase chain reaction amplification and DNA microarray detection. *Analytical Chemistry* **76**, 1824-1831.

[223] Liu D., Perdue R. K., Sun L., Crooks R. M. (2004) Immobilisation of DNA onto poly(dimethylsiloxane) surfaces and application to a microelectrochemical enzyme-amplified DNA Hybridisation Assay. *Langmuir* **20**, 5905-5910.

[224] Fan Z. H., Mangru S., Granzow R., Heaney P., Ho W., Dong Q., Kumar R. (1999) Dynamic DNA hybridisation on a chip using paramagnetic beads. *Analytical Chemistry* **71**, 4851-4859.

[225] Hayes M. A., Polson N. A., Phayre A. N., Garcia A. A. (2001) Flow-based microimmunoassay. *Analytical Chemistry* **73**, 5896-5902.

[226] Gabig-Ciminska M., Holmgren A., Andresen H., Bundvig Barken K., Wümpelmannb M., Albers J., Hintsche R., Breitenstein A., Neubauer P., Lose M., Czyzf A., Wegrzyn G., Silfversparre G., Jürgen B., Schweder T., Enfors S. O. (2004) Electric chips for rapid detection and quantification of nucleic acids. *Biosensors and Bioelectronics* **19**, 537–546.

[227] Kwakye S., Goral V. N., Baeumner A. J. (2006) Electrochemical microfluidic biosensor for nucleic acid detection with integrated minipotentiostat. *Biosensors Bioelectronics* **21**, 2217–2223.

[228] Lakshmi D., Whitcombe M. J., Davis F., Chianella I., Piletska E. V., Guerreiro A., Subrahmanyam S., Brito P. S., Fowler S. A., Piletsky S. A. (2009) Chimeric polymers formed from a monomer capable of free radical, oxidative and electrochemical polymerisation. *Chemical Communications*, 2759-2761.

[229] Lakshmi D., Bossi A., Whitcombe M. J., Davis F., Chianella I., Fowler S. A., Subrahmanyam S., Piletska E. V., Piletsky S. A. (2009) Electrochemical sensor for catechol and dopamine based on a catalytic molecularly imprinted polymer-conducting polymer hybrid recognition element. *Analytical Chemistry* **81**, 3576-3584.

[230] Holzhauser T., Wangorsh A., S.Vieths (2000) Polymerase chain reaction (PCR) for detection of potebtially allergenic hazelnut residues in complex food matrixes. *European Food Research and Technologies* **211**, 360-365.

[231] Skoog D. A., West D. M., Holler F. J., Crouch S. R. (2004) *Fundamentals of Analytical Chemistry,* 8th ed., Thomson Brooks/Cole, USA.

[232] Bard A. J., Faulkner L. R. (2001) *Electrochemical Methods*, 2nd ed., John Wiley & Sons, Inc., USA.

[233] Wang J. (2000) *Analytical electrochemistry*, 2nd ed., John Wiley & Sons, Inc., USA.

[234] Laschi S., Palchetti I., Marrazza G., Mascini M. (2006) Development of disposable low density screen-printed electrode arrays for simultaneous electrochemical measurements of the hybridisation reaction. *Journal of Electroanalytical Chemistry* **593**, 211-218.

[235] Millan K.M., Mikkelsen S.R. (1993) Sequence-Selective biosensor for DNA based on hybridisation indicators. *Analytical Chemistry* **65**, 2317-2323.

[236] Piletsky S. A., Nicholls I. A., Rozhko M. I., Sergeyeva T. A., Piletska E. V., El'Skaya A. V., Karube I. (2005) Molecularly imprinted polymers – tyrosinase mimics. *Ukrainskii Biokhimicheskii Zhurnal* **77**, 63–67.

[237] Emmenegger C., Mauron P., Zuttel A., Nutzenadel C., Schneuwly A., Gallay R., Schlapbach L. (2000) Carbon nanotube synthesised on metallic substrates, *Applied Surface Science* **162-163**, 452-456.

[238] Trojanowicz M. (2006) Analytical applications of carbon nanotubes: a review. *Trends in analytical chemistry* **25**, 480-489.

[239] Wirth C.T., Hofmann S., Robertson J. (2008) Surface properties of vertically aligned carbon nanotube arrays. *Diamond & Related Materials* **17**, 1518–1524.

[240] Musso S., Porro S., Rovere M., Chiodoni A., Tagliaferro A. (2007) Physical and mechanical properties of thick self-standing layers of multiwall carbon nanotubes. *Diamond & Related Materials* **16** 1174–1178.

[241] Wang S. G., Wang R., Sellin P. J., Zhang Q. (2004) DNA biosensors based on self-assembled carbon nanotubes. *Biochemical and Biophysical Research Communications* **325**, 1433-1437.

[242] Kyung S., Lee Y., Kim C., Lee J., Yeom G. (2006) Deposition of carbon nanotubes by capillary-type atmospheric pressure PECVD. *Thin Solid Films* **506– 507**, 268 – 273.

[243] Teng F. Y., Ting J. M., Sharma S. P., Liao K. H. (2008) Growth of CNTs on Fe-Si catalyst prepared on Si and Al coated Si substrates. *Nanotechnology* **19**, 95607-95613.

[244] Li J., Cassell A., Delzeit L., Han J., Meyyappan M. (2002) Novel three-dimensional electrodes: electrochemical properties of carbon nanotube ensembles. *Journal of Physical Chemistry B* **106**, 9299-9305.

[245] Daniel S., Rao T. P., Rao K. S., Rani S. U., Naidu G.R.K., Lee H.-Y., Kawai T. (2007) A review of DNA functionalized/grafted carbon nanotubes and their characterization. *Sensors and Actuators B: Chemical* **122**, 2, 672-682.

[246] Staros J.V., Wright R.W., Swingle D.M. (1986) Enhancement by *N*-hydroxysulfosuccinimide of water-soluble carbodiimide-mediated coupling reactions. *Analytical Biochemistry* **156**, 220.

[247] Wang Z., Liu J., Liang Q., Wang Y., Luo G. (2002) Carbon nanotube-modified electrodes for the simultaneous determination of dopamine and ascorbic acid. *Analyst* **127**, 653–658.

[248] Cai H., Cao X., Jiang Y., He P., Fang Y. (2003) Carbon nanotube-enhanced electrochemical DNA biosensor for DNA hybidisation detection. *Analytical and Bioanalytical Chemistry* **375**, 287-293.

[249] Berti F. (2006) Determination of allergens in food using electrochemical genosensors. (Master degree thesis in Chemistry, University of Florence, Italy. Supervisor: Prof.ssa G. Marrazza).

[250] Mermet J. M., Otto M., Valcarcel M. (2006) *Analytical chemistry : a modern approach to analytical science* 2nd ed., founding editors: R. Kellner, H. M. Widmer, Wiley VHC, Germany.

[251] Pumera M., Merkoci A., Alegret S. (2006) New materials for electrochemical sensing VII. Microfluidic chip platforms. *Trends in Analytical Chemistry* **25**, 219-235.

[252] Kwakye S., Baeumner A. (2003) A microfluidic biosensor based on nucleic acid sequence recognition. *Analytical and Bioanalytical Chemistry* **376**, 1062–1068.

[253] Goral V. N., Zaytseva N. V., Baeumner A. J. (2006) Electrochemical microfluidic biosensor for the detection of nucleic acid sequences. *Lab on a Chip* **6**, 414–421.

[254] Lindfors T., Ivaska A. (2002) Potentiometric and UV/vis characterisation of N-substituted polyanilines. *Journal of Electroanalytical Chemistry* **535** 65-74.

[255] Mazzotta E., Picca R.A., Malitesta C.,. Piletsky S.A, Piletska E.V. (2008) Development of a sensor prepared by entrapment of MIP particles in electrosynthesised polymer films for electrochemical detection of ephedrine *Biosensors and Bioelectronics* **23**,1152-1156.

[256] Jin M., Yu Z., Xia Y. (2006) Electrochemical and spectroelectrochemical studies on aniline in organic medium and its antiknock mechanism. *Russian Journal of Electrochemistry* **42**, 9, 964-968.

[257] Martin C. R. (1995) Template synthesis of electronically conductive polymer nanostructures. *Accounts of Chemical Research* **28**, 61-68.

[258] Vernon-Parry K. D. (2000) Scanning Electron Microscopy: an introduction. *III-Vs Review* **13**, 4, 40-44.

[259] Vernon-Parry K. D. (2000) TEM: an introduction. *III-Vs Review* **13**, 6, 36-40.

[260] Koval I. A., Gamez P., Belle C., Selmeczi K., Reedijk J. (2006) Synthetic models of the active site of catechol oxidase: mechanistic studies. *Chemical Society Reviews* **35**, 814–840.

[261] Onnerfjord P., Emnus J., Marko-Varga G., Gorton L., Ortega F., Dominguez E. (1995) Tyrosinase graphite-epoxy based composite electrodes for detection of phenols. *Biosensors & Bioelectronics* **10,** 607-619.

[262] Quan D., Shin W. (2004) Amperometric detection of catechol and catecholamines by immobilized laccase from DeniLite. *Electroanalysis* **16**, 1576-1582.

[263] Carralero Sanz V., Luz Mena M., Gonzalez-Cortés A., Yànez-Sedeno P.,. Pingarròn J.M (2005) Development of a tyrosinase biosensor based on gold nanoparticles-modified glassy carbon electrodes. Application to the measurement of a bioelectrochemical polyphenols index in wines. *Analytica Chimica Acta* **528**,1–8.

PUBLICATIONS

1. Berti F., Laschi S., Palchetti I., Rossier J. S., Reymond F., Mascini M., Marrazza G. (2009) Microfluidic-based electrochemical genosensor coupled to magnetic beads for hybridization detection. *Talanta* **77**, 3, 971-978.

2. Berti F., Lozzi L., Palchetti I., Santucci S., Marrazza G. (2009) Aligned carbon nanotube thin films for DNA electrochemical sensing. *Electrochimica Acta* **54**, 22, 5035-5041.

3. Berti F., Palchetti I., Marrazza G., Mascini M., Lozzi L., Santucci S., Baratto C., Comini E., Todros S., Faglia G., Sberveglieri G. (2008) New nanostructures for genosensing. In: *Sensors and Microsystems, Proceedings of 13th italian conference, Rome Italy, 19 - 21 February 2008*, World Scientific Publishing, Singapore, p. 63-67.

-

4. Palchetti I., Berti F., Laschi S., Marrazza G., Mascini M. Electrochemical characterization of PNA/DNA hybridized layer using SECM and EIS techniques. In: *Sensors and Microsystems, AISEM 2009 Proceedings, Series: Lecture Notes in Electrical Engineering , Vol. 54*, Springer, Germany (in press, december 2009).

5. Berti F., Todros S., Lakshmi D.,. Whitcombe M. J, Chianella I., Ferroni M., Marrazza G., Piletsky S. A., Turner A. P. F. Quasi-monodimensional polyaniline nanostructures for enhanced molecularly imprinted polymer-based sensing (submitted to *Biosensors and Bioelectronics*, december 2009).

Talanta 77 (2009) 971–978

Contents lists available at ScienceDirect

Talanta

journal homepage: www.elsevier.com/locate/talanta

Microfluidic-based electrochemical genosensor coupled to magnetic beads for hybridization detection

Francesca Berti[a], Serena Laschi[a], Ilaria Palchetti[a], Joël S. Rossier[b], Frédéric Reymond[b], Marco Mascini[a,c], Giovanna Marrazza[a,*]

[a] Università degli Studi di Firenze, Dipartimento di Chimica, Via della Lastruccia 3, 50019 Sesto Fiorentino, Italy
[b] DiagnoSwiss S.A., Rte de l'Ile-au-Bois 2, 1870 Monthey, Switzerland
[c] Istituto Nazionale Biostrutture e Biosistemi (INBB), Unit of Florence, Viale delle Medaglie d'Oro 305, 00136, Roma, Italy

ARTICLE INFO

Article history:
Received 19 March 2008
Received in revised form 21 July 2008
Accepted 26 July 2008
Available online 14 August 2008

Keywords:
Electroanalytical methods
Genosensor
Magnetic beads
Microfluidics
Microfabrication
Nanoelectrode array
Allergen detection

ABSTRACT

This paper describes the development of a rapid and sensitive enzyme-linked electrochemical genosensor using a novel microfluidic-based platform. In this work, hybridization was performed on streptavidin-coated paramagnetic micro-beads functionalized with a biotinylated capture probe. The complementary sequence was then recognized via sandwich hybridization with a capture probe and a biotinylated signaling probe. After labeling the biotinylated hybrid with a streptavidin–alkaline phosphatase conjugate, the beads were introduced in a disposable cartridge composed of eight parallel microchannels etched in a polyimide substrate. The modified beads were trapped with a magnet addressing each microchannel individually. The presence of microelectrodes in each channel allowed direct electrochemical detection of the enzymatic product within the microchannel. Detection was performed in parallel within the eight microchannels, giving rise to the possibility of performing a multiparameter assay. Quantitative determinations of the analyte concentrations were obtained by following the kinetics of the enzymatic reaction in each channel. The chip was regenerated after each assay by removing the magnet and thus releasing the magnetic beads. The system was applied to the analytical detection of PCR amplified samples with a RSD% = 6. A detection limit of 0.2 nM was evaluated.

1. Introduction

In the last decade, several procedures and applications have been developed in order to obtain simple and portable devices for DNA diagnostics. In this context electrochemical genosensors couple the selectivity of the hybridization event with the sensitivity, compatibility with micro-fabrication, low cost and portability of electrochemical devices [1]. However, a recurring problem with electrochemical DNA detection is the background interference. The absorption of non-specific DNA sequences or enzymatic labels at the electrode surface, in fact, can reduce the sensitivity of the assay. To overcome this problem, in the past few years many researchers exploited the possibility of performing the hybridization event on the surface of paramagnetic micro- and nano-beads and several formats of magnetic bead-based electrochemical genosensors have been reported in literature [2–9]. Both label-free and enzyme-linked methods have been proposed by Wang et al. [2,3,6]. Palecek et al. [4] showed an enzyme-linked immunoassay for the detection of DNA hybridization event performed on paramagnetic beads with covalently bound a $(dT)_{25}$ probe, able to hybridize with target DNAs containing adenine stretches. Target DNAs were modified with osmium tetroxide,2,2′-bipyridine and the immunogenic DNA-Os, bipy adducts were determined by enzyme-linked immunoassay or, alternatively, by direct measurement of the Osmium signal by square wave voltammetry. Another interesting way to amplify the electrical signal was found by Kawde and Wang [7], who achieved a detection limit of 0.1 ng/mL using oligonucleotides functionalized with polymeric beads carrying gold nanoparticles. Lermo et al. [8] developed a genomagnetic assay for the detection of food pathogens based on a graphite–epoxy composite magneto electrode (m-GEC) as electrochemical transducer. The assay was performed in a sandwich format by double labeling the amplicon ends during PCR with a biotinylated capture probe, to achieve the immobilization on streptavidin-coated magnetic beads and a digoxigenin signaling probe, to achieve further labeling with the enzyme marker (anti-digoxigenin horseradish peroxidase).

These examples show interesting features; however, a significant challenge for all biosensor systems is minimizing sample preparation, requirements, operational complexity and time. Microfluidic-based platforms show great potential in responding

* Corresponding author. Tel.: +39 0554573320; fax: +39 0554573396.
E-mail address: giovanna.marrazza@unifi.it (G. Marrazza).

0039-9140/$ – see front matter © 2008 Elsevier B.V. All rights reserved.
doi:10.1016/j.talanta.2008.07.064

to these demands due to significant decrease in sample/reagent consumption and cost, and dramatically reduction in time [10]. Therefore, microfluidic devices have found great application in the proteomic [11,12] and genomic area [13,14]. Further advantages have been demonstrated by incorporating paramagnetic beads as transportable solid support [15–17]: analytes were captured by probe (i.e. DNA)-modified beads in flow through format. Small-diameter particles, in fact, help to enhance the surface area-to-volume ratio thus increasing the sensitivity. Moreover, magnetic properties greatly facilitate the delivery and removal of reagents through the microfluidic channels.

In this work, we report the development of a rapid and sensitive enzyme-linked electrochemical genosensor using a commercially available microfluidic-based platform. This was obtained by integrating the existing technology with a new electroanalytical procedure based on the use of paramagnetic beads. The proposed assay allowed the rapid analysis of PCR amplicons.

Only few examples of analytical procedures based on microfluidic platform coupled to paramagnetic beads for hybridization electrochemical detection were reported in literature [18,19]. Baeumner and co-workers [18] reported an interesting approach based on liposomes entrapping the electrochemical marker (ferro/ferricyanide couple).

The novelty of the proposed procedure was the combination of a sensitive electrochemical platform and a proper microfluidic with a simple and effective enzyme signal amplification technology.

In our approach, streptavidin-coated paramagnetic micro-beads were modified with a biotinylated capture probe. The complementary sequence was then recognized via sandwich hybridization with a capture probe and a biotinylated signaling probe. After labeling the biotinylated hybrid with a streptavidin–alkaline phosphatase conjugate, the particles were introduced in a disposable cartridge composed of eight parallel microchannels etched in a polyimide substrate (called chip) [20]. The modified particles were trapped with a magnet addressing each microchannel individually. The presence of microelectrodes in each channel allowed direct electrochemical detection of the enzymatic product within the microchannel. Detection was performed in parallel within the eight microchannels, giving rise to the possibility of performing a multiparameter assay. Quantitative determinations of the analyte concentrations were obtained by following the kinetics of the enzymatic reaction in each channel. The chip was regenerated after each assay by removing the magnet and thus releasing the magnetic beads. The system was applied to the analytical detection of PCR amplified samples. Our attention was focused on the detection of a 182 bp fragment of Cor a 1.04, the major hazelnut allergen [21–25].

The assay was also carried out using disposable electrochemical sensors as electrochemical transducers to optimize some parameters such as hybridization time, enzyme concentration and incubation.

2. Materials and methods

2.1. Reagents

Dithiothreitol (DTT), streptavidin–alkaline phosphatase, α-naphthyl phosphate, bovine serum albumin (BSA), magnesium chloride and diethanolamine were obtained from Sigma–Aldrich. Disodium hydrogenphosphate, ethylendiamine tetraacetic acid (EDTA) and potassium chloride were purchased from Merck. MilliQ water was used throughout this work. TE buffer 20× (200 mmol/L Tris/HCl; 20 mmol/L EDTA; pH 7.5), Picogreen and λ-DNA standard solution (100 μg/mL), used for fluorescent measurements, were obtained from Molecular Probes.

p-Aminophenyl phosphate was purchased from DiagnoSwiss S. A. (Monthey, Switzerland). Streptavidin-coated paramagnetic beads (iron oxide particles with the diameter of approximately 1.0 ± 0.5 μm) were purchased from Promega (USA). Synthetic oligonucleotides were obtained from MWG Biotech AG. Genomic DNA from hazelnut was obtained using the extraction kit Sure Food PREP-Allergen (Congen). *Taq* polymerase, dNTP mixture and PCR buffer were obtained from Takara. The sequences of synthetic oligonucleotides, PCR primers and the PCR amplicon are reported below:

Capture probe (24 mer): biotin-5′-GGA GAT CGA CCA CGC AAA CTT CAA-3′ Signaling probe (20 mer): 5′-ATA CTG CTA CAG CAT CAT CG-TEG-biotin-3′ where TEG (tetra-ethyleneglycol) was used as spacer arm Forward primer (24 mer): 5′-GGA GAT CGA CCA CGC AAA CTT CAA-3′ Reverse primer (23 mer): 5′-CCT CCT CAT TGA TTG AAG CGT TG-3′ PCR amplified fragment of the Cor a 1.04 gene (182 bp) of hazelnut: 5′-GGAGATCGACCACGCAAACTTCAAATACTG-CTACAGCATCATCGAGGGAGGTCCA TTGGGGCACACACTGGAGAAGA-TCTCTTACGAGATCAAGATGGCGGCAGCCCCTCATGGAGGAGGATCCA TCTTGAAGATCACCAGCAAGTACCACACCAAGGGCAACGCTTCAATCAA TGAGGAGG-3′.

2.2. Disposable screen-printed electrodes

Screen-printed electrochemical cell (SPEC) consists of a carbon working electrode, a carbon counter electrode and a silver pseudo-reference electrode. Materials and procedures to screen-print the transducers are described elsewhere [26].

The DPV electrochemical measurements were performed with μAutolab type II PGSTAT with a GPES 4.9 software package (Metrohm, Rome, Italy). All potentials were referred to the Ag/AgCl pseudo-reference electrode. All experiments were carried out at room temperature (25 °C).

To perform electrochemical measurement SPECs were kept horizontally and a magnet holding block was placed on the bottom part of the electrode, to better localize the beads onto the working surface. Then a known volume of a solution containing the enzymatic substrate was added on the SPEC surface to close the electrochemical cell. In further sections these disposable electrochemical sensors will be called “drop-on system”.

2.3. Microfluidic-based platform

A microfluidic-based platform, produced by DiagnoSwiss S.A., was used. This platform consists of a disposable cartridge called ImmuChip™, an instrument called ImmuSpeed™ and its associated software ImmuSoft™.

ImmuChip™ consists of eight parallel microchannels etched in a polyimide substrate at distances compatible with conventional 96-well plate automation [11]. The fabrication process of the microchannel systems was described elsewhere [11,12]. Each microchannel contains a housing with a sample deposition reservoir (well), and it was etched in a polyimide body with inlet/outlet in contact with microelectrode tracks. The microchannels have a length of 1 cm and a total volume of 65 nL. The upper part of each channel contains an array of 48 gold working microelectrodes. A counter electrode and an Ag/AgCl pseudo-reference electrode are placed at the bottom of the well, near the channel entrance. ImmuChip™, called simply chip throughout the text, is shown in the Fig. 1A.

ImmuSpeed™ is composed of an interface to plug the disposable cartridge, a temperature controller, a multichannel pumping device and valves as well as a multiplexer electrochemical detector for sequential detection occurring in each of the eight channels (Fig. 1B).

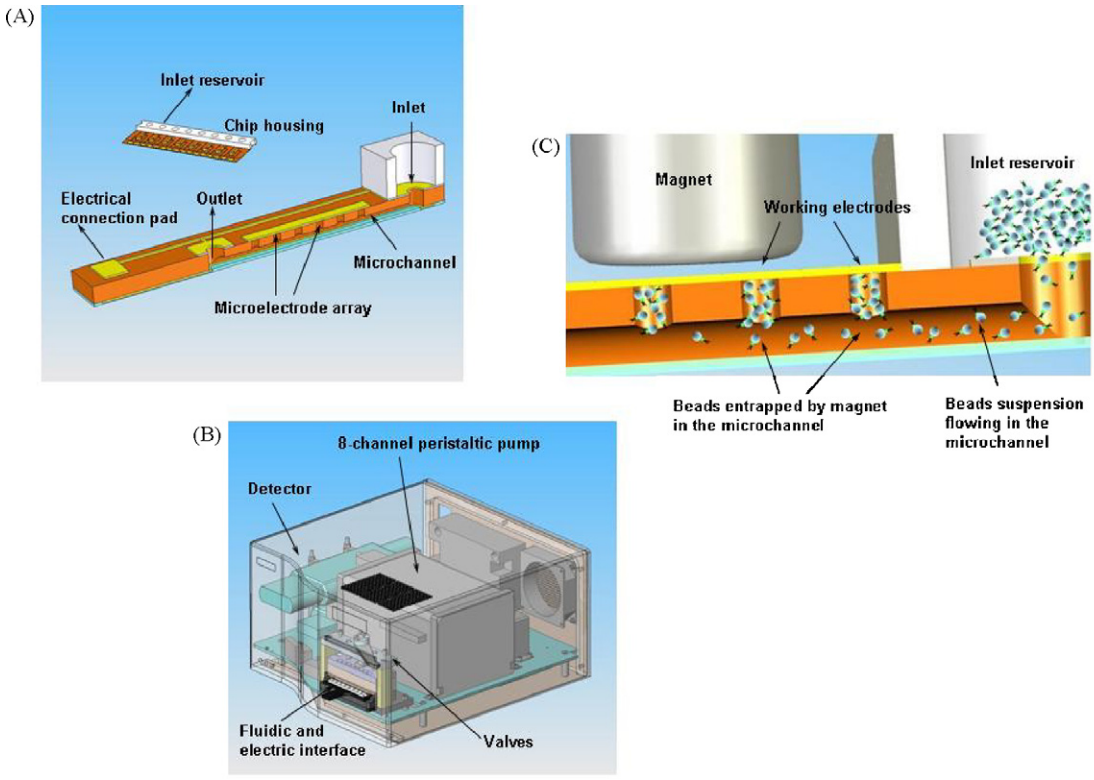

Fig. 1. (A) Technical drawing of the chip: ImmuChip™; (B) technical drawing of the microfluidic-based platform ImmuSpeed™; (C) technical drawing of a microchannel cross-section with flowing magnetic beads being captured by a magnet.

A special software (ImmuSoft™) has been created to integrate the fluidic and the electrochemical detection. The software enables the application of independent protocols in the different channels. Sample and reagent solutions are aspirated from the inlet reservoir through the reaction channel to the waste, but the solution flow can be directed in both directions, allowing the construction of protocols with back flow. The fluidic can also be regulated in order to alternate times in which the liquid flows into the channels with times where the solution remains static: in this case parameters as well as the time during which the liquid should flow through the channels, the flow rate and the turnover at which this mode should be repeated, in order to have more "loading cycles", can be also varied. This last procedure allows to increase the contact time of the solution with the well of channels and ensures an efficient steady state of the solutions during the incubation and/or detection steps.

An electrochemical detection step is then added to complete the protocol. This is performed by real-time chronoamperometric technique, in which the kinetics of the enzyme-label reaction are followed, by measuring the current alternatively on each channel and then reporting it vs. time. Detection parameters are introduced to the protocol by the user. Apart from the applied potential, parameters that can be tuned are the time interval between two chronoamperometric measurements as well as the number of such measurements cycles, which are influencing the duration of each measurement (acquisition time).

In this particular application, the chip was integrated with a dedicated magnet to capture the beads into the channel, as described in Fig. 1C. Eight cylinder magnets, supported in a bar, were inserted between the chip and instrument interface in order to capture the beads flowing through the channel at the electrode position.

All experiments were carried out at 37 °C.

2.4. DNA modification of streptavidin-coated paramagnetic beads

The modification of the beads with biotinylated capture probe was carried out on aliquots of 0.75 mL, containing 1 mg/mL of beads. The beads were washed three times with 600 μL of phosphate buffer 0.5 M, pH 7.0 (using a magnetic particle concentrator – MagneSphere Magnetic Separation Stand, Promega) and re-suspended in 500 μL of buffer containing 1.0 nmol of capture probe/mg of beads. After an incubation of 30 min, under continuous mixing, the beads were washed three times with phosphate buffer. Finally, the modified beads were incubated for 15 min with 500 μL of 500 μM solution of biotin in phosphate buffer, to block the remaining streptavidin active sites on the probe-functionalized surface, in order to prevent the undesired binding of other biotinylated oligonucleotides. After the treatment, the beads were then washed three times with phosphate buffer and re-suspended to 1 mg/mL in buffer. The modified beads can be stored at 4 °C until use [6]. Their stability was experimentally demonstrated by hybridization experiments performed using the same aliquot of beads freshly modified, after 1 week and after 1 month. By comparing signals obtained for a 5 nM oligonucleotide target sequence (100 ± 4 nA for freshly modified beads, 95 ± 1 nA after 1 week, 90 ± 2 nA after 1 month) only a 10% decrease was observed after 1 month.

2.5. PCR amplification

The conditions for the PCR amplification of the gene sequence codifying for Cor a 1.04 allergen were adapted from the procedure reported in literature [24]. The DNA template was extracted from raw hazelnuts using the commercial kit Sure Food PREP-Allergen (Congen), according to the manufacturer's instructions. The PCR reaction was carried out in a final volume of 50 μL containing PCR buffer 1× 1.5 mM $MgCl_2$, 1.2 U/mL of *Taq* polymerase, 200 μM of

dNTPs (deoxyribonucleotide triphosphates), 0.25 μM of forward primer, 0.25 μM of reverse primer and 500 ng of genomic DNA. The PCR was performed with a MJ Research PTC 150 thermocycler (MJ Research Inc.) using the following conditions: activation of *Taq* polymerase at 95 °C for 5 min, followed by a 40 two-step cycles (94 °C for 30 s, 63 °C for 30 s) and a final extension at 72 °C for 10 min. Prior to use, PCR amplicons were purified using Millipore Montage PCR centrifugal filter devices according to the manufacturer's protocol. Their concentration was finally determined by fluorescence measurements using the Picogreen dye and a TD-700 fluorometer (Analytical Control).

2.6. Hybridization procedure

Hybridization experiments were carried out in a sandwich-like format (see Fig. 2). Synthetic target and PCR amplicons were diluted with a solution 0.15 μM of biotinylated signaling probe in phosphate buffer. In the case of PCR amplicon, the double-stranded DNA was thermally denaturated by using a boiling water bath (5 min at 100 °C); amplicon strand re-annealing was retarded by cooling the sample in an ice-water bath for 1 min. Both the PCR blank and non-complementary PCR products were used as negative controls. For every assay 20 μL of probe-modified beads were employed. Using the magnetic particle concentrator, the buffer was removed carefully and then the beads were incubated with 50 μL of the hybridization solution for 15 min. After hybridization, the beads were washed three times with 100 μL of DEA buffer (0.1 M diethanolamine, 1 mM $MgCl_2$, 0.1 M KCl; pH 9.6), to remove non-specifically adsorbed sequences.

2.7. Labeling with alkaline phosphatase

After the hybridization and washing steps, the beads were incubated with 50 μL of a solution containing 0.75 U/mL of the streptavidin–alkaline phosphatase conjugate and 10 mg/mL of BSA (blocking agent) in DEA buffer. After 20 min, beads were washed three times with 100 μL of DEA buffer.

2.8. Electrochemical detection: drop-on system

After washing, the beads were re-suspended in 25 μL. The electrochemical measurements were performed by placing a magnetic particle concentrator under the SPEC; 10 μL of enzyme-labeled bead suspension was deposited on the working electrode surface, and the liquid was carefully removed with a pipette without touching the electrodes. Then, the planar electrochemical cell was covered with 50 μL of 1 mg/mL α-naphthyl phosphate in DEA buffer. After 5 min, the electrochemical signal of the enzymatically produced α-naphthol was measured by DPV (modulation time 0.05 s; interval time 0.15 s; step potential 5 mV; modulation amplitude 70 mV; potential scan from 0 to +0.6 V). Upon scanning the potential, the α-naphthol was irreversibly converted into an electro polymerized derivative; the height of its oxidation peak was taken as the analytical signal. Reported results are the average of at least three measurements and the error bars correspond to the standard deviation.

2.9. Electrochemical detection: microfluidic-based platform

After washing, the beads were re-suspended in 135 μL. A volume of 20 μL of bead suspension was added in each inlet reservoir of the ImmuChip™. The solution was then introduced in the microchannels by applying the optimized loading cycles; during the loading cycles, a suitable magnet was used in order to allow for the blocking of the beads within each microchannel. Once all the suspensions were introduced and the beads captured, the substrate solution was added. Following the manufacturer's instructions, *p*-aminophenyl phosphate (10 mM in DEA buffer) was used as enzymatic substrate.

The chronoamperometric measurement of the enzyme kinetics was performed in a static mode, i.e. without flow. The eight channels were then sequentially measured, each 2 s, at a potential of +250 mV vs. Ag/AgCl, for a total acquisition time of 3 min; in this way many measuring cycles are recorded, and a plot of current as function of time is obtained for each channel. The slope of the linear portion of the plot, which is a direct measure of the *p*-aminophenol concentration and hence of the enzyme concentration, was used as analytical data. An example of enzyme kinetics acquisition data, obtained by adsorbing only alkaline phosphatase enzyme in the microchannels, is reported in the Fig. 3. The data elaboration was performed using the software incorporated in the DataFitX fitting tool (Oakdale Engineering, USA).

3. Results and discussion

3.1. Optimization of magnetic bead-genosensor assay using drop-on system

The magnetic beads assay scheme is shown in Fig. 2. Preliminary experiments were performed using disposable electrochemical sensors in order to optimize some parameters (i.e. modification of beads, assay times and procedures). This allowed us to control the reliability of the DNA beads modification process with an experimental set-up already tested for other analytical applications [27] and thus by avoiding any effect due to flow conditions. The experiments were performed using 10 nM solution of hazelnut amplicon corresponding to Cor a 1.04 gene.

The influence of the probe concentration was firstly investigated. The declared binding capacity of paramagnetic beads is 0.75 nmol of biotinylated oligonucleotides/mg of beads. However, in the analysis of long, double stranded sequences, as PCR products, the base-pair recognition might be decreased by electrostatic repulsions and the high steric interference. By varying the probe concentration, different densities of biorecognition sites can be obtained on the beads with, consequently, variations in hybridization efficiency. The experiment was performed by modifying five aliquots of beads with different concentrations of capture probe solution (0.15, 0.75, 1.0, 3.2, 7.5 nmol/mg). Results obtained (not shown) demonstrated that using a solution of 1 nmol/mg a good compromise between intensity of signal and amount of employed reagents could be achieved. The analytical signal obtained was, in fact, $1.3 \times 10^{-8} \pm 2 \times 10^{-9}$ A, whereas for lowest concentration tested (0.15 nmol/mg) was $0.70 \times 10^{-8} \pm 3 \times 10^{-9}$ A and for the highest (7.5 nmol/mg) a value of $1.5 \times 10^{-8} \pm 3 \times 10^{-9}$ A was obtained.

Afterwards, the hybridization time was optimized. Probe-modified and biotin-blocked beads (20 μg) were incubated with 50 μL of the hybridization solution for 10, 15, 30, 45, 60 min. As reported in Fig. 4, the hybridization occurred with maximum efficiency after 15 min. The reported results exhibit very low specific vs. non-specific signal ratio. Thus, 15 min of incubation time was used for further measurements.

Then, the labeling step was investigated. Thus, five aliquots of beads, modified with biotinylated hybrid, were exposed to 50 μL of solution containing different concentrations of streptavidin–alkaline phosphatase and 10 mg/mL of BSA in DEA buffer. As reported in Fig. 5, signal shows a dramatic increase with the enzyme concentration. Only for concentrations higher than 0.75 U/mL a considerable signal amplification can be observed. Probably for a small amount of enzyme, which is moreover dis-

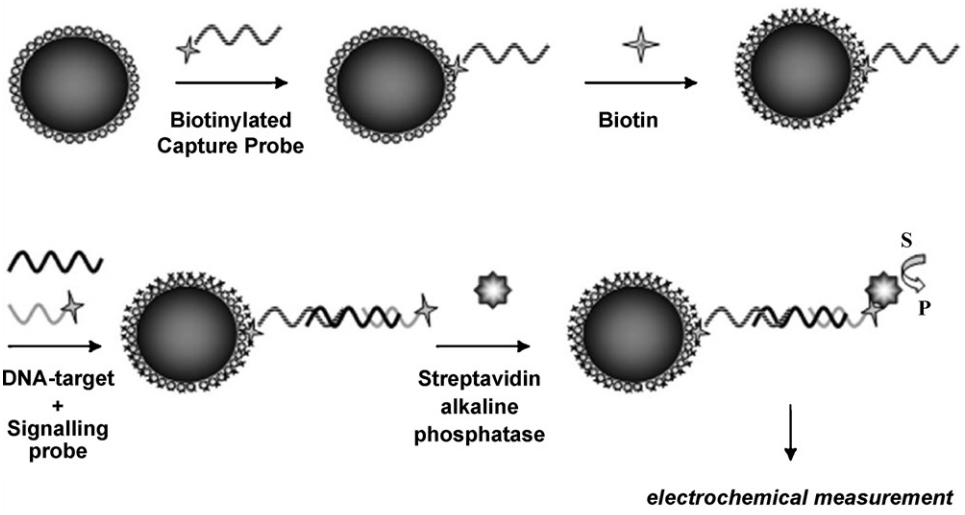

Fig. 2. Scheme of the genomagnetic assay: streptavidin-coated paramagnetic microparticles were functionalized with a biotinylated capture probe and the remaining streptavidin active sites were blocked with biotin. The complementary sequence was hybridized with capture probe in the presence of a biotinylated signaling probe. The biotinylated hybrid was labeled with a streptavin–alkaline phosphatase conjugate. Subsequently, the particles were magnetically absorbed onto the working electrode. The electrochemical cell was then covered with the substrate and the enzymatic product was measured.

persed in a highly viscous solution (BSA), the kinetic of association with biotinylated hybrid is too slow. The best specific vs. non-specific signal ratio (20:1) was obtained for a concentration of 0.75 U/mL of streptavidin–alkaline phosphatase. This concentration was used for further experiments. The influence of the enzyme–biotin association time on analytical signal was finally examined. Results are showed in Fig. 6. The kinetics of reaction appear very fast since high analytical signal can be observed after very short times. The optimal value was found to be 10 min for the enzyme–biotin association time and no relevant increasing of the signal can be observed for longer periods.

A calibration experiment of PCR amplicons was finally performed using the optimized conditions. The voltammetric response increased with the target concentration up to 10 nmol/L ($r^2 = 0.98$), then slowly decreased (Fig. 7). This behavior has been elsewhere explained as a consequence of the re-annealing of the two complementary strands [28]. When the amount of target in solution is relatively high, random collisions of reagents make re-annealing of the two complementary sequences favored over formation of the probe-amplicon hybrid. The non-specific signal, obtained using a non-complementary sequence, resulted negligible even at the highest investigated concentration, thus confirming the good selectivity of the genosensor.

The reproducibility of the measurements (evaluated as relative standard deviation over 8 results for a 10 nmol/L solution) was 8%.

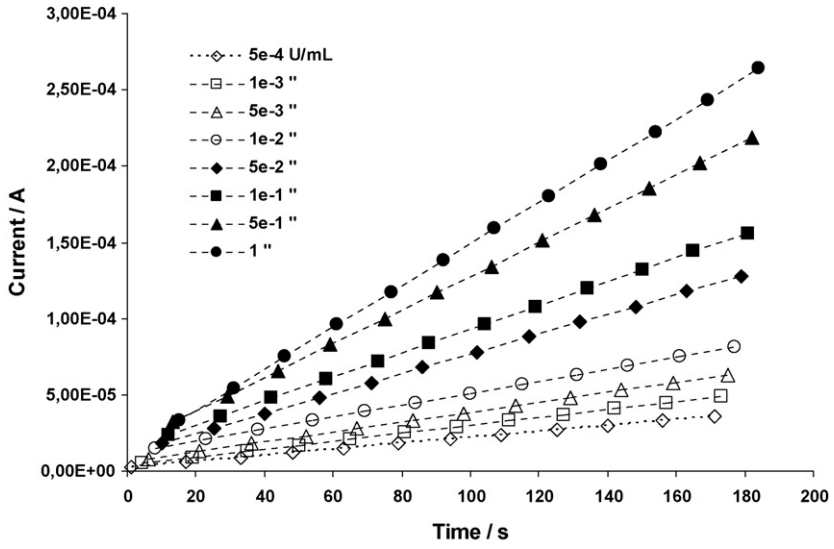

Fig. 3. Chrono-amperometric detection of enzyme kinetics in a chip. The experiment was performed by adsorbing on the walls of the microchannels different amounts of alkaline phosphatase (from 1 to 5 10^{-4} U/mL, in channel from 1 to 8) and then introducing the enzyme substrate. Each symbol represents a single current acquisition value. Data were then elaborated using the DataFitX fitting tool, obtaining for each channel a plot of current as a function of time. The slope of the linear portion of the plot, which is a direct measure of the *p*-aminophenol concentration and hence of the enzyme concentration, was used as analytical data. The chrono-amperometric detection was performed at +250 mV vs. Ag/AgCl.

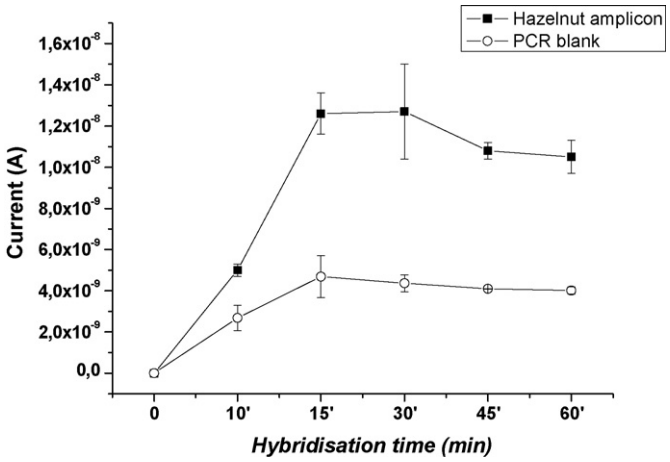

Fig. 4. Influence of hybridization time on the analytical signal. 20 μg of probe-modified and biotin-blocked beads were incubated with 50 μL of the hybridization solution for 15, 30, 45, 60 min. The experiments were performed using drop-on system. See detail in the text.

3.2. Procedure optimization using microfluidic-based platform

Key parameters to test the magnetic bead-based genosensor in the microfluidic-based platform were the procedure for bead capture in the microchannel of the chip and protocols for the electrochemical evaluation of the enzyme kinetic. This set of experiments was performed using beads modified with a target concentration of 10 nM and the assay conditions as optimized in paragraph 3.1.

The first set of experiments was devoted to develop a suitable procedure for beads capture within the microchannels. For this reason, two different loading operations were compared. The experiments were performed by depositing a volume of 20 μL of beads suspension into each of the eight inlet reservoirs of a chip. In the first loading protocol, after placing the magnet, as illustrated in Fig. 1C, a flow rate of 10 μL/min was applied for 2 min until the bead suspension was completely introduced into each channel. The flow was, then, reversed and kept at a rate of 5 μL/min in order to allow the complete capture of the beads. After 4 min, the solution was removed from the wells, and 20 μL of 20 mM *p*-aminophenyl phosphate was added and introduced into the channel at a flow rate of 2 μL/min. After 30 s, the flow was stopped and sequential chronoamperometric measurements of 2 s for a total time of 6 min were carried out. The same experiment was performed with two different bead suspension amounts (1 and 3 mg/mL, respectively); results demonstrated that this strategy was characterized by low reproducibility for both amounts and it was considered as not useful (data not shown). Thus, more loading cycles were introduced and the reverse phase was eliminated, in order to increase the efficiency of the assay. In this approach, each loading step comprised 2 s at 2 μL/min flow through and 3 s of steady state without flow. A total number of 100 loading cycles was used, and then the electrochemical detection step was carried out as previously. Four different

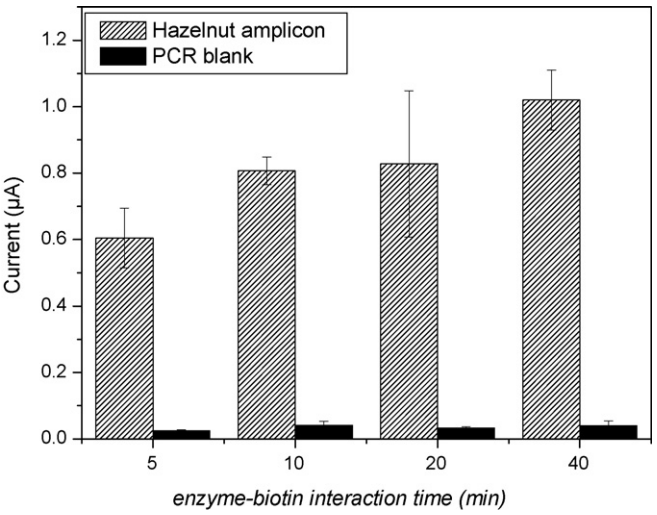

Fig. 6. Influence of enzyme–biotin interaction time on the analytical signal. After the hybridization step, beads were incubated with 50 μl of solution containing 0.75 of streptavidin-alkaline phosphatase and 10 mg/ml of BSA in DEA buffer for different times (5, 10, 20, 40 min.). Then, the cell was covered with 50 μL of 1 mg/ml α-naphthyl phosphate in DEA buffer and incubate for 5 min. The experiments were performed using drop-on system. See detail in the text.

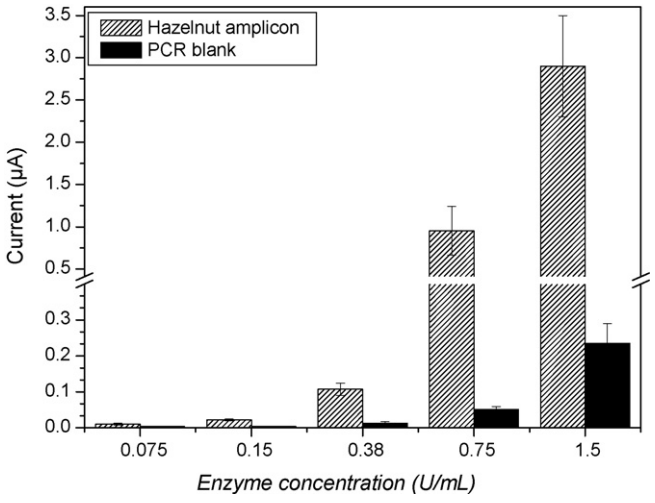

Fig. 5. Influence of enzymatic conjugate concentration on the analytical signal. After the hybridization step, beads were incubated with 50 μl of solution containing different concentrations (0.075, 0.15, 0.38, 0.75, 1.5 U/ml) of the streptavidin–alkaline phosphatase conjugate and 10 mg/ml of BSA (blocking agent) in DEA buffer for 20 min. The experiments were performed using drop-on system. See detail in the text.

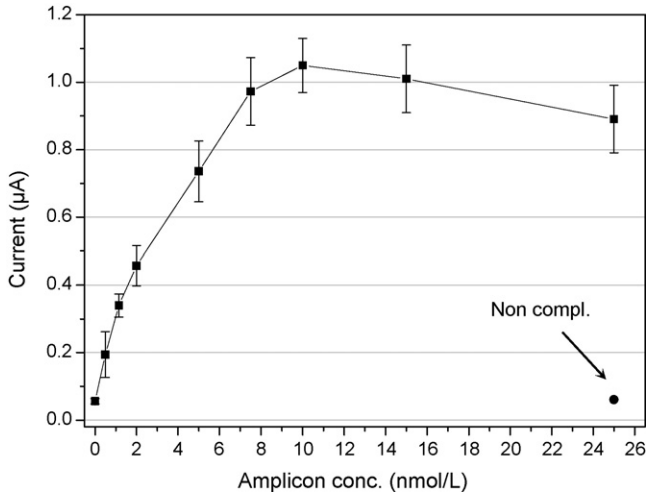

Fig. 7. Calibration plot for Cor a 1.04 amplicons. Probe-modified and biotin-blocked beads were incubated for 15 min with 50 μL of thermally denatured target solutions, diluted to the desired concentration (0, 1, 2, 5, 7.5, 10, 15, 25 nmol/L) with a solution 0.15 μM of a biotinylated signaling probe in phosphate buffer. The experiments were performed using drop-on system. See detail in the text.

Table 1
Evaluation of *p*-aminophenyl phosphate concentration on the sensitivity of the assay

PAPP concentration (mM)	Acquisition time: 3 min	
	Linear slope (μA/s)	r^2
20	$(9.4 \pm 0.3) \times 10^{-8}$	0.999
10	$(4.2 \pm 0.6) \times 10^{-6}$	0.990
5	$(5.1 \pm 1.2) \times 10^{-7}$	0.55

Experiments were performed with the microfluidic-based electrochemical platform. Other details in the text.

bead suspensions (0.15, 0.5, 1.0, 3.0 mg/mL) were tested. The higher sensitivity was obtained by decreasing the beads amount (data not shown). These results could be due to the fact that high amount of beads reduced the flow efficiency into the microchannels. For 0.5 mg/mL beads suspension, a sensitivity of $(4 \pm 1) \times 10^{-6}$ A/nM was observed; this was the highest sensitivity obtained, but associated with a large standard deviation (RSD% = 25). The best result was obtained for a concentration of 0.15 mg/mL, where a lower slope was observed (2×10^{-6} A/nM) but with the highest reproducibility (RSD% = 10, $n = 8$). This amount of beads was then used for further experiments.

Finally, the concentration of *p*-aminophenyl phosphate was optimized in order to get the higher sensitivity and to avoid the inhibition of the enzymatic activity due to the substrate concentration excess. During the electrochemical measurement step, three different *p*-aminophenyl phosphate concentrations were used, in combination with two different acquisition times, 6 and 3 min, respectively. In the case of 6 min it was found that, between the three *p*-aminophenyl phosphate concentrations tested (20, 10 and 0.5 mM), a linear slope trend ($r^2 = 0.999$) was obtained only for the 20 mM concentration. Otherwise, by decreasing the data acquisition time from 6 to 3 min, a higher sensitivity with a good linear correlation ($r^2 = 0.990$) was obtained for 10 mM as substrate concentration (Table 1). Thus, this concentration was then used for the assay, taking advantage from the minor reagent consumption coupled with a shorter detection time.

3.3. Analysis of PCR-amplified samples

Experiments of PCR amplicons were then performed. Different amplicon concentrations (0, 2, 5, 10, 15, 20, 30 nM) and a 30 nM of non-specific sequence solution were analyzed. Each concentration was tested in a different channel. After measurement, the magnet was removed and the microchannels were washed with deionized water for 5 min with a flow rate of 5 μL/min. Then, fresh aliquots of beads were added in the microchannels and measurements were repeated. This procedure was performed for three times. As reported in Fig. 8, the response increased with the target concentration up to 10 nmol/L, and then slowly decreased. This behavior was the same observed with "drop-on sensor" system (Fig. 7), even if the electrochemical measurement procedure was different. In our opinion, the key factor to explain this trend is that the bead modification process (i.e. capture probe concentration, target hybridization time, enzyme concentration) was the same for both the measurement strategies.

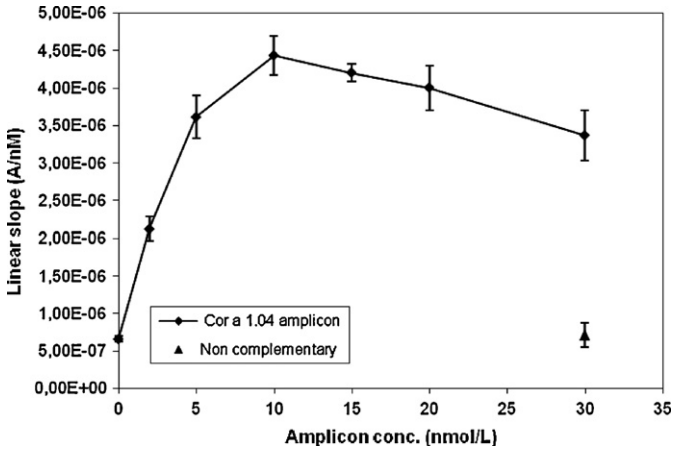

Fig. 8. Calibration plot for Cor a 1.04 amplicons. Probe-modified and biotin-blocked beads were incubated for 15 min with 50 μL of thermally denatured target solutions, diluted to the desired concentration. Experiments were performed with the microfluidic-based electrochemical platform. Other details in the text.

The overall procedure (including sample amplification, target hybridization and labeling, measurement, data presentation) takes approximately 90 min.

The reproducibility of the measurements (evaluated as relative standard deviation over three results for 10 nM solution) was 6%.

We demonstrated that target concentrations at nM levels can be easily detected. Moreover, the reliability of the method was also demonstrated, with the low signal of the non-specific sequence ($7 \pm 2 \times 10^{-7}$ A/nM).

A detection limit of 0.2 nM was calculated considering the slope of the linear portion of the calibration curve (0–5 nM), fitting in the following equation $Y = 6 \times 10^{-7}X + 9 \times 10^{-7}$ the mean of the blank solution response plus three times its standard deviation.

4. Conclusions

In this work a rapid and sensitive enzyme-linked electrochemical genomagnetic assay using a microfluidic system was developed. The integration of microfluidic-based platform with a new analytical procedure based on the use of paramagnetic beads allowed the possibility to measure nM level of DNA sequences, with high reproducibility. The hybridization reaction has been carried out on probe-modified paramagnetic micro-particles, freely moving in solution, thus favoring random collisions between reagents. Moreover, magnetic properties of the particles allow an easy separation from the solution with the consequent possibility of avoiding the absorption of non-specific DNA sequences or enzymatic labels at the electrode surface.

Further work will be devoted to investigate the possibility of automation of beads modification and integration in the microfluidic-based platform, in line with the concept of Lab-on – a chip technology. Even if the procedure was demonstrated with DNA sequences, however other affinity biomolecules such as aptamers or classical antibodies can undoubtedly benefit from the use of paramagnetic beads integrated in a microfluidic-based platform, using the set-up developed in this work.

References

[1] F. Lucarelli, G. Marrazza, A.P.F. Turner, M. Mascini, Biosens. Bioelectron. 19 (2004) 515.
[2] J. Wang, A. Kawde, A. Erdem, M. Salzar, Analyst 126 (2001) 2020.
[3] J. Wang, R. Polsky, D. Xu, Langmuir 17 (2001) 5739.
[4] E. Palecek, S. Billovà, L. Havran, R. Kizek, A. Miculkova, F. Jelen, Talanta 56 (2002) 919.
[5] E. Palecek, M. Fojta, Talanta 74 (2007) 276.
[6] J. Wang, D. Xu, A. Erdem, R. Polsky, M.A. Salazar, Talanta 56 (2002) 931.
[7] A.N. Kawde, J. Wang, Electroanalysis 16 (2004) 101.
[8] A. Lermo, S. Campoy, J. Barbè, S. Hernadez, S. Alegret, M.I. Pividori, Biosens. Bioelectron. 22 (2007) 2010.
[9] A. Erdem, D.O. Ariksoysal, H. Karadeniz, P. Kara, A. Sengonul, A.A. Sayiner, M. Ozsoz, Electrochem. Commun. 7 (2005) 815.
[10] M. Pumera, A. Merkoci, S. Alegret, Trends Anal. Chem. 25 (2006) 219.
[11] J.S. Rossier, C. Vollet, A. Carnal, G. Lagger, V. Gobry, H.H. Girault, P. Michel, F. Reynold, Lab. Chip 2 (2002) 145.
[12] J.S. Rossier, F. Reymond F, in: Alegret and Merkoçi (Eds.), Comprehensive Analytical Chemistry, vol. 49, Elsevier, pp. 885–905.

[13] R.H. Liu, J. Yang, R. Lenigk, J. Bonanno, P. Grodzinski, Anal. Chem. 76 (2004) 1824.
[14] D. Liu, R.K. Perdue, L. Sun, R.M. Crooks, Langmuir 20 (2004) 5905.
[15] Z.H. Fan, S. Mangru, R. Granzow, P. Heaney, W. Ho, Q. Dong, R. Kumar, Anal. Chem. 71 (1999) 4851.
[16] M.A. Hayes, N.A. Polson, A.N. Phayre, A.A. Garcia, Anal. Chem. 73 (2001) 5896.
[17] H. Zhang, S.M. Mitrovsky, R. Nuzzo, Anal. Chem. 79 (2007) 9014.
[18] S. Kwakye, V.N. Goral, A.J. Baeumner, Biosens. Bioelectron. 21 (2006) 2217–2223.
[19] V.N. Goral, N.V. Zaytseva, A.J. Baeumner, Lab. Chip 6 (2006) 414–421.
[20] D. Hoegger, P. Morier, C. Vollet, D. Heini, F. Reymond, J.S. Rossier, Anal. Bioanal. Chem. 387 (2007) 267.
[21] M. Besler, Trends Anal. Chem. 20 (2001) 662.
[22] A. Germini, E. Scaravelli, F. Lesignoli, S. Sforza, R. Corradini, R. Marchelli, Eur. Food Res. Technol. 220 (2005) 619.
[23] H. Hird, J. Lloyd, R. Goodier, J. Brown, P. Reece, Eur. Food Res. Technol. 217 (2003) 265.
[24] T. Holzhauser, A. Wangorsh, S. Vieths, Eur. Food Res. Technol. 211 (2000) 360.
[25] O. Stephan, S. Vieths, J. Agric. Food Chem. 52 (2004) 3754.
[26] S. Laschi, I. Palchetti, G. Marrazza, M. Mascini, J. Electroanal. Chem. 593 (2006) 211–218.
[27] S. Centi, E. Silva, S. Laschi, I. Palchetti, M. Mascini, Anal. Chim. Acta 594 (2007) 9.
[28] M.L. Del Giallo, F. Lucarelli, E. Cosulich, E. Pistarino, B. Santamaria, G. Marrazza, M. Mascini, Anal. Chem. 77 (2005) 6324.

Electrochimica Acta 54 (2009) 5035–5041

Contents lists available at ScienceDirect

Electrochimica Acta

journal homepage: www.elsevier.com/locate/electacta

Aligned carbon nanotube thin films for DNA electrochemical sensing

F. Berti [a], L. Lozzi [b], I. Palchetti [a], S. Santucci [b], G. Marrazza [a,*]

[a] Department of Chemistry, University of Florence, Via della Lastruccia 3, Sesto Fiorentino (Firenze) 50019, Italy
[b] Department of Physics, University of L'Aquila, Coppito, L'Aquila 67100, Italy

ARTICLE INFO

Article history:
Received 30 October 2008
Received in revised form 8 January 2009
Accepted 9 January 2009
Available online 21 January 2009

Keywords:
CNT
CVD
DNA
Genosensor
DPV

ABSTRACT

Carbon nanotubes are interesting materials for DNA electrochemical sensing due to their unique electric properties: high surface area, fast heterogeneous electron transfer, and electrochemical stability. In this work aligned Carbon NanoTube (CNT) thin films were designed and tested as candidate platforms for DNA immobilization and for the development of an electrochemical genosensor.

The films were prepared by Chemical Vapor Deposition (CVD) using acetylene and ammonia as precursor gases and nickel particles as catalyst. A preliminary electrochemical characterization was performed using cyclic voltammetry since, so far, these films have been used only for gas sensing. The surfaces were then covalently functionalized with a DNA oligonucleotide probe, complementary to the sequence of the most common inserts in the GMOs: the Promoter 35S. The genosensor format involved the immobilization of the probe onto the sensor surface, the hybridization with the target-sequence and the electrochemical detection of the duplex formation. Careful attention was paid to the probe immobilization conditions in order to minimize the signal due to non-specifically adsorbed sequences. For the detection of the hybridization event both label-free and enzyme-labelled methods were investigated. In case of the enzyme-labelled method a target concentration at nanomolar level can be easily detected, with a linear response from 50 nM to 200 nM, whereas the label-free method showed a linear response between 0.5 μM and 10 μM. The reproducibility was 11% and 20% with the enzyme-labelled method and the label-free method, respectively. The batch-to-batch reproducibility of the different sensors was also evaluated.

1. Introduction

Recent advances in nanotechnology have led to the synthesis of novel functional materials, such as nanowires, nanotubes and nanocrystals, ideal building blocks for emerging nanoscale biosensor devices. The ability to tailor the size and structure and hence the properties of nanomaterials offers excellent prospects for designing novel sensing systems and enhancing the performance of bioanalytical assays [1].

In this paper we designed and tested new vertical aligned MultiWalled Carbon NanoTube (MWCNT) thin films for DNA electrochemical sensing. Since their discovery in 1991 [2], Carbon NanoTubes (CNTs) have generated great interest for applications in electrochemical devices due to their interesting and technologically important combination of properties such as high surface area, fast heterogeneous electron transfer, chemical stability, easiness of miniaturization [3–5].

As widely reviewed [1,6–8], many genosensors have been developed employing CNTs as platform for DNA immobilization and electrochemical transduction. In particular, in the last five years, highly encouraging results have been obtained by modifying carbon electrode surfaces (mainly glassy carbon and carbon paste) with a dispersion of CNTs in polymers or solvents [9–16]. Further advantages may come from the employment of electrode surface based on highly ordered and vertically aligned carbon nanotube. The vertical orientation of the nanostructures, in fact, facilitates the loading of DNA probe as well as the access of the analyte towards the immobilized probe, thus increasing the sensitivity of the analysis. Moreover, the technologies required for the construction of such surfaces are compatible with device miniaturization thus allowing the realization of nanoelectrodes or nanoarray, with a further increase in the sensitivity of the measurements. Despite these advantages, there are still few papers [17–20] reporting the application of well-oriented CNTs film for DNA electrochemical biosensing. In those papers MWCNT were prepared by plasma treatment on gold after pyrolysis of Fe(II) phthalocyanine [19] as well as grown by Plasma-Enhanced Chemical Vapor Deposition (PECVD) and encapsulation with tetraethoxysilane [17,18]. In the present paper, vertically aligned carbon nanotubes were obtained by thermal CVD. Thermal CVD is a much more accessible method for CNT

* Corresponding author. Tel.: +39 0554573320; fax: +39 0554573396.
E-mail address: giovanna.marrazza@unifi.it (G. Marrazza).

0013-4686/$ – see front matter © 2009 Elsevier Ltd. All rights reserved.
doi:10.1016/j.electacta.2009.01.038

growth, requiring only a basic tube furnace and gas manifold. Moreover, it has advantages in terms of sample sizes and numbers of samples that can be prepared per run.

Self-assembled aligned MWCNT thin films were prepared by CVD onto insulators (SiO_2 or Si_3N_4) and metallic (Al) substrates, using acetylene and ammonia as precursor gases and nickel particles as catalyst. So far these devices themselves have been used only for gas sensing (based on changes in the electrical resistance of the CNT film) for the detection of nitrogen dioxide [21,22], ammonia and ethanol [23]. In order to determine the most suitable film format for genosensor development, different growing substrates and temperatures, were tested. On this purpose, a preliminary characterization was performed using cyclic voltammetry (CV), in order to investigate their electrochemical behavior in solution. This screening showed that nanostructures grown on an aluminum substrate at 700 °C exhibited the best performances for genosensing.

Subsequently the genosensor was developed using synthetic oligonucleotides related to the 35S promoter, a typical genetic construct present in the majority of GMOs [24], target of great interest in biosensor-based food analysis [25–28]. The nanostructured surface was functionalized with an oligonucleotide DNA probe by covalent immobilization. For the detection of the hybridization event both label-free and enzyme-linked methods were investigated.

A label-free approach greatly simplifies the sensing protocol and allows avoiding the utilization of toxic or carcinogenic compounds, usually used as indicators. The assay is based on the measurement of the intrinsic electrochemical signal of the guanine moiety [29–31]. An inosine-modified (guanine-free) probe was immobilized onto the sensor. After the hybridization, the duplex formation was detected by measuring the oxidation signal of guanine, present only in the target sequence. After elaborating the experimental procedure the analytical performance of the assay was tested out by measuring different concentrations of target and controlling the non-specific signal.

In order to improve the selectivity and the sensitivity of the assay an enzyme-linked approach was also studied. In this way the biocatalytic activity of the enzyme can be exploited to amplify the hybridization signal [26]. After probe immobilization, the genosensor was hybridized with a biotinylated complementary sequence. The enzymatic conjugate streptavidin alkaline phosphatase was coupled to the hybrid through streptavidin–biotin bond and the electroactive product of enzymatic hydrolysis, p-amino phenol was detected by DPV (differential pulse voltammetry).

2. Experimental

2.1. Chemicals

Acetic acid, sodium acetate, potassium chloride, potassium ferricyanide and nitric acid were obtained from Merck (Italy); *N*-(3-dimethylaminopropyl)-*N*′-ethylcarbodiimide hydrochloride (EDAC), hydroquinone, urea, streptavidin–alkaline phosphatase, bovine serum albumin (BSA), magnesium chloride and diethanolamine were purchased from Sigma–Aldrich (Italy); N-hydroxysuccinimide and sodium dodecyl sulphate (SDS) were obtained from Fluka (Italy); p-aminophenyl phosphate was purchased from DiagnoSwiss (Switzerland). All the solutions were prepared using MilliQ grade water.

The genosensor has been developed using synthetic oligonucleotides (MWG Biotech, Germany) related to the 35 S promoter. The sequences are reported below:

DNA probe (25 mer): 5′-NH_2–$(CH_2)_6$-GGCCATCGTTGAAGATGCCTCTGCC-3′;
inosine-substituted DNA probe (25 mer): 5′-NH_2–$(CH_2)_6$-IICCATCITTIAAIATICCTCTICC-3′;

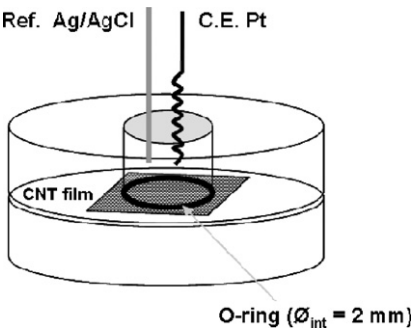

Fig. 1. Scheme of the plexiglass well cell used through all the electrochemical experiments. An o-ring delimited a circular working electrode surface (Ø = 2 mm) on the CNT film.

Target (25 mer): 5′-GGCAGAGGCATCTTCAACGATGGCC-3′;
Biotinylated target (25 mer): 5′-biotin-TEG-GGCAGAGGCATCTTCAACGATGGCC-3′;
Non-complementary sequence (24 mer): 5′-GGA GAT CGA CCA CGC AAA CTT CAA-3′;
Non-complementary biotinylated sequence (24 mer): 5′-biotin-TEG-AGG CCC TGC GAG CAA CAT CTC ATG-3′.

2.2. Electrochemical apparatus

Electrochemical experiments were performed with an AUTOLAB PGSTAT 30(2) digital potentiostat/galvanostat with a GPES 4.8 software package (EcoChemie, Netherlands). A Plexiglass three electrode well cell (made in our laboratory) with the carbon nanotube thin film as working electrode (Ø = 2 mm), an Ag/AgCl wire as reference electrode and a platinum coil as counter electrode was employed (Fig. 1).

2.3. CNT thin film fabrication

Multiwalled carbon nanotube thin films were obtained by chemical vapor deposition using acetylene and ammonia as precursor gases and nickel particles as catalyst.

Different substrates were used, commercially available SiO_2 and Si_3N_4 layers (100 and 150 nm thick, respectively) on silicon, as well as Al (100 nm) layer grown by sputtering onto a Si substrate, with a thin native silicon dioxide layer. A thin (3 nm) film of Ni catalyst was deposited by high vacuum (10^{-6} Torr) thermal evaporation onto the substrate. Then the substrate was introduced in the CVD reactor. The CVD reactor was pumped down up to about 10^{-6} Torr, mainly to remove oxygen. Then, the pressure was raised up to about 3 Torr introducing ammonia (100 standard cubic centimeter for minute, sccm) and the substrate was heated to 700° for 20 min in ammonia environment to induce the cluster formation of the catalyst layer and to remove the nickel oxide layer due to the air exposure of the sample during the transfer from the evaporation system to the CVD reactor. Keeping the ammonia flux unchanged, acetylene was flown (20 sccm) for 10 min thus enabling the CNT growth. Two different CNT growing temperatures, 500 °C and 700 °C, were used. In the case of MWCNT grown on SiO_2 and Si_3N_4 substrate a gold film was also deposited by thermal evaporation on one side of the film, for the realization of the metallic contact.

All the samples were morphologically characterized by means of a scanning electron microscope equipped with a field emission gun (FEG-SEM) (Fig. 2a and b).

2.4. Functionalization of the sensor surface

Each cycle of measurement consisted of three steps: DNA-probe immobilization, hybridization, electrochemical investigation of the

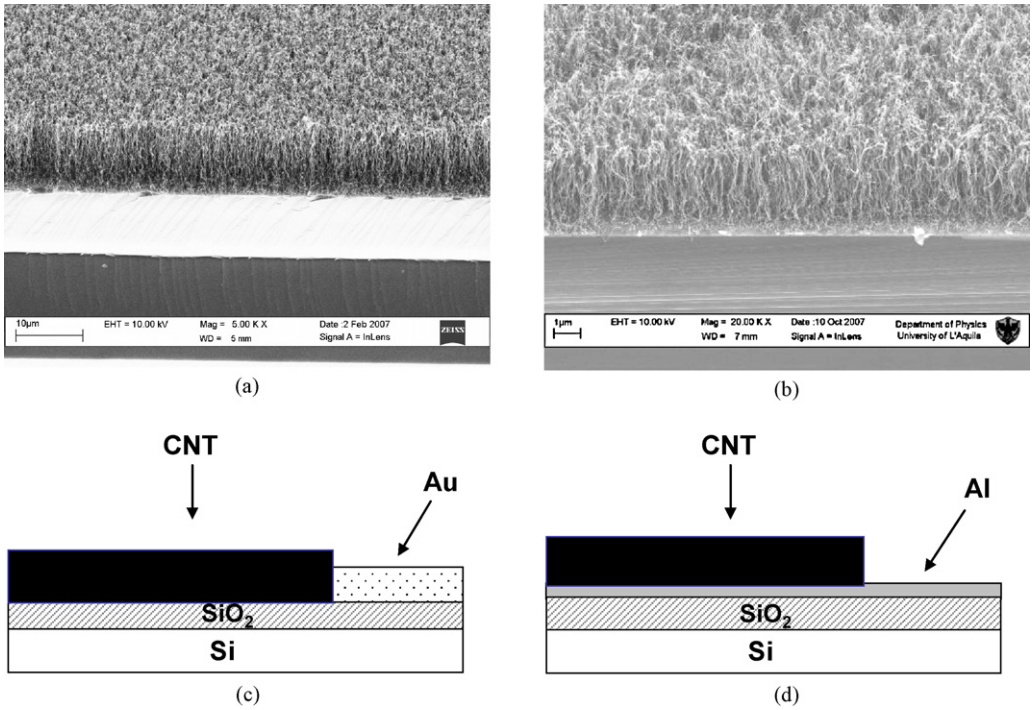

Fig. 2. Aligned carbon nanotube thin films obtained by CVD. (a) SEM image of the CNT film grown on a SiO_2 substrate (CNT/Ni/SiO_2). (b) SEM image of the CNT film grown on an Al/SiO_2 substrate (CNT/Ni/Al/SiO_2). (c) Scheme of CNT/Ni/SiO_2. (d) Scheme of CNT/Ni/Al/SiO_2.

surface. After biosensor regeneration a new cycle was performed. Synthetic guanine containing as well as inosine-modified oligonucleotides, having a C6 spacer and a terminal amino group, were covalently immobilized onto CNTs. Carboxylic groups were introduced onto the carbon nanotubes by oxidation. Then, they were activated by interaction with 30 μL of an aqueous solution containing 5 mmol/L EDAC and 8 mmol/L NHS for 1 h [32]. Finally, 30 μL of capture-probe 10 μM in phosphate buffer 0.5 M, pH 7.0, were deposited overnight (∼16 h). The immobilization proceeded through the formation of amide bonds between the carboxylic functionality at the electrode surface and the amino-terminal end of the oligonucleotides. The residual reactive groups were blocked by depositing 30 μL of ethanolamine 100 mM for 20 min. Then the biosensor was rinsed three times with 100 μL of phosphate buffer.

2.5. Label-free hybridization assay

The inosine-substituted immobilized probe was hybridized for 30 min with 30 μL of a convenient amount of guanine containing oligonucleotide target in phosphate buffer 0.5 M, pH 7.0. An analogue solution of non-complementary sequence was employed as control of the non-specific signal. After 20 min the sensor was washed three times with 100 μL of acetate buffer 0.25 M, pH 4.7 (containing 10 mM of potassium chloride). The guanine electrochemical oxidation was performed by DPV, after closing the circuit with 50 μL of acetate buffer (modulation time, 0.05 s; interval time, 0.15 s; step potential, 5 mV; modulation amplitude, 70 mV).

Finally the genosensor was regenerated with 50 μL of a denaturant solution containing urea 5 M and sodium dodecyl sulphate (SDS) 0.05%, for 5 min.

2.6. Enzyme-linked hybridization assay

The hybridization experiments were carried out using a biotinylated target. Control experiments were carried out using non-complementary biotinylated sequences to evaluate the non-specific signal. The probe-modified sensor was incubated for 30 min with 30 μL of oligonucleotide target solution, diluted to the desired concentration with phosphate buffer 0.5 M, pH 7.0. After hybridization, the sensor was washed three times with 100 μL of DEA buffer (0.1 M diethanolamine, 1 mM $MgCl_2$, 0.1 M KCl; pH 9.6) and incubated with 30 μL of a solution containing 0.75 U/mL of the streptavidin–alkaline phosphatase conjugate and 10 mg/ml of BSA (blocking agent) in DEA buffer. After 20 min the surface was washed three times with 100 μL of DEA buffer. The electrochemical measurements were performed by closing the circuit with 50 μL of DEA buffer containing 1 mg/mL of enzymatic substrate, p-amino phenyl phosphate. After 10 min, the electrochemical signal of the enzymatically produced p-amino phenol was measured by DPV (modulation time, 0.05 s; interval time, 0.15 s; step potential, 5 mV; modulation amplitude, 70 mV).

The regeneration of the genosensor surface was performed by washing the surface with distilled water to remove the enzymatic product and by treating with 50 μL of a denaturant solution containing Urea 5 M and SDS 0.05%, for 5 min.

3. Results and discussion

3.1. CNT-film characterization

Different patterns of CNT films (Table 1), growth on different substrates (SiO_2, Si_3N_4, Al), at different temperatures (500 °C,

Table 1
List of the sensor tested for the genosensor development.

Sensor	Growing temperature
CNT/Ni/SiO_2	500 °C
CNT/Ni/SiO_2	700 °C
CNT/Ni/Si_3N_4	500 °C
CNT/Ni/Si_3N_4	700 °C
CNT/Ni/Al/SiO_2	500 °C
CNT/Ni/Al/SiO_2	700 °C

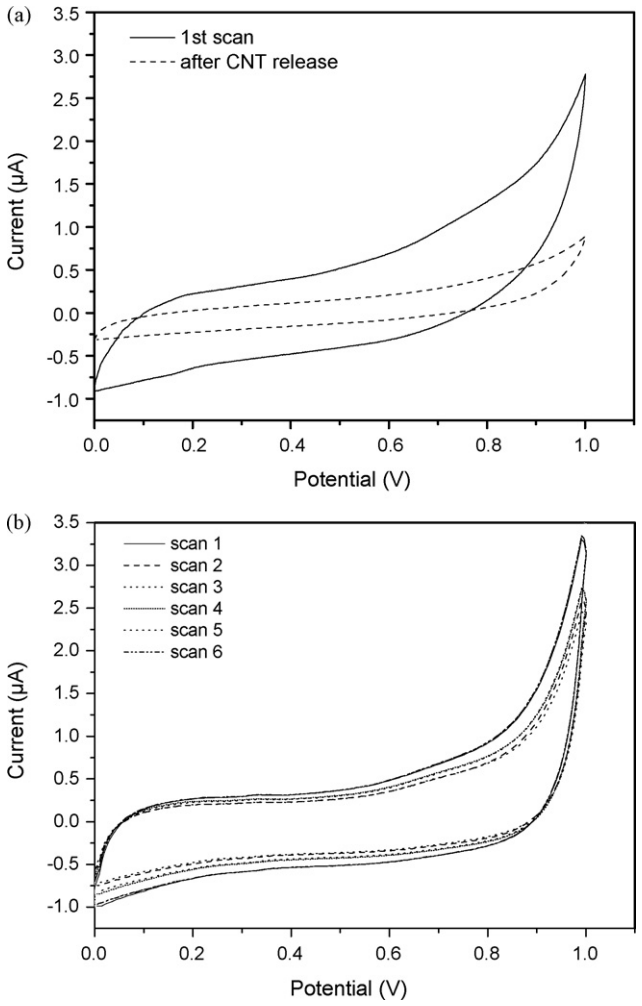

Fig. 3. Evaluation of CNT adhesion during electrochemical measurements in solution. (a) CNT/Ni/SiO_2 (700 °C): CV of acetate buffer 0.25 M with KCl 10 mM, before (solid line) and after (dashed line) CNT release. (b) CNT/Ni/Al/SiO_2 (700 °C): CV of acetate buffer 0.25 M with KCl 10 mM, six consecutive scans. (CV parameters: start potential 0.7 V, first vertex potential −0.5 V, second vertex potential 0.7 V, step potential 0.0244 V, scan rate 0.05 V s^{-1}; potential vs. Ag/AgCl, KCl 0.01 M.)

700 °C) were tested. All the CNT films were firstly characterized by Cyclic Voltammetric (CV) scans in buffer solution. The first kind of sensor (Fig. 1c) was obtained on SiO_2 substrates (CNT/Ni/SiO_2) by first evaporating gold contacts, then depositing the catalyst particles; finally the CNTs were grown. These sensors showed remarkable problems of adhesion once in solution and CNTs were released after few potential scans. Besides being clearly visible by an optical inspection, this phenomenon was also demonstrated by comparing CV scans recorded before and after CNT release. As reported in Fig. 3a, a decrease in the capacitive current was observed. It is obvious that the mechanical resistance of the surface and, in particular, the adhesion of CNTs at the growing substrate is crucial. The release of nanotubes during the assay changes the surface properties with consequent loss of reliability of the measurements.

A little improvement in CNT adhesion was achieved, for both the temperatures applied, by changing the growing substrate with Si_3N_4 (CNT/Ni/Si_3N_4). However also in this case CNTs were released increasing the number of CV scans. The introduction of an aluminum layer on the SiO_2 substrate (CNT/Ni/Al/SiO_2, Fig. 1d), which serves as growing substrate as well as electrical contact, allowed to improve film stability. As reported in literature [33] carbon nanotube synthesized on metallic substrates have been demonstrated

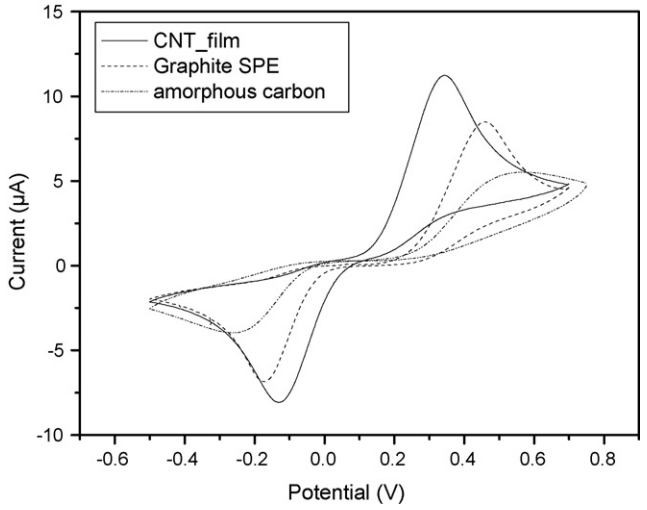

Fig. 4. CV of 1 mM hydroquinone in acetate buffer 0.25 M with KCl 10 mM (CV parameters: start potential 0.7 V, first vertex potential −0.5 V, second vertex potential 0.7 V, step potential 0.0244 V, scan rate 0.05 V s^{-1}; potential vs. Ag/AgCl, KCl 0.01 M). Signals obtained using CNT films (solid line), carbon screen-printed electrodes (dashed line) and sensors processed in the CVD reactor, in the absence of one of the precursor gases, thus obtaining only amorphous carbon on the surface (dot line).

to exhibit excellent properties as electrode materials. CNTs growth at 500 °C were weakly adhered at the surface so they were released in solution just after the immobilization step but a high stability was achieved using films growth at 700 °C. This increase in stability has been explained considering that, as at 700 °C aluminum is melted, a partial inclusion of Ni particles into the metal may root CNTs deeper in the Al substrate [34]. This improvement has been experimentally demonstrated. As shown in Fig. 3b, even after six subsequent CV scans, no significant variation in the capacitive current can be observed.

Thus CNT/Ni/Al/SiO_2 was used for all further experiments.

In order to investigate the electron-transfer properties of these sensors in solution, CV experiments were performed. For this purpose two different redox mediators such as potassium ferricyanide and hydroquinone were used. Signals obtained using CNT films were compared with the ones obtained using carbon screen-printed electrodes (CSPE), with the same geometric area, and an amorphous carbon sensor obtained by processing the substrate in the CVD reactor, in the absence of one of the precursor gases. As known, for a nernstian wave the ratio of peak currents (i_{pa}/i_{pc}) is 1, regardless of scan rate, and the separation of peak potential (ΔE_p) is always close to $59/n$ mV (where n is the number of exchanged electrons) [35]. An increase in the reversibility was observed at CNT-film surfaces for all the mediators tested thus demonstrating that the presence of nanostructures enhance the electron transfer at the electrode–solution interface. When using potassium ferricyanide as redox mediator the improvement of i_{pa}/i_{pc} and ΔE_p were less remarkable (i_{pa}/i_{pc} = 1.23 for the amorphous carbon surface, 1.18 for CSPE, 1.08 for the CNT film; ΔE_p = 307 mV for the amorphous carbon surface, 264 mV for CSPE, 188 mV for the CNT film). The increase in reversibility was more pronounced in the case of hydroquinone (Fig. 4). The values obtained show an improvement in the ratio of peak currents and a significant decrease in the separation of peak potential of about 100 mV with respect to carbon electrode and about 400 mV with respect to the amorphous carbon surface (i_{pa}/i_{pc} = 1.47 for the amorphous carbon surface, 1.08 for CSPE, 1.02 for the CNT film; ΔE_p = 869 mV for the amorphous carbon surface, 576 mV for CSPE, 467 mV for the CNT film). The increase in the reversibility have been elsewhere explained considering CNTs as "conductive wires" which establish an electrical channel between

the electrode and the redox couple solution thus accelerating the electron transfer and decreasing the surface resistance [36].

3.2. Development of the genosensor

3.2.1. Optimization of the immobilization conditions

As the electrochemical characterization demonstrated highly promising electrical properties, CNT films were then investigated as platforms for DNA immobilization and electrochemical transduction. Firstly, the oligonucleotide immobilization conditions were deeply studied. In fact, control of the surface chemistry and coverage is essential for assuring high reactivity, orientation, accessibility and stability of the surface-confined probe as well as for minimizing non-specific adsorption events. Two properties of CNT films make them particularly suitable to serve those purposes: the well alignment of nanostructures and the high reactivity of their fullerene-like tips which allow an easy end-modification of the nanotubes with functional groups (e.g. —COOH, —OH, —C=O) [37]. Thus amino-linked DNA probe was covalently immobilized by the classical method of diimide activated amidation after introducing carboxylic groups on the nanotube ends by oxidation. A DPV scan of the immobilized probe is reported in Fig. 5 (solid line) where oxidation peaks of guanine (E_{peak} = 0.91 V vs. Ag/AgCl) and adenine (E_{peak} = 1.3 V vs. Ag/AgCl) can be observed. Dashed line represent the DPV scan obtained after applying the same immobilization protocol for the functionalization of an amorphous carbon sensor. The absence of any oxidation peak of the purine bases demonstrates that no chemisorption event occurs in the absence of nanostructures or at the underlying growing aluminum substrate. Aspecific signals due to adsorbed DNA molecules on the electrode surface were minimized by washing with phosphate buffer and blocking the residual carboxylic reactive groups with ethanolamine.

Moreover, a strategy of regeneration of the genosensor was developed in order to perform different analysis using the same functionalized surface. In particular, the immobilized probe was regenerated by denaturing the hybrid with an aqueous solution containing urea 5 M and SDS 0.05%. In this way up to five cycles of hybridization/denaturation were performed using the same sensor, thus confirming the stability of the film and the robustness of the immobilization chemistry.

Then, the influence of the probe concentration on the hybridization reaction was investigated. Electrode surfaces with lower probe densities show, in fact, a limited number of biorecognition sites, whereas higher surface densities can cause steric and electrostatic interference between packed probes and the incoming target DNA fragment [38]. The optimal surface coverage was experimentally assessed by performing label-free hybridization experiments varying the capture probe concentration in a range between 1 μM and 20 μM. The higher hybridization yield was obtained using a 10 μM solution of amino-linked probe (Guanine oxidation peak height vs. Ag/AgCl: i_p = 247 nA for target 1 μM, i_p = 51.4 nA for a 1 μM non complementary sequence, specific vs. nonspecific ratio ~1:5), so this concentration was chosen for further measurements.

3.2.2. Label-free assay

Two different approaches were investigated for the electrochemical detection of the hybridization reaction. The first, a label-free assay, was based on the intrinsic electrochemical activity of the guanine moiety. The format involved the immobilization of an inosine-modified (guanine-free) probe onto the sensor. The inosine moiety preferentially formed base-pair with the cytosine residue, but its oxidation signal is well separated from that of guanine ($\Delta E_p \sim 400$ mV). After hybridization, duplex formation is indicated by the oxidation signal of the guanine bases, present only in the target sequence. The performances of the so-obtained genosensor were investigated by testing different amounts of DNA target. The experiments were performed on a single probe-modified CNT film by subsequent cycles of hybridization/denaturation. As reported in Fig. 6, guanine oxidation peaks recorded in the presence of different DNA target, in a concentration range between 0 μM and 10 μM, exhibited a good directly proportional relationship between concentration (from 0.5 μM to 10 μM) and electrochemical response (from the linear fit of data: $y = 0.95x + 1.14$, $R = 0.99$). The non-specific signal, obtained using a non-complementary sequence (10 μM), resulted more than three times lower than the lowest investigated concentration, thus confirming the selectivity of the genosensor.

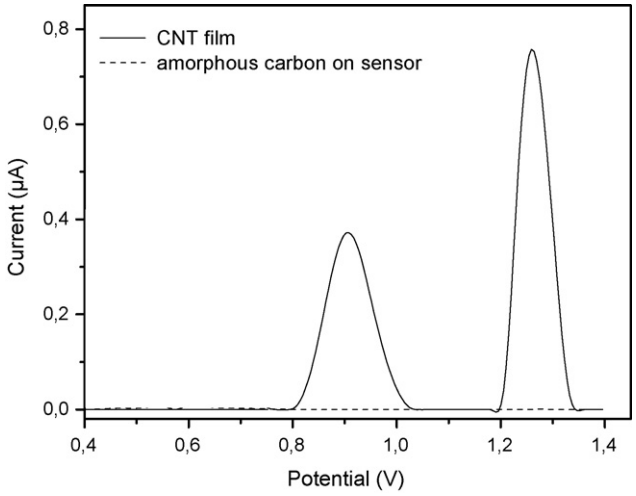

Fig. 5. Guanine and adenine oxidation peaks obtained after the immobilization of DNA probe (10 μM) on CNT film (solid line) and on an amorphous carbon sensor (dashed line). DPV measurements performed in acetate buffer 0.25 M with KCl 0.01 M (DPV parameters: modulation time, 0.05 s; interval time, 0.15 s; step potential, 5 mV; modulation amplitude, 70 mV; potential vs. Ag/AgCl, KCl 0.01 M).

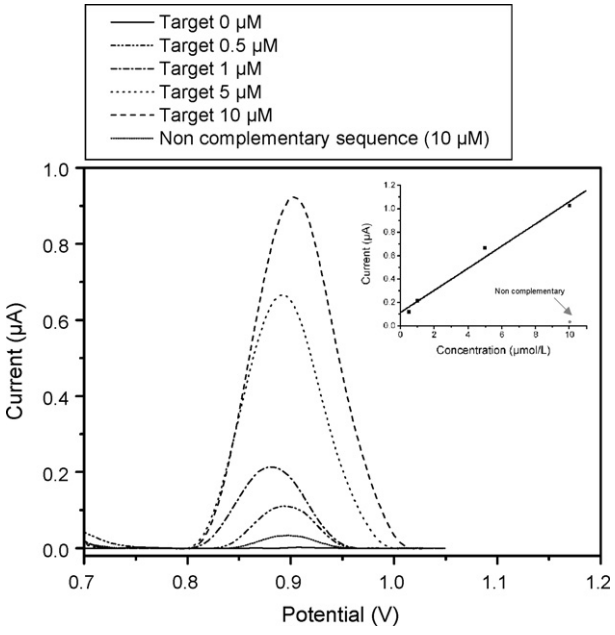

Fig. 6. Guanine oxidation peaks obtained after the hybridization with DNA target (concentration range, 0–10 μM) and non-complementary oligonucleotide (10 μM). Measurements were performed in 50 μL of acetate buffer 0.25 M + KCl 10 mM. (DPV parameters: modulation time, 0.05 s; interval time, 0.15 s; step potential, 5 mV; modulation amplitude, 70 mV; potential vs. Ag/AgCl, KCl 0.01 M). For "target 0 μM" no peak was observed, thus this value was not considered in the linear fit.

The reproducibility of the measurements (evaluated as relative standard deviation over five measurements for a 1 μmol/L solution) was 20% within the same sensor (for successive cycle of hybridization), 26% when using different sensors.

3.2.3. Enzyme-linked assay

An enzyme-linked approach was also developed. The biocatalytic activity of the enzyme label causes a great amplification of the hybridization signal, thus increasing the sensitivity of DNA electrochemical detection. Moreover, non-specific signals can be minimized by using an appropriate enzymatic conjugate (streptavidin–AP) coupled with an efficient blocking agent (BSA) [26].

After the immobilization, the probe was hybridized with a biotinylated target. The biotinylated hybrid was then labelled with streptavidin–alkaline phosphatase and incubated with a substrate, whose product of enzymatic hydrolysis is electroactive and can be detected by DPV. p-Amino-phenyl phosphate was selected among other substrates because the oxidation product, p-amino phenol, doesn't form electropolymerized products and can be easily washed away thus allowing the reusability of the sensor.

The performances of the enzyme-labelled format were tested recording enzymatic product signals obtained in the presence of different concentrations of DNA target. As reported in Fig. 7, the voltammetric response increased linearly with the target concentration up to 200 nmol/L (from the linear fit of data: $y = 0.02x + 0.31$, $R = 0.98$). The non-specific signal, obtained using a non-complementary sequence, resulted negligible even at the highest investigated concentration (200 nM), thus confirming the good selectivity of the genosensor. Thus target concentrations at nanomolar levels can be easily detected.

In this case the reproducibility of the measurements (evaluated as relative standard deviation over five results for a 1 μmol/L solution) was 11% within the same sensor (for successive cycle of hybridization), 18% when using different sensors.

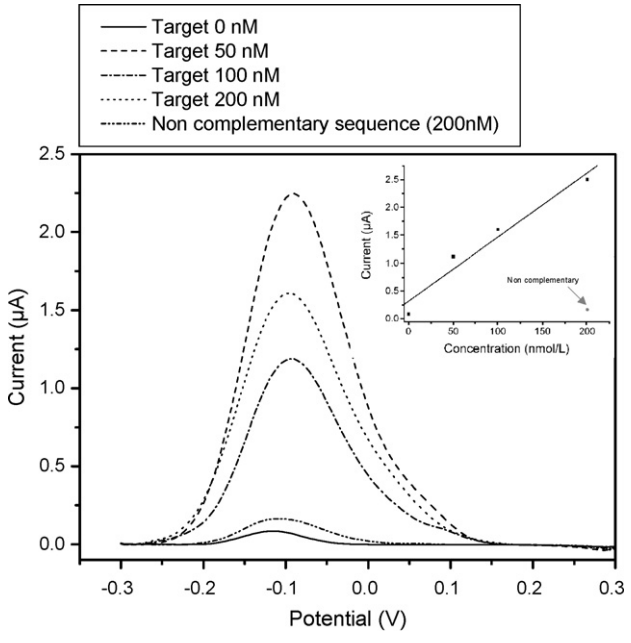

Fig. 7. p-Amino phenol oxidation peaks obtained after the hybridization with DNA target (concentration range 0–500 nM) and non-complementary oligonucleotide (500 nM). Measurements were performed in 400 μL of DEA buffer containing 1 mg/mL of p-amino phenyl phosphate after 15 min of incubation with the enzyme-labelled hybrid. (DPV parameters: modulation time, 0.05 s; interval time, 0.15 s; step potential, 5 mV; modulation amplitude, 70 mV; potential vs. Ag/AgCl, KCl 0.01 M.)

4. Conclusions

In this work, CNT thin films were optimized for the electrochemical detection of gene sequences by DNA hybridization at the sensor-liquid interface. The physical and electrochemical characterization of the surfaces demonstrated the well alignment of the nanostructures and highly improved electron transfer properties with respect to other carbon based electrodes. The screening of different models of CNT films, prepared by CVD, showed that nanostructures grown on an aluminum substrate at 700 °C exhibited the best performances for genosensor realization.

A model genosensor was developed using synthetic oligonucleotides related to the 35S promoter, a typical genetic construct present in the majority of GMOs. The nanostructured surface was functionalized with the oligonucleotide DNA probe by covalent immobilization. For the detection of the hybridization event a label-free assay was initially developed achieving good levels of sensibility and selectivity. In order to improve the sensitivity of the assay an enzyme-linked approach was also studied, thus increasing the sensibility of the measurement of nearly one order of magnitude.

In summary, we have demonstrated a new electrochemical platform based on vertically aligned CNT films for ultrasensitive DNA detection.

Combining such an electrode platform with enzyme labeling, a detection limit in the nanomolar range of oligonucleotide targets is achieved. This concentration level is sufficient for most applications involving gene expression and sequence analysis. Moreover, the reliability of the method is also demonstrated, with the low nonspecific signal. Thus, a highly sequence specific (single base mismatch) DNA analysis can be accomplished. This platform may be also applicable to the detection of trace redox chemicals (i.e. heavy metals, toxic contaminants, drugs, etc), immunoassay based detection scheme and as electrochemical detectors in microfluidic devices.

Acknowledgement

This work has been partly supported by the Ministero dell'Istruzione, dell'Università e della Ricerca PRIN 2005 "Quasi mono dimensional nanosensors for label free ultra sensitive biological detection".

References

[1] J. Wang, Analyst 130 (2005) 421.
[2] S. Iijima, Nature 354 (1991) 56.
[3] R.H. Baughman, A. Zakhidov, W.A. De Heer, Science 297 (2002) 787.
[4] A. Merkoci, M. Pumera, X. Leopis, B. Péres, M. Del Valle, S. Alegret, Trends Anal. Chem. 4 (2005) 9.
[5] F. Valentini, S. Orlanducci, M.L. Terranova, A. Amine, G. Palleschi, Sens. Actuators B 100 (2004) 117.
[6] G.A. Rivas, M.D. Rubianes, M.C. Rodrìguez, N.F. Ferreyra, G.L. Luque, M.L. Pedano, S.A. Miscoria, C. Parrado, Talanta 74 (2007) 291.
[7] M. Pumera, S. Sanchez, I. Ichinose, J. Tang, Sens. Actuators B 123 (2007) 1195.
[8] S. Daniel, T. Rao, K.S. Rao, S.U. Rani, G.R.K. Naidu, H.Y. Lee, T. Kawai, Sens. Actuators B: Chem. 122 (2) (2007) 672–682.
[9] J. Wang, A. Kawde, M. Musameh, Analyst 128 (2003) 912.
[10] H. Cai, X. Cao, Y. Jiang, P. He, Y. Fang, Anal. Bioanal. Chem. 375 (2003) 287.
[11] A. Erdem, P. Papakonstantinou, H. Murphy, Anal. Chem. 78 (2006) 6656.
[12] Y. Yang, Z. Wang, M. Yang, J. Li, F. Zheng, G. Shen, R. Yu, Anal. Chim. Acta 584 (2007) 268.
[13] H. Wei, Y. Du, J. Kang, E. Wang, Electrochem. Commun. 9 (2007) 1474.
[14] C. Jiang, T. Yang, K. Jiao, H. Gao, Electrochim. Acta 53 (2008) 2917.
[15] H. Qi, X. Li, P. Chen, C. Zhang, Talanta 72 (2007) 1030.
[16] K. Kerman, M. Saito, S. Yamamura, Y. Takamura, E. Tamiya, Trends Anal. Chem. 27 (2008) 7.
[17] J. Li, H.T. Ng, A. Cassell, W. Fan, H. Chen, Q. Ye, J. Koehne, J. Han, M. Meyyappan, Nano Lett. 5 (2003) 597.
[18] J. Koehne, H. Chen, J. Li, A.M. Cassell, Q. Ye, H.T. Ng, J. Han, M. Meyyappan, Nanotechnology 14 (2003) 1239.
[19] P. He, L. Dai, Chem. Commun. 3 (2004) 348.

[20] S.G. Wang, R. Wang, P.J. Sellin, Q. Zhang, Biochem. Biophys. Res. Commun. 325 (2004) 1433.
[21] L. Valentini, I. Armentano, J.M. Kenny, C. Cantalini, L. Lozzi, S. Santucci, Appl. Phys. Lett. 82 (2003) 961.
[22] L. Valentini, L. Lozzi, C. Cantalini, I. Armentano, J.M. Kenny, L. Ottaviano, S. Santucci, Thin Solid Films 436 (2003) 95.
[23] L. Valentini, C. Cantalini, I. Armentano, J.M. Kenny, L. Lozzi, S. Santucci, Diamonds Relat. Mater. 13 (2004) 1301.
[24] K. Pietsch, U. Waiblinger, P. Brodmann, A. Wurzl, Deutsche Lebensmittel RundschauHelf 2 (1997) 35.
[25] F. Lucarelli, G. Marrazza, M. Mascini, Biosens. Bioelectron. 20 (2005) 2001.
[26] I. Palchetti, S. Laschi, G. Marrazza, M. Mascini, Anal. Chem. 79 (18) (2007) 7206.
[27] B. Meric, K. Kerman, G. Marrazza, I. Palchetti, M. Mascini, M. Ozsoz, Food Control 15 (2004) 621.
[28] I. Mannelli, M. Minunni, S. Tombelli, M. Mascini, Biosens. Bioelectron. 18 (2003) 129.
[29] E. Palec˘ek, M. Fojta, M. Tomschik, J. Wang, Biosens. Bioelectron. 13 (1998) 621.
[30] J. Wang, A.N. Kawde, Anal. Chim. Acta 431 (2001) 219.
[31] P. Kara, D. Ozkan, A. Erdem, K. Kerman, S. Pehlivan, F. Ozkinay, D. Unuvar, G. Itirli, M. Ozsoz, Clin. Chim. Acta 336 (2003) 57.
[32] K.M. Millan, S.R. Mikkelsen, Anal. Chem. 65 (1993) 2317.
[33] C. Emmenegger, P. Mauron, A. Zuttel, C. Nutzenadel, A. Schneuwly, R. Gallay, L. Schlapbach, Appl. Surf. Sci. 162–163 (2000) 452.
[34] F.Y. Teng, J.M. Ting, S.P. Sharma, K.H. Liao, Nanotechnology 19 (2008) 095607.
[35] A.J. Bard, L.R. Faulkner, Electrochemical Methods: Fundamentals and Applications, Wiley, Somerset, NJ, 2001.
[36] J. Li, A. Cassell, L. Delzeit, J. Han, M. Meyyappan, J. Phys. Chem. B 106 (2002) 9299.
[37] M. Trojanowicz, Trends Anal. Chem. 25 (5) (2006) 480.
[38] F. Farabullini, F. Lucarelli, I. Palchetti, G. Marrazza, M. Mascini, Biosens. Bioelectron. 22 (2007) 1544.

NEW NANOSTRUCTURES FOR GENOSENSING

F.BERTI[1], I. PALCHETTI[1], G. MARRAZZA[1*], M. MASCINI[1], L. LOZZI[2], S. SANTUCCI[2], C. BARATTO[3], E. COMINI[3], S. TODROS[3], G. FAGLIA[3], G. SBERVEGLIERI[3]

[1]*Department of Chemistry, University of Florence, Florence, Italy.*
[2]*INFM, Department of Physics, University of L'Aquila, L'Aquila, Italy*
[3] *CNR-INFM SENSOR, Dept. of Chemistry and Physics, University of Brescia, Italy.*

Abstract

Recent advances in nanotechnology have attracted immense attention due to the possibility of creating functional materials, devices and systems by controlling matter at atomic and molecular scales. In this context, nanostructured electrode surfaces show an interesting and technologically important combination of properties such as high surface area, good electrical properties, chemical stability and easiness of miniaturization. In the present work, carbon nanotubes (CNT) and tin oxide nanostructured thin films were designed and tested as candidate electrical genosensors. Self-assembled CNT films were prepared by Chemical Vapor Deposition (CVD). Electrodes based on SnO_2 thin films and nanowires were prepared by RF magnetron sputtering on Al_2O_3 substrates.
Sensors were functionalized using oligonucleotides related to the most common inserts in the GMOs: the Promoter 35S. In particular, this paper describes the development of an enzyme-labelled genosensor using CNT thin films.

1. Introduction

Nanoscale materials are emerging as promising building blocks for the development of nano-structured genosensor devices. Among them, carbon nanotube electrodes play an important role in DNA electrochemical sensing due to their unique electric properties: high surface area, fast heterogeneous electron transfer, electrochemical stability, easiness of miniaturization [1].
Further advantages may come from the employment of highly ordered and vertically aligned carbon nanotube surfaces, like the sensors developed in this

* Corresponding author. *E-mail address:* giovanna.marrazza@unifi.it

work. The vertical orientation of the nanostructures, in fact, facilitates the access of the analyte towards the immobilized probe. Thus the aim of the present work was the investigation of new vertically organized CNTs surfaces as candidate platforms for DNA biosensor development.
Self-assembled aligned CNT thin films were prepared, in Santucci's laboratory, by Chemical Vapor Deposition (CVD) onto silicon oxide and aluminum substrates, using acetylene and ammonia as precursor gases and nickel particles as catalyst. These devices have been used only for gas sensing [2]. Therefore an electrochemical characterization was performed using cyclic voltammetry in order to investigate their electron-transfer properties in solution.
The genosensor was developed using synthetic oligonucleotides related to the 35S promoter, a typical genetic construct present in the majority of GMOs. The nanostructured surface was functionalized with an oligonucleotide DNA-probe by covalent immobilization. For the detection of the hybridization event an enzyme-linked approach was optimized thus exploiting the bio-catalytic activity of the enzyme to amplify the hybridization signal [4]. After the immobilization of the probe, the method involved the hybridization with a biotinylated target and the labelling with the enzymatic conjugate streptavidin alkaline phosphatase. The enzyme was then incubated with p-amino phenyl phosphate, and the product of enzymatic hydrolysis, detected by DPV.

2. Experimental

2.1 Chemicals

Acetic acid, sodium acetate, potassium chloride, nitric acid were obtained from Merck; *N*-(3-dimethylaminopropyl)-*N*′-ethylcarbodiimide hydrochloride (EDAC), urea, streptavidin-alkaline phosphatase, bovine serum albumin (BSA), magnesium chloride and diethanolamine were purchased from Sigma-Aldrich; N-hydroxysuccinimide (NHS) and sodium dodecyl sulphate (SDS) were obtained from Fluka; p-amino phenyl phosphate was purchased from DiagnoSwiss (Switzerland). All the solutions were prepared using MilliQ water.
The genosensor has been developed using synthetic oligonucleotides (MWG Biotech, Germany) related to the 35S promoter. The sequences of DNA probe (CP), target sequence (T35S) and a non complementary oligonucleotide (NC) are reported below:
CP (25 mer): 5'-NH_2-$(CH_2)_6$-GCCATCGTTGAAGATGCCTCTGCC-3'
T35S (25 mer): 5'-biotin-TEG-GGCAGAGGCATCTTCAACGATGGCC-3'
NC (24 mer): 5'-GGAGATCGACCACGCAAACTTCAA-3'

2.2 Apparatus

Electrochemical experiments were performed with a AUTOLAB PGSTAT 30(2) digital potentiostat/galvanostat with a GPES 4.8 software package (Eco Chemie). A three electrode well cell with the CNT thin film as working electrode (Ø = 4 mm), an Ag/AgCl wire as reference electrode and a platinum coil as counter electrode was employed. Carbon nanotube thin films were obtained in the laboratory by chemical vapour deposition (CVD), using acetylene and ammonia as precursor gases and nickel particles as catalyst [2].

2.4 DNA-probe immobilization

Synthetic oligonucleotides, having a C6 spacer and a terminal amino group, were covalently immobilized onto CNTs. Carboxylic groups were introduced onto the carbon nanotubes by oxidation and activated by interaction with 30µL of an aqueous solution containing 5mmol/L EDAC and 8 mmol/L NHS for 1 h. Finally, 30µL of capture-probe 10µM in phosphate buffer 0.5M pH 7.0, were deposited overnight. The immobilization proceeded through the formation of amide bonds between the carboxylic groups at the electrode surface and the amino-terminal end of the oligonucleotides. The residual reactive groups were blocked by depositing 30 µL of ethanolamine 100 mM for 20 minutes.

2.6 Hybridization assay

The probe-modified sensor was incubated with 30 µL of oligonucleotide target dissolved in phosphate buffer 0.5M pH 7.0, for 30 minutes. After hybridization, the sensor was incubated for 20 minutes with 30µl of a solution containing 0.75 U/ml of the streptavidin-alkaline phosphatase conjugate and 10mg/ml of BSA in DEA buffer (0.1 M diethanolamine, 1 mM $MgCl_2$, 0.1 M KCl; pH 9.6). The electrochemical measurements were performed by closing the circuit with 400 µL of DEA buffer containing 1mg/mL of p-amino phenyl phosphate. After 10 min, the electrochemical signal of the enzymatically produced p-amino phenol was measured by DPV (modulation time, 0.05 s; interval time, 0.15 s; step potential, 5mV; modulation amplitude, 70 mV). The regeneration of the immobilised probe was performed by treating with 50µL of a denaturant solution containing urea 5M and SDS 0.05%, for 5 minutes.

3. Results

Firstly the oligonucleotide immobilization conditions were deeply studied. Control of the surface chemistry and coverage, in fact, is essential for assuring high reactivity, orientation, accessibility and stability of the surface-confined

probe as well as for minimising non-specific adsorption events. Two properties of CNT-films make them particularly suitable to serve those purposes: the well alignment of nanostructures and the high reactivity of their fullerene-like tips which allow an easy end-functionalisation of the nanotubes. Thus amino-linked DNA-probe was covalently immobilized by the method of diimide-activated amidation, as reported in figure 1.

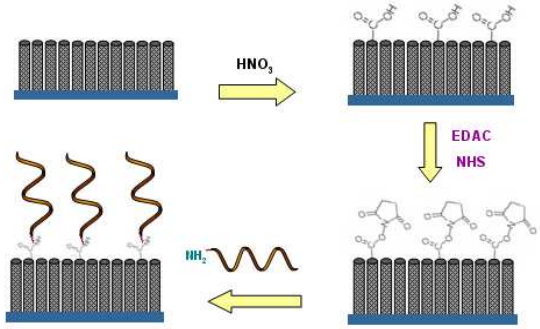

Figure 1. Scheme of DNA-probe immobilization

The optimal surface coverage was then experimentally assessed by varying the capture probe concentration in a range between 1 and 20μM. The higher hybridization yield was obtained using a 10 μM solution of amino-linked probe (specific vs non specific ratio ~1:5), so this concentration was chosen for further measurements.
The global performances of the genosensor were investigated by testing different amounts of DNA-target. The experiments were performed on a single probe-modified CNT-film by subsequent cycles of hybridization/denaturation. On that purpose p-amino phenyl phosphate was selected among other substrates because the hydrolysis product, p-amino phenol, doesn't electropolymerize and can be easily washed away thus allowing the reusability of the sensor.
p-amino phenol oxidation peaks, recorded in the presence of different concentrations of DNA-target (in the range 0-1μM), are reported in figure 2.

4. Discussion and conclusion

In this work, CNT thin films were developed in order be employed for the electrochemical detection of gene sequences by DNA hybridization at the sensor-liquid interface. A strategy of functionalisation was optimized in order to obtain a proper probe densities and orientation thus favoring the biorecognition event. The nanostructured surface was functionalized with the oligonucleotide DNA-probe by covalent immobilization. For the detection of the hybridization

event an enzyme linked assay was developed achieving satisfactory levels of sensibility and selectivity. Results reported in figure 2 exhibit a good proportional relationship between concentration and electrochemical response. The non-specific signal, obtained using a non-complementary (1µM), resulted negligible thus confirming the selectivity of the genosensor. Therefore CNT-films developed in this work resulted highly promising materials for the realization of nanostructured genosensors.

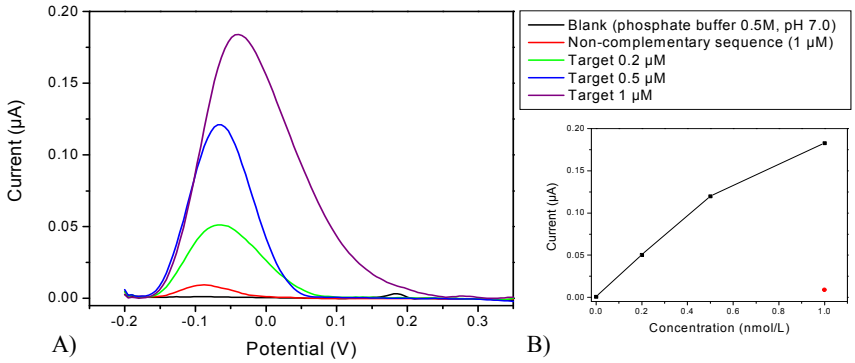

Figure 2. A) DPV p-amino phenol oxidation signal obtained after the hybridization with DNA target (concentration range 0-1µM) and non complementary oligonucleotide. B) calibration curve obtained by plotting the oxidation peak heights vs. target concentration.

Acknowledgements

This work has been partly supported by the Ministero dell'Istruzione, dell'Università e della Ricerca PRIN 2005 "Quasi mono dimensional nanosensors for label free ultra sensitive biological detection".

References

1. Merkoci, M. Pumera, X. Leopis, B. Péres, M. Del Valle, S. Alegret, *Trends in analytical Chemistry*, 4, 9 (2005).
2. L. Valentini, C. Cantalini, L. Lozzi, I. Armentano, J. M. Kenny, S. Santucci, *Materials Science and Engineering C*, 23, 523-529 (2003).
3. F. Bettazzi, F. Lucarelli, I. Palchetti, F. Berti, G.Marrazza, M. Mascini,, *Analytica Chimica Acta*, 6 1 4, 93–102 (2008).

ELECTROCHEMICAL CHARACTERIZATION OF PNA/DNA HYBRIDIZED LAYER USING SECM AND EIS TECHNIQUES

Ilaria Palchetti, Francesca Berti, Serena Laschi, Giovanna Marrazza, Marco Mascini

Dipartimento di Chimica, Università degli Studi di Firenze, Via della Lastruccia 3, 50019 Sesto Fiorentino (Fi), Italia, e-mail: ilaria.palchetti@unifi.it

The detection of DNA hybridization is of significant scientific and technological importance as testified by the growing interest in chip-based characterization of gene expression patterns and detection of pathogens. Recently, there has been an increasing interest for DNA sensors based on the SAMs (Self Assembled Monolayers) of Peptide Nucleic Acid (PNA) modified electrodes. PNA is a DNA mimic that has a neutral peptide-like backbone with nucleobases that allows the molecule to hybridize to complementary DNA strands with high affinity and specificity. In this communication, we present hybridization studies with DNA target oligonucleotides on a mixed monolayer of PNA and MCH (mercaptohexanol) on Au electrodes using EIS (Electrochemical Impedance Spectroscopy) and SECM (Scanning Electrochemical Microscopy). Preliminary results of PNA/DNA hybridization detection in a label free approach are reported.

1. Introduction

The use of nucleic acids recognition layers in biosensor design represents an exciting area in analytical chemistry [1]. Recently, probes produced by chemical changes to the backbone of naturally occurring DNA or RNA are used more and more in NA sensing techniques [2]. Among these, Peptide Nucleic Acid (PNA) are frequently used. Owing to its neutral backbone and proper interbase spacing, PNA binds to its complementary nucleic acid sequence (DNA or RNA) with higher affinity and specificity compared to traditional oligonucleotides. The neutral backbone also implies a lack of electrostatic repulsion between the PNA and DNA strands (compared to that existing between two negatively charged DNA oligomers), and hence a higher thermal stability of PNA/DNA duplexes. Electrochemical methods can conveniently be used in NA sensing to study and detect PNA/DNA hybridization in a label free approach. The immobilized PNA probes on the electrode surface are uncharged, and hence, do not affect the charge transfer from charged redox indicator, such as $K_4Fe(CN)_6$/ $K_3Fe(CN)_6$, to the electrode. Once DNA targets hybridize to PNA, the charge density at the sensor surface will be changed. Thus, one can use electrochemical techniques highly sensitive to the interfacial electron transfer, such as EIS or SECM, to conveniently monitor the PNA/DNA hybridization process. In this communication preliminary results of such studies using both the techniques are reported.

2. Experimental

Table 1 shows the thiol-terminated PNA probe and DNA target used in this study. Thiolated PNA was dissolved in 0.1% trifluoroacetic acid. Here, PNA-modified surfaces were obtained by exposing the gold substrates in a 15 μM (for SECM measurements) or 200 nM (for EIS measurements) PNA solution for

about 12 h. The surfaces were then treated further with 1 mM mercaptohexanol (MCH) solution for 30 min. EIS measurements were performed with an AUTOLAB PGSTAT 30(2) digital potentiostat/galvanostat, using a Ag/AgCl pseudo reference electrode and a Pt counter electrode. SECM measurements were performed with an Uniscan instrument SECM 270 (Uniscan, UK), using Au disk microelectrodes with 10 μm diameters (CH Instruments, UK) as amperometric SECM tip and $Hg/HgSO_4$ (CH Instruments, UK) as reference electrode.

Name	***Sequence***
Thiolated PNA	5' TAT TTA CGT GCT GCT A -$(CH)_6$-SH 3'
Fully complementary target	5' TAG CAG CAC GTA AAT A - TEG- biotin 3'
Non complementary sequence	5' AGG CCC TGC GAG CAA CAT CTC ATG–TEG-biotin 3'

Table 1. The sequences of PNA probe and DNA targets

3. Results and Discussion

3.1 PNA-DNA layer characterization by SECM

The first step of the detection scheme consists of the immobilization of thiol-tethered PNA by chemisorption; then the PNA chip is postassembled with MCH to increase hybridization efficiency and to avoid unspecific adsorption of target strands. When a gold surface is exposed to thiol-containing compounds (HS-R), by varying the terminal group of R, surface properties, including chemical and electrochemical reactivity, are different. Thus, an evaluation of the behavior of the HS-PNA/MCH mixed adsorbate was performed. Approach curves obtained in 1 mM $K_4Fe(CN)_6$ solution showed a positive feedback. This behavior demonstrated that mediators are not blocked by the PNA monolayer, mainly because the backbone of PNA contains no charged phosphate groups to repeal negatively charged mediators. After DNA hybridization the feedback effect is smaller, indicating the presence of negatively charged phosphate group and of electrostatic repulsion. However this effect is not pronounced as expected. Probably this behavior is due to defects of the PNA/DNA layer; as a consequence the DNA strands are so loosely arranged that their anionic phosphate groups could not really hinders $Fe(CN)_6^{3-}$ molecules to approach the Au surface to undergo redox recycling. However, approach curves recorded in ferrocenemethanol (data not shown) showed a positive feedback demonstrating that diffusion of this uncharged mediator proceeds virtually unimpeded.

3.2 PNA-DNA layer characterization by EIS

EIS experiments confirmed results obtained with SECM. Since the backbone of PNA contains no charged phosphate groups, the electron transfer resistance is

smaller in the case of the chip modified with thiol tethered PNA before the hybridization with the target DNA than after the hybridization. This is consistent with the electrostatic repulsion of the redox indicator from the electrode interface by the formation of the charged PNA/DNA duplexes, thereby introducing a barrier to electron transfer. The resistance increases with the DNA target concentration (data not shown), whereas is similar to the PNA layer only when a non complementary strand was studied.

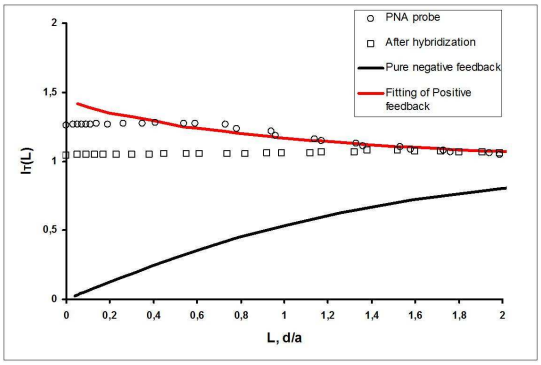

Figure 1. Approach curve experiments on a 15 µM HS-PNA modified gold substrate before and after hybridization with 30 µM DNA. The approach curves are obtained in $K_4Fe(CN)_6$ 1 mM solution in Tris-ClO_4 buffer 20 mM + $NaClO_4$ 50 mM, pH 8.6, over a modified chip, E_{tip} = + 0.100 V, E_s=OCP. For all the experiments a Au tip with a diameter of 10 µm was used. The black solid line is the SECM theoretical curve for pure negative feedback.

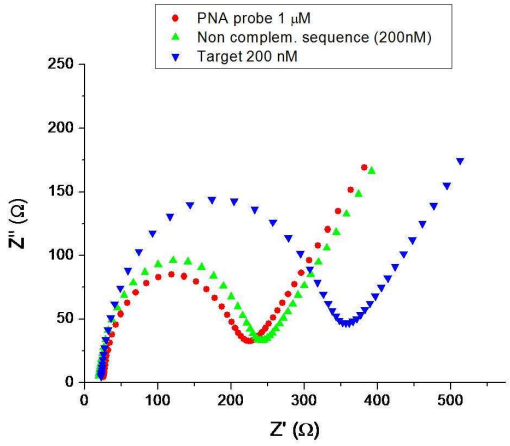

Figure 2. Nyquist Plot for PNA-modified gold substrates. Experimental parameters: redox probe, 2.5 mM $[Fe(CN)_6]^{3-/4-}$ (1:1) mixture in 1 M KCl; Bias potential, + 0.2 V; frequency range, 100 kHz-100 mHz; ac voltage amplitude, 10 mV. 0.2 µM HS-PNA gold modified substrate.

4. Conclusions

The data reported in this communication demonstrated that PNA/DNA hybridization can be detected with both EIS and SECM in a label free approach by using a negatively charged redox mediator.
However, SECM detection needs the formation of highly packed probe layer, this means high probe concentration and high target concentration. EIS detection can easily discriminate specific and non specific signal at nM range of target even using low concentration of probe.

Acknowledgments

Support from the Italian Government in the framework of the PRIN 2007 project.

References

[1] J. Wang, "DNA biosensors based on PNA recognition layer. A review", Biosensors & Bioelectronics, [13], pp. 757-762, 1998.
[2] Ilaria Palchetti and Marco Mascini "Nucleic acid biosensors for environmental pollution monitoring", Analyst, [133] pp. 825-964, 2008.

Elsevier Editorial System(tm) for Biosensors and Bioelectronics
Manuscript Draft

Manuscript Number: BIOS-D-09-01872

Title: QUASI-MONODIMENSIONAL POLYANILINE NANOSTRUCTURES FOR ENHANCED MOLECULARLY IMPRINTED POLYMER-BASED SENSING

Article Type: Full Length Article

Section/Category: Regular Papers

Keywords: Polyaniline, nanostructure, biosensor, molecularly imprinted polymers

Corresponding Author: prof Giovanna marrazza,

Corresponding Author's Institution:

First Author: Giovanna Marrazza, Prof.

Order of Authors: Giovanna Marrazza, Prof.; Francesca Berti, Dr; Silvia Todros, Dr; Dhana Lakshmi, Dr; Michael Whitcombe, Dr; Iva Chianella, Dr; Matteo Ferroni, Dr; Sergey A Piletsky , Prof; Anthony P Turner, Prof

QUASI-MONODIMENSIONAL POLYANILINE NANOSTRUCTURES FOR ENHANCED MOLECULARLY IMPRINTED POLYMER-BASED SENSING

Francesca Berti [a], Silvia Todros [b], Dhana Lakshmi [c], Michael J. Whitcombe [c], Iva Chianella [c], Matteo Ferroni [b], Sergey A. Piletsky [c], Anthony P. F. Turner [c] and Giovanna Marrazza [a 1]

[a] Department of Chemistry, University of Florence, via della Lastruccia 3, 50019 Sesto Fiorentino, Firenze, Italy

[b] CNR-INFM SENSOR Laboratory, Department of Physic and Chemistry, University of Brescia via Valotti 9, 25133 Brescia, Italy

[c] Cranfield Health, Cranfield University, Cranfield, Bedfordshire, MK43 0AL, UK

Keywords: Polyaniline, nanostructure, biosensor, molecularly imprinted polymers

Abstract

Nanomaterials are finding wide application in biomedical and bioanalytical devices. The rationale for this can be traced to the nanometre scale of most biological systems and the importance of molecular interaction, which make nanostructures intuitive candidates for integration into biosensing systems. Moreover, nanomaterials can greatly facilitate the miniaturisation of sensors and devices, delivering nanometre tolerances and / or dimensions resulting in better sensitivity, specificity and faster response times compared to current solutions. The main challenge in developing chemical sensors based on nanostructures is to realise a reliable electrical contact and to optimise transduction from active sites or receptors to the electrode.

[1] Corresponding author: Giovanna Marrazza
Department of Chemistry, University of Florence, via della Lastruccia 3, 50019 Sesto Fiorentino, Firenze, Italy
e-mail: giovanna.marrazza@unifi.it
Tel:+390554573320
Fax:+390554573396

In this work, we explore a simple, inexpensive and fast route to grow polyaniline (PANI) nanotubes, arranged in an ordered structure directly on an electrode surface, by electrochemical polymerisation using alumina nanoporous membranes as a template. The deposited nanostructures have been electrochemically and morphologically characterised and then employed to create a model molecularly imprinted polymer-sensor for catechol detection. The advantages of using nanostructures in this particular biosensing application have been evaluated by comparing the analytical performance of the sensor with an analogous non-nanostructured MIP-sensor that we had previously developed. A significantly lower limit of detection has been (one order of magnitude) thus demonstrating that the nanostructures enhance the analytical performance of the sensor.

1. Introduction

The last decade has witnessed a fast and prolific production of sensors and biosensors based on nanomaterials. The dimensions of nanostructures are comparable to the size of the molecules being sensed, and thus they represent ideal transducers which can also be interfaced with macroscopic instruments. Thus they facilitate the construction of miniaturised sensor devices with nanometre dimension resulting in better sensitivity, specificity and faster response compared to current solutions. The main challenge in developing chemical sensors based on nanostructures is to realise reliable electrical contact and to optimise transduction from active sites or receptors, to the electrode.

In this work, we grew polyaniline (PANI) nanostructures in an ordered arrangement directly on an electrode surface by electrochemical polymerisation, using alumina nanoporous membranes as template. The PANI nanostructures were then used as a functional substrate for the development of a molecularly imprinted polymer-based sensor, thus exploiting the intrinsic advantages of

nanostructures as optimal transducers together with the well known benefits of molecularly imprinted polymers as receptors.

Polyaniline is a conductive polymer, a class of molecules which have found a large number of applications in the field of chemical and biochemical sensing over the last three decades (Bidan, 1992). Their intrinsic conductivity results from the formation of charge carriers ("doping") upon oxidising (p-doping) or reducing (n-doping) their conjugated backbone (Lange et al., 2008). In this way they assume the electrical properties of metals, while having the characteristics of organic polymers such as light weight, resistance to corrosion, flexibility and lower cost of fabrication (Palaniappan and John, 2008). Moreover, when formed as nanostructures, conductive polymers are enriched with further appealing properties, i.e. ease of preparation by chemical or electrochemical methods, sensitivity towards a wide range of analytes, great signal amplification due to their electrical conductivity and fast electron transfer rate. Compared to inorganic nanostructures, they are more amenable to both chemical modification in order to obtain high specificity towards different compounds and to fabrication procedures which greatly facilitate miniaturisation and array production (Yoon and Jang, 2009).

Among conducting polymers, PANI has generated great interest because it is inexpensive, easy to process and dope, has high conductivity and the raw materials for its synthesis are readily available (Ding et al., 2008). However, the performance of the conventional PANI films is strongly dependant on thickness: the higher the thickness, the poorer is the diffusion of analytes towards the sensing element and consequently the sensitivity of measurements decreases (Zhang and Wang, 2006). For this reason, considerable attention has been paid in the realisation of one-dimensional polymer nanostructures which, due to their greater exposure area, offer the possibility of enhancing the diffusion of analyte towards the transducer. Polyaniline nanofibre sensors have been employed in gas and chemical detection (Huang et al., 2004; Virji et al., 2004). In bioanalysis, high-

performance composites have been obtained by coupling PANI nanostructures with biologically functional materials such as enzymes, bio- or synthetic receptors, to obtain various catalytic (Morrin et al., 2005; Du et al., 2009; Zhao et al., 2009; Somerset et al., 2007) or affinity (Zhu et al., 2006; Chang et al., 2007; Zhou et al., 2009) biosensors.

Nanostructured PANI can be obtained by "template" or "template free" methods of synthesis, as widely reviewed (Kuchibhatla et al., 2007; Cho and Lee, 2008; Cao and Liu, 2008; Martin, 1996; Chen et al., 2008). Among template approaches, "soft template" and "hard template" strategies can be distinguished. In this work, a hard template method has been used. This technique involves the employment of physical templates such as nanoporous membranes (polycarbonate, silica or alumina). Monomer solution fills the cylindrical pores of the membrane, thus allowing the formation of monodisperse polymer nanocylinders or tubes with accurate control of length (in the order of microns) and diameter (between 10 and 200 nm) (Cho and Lee, 2008).

Polyaniline nanowires grown using this method were then used as functional substrates for the development of a molecular imprinted polymer-based sensor. Molecularly Imprinted Polymers (MIPs) are synthetic polymers with artificial recognition cavities (Mosbach, 1994; Hollinger and Hoogenboom, 1995; Wullf, 1993). The imprinting technique uses the target molecule as a template for synthesising polymers with specific recognition sites. Such artificial receptors have shape and chemical functionality matching those of the analyte and are thus capable of rebinding specifically the target molecules in preference to other closely related molecules (Piletsky and Turner, 2002). The use of these compounds as artificial receptors offers three main advantages: ease high affinity and selectivity (similar to those of natural receptors such as enzymes and antibodies); a unique stability, which cannot be found in natural biomolecules; and ease of preparation, suitable for mass production (Piletsky et al., 2006). However, most common imprinted polymers, mainly based on acrylic or vinylic compounds, are electrical insulators. This seriously limits their use as receptors in

electrochemical sensors because of the lack of a direct path for conduction from the active sites to the electrode. Different ways have been investigated to overcome this problem such as the formation of conductive and semi-conductive MIPs, such as imprinted polypyrrole, polyaniline (Deore et al., 1999; Sreenivasan, 2007) or the integration of MIPs with polymeric conductors, thus taking advantage of both materials (Mazzotta et al., 2008; Lakshmi et al., 2009a).

In this work, we applied a simple approach to a close integration between MIP and transducer. The idea was to develop a nanostructured sensor based on polyaniline nanowires or nanotubes grafted with MIP receptors. A novel hybrid material, N-phenylethylene diamine (NPEDMA) (Lakshmi et al., 2009b) was used as monomer, combining two orthogonal polymerisable functionalities, an aniline group and a methacrylamide. In this way, the polymerisation of NPEDMA resulted in a conductive layer which allowed direct electrical connection between the electrode and the MIP.

The conducting nanostructures were synthesised inside the pores of a membrane by electropolymerisation of the aniline function. The MIP, a Tyrosinase-mimicking polymer imprinted with catechol (Piletsky et al., 2005), was photochemically grafted over the polyaniline via iniferter activation of the methacrylamide groups. Thus, hybrid catalytic material electrodes were prepared and characterised. Finally the ability to detect catechol was evaluated.

2. Materials and methods

2.1 Chemicals

Catechol, resorcinol, hydroquinone, (-)-epinephrine, serotonin hydrochloride, ethylene glycol dimethacrylate (EGDMA), N-phenyl ethylenediamine, methacrylic anhydride, acetonitrile, dimethylformamide, perchloric acid, sodium hydroxide and methanol were purchased from Sigma-Aldrich (Gillingham, U.K.). Resorcinol was obtained from Fluka (Gillingham, U.K.). Iniferter

(diethyl dithiocarbamic acid benzyl ester) was purchased from TCI (Oxford, U.K.). Copper chloride and ethylenediaminetetraacetic acid (EDTA) were obtained from Fisher Scientific (Loughborough, UK). NMR solvents were obtained from Goss Scientific (Chelmsford, U.K.).Ultrapure water (Millipore) was used for preparing all the solutions.

2.2 Monomer (NPEDMA) preparation

N-phenylethylenediaminemethacrylamide (NPEDMA) monomer was prepared following a procedure reported by Lakshmi et al. (2009b). The monomer was characterised by recording ^{1}H-NMR spectra using deuterated chloroform ($CDCl_3$) as solvent (spectra not reported here).

2.3 Template synthesis of PANI nanostructures

Polyaniline nanostructures were electrochemically synthesised using nanoporous alumina membranes as template. A gold layer was sputtered (180", 20 mA, in Ar atmosphere, using an Auto sputter coater, Agar Scientific, Stansted, UK) on one side of an alumina nanoporous membrane employed as template (Whatman Anopore membrane, Ø = 0.02μm), in order to achieve electrical conductivity. The aniline monomer (NPEDMA) was electropolymerised by cycling the Au sputtered membrane between -0.4 V and +1.0 V (vs. Ag/AgCl, scan rate 50 mV s^{-1}, 10 cycles) in a solution of NPEDMA (2.4 mmol L^{-1} in methanol) in 50 mmol L^{-1} $HClO_4$. Finally, template was removed by dissolving the membrane in NaOH for 30 minutes.

2.4 Electrochemical apparatus

All electrochemical experiments were performed with an AUTOLAB PGSTAT 10 digital potentiostat/galvanostat with a GPES 4.8 software package (Eco Chemie, Utrecht, Netherland). A

plexiglass three electrode well cell (made in our laboratory) with the sputtered membrane as working electrode (Ø= 8 mm), an Ag/AgCl reference electrode and a platinum wire as counter electrode was employed. All the potentials were referred to the Ag/AgCl reference electrode. All the experiments were carried out at room temperature (25°C).

2.5 SEM characterisation

SEM analysis was carried out by field-emission LEO 1525 microscope, equipped with In-Lens detector (by LEO Inst., Nano Technology Systems Division of Carl Zeiss SMT, Germany) for secondary-electrons imaging, with a STEM detector (by KE Development, UK) on the back of the sample holder to acquire transmitted electron beam and with an X-rays detector (by Oxford Instruments Inca 250, UK) for EDX analysis.

2.6 Preparation of the MIP-sensor for catechol detection

Iniferter immobilisation: a solution of (0.0015g/10 mL acetonitrile) of diethyl dithiocarbamic acid benzyl ester, was prepared in a Petri dish (10-12 cm) and oxygen was removed from the solution by purging with argon for 10 minutes. After dipping the electropolymerised membranes in the iniferter solution, the Petri dish was covered with a flat glass plate, using some Parafilm to improve the adhesion and sealing. Irradiation with a Philips UV lamp, mounted at 8 cm from the surface of the samples, for 20 minutes, was used to photochemically attach the iniferter to PANI surface. The sample was then washed with methanol and dried in Argon gas.

MIP/NIP grafting: 375µmol (62.3 mg) of urocanic acid ethyl ester, 62.5 µmol (6.9 mg) of catechol and 1000 µmol of $CuCl_2$ (134.45 mg) were dissolved with 2.50 g DMF in a 30 mL thick walled tube glass followed by the addition of 1.20 g (6.06 mmol) of EGDMA. The reaction mixture was well

mixed and then sonicated for 10 minutes. The iniferter grafted electropolymerised membrane was dipped in the aforementioned reaction mixture in a small glass Petri dish. After the removal of the oxygen by purging with argon for 4 minutes, the Petri dish was covered with a flat glass plate sealed with Parafilm. Irradiation with UV light for 30 minutes (same exposure set-up as above) was then used to graft MIP on the samples. Following the same procedure, NIP (non-imprinted polymer) was also prepared using the same recipe without the addition of template (catechol).

2.7 Catechol detection

Different concentrations of catechol were detected by cyclic voltammetry (CV). Firstly 1 mL of $CuCl_2$ 5 mmol L^{-1} was added in the cell for 5 minutes. After washing with PBS, fresh solutions of catechol (in PBS, pH 7.4), were added to the electrochemical cell containing the Cu-loaded hybrid electrode. The CV was recorded applying the following parameters: start potential -0.5 V, first vertex potential 0.9 V, second vertex potential 0.5 V, step potential 0.01 V, scan rate 0.05 V s^{-1}; Potential vs. Ag/AgCl The height of the anodic peak was taken as analytical signal. Analogues that could be potential interferents were measured according to the same procedure.

3. Results and discussion

3.1. Synthesis of PANI nanostructures

Polyaniline nanostructures were electrochemically synthesised using nanoporous alumina membranes as template, a technique which has the advantage of careful control of the shape and dimensions of polymerised objects (Cho and Lee, 2008).

A recently designed aniline monomer, NPEDMA (Laksmhi et al., 2009b), was employed for nanostructure construction. The peculiarity of this compound is the simultaneous presence of orthogonal polymerisable moieties, an aniline group and a methacrylamide, which allow the growth of PANI nanostructures as well as an easy functionalisation with bioreceptors.

A gold layer was sputtered on one side of an alumina nanoporous membrane in order to achieve electrical conductivity. The aniline monomer was electropolymerised inside the pores of the membrane by CV, after making the membrane the working electrode in a three electrode well cell. Cycles of 5, 10 and 15 scans were tested in order to find the best condition for obtaining well defined nanowires. A low number of cycles resulted in incomplete filling of the pores while after too many scans, polymer tended to fill the pores and form a layer over the membrane. SEM characterisation (reported in the next paragraph) indicated that 10 cycles produced the best condition for growth.

Figure 1 shows 10 consecutive scans. A reversible redox couple, absent in the first scan and increasing with increasing number of cycles until a constant intensity, is observed at E_{pa}=400 mV and E_{pc}=200 mV; this can be attributed to the Leucoemeraldine (completely reduced form)-Emeraldine (partially oxidised form) transition (Linfords and Ivaska, 2002). An oxidation peak, without a corresponding cathodic peak on the reverse sweep, appeared at 650 mV and then decreased until disappearing with further increase in the number of the cycles. According to the literature (Jin et al., 2006), this can be ascribed to the oxidation of aniline to cation radicals, which are gradually deposited on the electrode surface, thus preventing aniline from being further oxidised.

Once electro-polymerised polyaniline was formed, the conductivity between the two sides of the membrane was measured in order to evaluate if the pores were filled with the conductive polymer or not. Firstly, resistance was measured between the two sides of the membrane, after having

sputtered one of them with a gold layer, thus demonstrating that even if a small amount of gold penetrates the pores it was not enough to contact the two sides. After electropolymerisation of aniline inside the pores, resistance values in the range 0.2-2.6 MΩ were recorded, thus demonstrating the presence of electrical "wires" connecting the two sides of the membrane.

Finally, template was removed by dissolving the membrane in NaOH, thus obtaining a ready-to-use PANI-nanowire array sensor with the gold layer as electrical contact. The sensor could potentially be exploited in many applications. The nanostructures could be grafted with receptors such as enzymes, antibodies or MIPs and used as affinity sensors. In this work, template membrane was kept as rigid framework for PANI wires. In our future activities, we are also planning to evaluate the feasibility of a nanostructured gas sensor obtained by sputtering a second gold contact on the other side of the membrane before its dissolution.

3.2. Morphological characterisation

In order to evaluate the morphology of the PANI nanostructures electro-polymerised through cyclic voltammetry (CV), Scanning Electron Microscopy (SEM), Scanning Transmission Electron Microscopy (STEM) and Energy Dispersive X-ray (EDX) analysis was carried out.

The SEM was operated at 1 - 3 kV accelerating voltage range, to prevent electrostatic charging of both alumina and polymer in the samples and to avoid polymer degradation under the impinging electron beam. Alumina membranes were analysed with SEM after electrochemical polymerisation of NPEDMA monomer following cyclic voltammetry (CV) with various numbers of cycles (5, 10, 15 cycles), in order to verify the presence of nanostructures grown inside the pores of the membranes and to understand the role of deposition time on material structure. The membranes were then dissolved in NaOH and analysed again, to obtain a morphological characterisation of the PANI nanostructures and to evaluate their durability after membrane dissolution. Comparing top

views of membranes before and after electro-polymerisation, it was clear that the pores were not completely filled by the polymer, even if some new structure could be found on the surface after the deposition. This effect was more pronounced the higher is the number of cycles used for the deposition: in 5-cycles samples there were no remarkable variations of the membrane surface morphology, in 10-cycles samples just a few small particles appeared, while after 15-cycles (SEM micrographs not shown here) a discontinuous film of polymer partially covered the membrane surface. For this reason, 10-cycles deposition was selected as the best conditions for growth.

The resulting structures after membrane dissolution can be seen in Figure 2, A and B, and in Figure 3, A. Polymer quasi-monodimensional nanostructures, of approximate diameter of 150 nm and length up to 50 microns, covered the surface uniformly. These structures were vertically aligned with respect to the substrate surface, even if after membrane dissolution small mechanical relaxation of the polymer could be observed. They were semiconductive, as could be deduced from weak charging effects under illumination with the electron beam, except in areas where some residuals of the alumina membrane were still present or the glass sample holder was uncovered. It was not clear from these images if these structures were nanowires/nanorods, i.e. the pores of the membrane were completely filled of polymer, or nanotubes with an empty core, i.e. the polymer started depositing on the pore surface towards the interior. To obtain a deeper understanding of this issue, Scanning Transmission Electron Microscopy (STEM) and Energy Dispersive X-ray (EDX) analysis and mapping were carried out.

Small portions of membranes were prepared in the shape of thin samples, transparent to high energy electrons, in order to perform STEM analysis: fragments of electro-polymerised membranes were placed on TEM grids and then dissolved in NaOH, resulting in single nanostructures suspended on the grid. The microscope was then operated at high voltage (20 kV). As can be clearly seen in Figure 3, B, STEM analysis showed the presence of dark areas near the centre of a single

nanostructure, imputable to the existence of porosities and with an empty core in the middle of the structures. Thus it can be inferred that these polymer nanostructures were tubes with a variable pore size, depending on the number of deposition cycles. This is consistent with literature reports that polymer generally nucleates and grows on the pore walls because of the electrostatic attraction between the growing polycationic polymer and anionic sites along the pore walls of the membrane itself (Martin, 1996).

EDX analysis (spectra not shown here) gave information on the elemental composition of the samples, showing the presence mainly of carbon, with a small amount of aluminum and oxygen, coming from residual Al_2O_3 of the template. For our purpose, it was interesting to map the most concentrated element, to obtain further information on the morphology of the nanostructures. Carbon mapping showed a broad profile (Figure 3 C), with a maximum near the core of the structure. In case of a nanotube, this profile appeared as a dual-peaked band, with a minimum in between corresponding to the empty core of the tube. However, if the pore was small (diameter of about 25 nm), a higher resolution would be necessary to distinguish the two peaks; it is thus possible that the small pore seen with STEM could not be discerned through EDX mapping.

3.3. MIP grafting of polyaniline nanostructures for catechol detection

The nanostructures produced were used in a model MIP biomimetic sensor for catechol detection, by adapting a procedure previously developed in our group by Lakshmi and co-workers (2009a). The intention was to compare sensors formed using a well optimised grafting method on our new nanostructures with the ones previously obtained on conventionally formed polymer structures. To our knowledge, this is the first MIP-sensor realised using a nanostructured conductive polymer-based platform for electrochemical transduction. The MIP composition had been previously developed by our team as a Tyrosinase-mimicking polymer, imprinted with catechol (Piletsky et al.,

2005). It is based on the simultaneous coordination of a catechol molecule with Cu(II) and the imidazole moiety of the functional monomer (urocanic acid ethyl ester), thus reproducing the active site of the enzyme tyrosinase, capable of oxidising o-diphenols to o-quinones, in the presence of oxygen. PANI nanowires were grafted with MIP and non-imprinted polymer (NIP) via iniferter activation of the methacrylamide groups (as reported in Paragraph 2.6), without removing the alumina membrane, in order to have a rigid framework which facilitated placement in the electrochemical cell. After grafting, the catechol employed as template in MIP construction was removed using EDTA. After loading with Cu(II) the sensors were ready to be employed.

The electrochemical behaviour of the nanostructured sensor in the presence of catechol was investigated by comparing CV scans before and after MIP grafting. Figure 4 shows CV scans of a 100 μmol L^{-1} solution of catechol in PBS buffer recorded using an Au-sputtered alumina membrane before electropolymerisation (dotted line), the same membrane after PANI nanostructures were grown (dashed line), and the MIP-grafted sensor (solid line). Oxidation and a reduction peaks are visible at 0.3 V and 0.1 V, respectively only with the MIP-grafted sensor, thus demonstrating that recognition and catalytic oxidation of catechol occur only in the presence of MIP and NPEDMA polymeric nanowires, which presumably facilitate electron exchange between the catalytic site and the electrode.

Moreover, compounds structurally related to catechol were also examined by CV, in order to evaluate cross reactivity, which might result in interference in a sensor. Results reported in Figure 5 show that even at concentrations ten-fold higher than a catechol reference solution, no peaks were detected for any of these compounds in the potential window of catechol oxidation, thus demonstrating the high selectivity of the sensor. The lack of interaction of resorcinol, hydroquinone and serotonin with the MIP is because these compounds are devoid of the ortho-dihydroxy motif required for the formation of the complex with copper (Lakshmi et al., 2009a). In case of ascorbic

acid and epinephrine, this lack of interaction was probably due to their lower propensity to oxidation or to steric hindrance, which prevents a good fit inside the recognition cavity.

The analytical performance of the sensor was investigated by producing a calibration curve correlating the catechol concentration (in the range 1-100 μmol L^{-1}) with the anodic peak current obtained by CV (Figure 6). The experiment was performed using the same sensor for different concentrations: immobilised catechol was removed with EDTA after each measurement and then another concentration was tested, after loading with Cu(II) in order to recreate the active site of tyrosinase. Each data point reported was calculated as the average reading from three different sensors. Corresponding data were collected using NIP control nanostructured electrodes.

As shown in Figure 6, sensors grafted with MIP exhibited a near linear response in the concentration range 0-5 μmol L^{-1}, then the signal increased more slowly, but still in proportion to concentration. In the case of non-imprinted control sensors, the signal was negligible, thus demonstrating the selectivity of the MIP. From the interpolation of the linear part of the curve (0-2 μmol L^{-1}), a limit of detection of 12 nmol L^{-1} for catechol was calculated using the following equation: $Y = 35.7\ X + 4.77$ ($R=0.97$) and considering the mean of the blank solution response plus three times its standard deviation (Mermet et al., 2006). These results were compared with analytical parameters previously obtained by Lakshmi et al. (2009a) who developed an analogous non-nanostructured MIP-sensor for catechol detection by depositing thin films of polymerised NPEDMA monomer on gold electrodes. Despite the wider range of linearity obtained in that case (228 nmol L^{-1}-144 μmol L^{-1}), in the present work a lower limit of detection was achieved (1 order of magnitude less), thus demonstrating that the presence of nanostructures increases the ability of the sensor to detect lower concentrations, due to the enhanced surface area.

4. Conclusions

A simple, inexpensive and rapid method for the formation of novel polyaniline nanostructures has been developed. These have been electrochemically and physically characterised (electrical conductivity measurements and morphological characterisation through SEM imaging). The PANI nanotubes had a diameter of 150 nm and length of up to 50 μm, uniformly covered the surface and were vertically aligned with respect to the substrate. Their high aspect-ratio is extremely favourable for sensing applications, because they provide an extended surface area of active sites and thus significantly increase sensitivity. This was illustrated by grafting molecularly imprinted polymers on polymer nanowires to create a specific and selective model MIP-sensor for catechol detection with a detection limit one order of magnitude lower (12 nmol L^{-1}) than an analogous non-nanostructured sensor. These results suggest that it this method could be used to create a wide range of high-performance sensors. In addition, the nanostructures could be connected directly to single or double electrical contacts for applications in chemical gas sensing by exploiting the variation in resistance of the polymer in the presence of different oxidising and reducing gases.

Acknowledgements

The authors would like to thank Prof. G. Faglia from CNR- INFM Sensor Lab, University of Brescia, for the helpful scientific supervision and support in the morphological characterisation, Dr. C. Baratto and Dr. F. Davis for their kind assistance and Prof. M. Mascini from University of Florence who gave us the possibility to collaborate, thanks to his long-term partnership with Cranfield University.

References

Bidan, G., 1992. Electro conducting conjugated polymers: new sensitive matrices to build up chemical or electrochemical sensors. A review. Sens. Actuators, B 6, 45–56.

Cao, G., Liu, D., 2008. Template-based synthesis of nanorod, nanowire, and nanotube arrays. Adv. Colloid Interface Sci. 136, 45–6.

Chang, H., Yuan, Y., Shi, N., Guan, Y., 2007. Electrochemical DNA biosensor based on conducting polyaniline nanotube array. Anal. Chem. 79, 5111-5115.

Chen, J., Xu, Y., Zheng, Y., Dai, L., Wu, H., 2008. The design, synthesis and characterisation of polyaniline nanophase materials. C. R. Chimie 11, 84-89.

Cho, S., Lee, S.B., 2008. Fast electrochemistry of conductive polymer nanotubes: synthesis, mechanism, and application. Acc. Chem. Res. 41, 699-707.

Deore, B., Chen, Z., Nagaoka, T., 1999. Overoxidized polypyrrole with dopant complementary cavities as a new molecularly imprinted polymer matrix. Anal. Sci. 15, 827-828.

Ding, S., Chao, D., Zhang, M., Zhang, W., 2008. Structure and electrochemical properties of polyamide and polyaniline. J. App. Polym. Sci. 107, 3408-3412.

Du, Z., Li, C., Li, L., Zhang, M., Xu, S., Wang, T., 2009. Simple fabrication of a sensitive hydrogen peroxide biosensor using enzymes immobilized in processable polyaniline nanofibers/chitosan film. Mater. Sci. Eng., C 29, 1794–1797.

Holliger, P., Hoogenboom, H.R., 1995. Artificial antibodies and enzymes: mimicking nature and beyond. Trends Biotechnol. 13, 7-9.

Huang, J., Virji, S., Weiller, B.H., Kaner, R.B., 2004. Nanostructured polyaniline sensors. Chem. Eur. J. 10, 1314–1319.

Jin, M., Yu, Z., Xia, Y., 2006. Electrochemical and spectroelectrochemical studies on aniline in organic medium and its antiknock mechanism. Russ. J. Electrochem. 42, 964-968.

Kuchibhatla, S.V.N.T., Karakoti, A.S., Bera, D., Seal, S., 2007. One dimensional nanostructured materials. Prog. Mater. Sci. 52, 699–913.

Lakshmi, D., Bossi, A., Withcombe, M. J., Davis, F., Chianella, I., Fowler, S.A., Subrahmanyam, S., Piletska, E.V., Piletsky, S.A., 2009a. Electrochemical sensor for catechol and dopamine based on a catalytic molecularly imprinted polymer-conducting polymer hybrid recognition element. Anal. Chem. 81, 3576-3584.

Lakshmi, D., Withcombe, M.J., Davis, F., Chianella, I., Piletska, E.V., Guerreiro, A., Subrahmanyam, S., Brito, P.S., Fowler, S.A., Piletsky, S.A., 2009b. Chimeric polymers formed from a monomer capable of free radical, oxidative and electrochemical polymerisation. Chem. Commun. 2759-2761.

Lange, U., Roznyatovskaya, N. V., Mirsky, V. M., 2008. Conducting polymers in chemical sensors and arrays. Anal. Chim. Acta 614**,** 1-26.

Lindfors, T., Ivaska, A., 2002. Potentiometric and UV/vis characterisation of N-substituted polyanilines. J. of Electroanal. Chem. 535, 65-74.

Martin, C.R., 1996. Membrane-Based Synthesis of Nanomaterials. Chem. Mater. 8, 1739-1746.

Mazzotta, E., Picca, R.A., Malitesta, C., Piletsky, S.A., Piletska, E.V., 2008. Development of a sensor prepared by entrapment of MIP particles in electrosynthesised polymer films for electrochemical detection of ephedrine. Biosens. Bioelectron. 23, 1152-1156.

Mermet, J.M., Otto, M., Valcarcel, M., 2006. Analytical chemistry : a modern approach to analytical science, founding editors: R. Kellner, H. M. Widmer, second ed., Wiley VHC, Germany.

Morrin, A., Ngamna, O., Killard, A.J., Moulton, S.E., Smyth, M.R., Fallace, G.G., 2005. An amperometric enzyme biosensor fabricated from polyaniline nanoparticles. Electroanalysis 17, 423-430.

Mosbach, K., 1994. Molecular Imprinting. Trends Biochem. Sci. 19, 9-14.

Palaniappan, S., John, A., 2008. Polyaniline materials by emulsion polymerisation pathway. Progr. Polym. Sci. 33, 732-758.

Piletsky, S.A., Nicholls, I.A., Rozhko, M.I., Sergeyeva, T.A., Piletska, E.V., El'Skaya, A.V., Karube, I., 2005. Molecularly imprinted polymers – tyrosinase mimics. Ukr. Biokhim. Zh. 77, 63–67.

Piletsky, S.A., Turner, A.P.F., 2002. Electrochemical sensors based on molecularly imprinted polymers. Electroanalysis 14, 317–23.

Piletsky, S.A., Turner, N.W., Laitenberger, P., 2006. Molecularly imprinted polymers in clinical diagnostics—Future potential and existing problems. Med. Eng .Phys. 28, 971–977.

Somerset, V., Klink, M., Akinyeye, R., Michira, I., Sekota, M., Al-Ahmed, A., Baker, P., Iwuoha, E., 2007. Spectroelectrochemical reactivities of novel polyaniline nanotube pesticide biosensors. Macromol. Symp. 255, 36–49.

Sreenivasan, K., 2007. Synthesis and evaluation of multiply templated molecularly imprinted polyaniline. J. Mater. Sci. 42, 7575-1578.

Virji, S., Huang, J., Kaner, R.B., Weiller, B.H., 2004. Polyaniline nanofiber gas sensors: examination of response mechanism. Nano Lett. 4, 491–496.

Wullf, G., 1993. The role of binding-site interactions in the molecular imprinting of polymers. Trends Biotechnol. 11, 85-87.

Yoon, H., Jang, J., 2009. Conducting-polymer nanomaterials for high-performance sensor applications: issues and challenges. Adv. Funct. Mater. 19, 1567–1576.

Zhang, D., Wang, Y., 2006. Synthesis and applications of one-dimensional nano-structured polyaniline: an overview. Mater. Sci. Eng., B 134, 9-19.

Zhao, M., Wu, X., Cai, C., 2009. Polyaniline nanofibers: synthesis, characterisation and application to direct electron transfer of glucose oxidase. J. Phys. Chem. C 113, 4987–4996.

Zhou, N., Yang, T., Jiang, C., Du, M., Jiao, K., 2009. Highly sensitive electrochemical impedance spectroscopic detection of DNA hybridisation based on Au_{nano}–CNT/PANI nano films. Talanta 77, 1021–1026.

Zhu, N., Chang, Z., Heb, P., Fang, Y., 2006. Electrochemically fabricated polyaniline nanowire-modified electrode for voltammetric detection of DNA hybridisation. Electrochim. Acta 51, 3758–3762.

Figure captions

Figure 1. CV scan of a solution containing NPEDMA 2.4 mmol L^{-1} in $HClO_4$ 50 mmol L^{-1} (Parameters: initial potential -0.4 V, final potential 1.0 V, scan rate 50 mV s^{-1}, 10 cycles, Potential vs Ag/AgCl).

Figure 2. SEM image of (A) top view of PANI nanostructures, after template dissolution (some residuals of the template still present); (B) vertically aligned PANI nanostructures, after and template dissolution, cross-sectional view. The length of the structures is proximately the same of the template thickness (nominal value 60 μm).

Figure 3. (A) SEM images of single PANI nanotube (sample prepared on TEM grid for STEM analysis), several microns long; (B) STEM image of single PANI nanotubes; (C) carbon mapping profile along the section of the nanostructure.

Figure 4. CV of 100 μmol L^{-1} catechol in PBS 10 mmol L^{-1}, pH 7.4, after loading with 5 mmol L^{-1} $CuCl_2$ for 5' (CV parameters: start potential -0.5 V, first vertex potential 0.9 V, second vertex potential -0.5 V, step potential 0.01 V, scan rate 0.05 V s^{-1}; Potential vs. Ag/AgCl). Signals obtained using MIP-grafted sensor (solid line), Au-sputtered alumina membrane before electropolymerisation (dotted line), sensor after the growth of PANI nanostructures (dashed line).

Figure 5. CV of catechol and structural analogues that are potentially interfering compounds. All the solutions were prepared using PBS 10 mmol L^{-1}, pH 7.4 and cycled after loading the sensor with 5 mmol L^{-1} $CuCl_2$ for 5' (CV parameters: start potential -0.5 V, first vertex potential 0.9 V, second vertex potential -0.5 V, step potential 0.01 V, scan rate 0.05 V s^{-1}; Potential vs. Ag/AgCl).

Figure 6. Calibration plot of anodic peak current vs catechol concentration for MIP-sensor and corresponding data obtained a non imprinted control sensor. All the solution were prepared using PBS 10 mmol L^{-1}, pH 7.4 and cycled after loading the sensor with 5 mmol L^{-1} $CuCl_2$ for 5'. Inset: linear fit of the linea part of the curve (0-2 µM): Y = 35.7 X + 4.77, R = 0.97. Each data point represents the average from three different sensors. (CV parameters: start potential -0.5 V, first vertex potential 0.9 V, second vertex potential -0.5 V, step potential 0.01 V, scan rate 0.05 V s^{-1}; Potential vs. Ag/AgCl).

Figure(s)

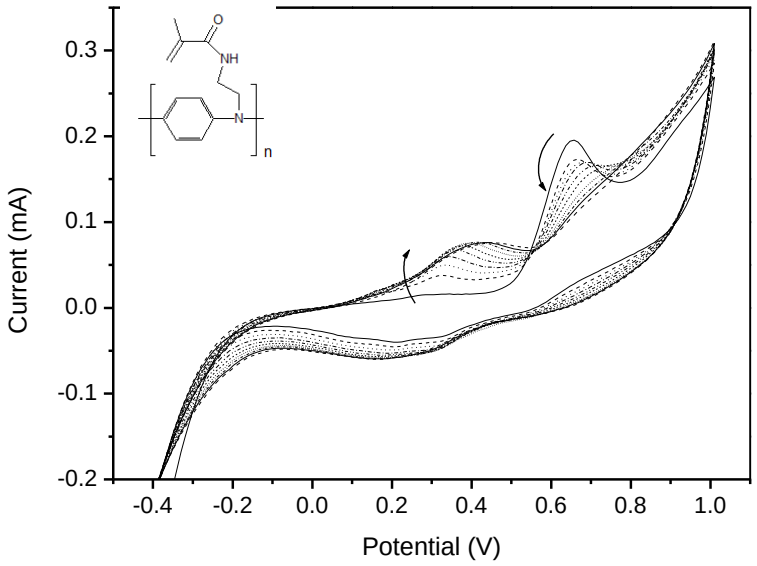

Figure 1.

Figure(s)

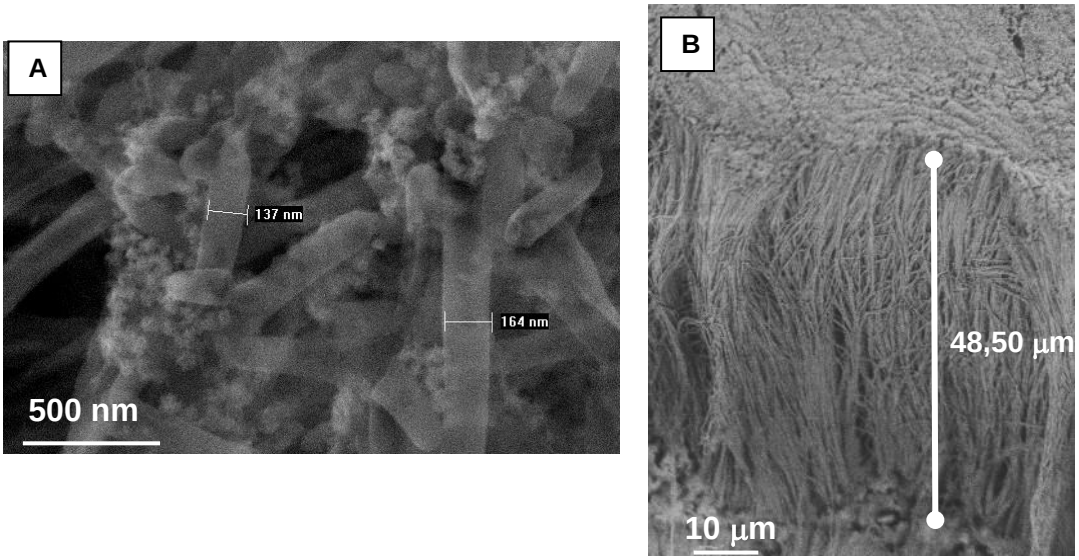

Figure 2.

Figure(s)

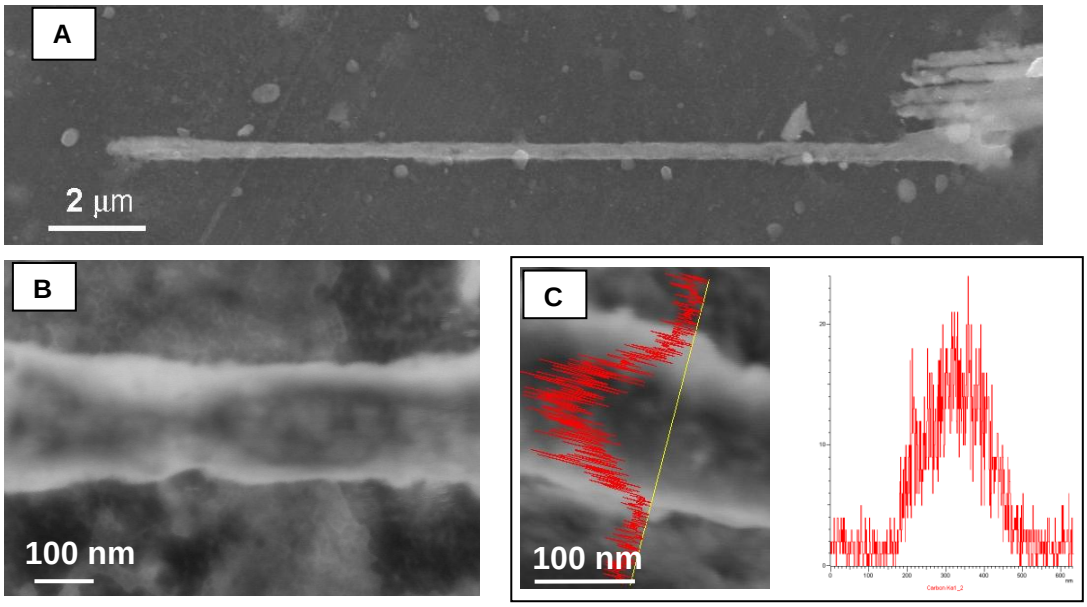

Figure 3.

Figure(s)

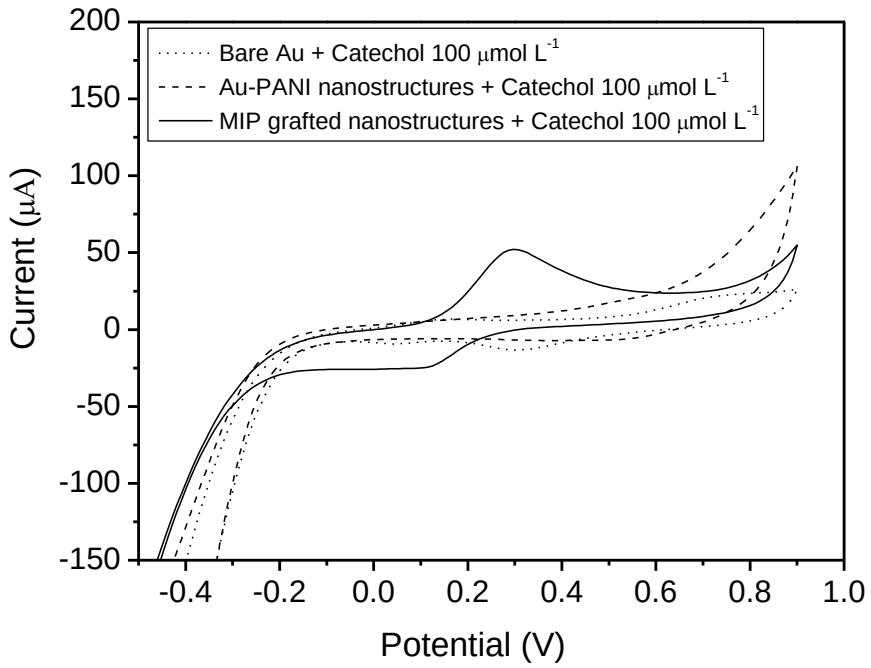

Figure 4.

Figure(s)

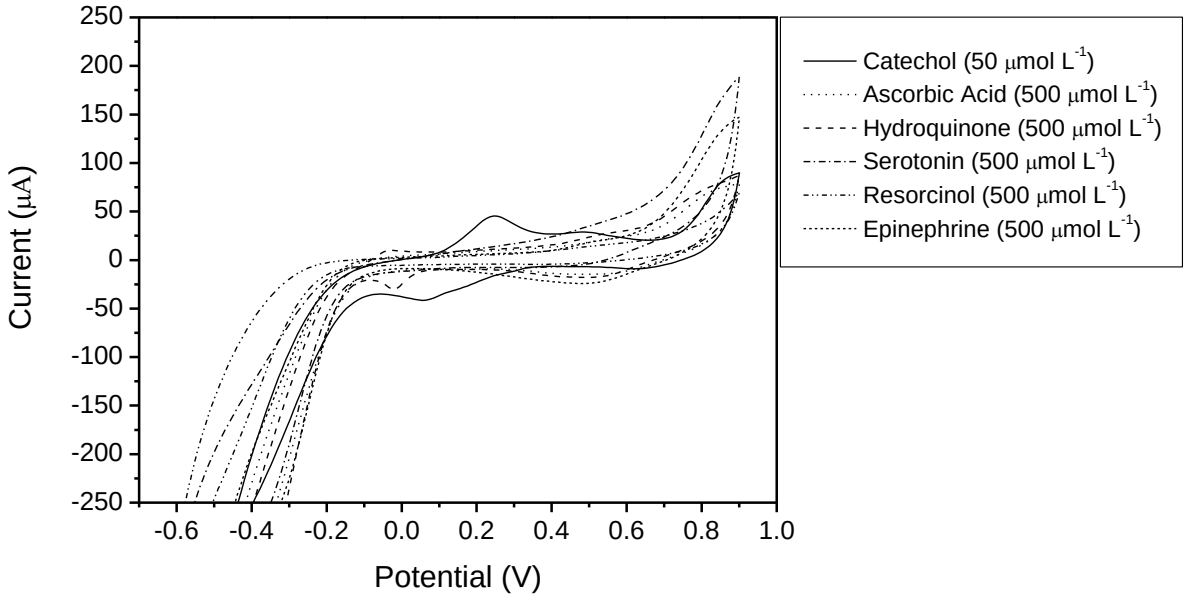

Figure 5.

Figure(s)

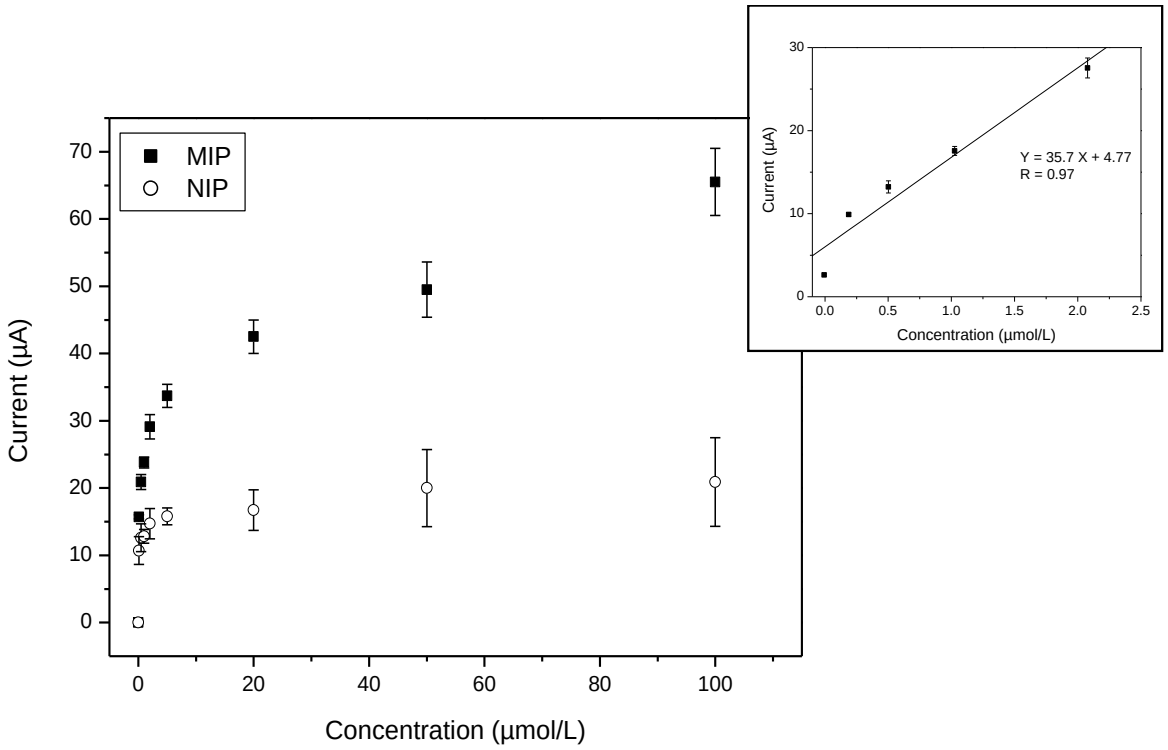

Figure 6.

Università degli Studi di Firenze

Dipartimento di Chimica

Prof. Giovanna Marrazza
Università degli Studi di Firenze
Dipartimento di Chimica
via della Lastruccia, 3
50019 Sesto Fiorentino (Fi)
Italy
e-mail address giovanna.marrazza@unifi.it

Sesto Fiorentino, 16/12/09

Dear Editor,

I am submitting the manuscript entitled:

"**Quasi-monodimensional polyaniline nanostructures for enhanced molecularly imprinted polymer-based sensing".**

The corresponding author is Giovanna Marrazza.

The co-authors are: Francesca Berti, Silvia Todros, Dhana Lakshmi, Michael J. Whitcombe, Iva Chianella, Matteo Ferroni, Sergey A. Piletsky, Anthony P. F. Turner.

The paper should be published as a Full Paper.

This manuscript (or any part of it) has not been previously published and is not under consideration for publication in other Journals.

Thank you for your consideration. I am looking forward to hear from you.

Best regards

Prof. Giovanna Marrazza